The Role of Interleukin-6 in the Regulation of Glucose Sensing in Hypothalamic GT1-7 Neurons

Geoffrey T. Denwood

Thesis Submitted for the Degree of

Doctor of Philosophy

October 2015

Table of Contents

List of Figures

List of Tables

Abbreviations

2-DG	2-deoxyglucose
5-TG	5-thioglucose
AgRP	agouti-related peptide
AMPK	AMP-activated protein kinase
ANOVA	analysis of variance
AP-1	activator protein 1
AP	area postrema
ARC	arcute nucleus of the hypothalamus
BAT	brown adipose tissue
BBB	blood brain barrier
BLM	basolateral region
BSA	bovine serum albumin
C/EBPβ	CCAAT enhancer binding protein β
CAMKKβ	calcium/calmodulin-dependent kinase kinase-β
cAMP	cyclic AMP
CNS	central nervous system
Co-IP	co-immunoprecipitation
COX	cytochrome c oxidase
CREB	cAMP response-element binding protein
CRH	corticotrophin-releasing hormone
CRHR	CRH receptor
CRP	C-reactive protein
CRR	counter regulatory response
CSF	cerebrospinal fluid
DM	diabetes mellitus
DMNX	dorsal motor nucleus of the vagus
DVC	dorsal vagal complex
ECAR	extracellular acidification rate
EPAC	exchange proteins activated by cAMP
ERK	extracellular signal regulated kinase
ETC	electron transport chain

FCCP	carbonyl cyanide-p-trifluoromethoxyphenylhydrazone
FRET	fluorescence resonance energy transfer
GABA	γ-aminobutyric acid
GE	glucose-excited
GFAP	glial fibrillary acidic protein
GH	growth hormone
GHRH	growth hormone releasing hormone
GI	glucose-inhibited
GK	glucokinase
GLUT	glucose transporter
GnRH	gonadotropin-releasing hormone
gp130	glycoprotein 130
HBSS	Hank's balanced salt solution
HFD	high fat diet
HK	hexokinase
hrIL-6	human recombinant IL-6
HSP60	heat shock protein 60
HSV1	herpes virus type 1
IP	intraperitoneal
IC_{50}	half maximal inhibitory concentration
ICV	intracerebroventricular
IL-6	interleukin-6
IL-6Rα	IL-6 α-receptor
IP	immunoprecipitation
IRS	insulin receptor substrate
iWAT	inguinal white adipose tissue
JAK	Janus kinase
K_{ATP}	ATP-sensitive potassium channels
LH	lateral hypothalamus
LKB1	liver kinase B1
MAN	medial amygdala nucleus
MAPK	mitogen activated protein kinase

MCH	melanin-concentrating hormone
MCL-1	myeloid cell leukemia-1
MCTs	monocarboxylate transporters
MOI	multiplicity of infection
NBD2	nuclear binding domain 2
NCX	sodium calcium exchanger
NO	nitric oxide
NPY	neuropeptide Y
NPC	neural precursor cells
NTS	nucleus of the tractus solitarius
OCR	oxygen consumption rate
OGD	oxygen and glucose deprivation
OSM	oncostatin M
OSMR	oncostatin M receptor
PBS	phosphate buffered saline
PDH	pyruvate dehydrogenase
PFKFB	6-phosphofructo-2-kinase/fructose-2,6-bisphosphatase
PGC1α	peroxisome proliferator-activated receptor γ coactivator 1-α
PHB1	prohibitin 1
PHHI	persistent hyperinsulinaemic hypoglycaemia of infancy
PI3K	phosphatidylinositol-4,5-bisphosphate 3-kinase
PIP2	phosphatidylinositol 4,5-bisphosphate
PKA	protein kinase A
PKB	protein kinase B or AKT
PKM2	pyruvate kinase muscle 2
PLL	poly-L-lysine
POMC	pro-opiomelanocortin
PVN	paraventricular nucleus of the hypothalamus
qRT-PCR	quantitative real time polymerase chain reaction
SDS-PAGE	sodium dodecyl sulphate polyacrylamide gel

	electrophoresis
SEM	standard error of the mean
SF-1	steroidogenic factor-1
SGLT	sodium-glucose linked transporter
SHP2	SH2-domain-containing tyrosine phosphatase
shRNA	small hairpin RNA
SOCS	suppressor of cytokine signalling
STAT	signal transducer and activator of transcription
STK11	serine/threonine kinase 11
SUR	sulphonylurea receptor
T172	threonine 172
T1D	type 1 diabetes
T2D	type 2 diabetes
TBST	tris-buffered saline with tween
TRPs	tandem pore K^+ channels
TU	transducing units
UCN1-3	urocortins 1-3
UCP	uncoupling protein
VDCC	voltage-dependent calcium channels
VL-VMN	ventrolateral-ventromedial nucleus
V_m	membrane potential
VMH	ventromedial hypothalamus
YFP	yellow fluorescent protein

Acknowledgments

Firstly, I would like to acknowledge my supervisors Professors Rory McCrimmon and Michael Ashford for giving me the opportunity to conduct this research and supporting me during my time under their supervision. I would also like to acknowledge my thesis monitoring committee, particularly Drs Calum Sutherland and Will Fuller for their support and willingness to help. I especially would like to thank Dr Will Fuller for teaching me the immunoprecipitation technique.

All members of the McCrimmon and Ashford labs past and present deserve acknowledgement for their help, advice and friendship, particular Kenneth and Craig. Special thanks go to Kathryn Wright for her contributions to this work.

Thank you to Dr Alison McNeilly for constant encouragement and company on the late shifts – the night is yet young!

Special thanks to Drs John Findlay and Elizabeth Haythorne for their friendship and caring nature throughout, and my PhD peers Polly, Susan and Fiona for helping me survive and keep going and providing good times outside of the lab.

I can't express my gratitude enough to Lauren Tebay, without whom, there simply would not be the physical thesis, with special commendations to Susan and Alison as well for their tireless efforts.

Thank you to Mum, Dad and Fay for the belief you've shown in me and for giving me the encouragement to stick in. Thanks also to Gran who I know would be very proud and want a copy of this work.

Amy, thank you for your unwavering support, unconditional loyalty and understanding, for taking care of me and helping me to remember that everything will be ok. I owe you one!

Declaration

I declare that this thesis is based on results obtained from investigations which I have personally carried out in the Division of Cardiovascular and Diabetes Medicine within the Medical Research Institute in the University of Dundee from October 2011 to September 2015 using funding provided by the Juvenile Diabetes Research Foundation I declare that the entire thesis is my own composition. Any work other than my own is clearly stated in the text and acknowledged with reference to any relevant investigators or contributors. This thesis has never been presented previously, in whole or in part, for the award of any higher degree. I have consulted all the references cited within the text of this thesis.

Signed Date ……

I confirm that Geoffrey Denwood has spent the equivalent of at least 9 terms in the Division of Cardiovascular and Diabetes Medicine, Medical Research Institute, University of Dundee, and that he has fulfilled the condition of the University of Dundee, thereby qualifying him to submit this thesis in application for the degree of Doctor of Philosophy.

Signed  Date:…….

Summary

Hypoglycaemia is the major complication associated with insulin therapy in type 1 diabetes. Repeated exposure to hypoglycaemia leads to suppression of normal counter regulatory responses (CRR) to subsequent hypoglycaemia, which increases the risk of severe episodes of hypoglycaemia. Studies have demonstrated the important role the brain plays in the regulation of whole body glucose homeostasis, including a vital role in mounting the CRR. Detection of hypoglycaemia by specialised glucose-sensing neurons of the hypothalamus is critical for initiating the associated CRR. It is believed that defective CRRs are mediated by brain adaptations leading to impaired central glucose sensing, although the mechanisms by which these occur remain unknown. Hypoglycaemia evokes a significant systemic and central stress response with an increase in inflammatory mediators including interleukin-6 (IL-6). The aim of the current study was to investigate whether IL-6 played a role in the regulation of central glucose sensing. This was addressed by examining the effects of IL-6 exposure on electrophysiological and biochemical responses in hypothalamic glucose-excited GT1-7 neurons. Antecedent exposure to IL-6 induced defective glucose sensing of subsequent hypoglycaemia, with a role for the exchange protein activated by cAMP (EPAC) implicated in this observation. The results obtained suggest that EPAC may mediate this effect by enhancing the sensitivity of ATP-sensitive potassium (K_{ATP}) channels to ATP-mediated inhibition following IL-6 exposure. The current results identify IL-6 and EPAC2 as novel mediators of defective hypothalamic glucose sensing, suggesting they may contribute to the development of blunted CRR observed with recurrent hypoglycaemia exposure.

1 Introduction

1.1 Diabetes

Diabetes Mellitus (DM) describes a metabolic disorder of multiple causes characterised by chronic hyperglycaemia with disturbances of carbohydrate, fat and protein metabolism resulting from defects in insulin secretion and or action (WHO, About Diabetes, retrieved July 24th 2015). Diabetes leads to damage, dysfunction and failure of multiple organs.

The two main types of diabetes are Type 1 Diabetes (T1D) and Type 2 Diabetes (T2D). T1D is an autoimmune disease that usually, but not exclusively, develops in childhood and is characterised by destruction of the pancreatic beta-cells leading to an absence of endogenous insulin. This type of diabetes represents 10% of all DM worldwide. The other 90% of DM is T2D, which usually develops in adulthood and is related to obesity, sedentary lifestyle and the consumption of unhealthy, high-fat and high-sugar diets (WHO, About Diabetes, retrieved July 24th 2015). Weight loss and physical activity are effective therapies for T2D.

Chronic hyperglycaemia leads to microvascular and macrovascular disease including retinopathy, nephropathy and neuropathy and increases the risk of cardiovascular disease (Yan 2014; Laakso & Kuusisto 2014). Regaining glycaemic control to limit hyperglycaemia has been shown to prevent or delay hyperglycaemia associated complications. However, the use of sulphonylurea drugs to increase insulin secretion or administration of exogenous insulin to achieve this can lead to unregulated hyperinsulinaemia, which poses the significant risk of hypoglycaemia.

1.2 Hypoglycaemia in Diabetes

It is estimated that 285 million people worldwide had diabetes in 2010, and the number of sufferers is predicted to increase by ~50% to 438 million people by the year 2030 (Cryer 2013). Improving glycaemic control by lowering blood glucose concentrations closer to the non-diabetic range in patients delays the microvascular (retinopathy, nephropathy, and neuropathy) and macrovascular (coronary, cerebral, and peripheral atherosclerosis) complications of type 1 and 2 diabetes. However, the use of sulphonylureas or insulin administration to achieve this introduces the considerable risk of hypoglycaemia, which is widely regarded as the major complication of improving

glycaemic control in patients with T1D and many with advanced stage T2D. The maintenance of circulating plasma glucose levels in the normal physiological range of 4-6 mM is critical as the brain relies almost exclusively on blood glucose as its primary source of energy and accounts for 60-80% of total body glucose uptake (Wasserman 2009; Zierler 1999). When blood glucose falls below 3 mM symptoms such as nervousness and irritability will ensue, and hypoglycaemia allowed to continue unchallenged will lead to impaired cognitive and motor function, coma and death (Donovan & Watts 2014). Unlike complications associated with chronic hyperglycaemia, acute hypoglycaemia can mediate negative effects within minutes (Donovan & Watts 2014). Hypoglycaemia impairs defences against subsequent hypoglycaemia and thus causes a vicious cycle of recurrent hypoglycaemia (Cryer 2013). In healthy individuals a very effective combination of behavioural and physiological responses to hypoglycaemia act rapidly to restore euglycaemia upon detection of falling plasma glucose levels, however these counter regulatory responses (CRR) are compromised in diabetes. Attenuated epinephrine and sympathetic neural responses to falling glucose levels play a key role in the pathophysiology of T1D and advanced stage T2D in the absence of normal insulin and glucagon responses.

Hypoglycaemia is a huge detriment to the lives of patients with T1D. They suffer immeasurable episodes of asymptomatic hypoglycaemia, an average of two symptomatic episodes per week and an average of one episode of severe hypoglycaemia requiring the assistance of another person each year. A 2007 study found that duration of T1D did not influence the prevalence or incidence of mild hypoglycaemia (UK Hypoglycaemia Study Group 2007). However, in the same study, the long-duration T1D group experienced the highest frequency of severe episodes of hypoglycaemia (UK Hypoglycaemia Study Group 2007). In T2D, the administration of sulphonylureas to increase insulin secretion or exogenous insulin can cause therapeutic hyperinsulinaemia independent of the plasma glucose level, and therefore hypoglycaemia. However, studies have shown that hypoglycaemia frequency in T2D is much lower than that seen in T1D, with Donnelly *et al*. reporting that participants with T1D in their trial had a rate of 42.89 episodes of hypoglycaemia per patient year compared to a rate of 16.37 episodes of hypoglycaemia per patient year in the T2D cohort (Donnelly et al. 2005). As insulin secretion and action is impaired increasingly with duration of T2D, hypoglycaemia becomes more limiting to glycaemic control (Cryer 2013). The UK Hypoglycaemia Study Group reported that the frequency of severe hypoglycaemia

increases with the duration of insulin therapy in T2D, such that the incidence of mild and severe hypoglycaemia for T2D patients on insulin for more than 5 years was similar to that for T1D patients with short disease duration (UK Hypoglycaemia Study Group 2007).

1.3 Physiology and Pathophysiology of Defence Against Hypoglycaemia

As previously mentioned, physiological and behavioural responses combine to prevent or correct the incidence of clinical hypoglycaemia in healthy individuals. Physiological responses are primarily decreased endogenous insulin secretion as plasma glucose levels fall within the physiological range and increased glucagon secretion, and if glucose continues to fall, increased epinephrine responses as glucose levels fall below the physiological range. These responses act to increase hepatic glucose production and decrease glucose clearance by insulin-sensitive tissues such as skeletal muscle; therefore leading to an increase in plasma glucose levels. All CRR hormones are initiated at blood glucose levels just below the normal range, i.e., 3.6-3.8 mM (Cryer 1997). The behavioural component of the CRR leads to the ingestion of carbohydrates that is prompted by symptoms of hypoglycaemia; critical for patient awareness of hypoglycaemia.

In T1D three major defects in this homeostatic response contribute to the high frequency of hypoglycaemia observed. Firstly, T1D is characterised by an absence of insulin due to auto-immune destruction of the pancreatic beta-cells and the administration of exogenous insulin can lead to the development of unregulated and sustained hyperinsulinaemia (McCrimmon & Sherwin 2010). Secondly, reduced or absent glucagon, the principal rapid-acting CRR hormone, results in considerable impairment of glucose recovery from hypoglycaemia (Gerich et al. 1973). The cause of suppressed glucagon responses to hypoglycaemia in individuals with T1D is still disputed and a number of both intra- and extra-pancreatic factors have been implicated in this defect, including beta to alpha-cell signalling (Fukuda et al. 1988) and ventromedial hypothalamus (VMH)-mediated effects of insulin (Paranjape et al. 2010). Thirdly, a reduced autonomic response to hypoglycaemia affects the majority of patients with T1D by 10 years of disease duration (Mokan et al. 1994). Hypoglycaemia normally activates the autonomic nervous system leading to increased hepatic glucose production and reduced glucose uptake from the circulation in peripheral tissues.

Activation of the sympathetic nervous system stimulates glycogenolysis and gluconeogenesis in the liver, processes that are important in the correction of falling plasma glucose levels. The autonomic response is closely associated with the generation of symptomatic responses to hypoglycaemia and therefore impairment of this response can lead to reduced awareness of hypoglycaemia due to lack of symptoms (McCrimmon & Sherwin 2010). The major driver of reduced autonomic responses to hypoglycaemia is antecedent hypoglycaemia itself, thus leading to a vicious cycle of hypoglycaemia in patients with T1D (Heller & Cryer 1991).

The barrier of hypoglycaemia can range from being a nuisance to being life-threatening (Cryer 2013). Fortunately, the incidence of prolonged, profound hypoglycaemia that can result in serious brain injury is rare, however, hypoglycaemia can be fatal, with percentage estimates of hypoglycaemia mortality rates ranging from 2-10% (Feltbower 2008; Skrivarhaug et al. 2006).

1.4 Hypoglycaemia Detection

To initiate the vital CRR to correct hypoglycaemia, it first must be rapidly detected. Specialised glucose sensors are distributed at multiple sites throughout the body that are capable of detecting decreases in glucose levels, and activation of these sensors results in stimulation of CRR (Verberne et al. 2014). Although there are peripheral glucose sensors situated in the pancreas (beta-cell), the hepatic portal vein, the gut and the carotid body, overwhelming evidence implicates central nervous system (CNS) glucose sensing as being critical in inducing CRR to hypoglycaemia.

The brain has been recognised as an important regulator of glucose homeostasis since Claude Bernard's initial observation that a puncture of the floor of the fourth ventricle of dogs induced diabetes (Thorens 2012). Later, Jean Mayer proposed the glucostatic hypothesis, stating that feeding behaviour is regulated by central glucose sensing (Mayer 1953). Subsequent lesioning experiments demonstrated the importance of distinct hypothalamic nuclei and their involvement in the regulation of feeding and fasting. Lesioning of the lateral hypothalamus reduced feeding and body weight, whereas lesion of the VMH induced hyperphagia and hyperinsulinaemia (Hoebel 1965; King 2006). The use of gold thioglucose, which causes the destruction of VMH neurons, induces obesity; an effect providing evidence for central glucose responsive structures as the toxic effect of gold thioglucose is not replicated when gold is

conjugated with other metabolites or nutrients, suggesting a specific effect on glucose-sensitive neurons (Thorens 2012).

Studies in dogs demonstrated that maintaining brain glucose levels during systemic hypoglycaemia resulted in a reduced neurohumoral reaction to the hypoglycaemic challenge, suggesting that it was the fall in glucose within the brain that triggered the process leading to counter regulation (Frizzell et al. 1993; Biggers et al. 1989). The importance of the VMH in the mounting of the CRR to hypoglycaemia was demonstrated by studies using 2-deoxyglucose (2-DG) to induce neuroglucopenia in rats, stimulating the CRR (Borg et al. 1995). Furthermore, studies involving lesioning of the VMH by stereotaxic injection of ibotenic acid reduced counter regulation (Borg et al. 1994). Similarly, maintenance of VMH glucose levels during hypoglycaemia reduced counter regulation (Borg et al. 1997). Furthermore, mice with VMH specific deletion of the vesicular glutamate transporter, VGLUT2, in steroidogenic factor-1 (SF-1) expressing neurons had a marked defect in glucagon secretion in response to fasting or hypoglycaemia, suggesting that glutametergic neurons of the VMH are required for the CRR (Tong et al. 2007).

Brain nutrient sensors need to be able to rapidly and accurately detect changes in blood glucose. Specialised glucose-sensing neurons with this inherent property were first described in the 1960s by Anand BK *et al.* and Oomura *et al.* (Oomura & Yoshimatsu 1984; Anand et al. 1964). These neurons were reported to not only use glucose as a fuel source but also as a signalling molecule to regulate their activity. These neurons are classified as being either glucose-excited (GE) or glucose-inhibited (GI), increasing or decreasing their activity in response to glucose respectively. GE and GI neurons are present in the arcute (ARC), ventromedial (VMH), paraventricular (PVN) and lateral hypothalamic (LH) nuclei (Silver & Erecińska 1998; Wang et al. 2004).

The ARC is an important site for the integration of hormonal, nutritional and neuronal signals comprising neurons expressing anorexigenic and orexigenic peptides (Kohno & Yada 2012). Neurons in the ARC as well as the PVN and the LH are involved in the regulation of peripheral metabolism through regulation of the activity of the sympathetic and parasympathetic branches of the autonomic nervous system (Thorens 2012). Neurons in this circuitry are regulated by hormones including ghrelin, insulin and leptin as well as nutrients such as lipids, amino acids and glucose (Gale et al. 2004; Schwartz 2000). Importantly, glucose has been found to inhibit 40% of orexigenic

neuropeptide Y (NPY)-expressing neurons, while anorexigenic pro-opiomelanocortin (POMC) neurons are GE neurons and orexin neurons in the LH are GI (Thorens 2012).

1.4.1 Non-Hypothalamic Glucose Sensing

In studies similar to those performed in the VMH, the importance of the hindbrain structures involved in glucose-dependent regulation of feeding and glucose homeostasis, including the dorsal vagal complex (DVC), area postrema (AP), nucleus of the tractus solitarius (NTS), dorsal motor nucleus of the vagus (DMNX) and basolateral region (BLM), have been demonstrated by intracerebroventricular (ICV) injection of 2-DG, which only stimulates feeding if the cerebral aqueduct is open to allow access of the injected substance to the brainstem (Ritter et al. 1981) and the finding that 5-thioglucose (5-TG) can increase food intake when injected into the NTS, DMNX or BLM (Ritter et al. 2000). NTS neurons have been shown to be glucose sensitive in studies measuring their firing activity (Yettefti et al. 1995). NTS neurons project to the LH and PVN and neurons from the BLM project to the ARC, and destruction of the circuitry from the BLM to the ARC suppresses the effect of brainstem 2-DG injection to increase food intake and regulate expression of orexigenic agouti-related peptide (AgRP) and NPY, suggesting a highly functional interrelationship between GS neurons from the brainstem and hypothalamus in the control of feeding (Fraley & Ritter 2003; Ritter et al. 2001).

The medial amygdala nucleus (MAN) was also identified as a novel, limbic glucose-sensing region, containing glucokinase (GK)-expressing glucose-sensing neurons that responded directly to alterations in glucose availability in both *in vitro* and *in vivo* experiments (Zhou et al. 2010).

1.4.2 Non-Neuronal Glucose Sensing

Non-neuronal glial cells such as astrocytes and tanycytes may also be involved in hypoglycaemia detection. Importantly, astrocytes have been shown to be important for neuronal support, and metabolic coupling between astrocytes and neurons has been described whereby glucose utilisation by neurons occurs subsequent to its initial uptake and metabolism by astrocytes that produces lactate. The lactate produced can then be transferred to neurons via specific monocarboxylate transporters (MCTs) and used by neurons for ATP generation (Magistretti et al. 1999; Pellerin et al. 2007). The coupling

of metabolism in this way between the two cell types may be important in the function of glucose sensing.

The increase in c-fos labelling of neurons and astrocytes in the ARC, PVN and NTS induced by intracarotid or brainstem injection of glucose or 2-DG can be blocked by administration of the astrocyte-specific glycolytic inhibitor methyl sulfoximide (Guillod-Maximin et al. 2004; Young et al. 2000) demonstrating the importance of astrocytic glucose metabolism in neuronal activation in response to glucose deprivation. C-fos labelling studies have demonstrated the involvement of astrocyte-derived lactate in the control of glucose-sensing neurons in the AP and NTS of the brainstem using an MCT inhibitor to prevent astrocyte to neuron shuttling of lactate, with the intervention leading to elevations in blood glucose concentrations (Briski & Patil 2005; Patil & Briski 2005; Patil & Briski 2005)

Tanycytes are another subpopulation of glial cells that line the lateral lower part and the floor of the third ventricle. They have extended basal processes that reach regions of the median eminence devoid of blood-brain barrier (BBB) and sometimes are in direct contact with microvessels present in the median eminence (Thorens 2012). These processes form contact with neurons of the ARC, particularly those expressing NPY (Thorens 2012). These cells are therefore optimally positioned to contact both the cerebrospinal fluid (CSF) and the general circulation and they express glucose transporter 2 (GLUT2) and GK (García et al. 2003; Millán et al. 2010), suggesting that they may be involved in glucose sensing. Coppola *et al*. demonstrated a functional link between tanycytes and NPY neurons of the ARC with the observation that a reaction catalysed by deiodinase II (DIO2) in tanycytes can effect glucose sensing by inducing uncoupling protein 2 (UCP2) expression in NPY neurons (Coppola et al. 2007).

1.5 Mechanisms of Glucose Sensing – Glucose Excited Neurons

GE neurons for the most part use metabolic sensing mechanisms, requiring the uptake and subsequent metabolism of glucose to regulate their activity. The mechanisms of glucose sensing by GE neurons are thought to be analogous to those of the pancreatic beta-cell, which depend on glucose metabolism and production of coupling factors predominantly from mitochondrial metabolism which induce depolarisation of the plasma membrane prior to Ca^{2+} entry and stimulated secretion (Thorens 2012). Briefly,

this pathway involves uptake of glucose through GLUT2, phosphorylation of glucose by GK and a subsequent rise in the intracellular ATP/ADP ratio, which induces closure of ATP-sensitive potassium channels (K_{ATP}) resulting in depolarisation of the cell membrane and opening of voltage-gated calcium channels (VDCCs), resulting in Ca^{2+} influx which triggers insulin secretion.

1.5.1 The Role of Glucose Transport in Glucose Sensing

The Thorens group have focused on the role of Glut2 in glucose sensing and have observed its expression in the mouse brain in neurons, astrocytes, tanycytes and endothelial cells (Arluison et al. 2004; Marty et al. 2007). However, co-localisation of Glut2 has not been observed in NPY, POMC, orexin or melanin-concentrating hormone (MCH) neurons of the hypothalamus (Mounien et al. 2010). Similarly, only low Glut2 expression has been confirmed by qRT-PCR in the rat ARC, VMH, PVN and LH (Li et al. 2003). In 2004, Kang *et al.* conducted a study using single-cell RT-PCR and were able to show expression of Glut2 in about 33% of GE, GI and non-glucose-sensing neurons studied (Kang et al. 2004). In support of a role for GLUT2 in the central glucose-sensing machinery, Roncero *et al.* did observe its expression co-localised with GK in the hypothalamus and brainstem (Roncero et al. 2004). To further identify Glut2 expressing cells in the brain, the Thorens lab developed a transgenic mouse with yellow fluorescent protein (YFP) labelled Glut2, and were able to determine that Glut2 was only expressed in neuronal cells (Mounien et al. 2010). These cells were located most abundantly in the LH, with only a few cells present in the VMH and no positive cells in the ARC. Further YFP expressing cells were located in NTS, DMNX and BLM of the brainstem. Encouragingly, the YFP positive cells were demonstrated to be glucose responsive as intraperitoneal (IP) glucose or 2-DG increased c-fos immunoreactivity in these cells (Thorens 2012).

The Thorens lab developed another elegant mouse model to investigate the role of Glut2 in glucose sensing, in which they genetically inactivated Glut2 and transgenically re-expressed Glut1 in the beta-cells to normalise glucose-stimulated insulin secretion (GSIS). These mice had a reduced glucagon response to hypoglycaemia which was able to be restored upon re-expression of Glut2 in astrocytes but not in neurons, which also restored c-fos activation in the DVC in response to IP 2-DG injection (Thorens et al. 2000; Marty et al. 2005). These findings lend support to the view that astrocyte-neuron metabolic coupling is required for appropriate hypoglycaemia detection and

associated CRR, although make the subsequent observations by Mounien *et al.* of Glut2 expression only in neurons puzzling (Mounien et al. 2010). Importantly in these studies, c-fos labelling in the VMN in response to 2-DG was observed to be similar in GLUT2 positive and GLUT2$^{-/-}$ animals, suggesting that GLUT2 is not involved in hypoglycaemia detection in the VMN.

There is evidence that Na^+-dependent glucose transporters SGLT1 and 3 are required for glucose to excite neuronal activity. ICV injection of phlorizin, a specific of inhibitor of SGLT1 enhances food intake in rats (Tsujii & Bray 1990) and inhibits activation of GE neurons in the VMH (Yang et al. 1999). Furthermore, a majority of isolated GE hypothalamic neurons can be activated by the SGLT1 substrate α-MDG and the activity of these neurons cannot be increased by tolbutamide, suggesting that the increased activity induced by α-MDG may not be K_{ATP}-dependent (O'Malley et al. 2006). Glucose has been shown to induce a large inward current in *Xenopus* oocytes expressing SGLT3 and the mRNA for this transporter is expressed in cultured hypothalamic neurons and adult hypothalamus suggesting it may also be involved in glucose sensing (O'Malley et al. 2006).

1.5.2 Role of Glucokinase in Glucose Sensing

Phosphorylation of glucose by the low affinity enzyme GK is the regulated step in glycolysis (Lenzen 2014). GK has a K_m in the physiological range of blood glucose and is expressed in pancreatic beta and alpha-cells, hepatocytes and neurons.

The expression of GK has been confirmed in the brain of mice (Jetton et al. 1994). Barry Levin's group attempted to further characterise GK expression in the brain and were able to demonstrate its co-localisation with certain neuropeptides (Lynch et al. 2000; Dunn-Meynell et al. 2002). Jeffrey Friedman's group generated an enhanced green fluorescent protein (EGFP)-tagged GK mouse line and confirmed GK expression in the hypothalamus and limbic regions of the brain (Stanley et al. 2013). Similarly to the studies previously described for Glut2, the EGFP-GK cells demonstrated increased c-fos immunoreactivity in response to 2-DG or glucose, confirming them to be responsive to alterations in glucose levels. By exploiting dual immunohistochemistry, GK was shown to be expressed in 36% of GI orexin positive LH neurons, in 20% of POMC and 28% of NPY/AgRP ARC neurons which are GE and GI respectively. GK expression was also observed in glial cells in this work (Stanley et al. 2013). Growth

hormone releasing hormone (GHRH) neurons were confirmed to express GK and were further studied with electrophysiology confirming that they were GI neurons, with their activity increasing with glucose deprivation (Stanley et al. 2013). Importantly, growth hormone (GH) is one of the CRR hormones released in response to hypoglycaemia, and the findings in this study suggest it may be secreted as a direct consequence of glucose sensing by GK positive GI neurons that express GHRH.

Hypothalamic brain slices and cultures have been studied *ex vivo* in order to investigate the effects of GK manipulation on glucose sensing (Kang et al. 2004; L. Kang et al. 2006; Yang et al. 1999; Yang et al. 2004). Interfering RNA mediated knockdown of GK in VMH preparations largely abolished GE and GI glucose sensing, while conversely GK activation of dissociated VMN glucose-sensing neurons amplified GE and GI response (L. Kang et al. 2006). Furthermore, infusion of GK activators into the VMN reduced glucagon responses to hypoglycaemia while the GK inhibitor alloxan or siRNA knockdown of GK increased epinephrine responses to hypoglycaemia (Levin et al. 2008).

The MAN was identified as a glucose-sensing brain region, with the presence of GK positive glucose-sensing neurons confirmed to have a role in increasing or decreasing the CRR to hypoglycaemia (Zhou et al. 2010). Also, with infusion of GK inhibitors, feeding responses to glucoprivation were stimulated, with ICV administration inducing a more robust response than IV, consolidating the importance of central glucose-sensing mechanisms in this phenomenon (Osundiji et al. 2010).

The Evans laboratory has investigated the role of GK in hyperglycaemia. They found that while infusion of glucose into the third ventricle during systemic glucose overload enhanced glucose handling with facilitated insulin release, infusion of the GK inhibitors glucosamine or mannoheptulose reduced glucose tolerance associated with a decrease in insulin release (Osundiji et al. 2012). Furthermore, brain delivery of the two GK inhibitors rapidly triggered robust feeding responses, a physiological response to glucose deprivation, which was more potent than when delivered intravenously (Osundiji et al. 2010).

Whether GK may mediate defective central glucose sensing observed in patients with compromised CRR to hypoglycaemia, particularly those with T1D, is unconfirmed. An increase in GK expression was observed in the rat VMN after hypoglycaemia, associated with a shift in the glucose responsiveness of GE neurons (L. Kang et al.

2008). An increase in GK or hexokinase (HK) expression, if involved in regulating glucose-sensing neurons, would be predicted to impair CRR to low glucose, or at least shift the threshold for activation of CRR to a lower glucose value.

1.5.3 Role of AMPK in Glucose Sensing

AMP-activated protein kinase (AMPK) is an ubiquitously expressed enzyme composed of a catalytic α subunit and regulatory β and γ subunits, often referred to as the "fuel gauge" of a cell. The α1 subunit of AMPK is ubiquitously expressed whereas the α2 subunit is mainly expressed in skeletal muscle, heart and liver. The α2 subunit however has also been shown in brain to be critical for angiogenesis of astrocytomas and for glucose sensing ability by specialised hypothalamic neurons (Neurath et al. 2006; Beall, Hamilton, et al. 2012). AMPK is activated by an increase in the cellular AMP/ATP ratio. This has led to the "fuel gauge" analogy whereby AMPK is activated when cellular ATP levels are depleted (Hardie & Carling 1997). AMPK can also be activated by increased calcium concentrations (even in energy-replete cells), an effect which involves calcium/calmodulin-dependent kinase kinase-β (CAMKKβ)-dependent phosphorylation of threonine 172 (T172) in the activation loop of the α subunit of AMPK. AMPK can also be activated by liver kinase B1 (LKB1) or serine/threonine kinase 11 (STK11), the TGFβ-associated kinase and by glucosamine (Lang & Föller 2014). AMPK can inhibit cell proliferation, counteract hypertrophy and stimulate autophagy.

Cotero and Routh observed no effect of manipulating AMPK activity on the glucose sensing capacity of GE neurons from the ventrolateral-ventromedial nucleus (VL-VMN) of rats. In their study, inducing hypoglycaemia in the presence of the AMPK inhibitor Compound C had no effect on membrane hyperpolarisation in response to 0.1 mM glucose which was comparable to the hyperpolarisation seen in the absence of Compound C. In support of this finding, there was no significant difference in action potential frequency in VL-VMH neurons in the presence or absence of the AMPK activator AICAR, suggesting that AMPK does not regulate glucose sensing in this cell type (Cotero & Routh 2009). In contrast, the Routh group also showed that in GI neurons of the VMN, application of AICAR mimicked the excitatory effect of low glucose on action potential frequency, suggesting that AMPK might play in a role in stimulated neuronal activity in GI neurons (Canabal et al. 2007).

In another study from the Routh lab focusing on NPY expressing GI neurons, phosphorylation of AMPK α2 was increased in rat VMH tissue preparations in response to a reduction in glucose from 2.5 mM to 0.7 mM for 30 minutes, suggesting activation of AMPK in response to glucose deprivation in the VMH (Murphy et al. 2009). AICAR incubation was found to increase the percentage of depolarised VMH neurons, and also further increase the number of depolarised VMH neurons in response to glucose reduction from 2.5 mM to 0.7 mM than glucose reduction alone in the absence of AICAR. The AMPK inhibitor Compound C was found to prevent VMH neuron depolarisation in response to glucose reduction suggesting the importance of AMPK in the ability of GI neurons to depolarise in response to decreases in glucose levels (Murphy et al. 2009; Murphy et al. 2009).

Thorens' group have also identified that GI neurons expressing GLUT2 in the NTS are activated by hypoglycaemia, a depolarising effect which can be blocked by Compound C (Lamy et al. 2014). When stimulated these neurons were found to increase glucagon secretion, suggesting they are part of the circuitry involved in linking hypoglycaemia detection to a CRR, which is dependent on AMPK.

In 2004, Robert Sherwin's group observed that VMH microinjection of the AMPK activator AICAR in rats markedly reduced the glucose infusion rate (GIR) required to maintain an insulin-induced hypoglycaemic plateau (McCrimmon et al. 2004). The group confirmed that this observation was due to increased endogenous glucose production in AICAR treated rats. However, levels of the main CRR hormones glucagon and epinephrine did not differ between the two treatment groups, somewhat unexpectedly, leading to the assumption that AMPK activation stimulates glucose production via a non-hormonally mediated signal (McCrimmon et al. 2004).

Barbara Khan's group used ICV injection of 2-DG to induce neuroglucopenia which induced a robust CRR and a rapid and potent activation of both α1 and α2 AMPK in the ARC, VMH and DMH (Alquier et al. 2007). In this study, the authors also used a recurrent 2-DG protocol to induce defective CRR and showed that this was associated with reduced α1 and α2 AMPK activation in the ARC and MH. Furthermore, injection of AICAR was able to partially restore the impaired CRR in recurrent 2-DG treated rats, reinforcing the importance for appropriate AMPK activation in mounting CRR to hypoglycaemia (Alquier et al. 2007).

The Sherwin lab extended their findings about the role of AMPK in hypothalamic glucose sensing in 2008 by demonstrating that knockdown of VMH AMPK α2 resulted in an increased requirement for exogenous glucose to maintain the hypoglycaemic plateau during a subsequent hyperinsulinaemic clamp study, reinforcing their finding that AMPK activation had the opposite effect to reduce the GIR during the same clamp (McCrimmon et al. 2008; McCrimmon et al. 2004). AMPK α2 knockdown reduced endogenous glucose production and increased peripheral glucose utilisation in this study. Furthermore, knockdown of AMPK α2 suppressed CRR hormone response during hypoglycaemic clamps with significant reductions in the secretion of glucagon and epinephrine observed. The group went on to show that in a rat recurrent hypoglycaemia model of T1D, VMH activation of AMPK with AICAR restored defective CRR hormonal responses to hypoglycaemia induced by the recurrent hypoglycaemia protocol, supporting a crucial role of AMPK in mounting the CRR to hypoglycaemia (Fan et al. 2009). The finding that modulation of hypothalamic AMPK can regulate glucose production has been confirmed by others (Yang et al. 2010).

Another study has demonstrated that injection of glucose into the third ventricle of the hypothalamus results in suppressed activation of AMPK as indexed by its phosphorylation status. The study also confirmed the phosphorylation of AMPK as an indicator of low energy status, as activation of AMPK with AICAR led to increased food intake after a 6 hour fast in wild-type (WT) mice (Zhang et al. 2011).

In GT1-7 cells, a GE population of mouse hypothalamic neurons, overexpression of GLUT2 has been found to increase cellular ATP levels associated with reduced AMPK phosphorylation (Li et al. 2006). Functionally, this study also demonstrated that GLUT2 overexpression attenuated the increase in AgRP mRNA expression and AMPK phosphorylation observed in response to 2-DG treatment, implicating a role for AMPK in the response to low glucose (Li et al. 2006). Another *in vitro* study using hypothalamic N-43/5 neurons showed that these were GE neurons that had increased intracellular calcium mobilisation in response to depolarising stimuli including high glucose, high potassium and the K_{ATP} antagonist tolbutamide (Cai et al. 2007). The depolarising stimuli suppressed AMPK phosphorylation in these cells which was associated with increased POMC expression, demonstrating an involvement of AMPK in the glucose-regulated expression of POMC.

Claret *et al.* showed the importance of functional α2 AMPK for glucose sensing in GE POMC neurons using electrophysiological recordings from mouse hypothalamic slices. In control POMC neurons a decrease in glucose from 2 mM to 0.1 mM resulted in reversible membrane hyperpolarisation, however this response was absent in POMC neurons lacking α2 AMPK (Claret et al. 2007). Similarly, AgRP neurons also failed to hyperpolarise appropriately to 0.1 mM glucose stimulus when α2 AMPK was knocked out. These data suggest that POMC and AgRP are GE neurons that require α2 AMPK for glucose responsiveness.

The importance of AMPK for pancreatic beta-cell glucose sensing capacity has been investigated *in vitro* using isolated pancreatic islets and the CRI-G1 beta-cell line (Beall et al. 2010). In line with previous studies detailed, loss of AMPK α2 from mouse islets resulted in defective hypoglycaemia sensing, an effect also seen with expression of a dominant negative form of AMPK (Beall et al. 2010). This finding was also confirmed in GT1-7 neurons, a population of GE mouse hypothalamic neurons, where AMPK α2 but not α1 knockdown resulted in reduced hypoglycaemia detection (Beall, Hamilton, et al. 2012).

1.5.4 Role of K_{ATP} in Glucose Sensing

1.5.4.1 Structure and Function of K_{ATP} Channels

K_{ATP} channels are expressed in multiple tissues including heart, skeletal muscle, vascular smooth muscle, pancreatic islet cells and brain where they function to couple the metabolic state of the cell to its membrane excitability (Ashcroft 1988). K_{ATP} channels are hetero-octameric structures of two different subunits that assemble in a 4:4 stoichiometry (Tarasov et al. 2004). The pore of the channel is formed by a tetramer of inwardly rectifying K^+ channel (Kir6.x) subunits, either Kir6.1 or 6.2. Each Kir6.x subunit is associated with a regulatory sulphonylurea receptor (SUR) subunit, either SUR1 or SUR2. Different combinations of these subunits are expressed to form functional channels in different tissues, with Kir6.2 and SUR1 constituting the channels expressed in pancreatic beta-cells and brain (Sakura et al. 1995; Kang et al. 2004). Although all four Kir6.2 subunits have an ATP binding site, ATP binding to a single Kir6.2 subunit is sufficient to close the channel (Markworth et al. 2000). The associated SUR1 subunit confers the channel sensitivity to the sulfonylurea class of drugs and K^+ channel openers, as well as to the stimulatory action of magnesium-ADP (MgADP) (Tarasov et al. 2004). SUR1 belongs to the ATP-binding cassette (ABC) transporter

family of proteins and, like its family members, has two cytosolic nucleotide-binding domains (NBDs). The channel is opened by binding of magnesium nucleotides (eg MgATP, MgADP) to the NBDs of SUR1 (Tarasov et al. 2004). Nucleotide regulation of the K_{ATP} channel is therefore complex, with activity inhibited by nucleotide binding to Kir6.2 and activated by Mg-nucleotide binding to SUR1 (Tarasov et al. 2004). Electrophysiological and biochemical experiments have been performed to characterise these channels and have revealed the nucleotide, pharmacological and intracellular signalling-mediated regulation of the channel gating (Aguilar-Bryan & Bryan 1999; Seino 1999; Dzeja & Terzic 1998).

1.5.4.2 Beta-Cell K_{ATP} Channels

In the pancreatic beta-cell, K_{ATP} channels function as metabolic sensors where they play a crucial role in GSIS by coupling pancreatic beta-cell metabolism to calcium entry (Tarasov et al. 2004). Insulin is secreted in response to an elevation of cytosolic calcium levels, which results from influx through VDCCs in the plasma membrane. The opening of these channels is controlled by membrane potential, which is in turn determined largely by the activity of K_{ATP} channels (Tarasov et al. 2004).

At substimulatory glucose levels, K_{ATP} channels are open and potassium (K^+) efflux through the channels maintains the resting membrane potential at a hyperpolarised level of around -70 mV. As glucose levels rise, uptake and metabolism is increased leading to an elevation in the ATP/ADP ratio, which closes K_{ATP} channels. The inhibition of K^+ efflux through K_{ATP} channels depolarises the cell membrane. A sufficient depolarisation will lead to activation of VDCCs, calcium influx and the trigger of insulin secretion (Tarasov et al. 2004). Therefore, opening of pancreatic beta-cell K_{ATP} channels inhibits insulin secretion where as closure initiates insulin release (Tarasov et al. 2004). In this manner, K_{ATP} channels link metabolic changes to electrical activity and membrane excitability of beta-cells (Miki & Seino 2005). Furthermore, the SUR1 subunit of beta-cell K_{ATP} channels is the molecular target of the anti-diabetic sulphonylurea drugs including glibenclamide and tolbutamide which are widely used to reduce hyperglycaemia in T2D, as these agents are capable of enhancing insulin secretion by closing K_{ATP} channels (Ashcroft & Rorsman 1990). Conversely, K_{ATP} channel openers like diazoxide can inhibit insulin secretion.

Genetic manipulation of K_{ATP} channels including knockout and transgenic animal models have further clarified the physiological and pathophysiological roles that they

play (Miki & Seino 2005). Kir6.2$^{-/-}$ mice have an absolute lack of beta-cell K_{ATP} channel activity, indicating that this subunit is essential for functional beta-cell K_{ATP} channels (Miki et al. 1998). Kir6.2 containing channels are important for GSIS as Kir6.2$^{-/-}$ mice have neonatal hypoglycaemia and inappropriately high insulin levels (Miki et al. 1998; Seino et al. 2000). Furthermore, membrane potential of beta-cells from Kir6.2$^{-/-}$ did not depolarise in response to high glucose, confirming that Kir6.2 containing K_{ATP} channels are essential for glucose mediated regulation of electrical excitability of beta-cells (Miki et al. 1998; Seino et al. 2000). Kir6.2$^{-/-}$ beta-cells also had abnormal intracellular calcium levels and failed to demonstrate a change in intracellular calcium levels upon treatment with tolbutamide, indicating a lack of functional K_{ATP} channels (Miki et al. 1998; Seino et al. 2000). Impaired insulin secretion was observed in these animals in response to oral glucose tolerance test as well as from isolated islets in response to both high glucose and tolbutamide (Miki et al. 1998; Seino et al. 2000). The lack of K_{ATP} channel activity and insulin secretory defects of these mice were also observed in SUR1$^{-/-}$, reinforcing the presence of Kir6.2/SUR1 K_{ATP} channels in pancreatic beta-cells (Seghers et al. 2000; Shiota 2002). SUR1$^{-/-}$ islets similarly had impaired glucose and tolbutamide stimulated insulin secretion.

Consolidating the glucose sensing and insulin secretory defects observed in Kir6.2$^{-/-}$ and SUR1$^{-/-}$ mice, inactivating mutations of beta-cell K_{ATP} channel genes cause a severe form of persistent hyperinsulinaemic hypoglycaemia of infancy (PHHI) (Glaser et al. 1994). K_{ATP} channel mutations in Kir6.2 and SUR1 are also responsible for a particular pathogenesis of T2D (Huopio et al. 2000; Gloyn et al. 2006) and a neonatal form of diabetes in humans (Gloyn et al. 2004).

1.5.4.3 Regulation of K_{ATP} Channels

Much of what is understood about the regulation of K_{ATP} channel activity has come from studies performed in pancreatic beta-cells.

K_{ATP} channels are regulated by the intracellular concentrations of nucleotides, particularly ATP and ADP, as well as by lipids such as phosphatidylinositides and long-chain acyl-CoA esters (Tarasov et al. 2004).

In the pancreatic beta-cell a substantial fraction of ATP (68%) and ADP (45%) is non-diffusible and contained in intracellular organelles, especially the insulin secretory granules (Detimary et al. 1995). Intracellular ATP has been measured in purified rat beta-cells indicating that it exists at a concentration of 2 mmol/l at rest and increases to

4 mmol/l upon stimulation with 10 mmol/l glucose (Detimary et al. 1998). In the same study intracellular ADP was measured at a concentration of 750 μmol/l in the absence of glucose and fell to 250 μmol/l in response to 10 mmol/l glucose (Detimary et al. 1998). Furthermore, glucose also causes a marked increase in phosphocreatine (PCr) and a fall in phosphate levels (Krippeit-Drews et al. 2003).

ATP-mediated K_{ATP} channel inhibition has been demonstrated in response to nutrients that elevate ATP such as glucose, as well as by supply of reducing equivalents directly to cytochrome C, the final step in the electron transport chain (ETC) (Duchen et al. 1993). In contrast, metabolic inhibition of mitochondria with rotenone, DNP and azide reduce ATP generation and activate K_{ATP} channels in pancreatic beta-cells (Tarasov et al. 2004). Furthermore, inhibition of ATP translocase by bongkrekic acid, which prevents ATP export from the mitochondria, also activates K_{ATP} channels (Kiranadi et al. 1991).

It is clear however that ATP is not the sole regulator of K_{ATP} channel activity, evidenced by the fact that the sensitivity of the K_{ATP} channel for ATP-mediated inhibition differs in inside-out patches and the intact cell (IC_{50} = 10-30 μmol/l and 0.8 mmol/l respectively) (Tarasov et al. 2004; Tucker et al. 1998; Schmid-Antomarchi et al. 1987). This data suggests that there are factors other than ATP in the intact cell that contribute to K_{ATP} channel regulation. Importantly, it may be possible that the submembrane ATP level may not be the same as the bulk concentration, potentially owing to the activity of membrane ATPases, for example the Na^+/K^+ ATPase (Tarasov et al. 2004). Similarly, ATP may provide a tonic level of inhibition against which metabolically generated changes in other substances regulate channel activity (Tarasov et al. 2004).

The sensitivity of the channel to ATP is regulated at least by phosphatidylinositol-4,5-bisphosphate (PIP2) and related phosphoinositides (PPIs), long-chain acyl-CoA esters (LC-CoAs) and MgADP (Tarasov et al. 2004). All of these decrease the ability of ATP to close the K_{ATP} channel.

Direct application of the PPIs PIP2 and PIP3 to excised patches has demonstrated that they interact with K_{ATP} channels to increase their open probability and reduce their ATP sensitivity (Fan & Makielski 1997; Baukrowitz et al. 1998). Furthermore, overexpression of phosphatidylinositol 5-kinase (PI5-K), which increases PIP2 levels, reduces the ATP sensitivity of the K_{ATP} channel (Shyng et al. 2000) whereas breakdown

of PIP2 by phospholipase C (PLC) increases channel ATP sensitivity (Xie et al. 1999). These effects are mediated by the Kir6.2 subunit (Baukrowitz et al. 1998). PPIs and ATP have been reported to occupy distinct binding sites on Kir6.2 (Schulze et al. 2003) but interact allosterically with ATP reducing the binding of PPIs and vice versa (Wang et al. 2002).

LC-CoAs also enhance the open probability of the K_{ATP} channel and reduce its ATP sensitivity by interaction with the Kir6.2 subunit (Larsson et al. 1996; Gribble et al. 1998) and appear to bind to the same site as PIP2 (Schulze et al. 2003). In the pancreatic beta-cell, elevations in LC-CoA can result from glucose metabolism and from free fatty acids (FFAs) delivered from the blood or released from endogenous stores (Deeney et al. 2000). Interestingly, LC-CoAs have been suggested to contribute to the reduced glucose sensitivity of the beta-cell observed in obese diabetic individuals due to chronic exposure to FFA leading to increased levels of LC-CoA which subsequently reduce the ATP sensitivity of the K_{ATP} channel inhibiting insulin secretion (Larsson et al. 1996; Tarasov et al. 2004). Alternatively, LC-CoAs may exert a tonic stimulatory effect on the K_{ATP} channel as they have been reported to inhibit ATP/ADP translocase and upregulate UCP2, which would decrease ATP production (Chan et al. 2004). As a result, glucose metabolism would not fully close K_{ATP} channels leading to defective insulin secretion (Tarasov et al. 2004).

MgADP shifts the ATP dose-response curve to higher ATP concentrations favouring an open state of the channel even at increased ATP levels (Kakei et al. 1986). However, metabolic changes affecting the level of MgADP have also been proposed to couple cell metabolism to channel activity. A mutation within NBD2 of SUR1 strongly reduces channel activation by MgADP, with channels expressing this mutation permanently closed even under conditions of low glucose (Nichols et al. 1996), indicating that MgADP interaction with SUR1 is important for appropriate channel opening. Other mutations in both Kir6.2 and SUR1 have been found to reduce MgADP activation and prevent channel activation by metabolic inhibition (Dunne et al. 2004; Shyng et al. 1997). Some have suggested that an ATP hydrolysis cycle at NBD2 generates bound MgADP and that changes in cell metabolism influence K_{ATP} channel activity by modulating the length of time that NBD2 remains in the MgADP-bound (active) state (Zingman et al. 2001; Tarasov et al. 2004). Under conditions of high metabolic activity, ADP levels will be low, so MgADP should dissociate rapidly from NBD2 causing channel activity to decrease (Tarasov et al. 2004). In contrast, as metabolic activity

reduces, the rise in intracellular ADP will slow the dissociation of MgADP from NBD2 and promote channel opening (Tarasov et al. 2004). This model suggests that SUR1 would be a sensor of the intracellular MgADP concentration. The alternative view however is that MgADP simply shifts the ATP dose-response curve for channel inhibition and that the changes in ATP levels in response to fluctuations in metabolic rate constitute the means by which metabolism regulates K_{ATP} channel activity (Tarasov et al. 2004).

Studies to delineate the contributions of MgADP and ATP to K_{ATP} channel regulation have been performed by expressing WT and mutant channel subunits in *Xenopus* oocytes. In these studies, addition of 3 mmol/l azide, which blocks mitochondrial metabolism and lowers cytosolic ATP, produces a large increase in WT K_{ATP} channel current (Tarasov et al. 2004; Gribble, Ashfield et al. 1997). Mutations in highly conserved residues in the NBDs of SUR1 abrogate nucleotide binding and abolish the ability of MgADP or MgATP to stimulate channel activity (Gribble, Tucker et al. 1997). Importantly, when Kir6.2 is co-expressed with SUR1 in which two key nucleotide-binding residues are mutated (SUR1-KAKM), azide is no longer able to stimulate channel activity (Tarasov et al. 2004). This finding suggests that a reduction in metabolically derived ATP is only able to activate K_{ATP} channels upon its hydrolysis to MgADP and interaction with the SUR1 subunit of the channel. However, MgADP can also shift the ATP concentration-course for ATP-mediated inhibition of the K_{ATP} channel, thus it is possible that the lack of metabolic activation of Kir6.2/SUR1-KAKM channels simply reflects a greater ATP sensitivity (due to the absence of MgADP mediated stimulation of the channel), keeping the channel closed even when ATP levels fall upon metabolic inhibition (Tarasov et al. 2004).

Mutation of K185 to aspartate in Kir6.2 causes a profound decrease in the ability of ATP to block K_{ATP} channels, with the IC_{50} for ATP-mediated inhibition increasing from 10 μmol/l to 1.9 mmol/l in Kir6.2-K185D channels (John et al. 2003). Oocytes expressing Kir6.2-K185D/SUR1 channels had large K_{ATP} currents under control conditions, which were increased further by metabolic poisoning with azide (Tarasov et al. 2004). Co-expression of Kir6.2-K185D with SUR1-KAKM in oocytes resulted in smaller whole-cell currents under control conditions than Kir6.2-K185D/SUR1 channels, indicating that the difference in resting currents must be due to the contribution of MgADP/MgATP to the regulation of K_{ATP} channel activity at SUR1. The observation that both Kir6.2-K185D/SUR1 and Kir6.2-K185D/SUR1-KAKM had

comparable IC_{50} for ATP-mediated inhibition of the channel (1.9 mmol/l and 2.0 mmol/l respectively) is consistent with the idea that cytosolic Mg-nucleotides induce a significant decrease in the apparent ATP sensitivity of the channel in the cell through regulation of SUR1 (Tarasov et al. 2004).

If K_{ATP} channel activation upon metabolic inhibition were to be mediated only by Mg-nucleotide interaction with SUR1, Kir6.2/SUR1-KAKM channels should not be activated by azide, as these channels are insensitive to MgADP stimulation. However, Tarasov *et al.* were able to demonstrate activation of Kir6.2-K185D/SUR1-KAKM channels by azide, suggesting that this increase in current must be due to a reduction in ATP levels sensed by Kir6.2 (Tarasov et al. 2004). These experiments suggest that changes in intracellular ATP couple beta-cell metabolism to K_{ATP} channel closure and that Kir6.2 serves as a metabolic sensor (Tarasov et al. 2004). They are also consistent with the notion that MgADP can shift the ATP dose-response curve for inhibition of K_{ATP} channels at Kir6.2 (Tarasov et al. 2004). The results do not rule out that alterations in the rate of MgATP hydrolysis to MgADP may also play a role in coupling cellular metabolism to K_{ATP} channel inhibition (Zingman et al. 2001; Tarasov et al. 2004).

In the pancreatic beta-cell, K_{ATP} activity may also be regulated by creatine and adenylate kinase shuttles, with creatine kinase (CK) linking ATP generation to K_{ATP} channel closure and adenylate kinase (AK) regulating K_{ATP} channel opening (Tarasov et al. 2004). The proposition is that in the microenvironment of the channel, AK could convert AMP and ATP to ADP and promote channel opening, whereas CK could catalyse the transfer of phosphate from PCr to ADP, producing creatine and ATP, and consequently induce channel closure (Tarasov et al. 2004). In support of these notions, PCr concentration increases in islets in response to glucose (Krippeit-Drews et al. 2003) and has been shown to reduce the ability of ADP to stimulate K_{ATP} channel activity in beta-cells (Tarasov et al. 2004). Importantly, in the heart CK has been shown to physically associate with the K_{ATP} channel (Crawford et al. 2001).

Regulation of the K_{ATP} channel is complex, with PPIs and LC-CoAs exerting tonic effects on the channel and adenine nucleotides modulating channel activity. Furthermore, additional factors that regulate levels of nucleotides in the immediate environment of the channel may further modulate channel activity.

1.5.4.4 Brain K_{ATP} Channels

K_{ATP} channels exist throughout the brain, including in the hippocampus, cortex, substantia nigra and high expression observed in the hypothalamus, including regions thought to be involved in glucose sensing such as the VMH (Ashford et al. 1990; Kang et al. 2004).

K_{ATP} channels are most abundantly expressed in the hypothalamus (Ashford et al. 1990), which is well established as a homeostatic centre involved in the regulation of energy metabolism, body weight and glucose levels (Levin 1999). Glucose-sensing neurons of the hypothalamus are depolarised by tolbutamide (Ashford et al. 1990) and the presence of K_{ATP} channels has been demonstrated in hypothalamic glucose responsive neurons of Zucker rats (Rowe et al. 1996).

Interestingly, the expression of K_{ATP} channel subunits Kir6.2 and SUR1 has been shown to be regulated by glucose in the mediobasal hypothalamus, with a downregulation of expression observed in response to hyperglycaemia (Acosta-Martínez & Levine 2007). Kong *et al.* demonstrated K_{ATP}-dependent, GE electrical activity in MCH expressing hypothalamic neurons (Kong et al. 2010). Amoroso *et al.*, characterised K_{ATP} channels in the substantia nigra of rats, observing increased γ-aminobutyric acid (GABA) release from slices in response to high potassium, glucose or the potent sulphonylurea gliquidone (Amoroso et al. 1990). In this study, K_{ATP} channels were also demonstrated to open in response to ATP depletion by oligomycin, a complex V mitochondrial ETC inhibitor, which was completely inhibited by gliquidone (Amoroso et al. 1990). Together, these data demonstrate that K_{ATP} channels are inhibited by high glucose levels and opened in response to energy deprivation.

Glucose-sensing neurons of the VMH have been shown to express Kir6.2 and SUR1 by RT-PCR and VMH neurons from Kir6.2$^{-/-}$ mice failed to alter their electrical activity in response to glucose during electrophysiological experiments demonstrating the importance of K_{ATP} channels for glucose sensing (Miki et al. 2001). Furthermore, Kir6.2$^{-/-}$ mice were found to have a compromised recovery from insulin-induced hypoglycaemia, suggesting that they have an impaired CRR. These mice were found to have markedly reduced glucagon secretion in response to hypoglycaemia compared to WT mice (Miki et al. 2001). Intriguingly, the glucagon response to low glucose was intact in isolated islets from Kir6.2$^{-/-}$, suggesting that the primary defect in the glucagon response was centrally mediated. In support of this notion, neuroglycopenia stimulates

glucagon secretion by activating autonomic neurons (Taborsky Jr et al. 1998). Importantly, 2-DG-induced neuroglycopenia failed to stimulate glucagon secretion in Kir6.2$^{-/-}$ demonstrating the critical importance of K_{ATP} channels in hypoglycaemia detection (Miki et al. 2001).

In a pilot study of ten patients, Stephanie Amiel's group found no effect of administering either diazoxide or glibenclamide compared to placebo on CRR hormone responses during a subsequent hypoglycaemic clamp procedure, suggesting that modulation of K_{ATP} channels did not affect hormonal CRRs to hypoglycaemia (Bingham et al. 2002). Importantly however, studies in conscious mice demonstrated that CRRs to hypoglycaemia were attenuated by brain delivery of sulphonylureas to close brain K_{ATP} channels (Evans et al. 2004). In this work, glibenclamide was infused directly into the VMH, as well as via the usual ICV method, confirming that epinephrine and glucagon responses to brain glucopenia or systemic hypoglycaemia were suppressed by VMH sulphonylureas (Evans et al. 2004). The data demonstrate that closing hypothalamic K_{ATP} channels during hypoglycaemia prevents the triggering of the protective hormonal CRR, thereby confirming that the open state of hypothalamic K_{ATP} channels is critical for glucose-sensing neurons to detect falling blood glucose levels and stimulate downstream CRRs against glucose deprivation (Evans et al. 2004). The following year, McCrimmon *et al.* were able to demonstrate that *in vivo* delivery of pharmacological agents that open or close the K_{ATP} channel within the VMH have opposite effects to enhance or suppress respectively the CRR to acute hypoglycaemia (McCrimmon et al. 2005). By using a Kir6.2/SUR1 selective K_{ATP} channel opener, NN414, the observed amplification of the CRR was proven to be mediated specifically by this isoform of K_{ATP} channel, confirming their involvement in the mechanism of VMH neuronal glucose sensing (McCrimmon et al. 2005). Importantly, this study also demonstrated that VMH injection of diazoxide to open K_{ATP} channels produced an amplification of hormonal CRRs and a reduction in the amount of exogenous glucose required to maintain a hyperinsulinaemic-hypoglycaemic clamp in rats with defective CRR caused by recurrent hypoglycaemia (McCrimmon et al. 2005). This data suggests that defective K_{ATP} opening to acute hypoglycaemia, induced by recurrent hypoglycaemia exposure, may be a mediator of defective CRR observed in T1D. A recent study in humans has demonstrated for the first time the potential utility of K_{ATP} channel activators, such as diazoxide, to improve CRRs to hypoglycaemia in individuals with T1D (George et al. 2015).

1.6 Defective Glucose Sensing in T1D

Defective central glucose-sensing mechanisms may be the root cause of defective CRR observed in T1D. Exposing hypothalamic but not hindbrain glucose-sensing regions to antecedent hypoglycaemia induces reduced CRR hormone responses to acute hypoglycaemia, with antecedent hypothalamic glucoprivation causing a defect similar to that in magnitude observed after recurrent hypoglycaemia (Sanders et al. 2007). Furthermore a single exposure to insulin-induced hypoglycaemia *in vivo* induces a left shift in the glucose responsiveness of VMH GE neurons to subsequent hypoglycaemia when studied *ex vivo*, resulting in hyperpolarisation of the cells only at lower glucose concentrations than controls (L. Kang et al. 2008).

1.6.1 Enhanced Glucose Metabolism

Evidence from rat studies shows that prolonged hypoglycaemia for one or two weeks increases GLUT1 or GLUT3 expression, raises glucose levels and enhances glucose uptake in the brain (Simpson et al. 1999; Duelli et al. 1999). Furthermore, as previously mentioned recurrent hypoglycaemia upregulates GK mRNA (L. Kang et al. 2008) and enhances HK activity as measured by increased glucose phosphorylation (Osundiji et al. 2010), while direct activation of GK suppresses the CRR to hypoglycaemia (Levin et al. 2008). These observations would be predicted to lead to enhanced glucose metabolism, preserving the intracellular energy status, increasing ATP levels and therefore leading to inhibition of K_{ATP} channels and a lack of activation of CRR to hypoglycaemia (Beall, Ashford, et al. 2012). Importantly, human studies suggest that after 56 hours of intermittent hypoglycaemia, brain glucose uptake is preserved in response to stepped hypoglycaemia, in contrast to the normal decrease in brain glucose uptake usually observed in response to hypoglycaemia (Boyle et al. 1994). This enhancement of brain glucose uptake would preserve energy status and impede activation of CRR to hypoglycaemia.

1.6.2 Alternate Fuel Usage

Alternatively, the metabolism of alternate fuel sources other than glucose, particular entailing a switch from glucose to lipid to metabolism, may underpin defective CRR to hypoglycaemia. Evidence supporting this hypothesis includes the finding of increased brain acetate concentration and utilisation during hypoglycaemia in patients with T1D

compared to control volunteers (Mason et al. 2006). Glycogen is stored in astrocytes and is mobilised during energy stress, being released as lactate, which can be transported to neurons to preserve their activity (Brown et al. 2004). Also, rats treated with a glycogen phosphorylase inhibitor under euglycaemic conditions, which permits accumulation of astrocyte glycogen stores, maintained brain activity significantly longer during hypoglycaemia than untreated rats with normal brain glycogen levels, demonstrating that glycogen can provide a central fuel source during hypoglycaemia (Suh et al. 2007). Brain glycogen content is reduced in mice, rats and humans during hypoglycaemia (Canada et al. 2011; Herzog et al. 2008; Lei & Gruetter 2006), demonstrating that glycogen is utilised and may serve as a temporary energy source (Beall, Ashford, et al. 2012). Lending further support to this finding is the measurement of increased glycogen content in rat hypothalamus after recurrent ICV 2-DG injections on three consecutive days (Alquier et al. 2007). These findings would be expected to delay the responses of glucose-sensing neurons to hypoglycaemia and impede initiation of the CRR (Beall, Ashford, et al. 2012). The increase of glycogen content in rat hypothalamus after recurrent 2-DG correlated with a delayed activation of AMPK in response to hypoglycaemia, suggesting that suppressed AMPK activity may be linked to delayed detection of glucose deprivation (Beall, Ashford, et al. 2012; Alquier et al. 2007). Local delivery of lactate into the VMH suppresses CRRs to systemically induced hypoglycaemia (Borg et al. 2003), and the uptake and utilisation of monocarboxylic acids is enhanced by antecedent hypoglycaemia (Herzog et al. 2013) and diabetes (Mason et al. 2006). It has been proposed that lactate suppresses CRRs to hypoglycaemia by increasing extracellular GABA levels in the VMH (Chan et al. 2013) presumably by increased activity of GE neurons. Data suggest that lactate affords neurons the capacity to maintain the same rate of glucose oxidation and TCA cycle activity during hypoglycaemia as under euglycaemic conditions (Herzog et al. 2013). This would lead to lactate mediated stimulation of GE neurons and silencing of GI neurons, presumably by inactivation of AMPK. Lactate recapitulated the effect of recurrent hypoglycaemia to decrease the glucose threshold at which GI neurons become active (Song & Routh 2006), therefore implicating a role for lactate in the impairment of glucose sensing in individuals with antecedent exposure to hypoglycaemia (Chan & Sherwin 2013).

1.6.3 Altered Hypothalamic Neurotransmission

There is also data implicating a role for GABA in the control of glucose sensing and CRR. GABA is an inhibitory neurotransmitter that may act downstream of K_{ATP} to modulate glucagon responses to hypoglycaemia (Ogunnowo-Bada et al. 2014). Studies showed that pharmacological closing of K_{ATP} increased VMN GABA levels while opening conversely decreased GABA levels, effects which were associated with suppressed or enhanced glucagon and other CRRs to hypoglycaemia (Chan et al. 2007; Chan et al. 2006). Furthermore, acute hypoglycaemia decreases VMH GABA levels while recurrent hypoglycaemia prevents the fall in GABA (Chan et al. 2008). Together these data permit speculation that K_{ATP} channel-expressing GE VMH neurons are GABAergic, and fail to hyperpolarise in response to low glucose following antecedent hypoglycaemia. Further promoting a role for GABA in the regulation of VMH glucose sensing, infusion of glucose into the VMH of rats suppressed glucagon and epinephrine responses to hypoglycaemia and altered VMH GABA levels, with the effects of glucose being antagonised by $GABA_A$ receptor inhibition (Zhu et al. 2010).

Glutamate is the predominant excitatory neurotransmitter in the CNS. One particular study has demonstrated that specific knockout VGLUT2, in SF-1 neurons of the VMH leads to loss of the glucagon response to hypoglycaemia, suggesting an integral role of glutamate neurotransmission in the stimulation of glucagon release (Tong et al. 2007). Another study has shown that EphA5 receptor signalling in the VMH can augment CRRs to hypoglycaemia by enhancing glutamatergic neurotransmission in the VMH (Murai & Pasquale 2011).

Serotonin has also been implicated in modulating CRRs to hypoglycaemia, with the serotonin selective reuptake inhibitor (SSRI) sertraline augmenting glucagon, epinephrine and norepinephrine responses to hypoglycaemia in rats (Sanders et al. 2008). Human studies have confirmed SSRI-mediated increases in catecholamine responses to hypoglycaemia (Briscoe et al. 2008; Briscoe et al. 2008).

1.6.4 Altered VMH Neuropeptide Input

Corticotrophin-releasing hormone (CRH) and urocortins 1-3 (UCN1-3) are neuropeptides that are capable of regulating the CRR to hypoglycaemia, with CRH via the CRH receptor 1 (CRHR1) amplifying, and UCN via the CRH receptor 2 (CRHR2) suppressing these responses (McCrimmon et al. 2006). UCN3 was shown to reduce

VMH glucose-sensing neuronal responses to hypoglycaemia, such that their electrical activity was only altered at a lower glucose threshold (McCrimmon et al. 2006). UCN3 positive nerve terminals innervate the VMH (Chen et al. 2011; Zhou et al. 2010) and therefore may be a mediator of defective CRRs to hypoglycaemia via their action to suppress VMH glucose sensing.

1.7 Mechanisms of Glucose Sensing – Glucose Inhibited Neurons

In VMH GI neurons, hypoglycaemia is thought to induce firing by a glucose metabolism-dependent signalling pathway. Kang *et al*. used single-cell RT-PCR analysis to demonstrate that different populations of GI neurons express Glut1, 2 and 3 so any of these transporters may be involved in glucose uptake in GI neurons (Kang et al. 2004). The same group has also identified the importance of GK for GI neuron glucose sensing (L. Kang et al. 2006). The mechanism of glucose sensing by VMH GI neurons proposed by Vanessa Routh's group is initially similar to that observed in GE neurons; namely an increase in the cellular AMP/ATP ratio in response to reduced glucose metabolism. This activates AMPK, which in turn triggers production of nitric oxide (NO) by endothelial nitric oxide synthase (eNOS), and the subsequent activation of guanylate cyclase by NO further activates AMPK. Contrastingly to GE neurons however, the subsequent regulation of the chloride conductance of cystic fibrosis transmembrane conductance regulator (CFTR) by AMPK is responsible for the induction of neuronal firing (Canabal et al. 2007; Murphy et al. 2009; Fioramonti et al. 2010).

Denis Burdakov's laboratory has also described orexin neurons from the LH as being GI but with glucose-sensing mechanisms distinct from those neurons described by Routh. Studies from the Burdakov group have reported that the activation of these neurons can be triggered by the non-metabolisable analogue 2-DG, that lactate cannot reproduce the glucose response and that GK inhibitors do not affect glucose sensing by these neurons (Dunn-Meynell et al. 2002; González et al. 2008). This led to the hypothesis that glucose activates a cell surface receptor that leads to regulation of channel activity, which was proposed to be controlled by tandem pore K^+ channels (TRPs) (Burdakov et al. 2006), but TRP knockout mice failed to directly support this hypothesis (Gonzàlez et al. 2009).

In GI neurons from the brainstem, electrophysiological studies have shown that they are activated in response to glucose removal by a signalling pathway that requires the presence of GK and the regulation of a K^+ current (Balfour et al. 2006; Balfour & Trapp 2007).

1.8 Interleukin-6 – Discovery and Function

Cytokines are secreted proteins which are involved in communication between cells of the immune system that also perform regulatory functions outside of this system (Schaper & Rose-John 2015). What is now called Interleukin-6 (IL-6) was originally identified as a novel mRNA in the 1980s, when two independent laboratories observed its expression after fibroblasts were stimulated with interferon-β (IFN-β) (Weissenbach et al. 1980; Sehgal & Sagar 1980). These groups called the discovery IFN-β2, and over the subsequent years, further groups worldwide also identified the same protein as a T-cell secreted factor involved in the stimulation of B-cells with varying nomenclature (Content et al. 1982; Haegeman et al. 1986; Hirano et al. 1986; Van Damme et al. 1987), before it was finally termed IL-6 (Yasukawa et al. 1987). The IL-6 mRNA encodes a secreted protein which consists of 184 amino acids which would translate into a protein of molecular weight around 21 kDa, however subsequent N-linked glycosylation means IL-6 exists as several isoforms of 21-28 kDa (Wolf et al. 2014). Glycosylation may be important for the stability or half-life of IL-6, but is not essential for its function, as non-glycosylated recombinant IL-6 produced in *Escherichia coli* (*E. coli*) is functional and is routinely used for *in vivo* and *in vitro* experiments (Wolf et al. 2014).

IL-6 is the strongest activator of the hepatic acute phase response which involves the expression of C-reactive protein (CRP), serum amyloid A (SAA), haptoglobin and α1-acid glycoprotein, which are secreted by hepatocytes during bacterial infections (Schaper & Rose-John 2015). IL-6 also plays a role in liver regeneration (Cressman et al. 1996), controls body weight (K. Wallenius et al. 2002), the development of local antibody responses (Ramsay et al. 1994) and has key roles in the CNS (Erta et al. 2012).

Over the last twenty years interest in the role of inflammation in a wide range of diseases not commonly thought of as immune-mediated disorders has led to studies that demonstrate that inflammatory mediators, such as IL-6, may not only be biomarkers of metabolic disease but may directly contribute to beta-cell dysfunction and insulin

resistance, among other pathologies (Kristiansen & Mandrup-Poulsen 2005). These will be addressed subsequently.

1.9 Interleukin-6 Signalling

IL-6 activates cells via a heterodimeric signalling complex consisting of the IL-6 α-receptor (IL-6Rα) and the signal transducing β-subunit glycoprotein 130 (gp130), which is shared with several other members of the IL-6 cytokine family (Wolf et al. 2014). The IL-6R exists in two forms, a membrane bound and a soluble version, which transduce classical and trans-signalling by IL-6 respectively. Gp130 of the IL-6R complex is ubiquitously expressed in all cell types, whereas the IL-6Rα subunit is predominantly expressed in hepatocytes, megakaryocytes and several leukocyte populations (Wolf et al. 2014). Studies have suggested that IL-6 trans-signalling via the soluble IL-6R accounts for the pro-inflammatory actions of IL-6, meaning that specific inhibition of this pathway, which does not mediate anti-inflammatory properties of classical membrane bound IL-6 signalling, could be a valuable therapeutic target to treat human inflammatory diseases (Rose-John 2012; Jones et al. 2011).

IL-6 signalling involves first the binding of IL-6 to its non-signalling α-receptor, which then permits recruitment of the signalling transducing gp130 subunit (Heinrich et al. 2003). As mentioned, there are multiple components of the IL-6 signalling system including membrane bound gp130 and IL-6Rα, as well as soluble forms of both proteins, sIL-6R and sgp130, making the biology of IL-6R signalling highly complex. For example, given the ubiquitous expression of gp130 on all cell types, a complex of IL-6 and sIL-6R can act agonistically rather than antagonistically, while sIL-6Rα potentiates the antagonistic activity of sgp130 (Heinrich et al. 2003).

1.10 sIL-6R and Trans-Signalling

As mentioned, classical signalling by IL-6 involves signal transduction via the formation of a signalling complex consisting of gp130 and IL-6Rα, where as in cell types lacking the IL-6Rα, trans-signalling is transferred via the combination of gp130 with the sIL-6R, which exists in human plasma at a concentration of 25-35 ng/ml (Chalaris et al. 2011). sIL-6R arises either via shedding of the membrane bound form due to proteolytic cleavage (Müllberg et al. 1993) or via alternative splicing of the IL-6R gene resulting in omission of the transmembrane domain coding exon (Muller-Newen et al. 1996; Wolf et al. 2014). In humans, an alternatively spliced mRNA has

been observed leading to translation of a sIL-6R protein (Lust et al. 1992). The pro-inflammatory consequences of IL-6 trans-signalling have already been targeted therapeutically, based on the efficacy of a naturally occurring soluble form of gp130 to inhibit trans-signalling (Jostock et al. 2001). Based on this data, the artificial fusion protein sgp130-Fc, a dimerisation of two sgp130 monomers and the Fc-part of a human IgG antibody, has been developed (Tenhumberg et al. 2008) and an optimised version of this inhibitor is at the time of writing being tested in phase I clinical trials (Jones et al. 2011; Wolf et al. 2014). This construct was shown to completely block IL-6 trans-signalling without affecting classical IL-6 signalling (Jostock et al. 2001). Sgp130-Fc is able to bind IL-6/sIL-6R complexes preventing trans-signalling via sequestering the IL-6/sIL-6R complexes.

Efforts to discover the cellular origin of the sIL-6R in mice have identified hepatocytes and myeloid cells, such as monocytes and macrophages, as the major contributors to sIL-6R levels, as a 30% or 63% reduction in circulating sIL-6R levels were observed with knockout of the IL-6R in hepatocytes and myeloid cells respectively (McFarland-Mancini et al. 2010). Interestingly, IL-$6^{-/-}$ mice were found to have a 50% reduction in sIL-6R levels, implicating a role for IL-6 itself in the regulation of cellular expression of IL-6R and subsequent sIL-6R generation (Coles et al. 2007). Sgp130 also exists as a component of IL-6 signalling, similarly formed via either alternative splicing or proteolytic cleavage resulting in shedding from the cell membrane. As of 2014, three different splice variants of sgp130 have been discovered, all of which are potent inhibitors of IL-6 trans-signalling (Jostock et al. 2001; Richards et al. 2006). Functionally, the ability of sgp130 to suppress trans-signalling is responsible for the anti-inflammatory effect of epigallocatechin-3-gallate, a compound studied in models of arthritis (Ahmed et al. 2006).

1.11 Signalling Cascades Activated by IL-6

Signalling by IL-6 is transduced by the Janus kinase/signal transducer and activator of transcription (JAK/STAT), mitogen-activated protein kinase (MAPK) and phosphatidylinositol-3-kinase (PI3K) pathways (Heinrich et al. 2003).

IL-6 via its receptor complex rapidly induces activation of tyrosine kinases of the Janus kinase (JAK) family, which are constitutively associated with the cytoplasmic tail region of gp130, by autophosphorylation (Heinrich et al. 2003; Schaper & Rose-John 2015). Gp130 binds to JAK1, JAK2 and tyrosine kinase 2 (TYK2), with JAK1 having

been demonstrated to play an essential role as cells lacking JAK1 have impaired IL-6 signal transduction (Guschin et al. 1995; Rodig et al. 1998). A second kinase family, the Src-family, has also been shown to be involved in IL-6 signalling, with a strong interaction of tyrosine protein kinase HCK and gp130 observed in response to IL-6 stimulation (Ernst et al. 1994). Studies have demonstrated HCK to be important for IL-6-dependent growth of myeloma cells (Hausherr et al. 2007) with MAPK involvement (Schaeffer et al. 2001).

The signal transducer and activator of transcription (STAT) family of proteins have a central role in IL-6-type cytokine signalling and their activation requires the transient association of the STATs with the cytokine receptors, homo- or heterodimerisation of tyrosine phosphorylated STATs and subsequent translocation of these dimers to the nucleus where they bind to the promoter regions of IL-6-inducible genes (Heinrich et al. 2003; Schaper & Rose-John 2015; Pranada et al. 2004). Once activated by autophosphorylation, JAK kinases phosphorylate tyrosine residues in the cytoplasmic region of gp130, leading to recruitment of STAT proteins. All IL-6-type family cytokines potently activate STAT3, which is phosphorylated on tyrosine 705 (Y705) via gp130 (Heinrich et al. 1998; Kaptein et al. 1996). STATs can then dimerise via their SH2 domains and translocate to the nucleus where they regulate transcription of target genes.

As well as tyrosine phosphorylation of STATs which leads to their nuclear translocation, STAT3 can also be phosphorylated at its serine 727 (S727) residue, with evidence suggesting a mitochondrial targeting and action of S727 phosphorylated STAT3 (Tian & An 2004; Wegrzyn et al. 2009; Gough et al. 2013).

The MAPK signalling cascade is also activated by IL-6, dependent on the SH2-domain-containing tyrosine phosphatase (SHP2)-binding site, Y759 of gp130 (Schiemann et al. 1997; Friederichs et al. 2001). Activation of the MAPK cascade by IL-6 involves the SHP2 linkage of the growth factor receptor bound protein/Son of Sevenless (Grb2-SOS) complex and/or Grb2-associated binder-1 (Gab1) to gp130 (Heinrich et al. 2003). SHP2 is rapidly recruited to tyrosine-phosphorylated gp130 and becomes phosphorylated in a JAK1-dependent manner (Schaper et al. 1998). Phosphorylated SHP2 can then interact with Grb2 (Fukada et al. 1996).

Gab1 is able to activate the Ras-Raf-MAPK cascade in response to IL-6. IL-6 stimulation leads to the tyrosine phosphorylation of Gab1 and its subsequent interaction

with SHP2 and PI3K, leading to activation of extracellular signal-regulated kinase 2 (ERK2) (Takahashi-Tezuka et al. 1998). The role of Gab1 in activating the MAPK cascade was confirmed in fibroblasts deficient in Gab1, which show a markedly reduced MAPK activity in response to IL-6 (Itoh et al. 2000). The balance between STAT3 and MAPK activation is crucial for the homeostasis of the organism and for controlled cell proliferation (Fukada et al. 1998; Fukada et al. 1996). Y759 of gp130 controls this balance, where its phosphorylation facilitates MAPK activation and dephosphorylation increases STAT3 activation (Schaper et al. 1998; Eulenfeld et al. 2012).

IL-6 also activates the PI3K signalling pathway. Studies have documented that IL-6 has both pro- and anti-apoptotic function that is dependent on activation of PI3K signalling in cancer cell lines (Hideshima et al. 2001; Jee et al. 2004). The adaptor protein Gab1 interacts with PI3K and therefore may couple gp130 to PI3K activation (Takahashi-Tezuka et al. 1998).

1.12 Negative Regulation of IL-6 Signalling

The recruitment of SHP2 to gp130 is also functionally important due to its phosphatase activity (Fischer et al. 2004). Binding of SHP2 to gp130 induces a conformational change in the former, leading to its enzymatic activity (Pluskey et al. 1995). As described above, SHP2 is important as an adaptor for IL-6-induced MAPK signalling, however, it also negatively regulates the JAK/STAT pathway (Lehmann et al. 2002). Lehmann *et al.* showed that overexpression of dominant-negative SHP2 mutants in COS-7 cells led to enhanced gp130, JAK, STAT and SHP2 phosphorylation, demonstrating the importance of SHP2 to negatively regulate these pathways (Lehmann et al. 2002). Co-immunoprecipitation (Co-IP) studies have demonstrated association of STAT3 and SHP2, suggesting STAT3 is a direct target for SHP2-mediated dephosphorylation (Gunaje & Bhat 2000). A role for protein tyrosine phosphatase ε C (PTPεC) in inhibition of IL-6-induced JAK/STAT signalling has been described (Tanuma et al. 2000), as well as one for protein tyrosine phosphatase 1B (PTP1B) (Myers et al. 2001).

The suppressor of cytokine signalling (SOCS) family of proteins are another mechanism of inhibition of IL-6-type family cytokine signalling (Yoshimura et al. 1995; Starr et al. 1997; Endo et al. 1997; Naka et al. 1997), and their expression is rapidly upregulated in response to IL-6 (Starr et al. 1997; Naka et al. 1997). SOCS proteins are induced via the JAK/STAT pathway and subsequently inhibit this pathway

at the level of JAKs in a classical negative feedback loop (Starr et al. 1997; Naka et al. 1997). SOCS3, potently induced by IL-6, has been found to bind to Y759 of gp130, which is also the residue that recruits SHP2 (Schmitz et al. 2000; Nicholson et al. 2000). Both SOCS3 mRNA and protein is induced rapidly in response to IL-6 stimulation and mediates negative regulation of IL-6 signalling via inhibition of the catalytic domain of JAKs (Endo et al. 1997; Starr et al. 1997; Naka et al. 1997; Sasaki et al. 1999; Kershaw et al. 2013). Sustained activation of IL-6 signalling is observed in the absence of SOCS3 (Yasukawa et al. 2003; Lang et al. 2003).

Furthermore, IL-6 signalling can be negatively regulated by receptor internalisation and subsequent protein degradation of the IL-6 receptor complex (Wang & Fuller 1994). Cells expressing gp130 mutants which do not internalise demonstrate more potent IL-6 signalling (Kortylewski et al. 1999).

1.13 Regulation of IL-6 Expression and Release

Plasma IL-6 levels are low in healthy humans existing in the region of 1-5 pg/ml (Agorastos et al. 2014). sIL-6R is found at concentrations in the range of 50-75 ng/ml and sgp130 is found around 400 ng/ml (Schaper & Rose-John 2015). Due to the presence of higher concentrations of sIL-6R and sgp130 in blood, secreted IL-6 will rapidly bind to sIL-6R that will immediately bind to sgp130 and be neutralised. In this way, the high concentrations of sIL-6R and sgp130 act as a buffer for IL-6 (Schaper & Rose-John 2015). In pathological conditions however, the concentration of sIL-6R and IL-6 increase rapidly (Nowell et al. 2003). During sepsis, IL-6 in the low μg/ml range have been reported (Waage 1989).

At the transcriptional level, the promoter region of the IL-6 gene has sequence motifs for the binding of activator protein 1 (AP-1), cyclic AMP (cAMP)-responsive element (CRE), CCAAT enhancer binding protein β (C/EBPβ, also termed NF-IL-6) and nuclear factor κ-light-chain-enhancer of activated B cells (NF-κB) (Wolf et al. 2014; Matsusaka & Fujikawa 1993; Ray et al. 1988; Ray et al. 1990; Asschert et al. 1999; Dendorfer et al. 1994). NF-κB mediated transcription of IL-6 has been observed in response to lipopolysaccharide (LPS), the pro-inflammatory cytokines tumour necrosis factor α (TNFα), IL-1α and IL-1β and viral infections (Sehgal et al. 1988; Fong et al. 1989; Kohase et al. 1987; Chen et al. 2005). Mutational analyses of the NF-κB binding site have demonstrated its importance for IL-6 gene expression induced by IL-1, TNFα and LPS (Shimizu et al. 1990; Libermann & Baltimore 1990). In a rodent model of

myocardial ischaemia/reperfusion injury, induction of IL-6 gene expression by C/EBPβ has been shown (Chandrasekar et al. 1999). Regulation of IL-6 mRNA has also been observed at the post transcriptional level both negatively (Iwasaki et al. 2011; Matsushita et al. 2009) and positively (Masuda et al. 2013) with microRNAs (miRNAs) also proposed to interfere with the expression of IL-6 (Rossato et al. 2012).

The membrane bound IL-6R expression has been shown to be regulated by steroid hormones and their synthetic derivatives (Wolf et al. 2014). Glucocorticoid treatment increases IL-6R mRNA and protein expression (Rose-John et al. 1990; Snyers et al. 1990). In hepatocytes, evidence suggests that IL-6 can enhance expression of its own membrane bound receptor in a positive feed-forward loop fashion, and also by IL-1 (Bauer et al. 1989). In contrast IL-6 was found to downregulate IL-6R expression in a natural killer cell line (Böttger et al. 2013)

Gp130 expression is also regulated by IL-6. Klouche *et al.* observed an increase in gp130 mRNA and surface protein expression in vascular smooth muscle cells following stimulation with an IL-6/sIL-6R complex, which also stimulated IL-6 secretion causing an autocrine stimulatory loop (Klouche et al. 1999). In a rat model of ischaemia and reperfusion, a significant upregulation of gp130 was found in the myocardium, accompanied by an increase in IL-6 and IL-6R expression, suggesting a role of IL-6 signalling in myocardial infarction (Chandrasekar et al. 1999). Fittingly, gp130 expression can be downregulated by the anti-inflammatory antibiotic minocycline, which led to blockade of the STAT3 and ERK1/2 pathways in human ovarian cancer cell lines (Ataie-Kachoie et al. 2013). ERK2 has been shown to bind to the gp130 promoter and regulate its expression, and inhibition of ERK2 prevents gp130 expression (Bonito et al. 2014). Since IL-6 can activate ERK1/2 signalling (Neurath & Finotto 2011), this suggests the presence of a feed-forward loop enhancing IL-6 signalling via an ERK2-mediated increase in gp130 expression. Conversely, gp130 expression has been shown to be downregulated by p38 MAPK mediated pro-inflammatory stimuli (Honke et al. 2014).

1.14 IL-6 in Diabetes

For T1D, the auto-immune nature of the destruction of pancreatic beta-cells is thought to result from an interaction of activated T cells and pro-inflammatory cytokines of the infiltrate, depicting a negative role of cytokines in the pathogenesis of the disease (Eizirik & Mandrup-Poulsen 2001). Having said this, the role of IL-6 in both human

and rodent diabetes is debated, with a lack of direct evidence for a deleterious role of IL-6 in the pathogenesis of T1D from human studies (Kristiansen & Mandrup-Poulsen 2005). It remains unclear as to whether IL-6 plays a role in beta-cell destruction, as direct evidence of a cytotoxic effect of IL-6 on beta-cells only exists *in vitro*, and contrastingly, cytoprotective effects have also been demonstrated in mouse islets and a beta-cell line (Choi et al. 2004; Oh et al. 2011). The likelihood is that the combination of factors from the beta-cells themselves and the immune infiltrate will converge to mediate beta-cell destruction.

In the context of T2D, work during the 1990s has suggested a potential role of immunological related mechanisms and associated factors in the development of peripheral insulin resistance as well as the progressive beta-cell failure observed in this disease (Pickup 2004; Kolb & Mandrup-Poulsen 2005). Low-grade inflammation has been shown to precede and be a risk factor for the development of T2D and intervening to reduce the inflammatory state has been shown to reduce the risk of developing T2D, implicating inflammation in the pathogenesis of this disease (Kolb & Mandrup-Poulsen 2005; Pickup 2004). Regarding the regulation of insulin secretion, which is impaired in T2D, IL-6 has been reported to inhibit GSIS from rodent islets (Wadt et al. 1998; Southern et al. 1990). Contrastingly, IL-$6^{-/-}$ mice have comparable fasting insulin levels as littermate control animals (Di Gregorio et al. 2004) but have been shown to develop mature onset obesity and disturbed glucose metabolism, but insulin was not investigated in this latter study (V. Wallenius et al. 2002). Interestingly, ICV but not IP replacement of IL-6 in the knockout animals increased energy expenditure (V. Wallenius et al. 2002) suggesting a role for central IL-6 in this regulation.

IL-6 appears to negatively regulate insulin signalling in peripheral tissues. In adipocyte cell lines IL-6 decreases insulin receptor substrate (IRS) phosphorylation and expression, decreases insulin receptor β subunit, inhibits insulin-induced phosphorylation of protein kinase B (PKB), increases expression of SOCS3 and reduces insulin-stimulated glucose transport by reducing GLUT4 expression (Rotter et al. 2003; Lagathu et al. 2003; Shi et al. 2004). Another study has however demonstrated an enhancement of glucose transport by IL-6 in 3T3-L1 adipocytes (Stouthard et al. 1996). In skeletal muscle, the human body's largest insulin-responsive organ, IL-6 has been shown to either enhance or have no effect on basal and insulin stimulated glucose uptake (Benrick et al. 2012; Carey et al., 2006; Geiger et al. 2007; Kim et al., 2004; Neill et al., 2013; Nieto-Vazquez & Ferna, 2008; Rotter Sopasakis et al. 2004; Yuen et

al. 2009). The data documenting the role of IL-6 on insulin sensitivity in liver is much more consistent. IL-6 activates the JAK/STAT signalling pathway leading to SOCS3 transcription and inhibition of insulin receptor autophosphorylation, tyrosine phosphorylation of IRS1 and 2 and decreased glycogen storage (Kristiansen & Mandrup-Poulsen 2005). These data demonstrate that IL-6 can reduce insulin sensitivity by impairing the insulin signalling pathway.

1.15 IL-6 in Metabolic Disease

The currently accepted paradigm regarding the role of pro-inflammatory cytokines in metabolic disease is that nutrient overload promotes inflammation and links the metabolic and immune systems, where inflammation may be pathological (Febbraio 2014). However, paradoxically, inflammation is an adaptive, protective and importantly, an energy consuming process, and therefore the roles of interleukins in metabolism and energy homeostasis is complex (Febbraio 2014). Evidence suggests that for several cytokines, including IL-6, although excess production is negative, blockade or insufficiency is equally undesirable (Febbraio 2014).

Given the observation that IL-6 is secreted from adipose tissue and macrophages and is elevated in obesity and metabolic disease (Hoene & Weigert 2007; Wellen & Hotamisligil 2005) it is generally assumed that elevations in IL-6 levels has negative effects on metabolism. As described earlier, IL-6 can induce insulin resistance, however the fact that it is released from skeletal muscle in response to beneficial, non-damaging muscle contraction (exercise) raises controversy regarding its negative implication in metabolic disease (Steensberg et al. 2000; Hiscock et al. 2004; Pedersen & Febbraio 2007). Furthermore, muscle derived IL-6 has cross tissue biological functions on liver, adipose, gut, pancreas and brain (Banzet et al. 2009; Wueest et al. 2014; Ellingsgaard et al. 2011; Shirazi et al. 2013). Importantly, IL-$6^{-/-}$ mice develop mature onset obesity, glucose intolerance and insulin resistance, implicating beneficial roles for IL-6 in protection against metabolic disease (V. Wallenius et al. 2002; Di Gregorio et al. 2004; Matthews et al. 2010).

In line with this, the Brüning lab demonstrated that mice with specific reduction of IL-6 signalling in hepatocytes had reduced insulin sensitivity and glucose tolerance, with liver-specific absence of IL-6 signalling affecting glucose uptake in adipose and muscle (Wunderlich et al. 2010). Furthermore, these animals had exaggerated inflammation and inflammatory signalling revealing a role for hepatic IL-6 signalling to limit hepatic

inflammation (Wunderlich et al. 2010). In another study from the same group, inactivation of IL-6 signalling specifically in myeloid cells induced exaggerated deterioration of glucose homeostasis during obesity due to enhanced insulin resistance (Mauer et al. 2014). An increase in inflammation was also observed with a shift in macrophage polarisation, identifying IL-6 as an important determinant of the alternative activation of macrophages and assigning the cytokine a role in limiting inflammation (Mauer et al. 2014).

IL-6 has been shown to be important for protection against bacterial infection mediated via classical signalling (Hoge et al. 2013; Sodenkamp et al. 2012) confirming the anti-inflammatory effects of this mode of signalling, while IL-6 trans-signalling is involved in the pathogenic infiltration of adipose tissue by macrophages in obesity, an effect which was prevented by inhibition of trans-signalling with sgp130-Fc (Kraakman et al. 2015), demonstrating the promiscuity of IL-6 and its signalling mechanisms in pathological states.

1.16 Inflammation, IL-6 and Hypoglycaemia

The link between hypoglycaemia and inflammation has been documented. Insulin-induced hypoglycaemic clamp studies in patients with T1D show that the pro-inflammatory cytokine IL-6 is significantly increased from baseline levels after one and two hours of hypoglycaemia (Ceriello et al. 2013a). Another insulin-induced hypoglycaemic study in healthy subjects resulted in significant increases in IL-6 at the nadir of the hypoglycaemia with elevated levels persisting four hours subsequently (Nematollahi et al. 2009).

Although Wright *et al.* found similar elevations in IL-6 in response to hypoglycaemic but also in the euglycaemic control clamp in their 2010 study (Wright et al. 2010), they described this response as inexplicable, and it contrasts with another study demonstrating increases in IL-6 in response to hypoglycaemia (Dotson et al. 2008). A comprehensive study using two hours of clamped hyperinsulinaemic euglycaemia and moderate hypoglycaemia measured increases in IL-6 during hypoglycaemia relative to euglycaemia and importantly, the magnitude of the increase observed in the control individuals in this study were comparable to those observed in the aforementioned studies by Dotson *et al.* and Nematollahi *et al.* (Gogitidze Joy et al. 2010).

To further support the increase in inflammation in response to hypoglycaemia, studies have also demonstrated increases in inflammatory mediators other than IL-6. Wright *et al.* demonstrated increases in endothelin-1 in response to hypoglycaemia in T1D patients, and although not a classical inflammatory component of the immune system, analogously, endothelins have been implicated in the pathogenesis of several disorders, including atherosclerosis, diabetes and hypertension (Wright et al. 2007). Furthermore, Galloway *et al.* demonstrated increases in CRP in response to insulin-induced hypoglycaemia in control individuals and those with T1D (Galloway et al. 2000)

As mentioned, the debate surrounding whether IL-6 exerts positive or negative effects is intense and unresolved. Nematollahi *et al.* proposed in their 2009 paper that "elevation of pro-inflammatory cytokines may be an adaptive response to acute stress for maintaining glucose homeostasis in glycemic excursions" (Nematollahi et al. 2009).

While the aforementioned hypoglycaemic clamp studies have demonstrated conclusively that IL-6 and other inflammatory mediators are increased peripherally in plasma in response to low glucose, whether there is a central source of IL-6 that may directly regulate CNS glucose-sensing mechanisms is less established. A 2001 study using populations of rat cortical mixed glial cells demonstrated accumulation of IL-6 mRNA as early as 15 minutes after exposure to glucose deprivation and this increase in mRNA was proven to be functional with an increase in release of IL-6 protein by the cultures after two hours of hypoxia and hypoglycaemia (Wang et al. 2001). This finding was consolidated by Choi SJ *et al.* who observed an increase in IL-6 mRNA and its secretion in mouse BV2 microglial cells as well as murine primary microglia in response to glucose deprivation (S. J. Choi et al. 2013).

Many studies utilise a combined oxygen and glucose deprivation (OGD) to model ischaemic stroke of brain tissue or central cell types such as astrocytes and microglia. Several of these studies have reported increases in IL-6 in response to this stimulus in the BV-2 murine microglial cell line, mouse primary cortical astrocytes, mouse astroglial cultures, rat brain cortical slices, rat astrocyte cultures and using *in vivo* models of cerebral ischaemia (Xiang et al. 2014; Niu et al. 2009; Gesuete et al. 2011; Contartese et al. 2012; Pan et al. 2014; Gertz et al. 2012). Unfortunately, none of these studies measured IL-6 increases in responses to glucose deprivation alone. Interestingly, although the majority of the aforementioned studies identify IL-6 as a marker of OGD, Redzic *et al.* demonstrated that microglia conditioned media, and

specifically TGFβ and IL-6, have cytoprotective effects on astrocyte, pericyte and brain endothelial cells exposed to OGD, suggesting that these two molecules mediate a protective mechanism against cell death following their secretion (Redzic et al. 2015).

1.17 GT1-7 Cells

The GT1 cell lines were developed by genetically targeting tumourigenesis to specific hypothalamic neurons in transgenic mice using the promoter region of the gonadotropin-releasing hormone (GnRH) gene to express the SV40 T-antigen (Tag) oncogene. This resulted in formation of neuronal tumours from which Mellon *et al*. developed clonal, differentiated, neurosecretory cell lines (Mellon et al. 1990). By targeting the expression of the potent oncogene to the GnRH promoter, anterior hypothalamic tumours were observed in two of the transgenic mice studied. Portions of one of these tumours from a mouse called GT-1 were taken for mRNA analysis and tissue culture, and it was confirmed by northern blot that the tumour tissue from this animal specifically expressed GnRH and Tag.

The authors went on to culture cells from the GT-1 tumour and over a six month period were able to separate out neuronal and glial cell types. Characteristic cultures of a pure cell population were established and cloned by serial dilution resulting in the GT1-1, GT1-3 and GT1-7 cell lines. Northern blotting was again used to confirm that the three cell lines still expressed GnRH as the pure cell population did. When attached to plastic the GT1- cell lines exhibited a distinct neuronal phenotype, including extension of lengthy neurites. Interestingly, the authors noticed that the neuronal phenotype was more profound when cells were cultured in the absence of serum, preventing cell division. GT1-7 cells were specifically shown to express the neuron-specific enolase (NSE) mRNA, and also mRNA for the neurofilament proteins. In contrast, GT1-7 cells do not express the astrocyte marker glial fibrillary acidic protein (GFAP). Furthermore, the neuroendocrine phenotype of the GT1-7 cells was confirmed to be limited to GnRH expression, with a lack of somatostatin, POMC, CRH and GHRH mRNA expression in these cells. Further confirmation of the neuronal phenotype of GT1-7 cells came in the finding of the mRNA for the synaptic vesicle associated protein VAMP-2, which is known to be expressed in the hypothalamus (Trimble et al. 1990). mRNA for the presynaptic membrane protein SNAP-25 was also found in GT1-7 cells, along with that for chromogranin B, a neuroendocrine secretory vesicle protein found in the brain. Taken together the expression of neuronal, neurosecretory and synaptic membrane

proteins in the GT1-7 cells confirms their identity as neurons and documents their differentiated state.

Functional confirmation of GnRH secretion was also confirmed in this paper. Firstly, GnRH protein was detected in the media of all three cultured cell lines (GT1-1, GT1-3 and GT1-7) by radioimmunoassay. The authors also used the GT1-7 cells to demonstrate that depolarisation by treatment with 56 mM potassium resulted in a four-fold increase in GnRH release compared to the basal measurable rate of GnRH secretion from these cells in 5.6 mM potassium. In a separate experiment, the sodium channel opener veratridine was used to depolarise GT1-7 cells causing a six-fold increase in GnRH release during a 15 minute time period. The veratridine response was blocked by a 30 minute pretreatment with tetrodotoxin demonstrating the presence of fast sodium channels that are necessary for the occurrence of propagated action potentials. In contrast, the GnRH release in response to depolarisation induced by high potassium was not blocked by tetrodotoxin, indicating that potassium stimulates GnRH release via a different mechanism to veratridine. Studies in hypothalamic brain slices demonstrating that high potassium releases GnRH via VDCCs support these findings.

The GT1-7 cell line has proved to be a highly useful model for studying hypothalamic neurons at the molecular level; cells which are known to play fundamental roles *in vivo* in the whole body homeostatic regulation of diverse functions such as energy homeostasis, food intake, reproductive function and metabolic regulation (Y.-H. Choi et al. 2013; Flanagan-Cato et al. 2001). Performing studies in GT1-7 cells permits the investigation of effects in an isolated population of hypothalamic neurons, independent from other neuronal innervation or glial cell influence.

The advantages of using GT1-7 cells are that the cell line can be readily cultured, dividing about every 24 hours, allowing rapid generation of cultures to perform studies. The cells are relatively robust and stand up well to electrophysiological examination providing reliable recordings with a well established resting membrane potential of ~ -50 mV. The cells are frequently used to investigate expression and secretion of the neurotransmitter GnRH, which cannot be easily done *in vivo,* and which from brain slice preparations is complicated by the heterogeneous nature of the cell types present. For the current studies, the validity of the GT1-7 cell model has been well characterised, as it is analogous to the pancreatic beta-cell and responsive to hypoglycaemia (Beall, Hamilton, et al. 2012). The GT1-7 cell line has also been demonstrated to express the

IL-6Rα at low levels (McCrimmon Laboratory, unpublished data). The model allows the detailed study of signalling pathways in isolated, metabolically-sensitive neurons which would otherwise be complex in intact hypothalami. The model allows distinction of whether effects observed on whole hypothalami are mediated via a direct action on neurons.

The disadvantages of the cell line are that culture conditions appear to have a considerable bearing on the responsiveness and phenotype of the cells. For example, it has been reported that the cells are of a more neuronal morphology under low serum conditions to inhibit cell division (Mellon et al. 1990). In my experience, the cells grow faster and appear healthier under high glucose conditions (25 mM), however this means that the cells have to be brought down to physiological glucose concentrations for experimentation. Since the physiological glucose concentration in the brain is 2.5 mM (Watts & Donovan 2010), this involves a large reduction in cultured glucose levels to achieve levels within the physiological range. This will likely induce a hypoglycaemic response in the cells meaning that cells either have to be reduced to lower glucose concentrations in a step wise manner or need to be allowed to recover and grow accustomed to 2.5 mM glucose conditions prior to experimentation. Another drawback of the GT1-7 cell line is that cellular protein content is low, meaning that experiments need to be performed on relatively large cultures of cells to yield enough cellular protein for subsequent analysis. Also, since the cell line is a tumour cell line, it is likely to be somewhat pathophysiological in phenotype. Our laboratory has determined that the glucose sensing phenotype of the GT1-7 cells exists transiently over a period of time in culture, such that glucose sensing experiments must be performed within a narrow passage range of the cells (p47-p60).

The GT1-7 cells were selected as the model for the current project as they are an easy to work with, homogenous, electrically active, hypothalamic GE neuronal cell line that permitted investigation of the direct effects of IL-6 on glucose-sensing neurons.

1.18 Hypothesis and Aims

The importance of CNS glucose sensing in the mounting of appropriate CRRs to hypoglycaemia, particularly by neurons of the VMH has been demonstrated. Several potential mediators of defective CRRs, induced by antecedent and recurrent hypoglycaemia and observed in T1D, have been proposed, many of which involve impairment of glucose-sensing neuronal function. There is a strong inflammatory

component associated with hypoglycaemia, but physiological roles for these inflammatory mediators in this setting remain undefined. IL-6 represents one of the most well characterised cytokines, and the aim of the current project was to investigate the hypothesis that IL-6 may play a role in the regulation of hypothalamic GS and therefore hypoglycaemia detection. The aims of the project were to determine if IL-6 regulated the activity of hypothalamic GE neurons and if so, the mechanisms by which this regulation occurred. Electrophysiological and biochemical analysis of an *in vitro* model of VMH GE neurons was employed to this end.

2 Materials and Methods

2.1 Cell Culture

GT1-7 cells were cultured in a category 1 biological safety rated cell culture facility and were maintained at 37°C in a 5% CO_2 incubator. In order to maintain cells in culture, they were grown in T75 stock flasks which were passaged every two to five days to maintain the cells at an optimal confluency of no greater than 80%. Since GT1-7 cells are non-adherent, all plasticware was pre-coated with poly-L-lysine (PLL) prior to cell seeding to facilitate attachment. This was achieved by incubating the plasticware at room temperature with an appropriate volume of PLL to cover the base at a concentration of 0.2 mg/ml (in dH_2O) for 30 minutes. PLL was removed and a phosphate buffered saline (PBS) rinse was performed prior to cell seeding.

To passage the cells, the stock media was removed from the T75 flask and a 10 ml 37°C PBS rinse was performed. 2 ml of 0.05% trypsin-EDTA was then applied to the flask and incubated at 37°C in a 5% CO_2 incubator for two-five minutes. Trypsinisation was inactivated by the addition of 3 ml of growth media to the flask. The resulting cell suspension was pipetted up and down thoroughly and used to rinse the base of the flask several times to ensure maximal retrieval of cells. The cell suspension was centrifuged at 800 rpm for 4 minutes in a 15 ml Falcon tube to pellet the cells. The media supernatant was removed to waste and the cell pellet was resuspended in 4-8 ml of growth media by thoroughly pipetting up and down. 1 ml of this cell suspension was added to a pre-PLL-coated T75 flask containing 10 ml of growth media to create a stock flask. If stock flasks required bulking up, or a higher density of cells was required in the stock flask, 2 ml of the cell suspension was added to a T75 flask containing 10 ml growth media. Stock flasks were given fresh growth media every 48 hours to replenish supply of glucose and other nutrients to the cells. To achieve this the media was removed from the flask and a fresh 10 ml of growth media was added.

Seeding protocols for experiments and assays differed depending on the specific assay being run, and will be discussed in detail according to the particular assay in the following methods.

Table 2.1: GT1-7 Culture Medias

Media	**Stock**	**Supplements**
25 mM Glucose Growth DMEM (Stock Media)	D5671 Dulbecco's Modified Eagle's Medium	25 mM D-glucose, 10% v/v Fetal Bovine Serum (Hyclone), 4 mM L-glutamine, 2% v/v penicillin-streptomycin (100,000 Units/ml)
2.5 mM Glucose Plating Media (Plating Media)	D11966 Dulbecco's Modified Eagle's Medium with 4 mM L-glutamine	2.5 mM D-glucose, 2% v/v Fetal Bovine Serum (Hyclone), 2% v/v penicillin-streptomycin (100,000 Units/ml)
2.5 mM Glucose Serum Free DMEM (Serum Free Media)	D11966 Dulbecco's Modified Eagle's Medium with 4 mM L-glutamine	2.5 mM D-glucose, 2% v/v penicillin-streptomycin (100,000 Units/ml)

2.2 Cell Seeding

2.2.1 Interleukin-6 (IL-6) Time Courses

GT1-7 cells were plated in 60 mm culture dishes at a density of 400,000 cells in 3 ml of plating media the night before experiments. On the day of the experiment, media was removed from the dishes and a PBS rinse performed prior to incubation in 3 ml of serum free media for two hours at 37°C in a 5% CO_2 incubator. This serum starve step was employed to ensure intracellular signalling cascades would be at a basal level of activation and comparable between experiments. After the two hour incubation the

serum free media was removed and a fresh 3 ml of serum free media was applied for the experiment. In the IL-6 timecourse experiments cells were treated with 20 ng/ml IL-6 (12 µl 5 µg/ml IL-6 stock dissolved in distilled H_2O) for five to 180 minutes. A control treatment was also performed in which cells were exposed to dH_2O alone for the longest time point of that particular experiment (e.g. 180 minutes). Treatments were performed in duplicate and were performed in a reverse format, such that 180 minute treatments were treated first and shorter time points were treated subsequently so all cells could be lysed at the same time point at the end of the experiment.

2.2.2 Antecedent IL-6 treatments

An antecedent IL-6 protocol was employed to mimic a pre-exposure to elevated IL-6 levels for subsequent observations of the effects this had on GT1-7 cells. GT1-7 cells were plated in 60 mm culture dishes at a density of 400,000 cells in 3 ml of plating media for biochemical experiments, or in 35 mm culture dishes at a density of 20,000 cells in 2 ml of plating media for electrophysiological experiments, the night before experiments. On the day of the antecedent exposure, plating media was removed from the dishes and a PBS rinse was performed prior to application of serum free media. Cells were then treated with either dH_2O vehicle control or 20 ng/ml IL-6 for three hours, incubated at 37°C in a 5% CO_2 incubator during this time. At the end of the treatment the media was removed and a PBS rinse performed prior to application of plating media overnight. The following day, the pre-exposed cell cultures were either investigated electrophysiologically (whole-cell and perforated patch clamp configuration), or underwent an acute hypoglycaemia treatment before being lysed. This involved media removal and a PBS rinse prior to application of either 2.5 mM glucose serum free media (euglycaemic control) or 0.1 mM glucose serum free media (hypoglycaemia) for 15 minutes. A 15 minute exposure of GT1-7 cells to 0.1 mM glucose has previously been shown to induce an increase in the phosphorylation of AMPK in these cells (Beall, Hamilton, et al. 2012). At the end of the 15 minute euglycaemic and hypoglycaemic treatments cells were lysed.

2.3 Cell Lysis for Western Blots

Cell lysis to harvest protein for subsequent analysis was performed in a 1x lysis buffer solution diluted in dH_2O from a 5x stock made up according to the recipe in Table 2.2.

Table 2.2: 5x Lysis Buffer 100 ml Stock

Tris HCl at pH 7.4	125 mM
NaF	250 M
NaCl	0.5 M
EDTA	5 mM
EGTA	25 mM
Triton X 100	5% v/v
NaPPi	50 mM

Prior to cell lysis, the 1x stock lysis buffer was supplemented with the protease inhibitors detailed in Table 2.3 and sucrose to increase osmolarity.

Table 2.3: 1x Lysis Buffer Supplements

Sucrose	92 mg/ml
2-mercaptoethanol	0.1% v/v
Benzamidine	1 mM
Na_3VO_4 (Heated at 95°C for five minutes prior to addition)	1 mM
PMSF	0.1 mM

Lysis buffer was always prepared on ice and vortexed prior to use. The amount of lysis buffer used varied depending on the number of cells being lysed and the surface area of the plasticware on which they were seeded. Table 2.3 demonstrates typical lysis buffer volumes used based on the plasticware being used with cells at a confluency of 70-80%.

Table 2.4: Lysis Buffer Volumes

Plasticware	**Surface Area (cm^2)**	**Lysis Buffer Volume (µl)**
6 well plate	10	50
60 mm plate	20	75
100 mm plate	60	150

To ensure sterility, cells were lysed in a tissue culture hood. The assay medium was removed from the plates and a 4°C PBS rinse was performed to remove as much of the assay medium as possible. The residual PBS was removed with a P1000 pipette. The appropriate volume of 1x lysis buffer was applied directly onto the base of the plastic and plates were scraped thoroughly with cell scrapers. The lysate was harvested and transferred to an eppendorf tube labelled appropriately and stored at -20°C.

2.3.1 Bradford Assay

A modified version of the well established Bradford protein assay (Bradford 1976) was used to determine the unknown protein concentrations of GT1-7 cell lysates. Cell lysates were thawed on ice and centrifuged at 13,000 rpm for 15 minutes at 4°C to pellet out the nuclear fraction. The resulting supernatant was transferred to a fresh eppendorf tube and the pellet was discarded. The Bradford assay utilised in this project was performed in a 96 well plate format. The unknown lysate protein concentrations were determined by extrapolating an absorbance value from a standard curve of known bovine serum albumin (BSA) absorbances of increasing concentration. Table 2.5 demonstrates the points of the standard curve used and how they were achieved.

Table 2.5: BSA Standard Curve for Bradford Assay

BSA Standard Curve (mg/ml)	**Volume of BSA stock (µl)**	**Volume of MilliQ dH_2O (µl)**
0	0	10
0.25	1.25 of 0.2 mg/ml stock	8.75
0.5	2.5 of 0.2 mg/ml stock	7.5
1	5 of 0.2 mg/ml stock	5
2	10 of 0.2 mg/ml stock	0
5	2.5 of 2 mg/ml stock	7.5
7	3.5 of 2 mg/ml stock	6.5

1 µl of the protein lysates to be assayed was diluted in 9 µl of MilliQ dH_2O and finally 250 µl of Bradford Reagent, warmed to room temperature, was added to all of the standard curve and lysate wells. The plate was incubated at room temperature for ten minutes to allow the Bradford Reagent to interact with the protein present. The absorbance values of the wells were then measured using an EnVision plate reader (PerkinElmer) at 595 nm. The absorbance values from the standard curve were plotted in Microsoft Excel and the unknown protein concentrations of the lysates were extrapolated using the gradient of the standard curve.

2.3.2 Sample Preparation for Western Blot

100 µl protein samples for analysis by Western blot were prepared to a final concentration of 1 µg/µl by diluting an appropriate volume of protein lysate with a 4x sample buffer stock (used at a working concentration of 1x) and MilliQ dH_2O. The recipe for the 4x sample buffer stock is shown in Table 2.6.

Table 2.6: 4x Sample Buffer Stock (12 ml)

0.5 M Tris at pH 6.8	4 ml
Glycerol	3.2 ml
20% Sodium Dodecyl Sulphate	3.2 ml
2-mercaptoethanol	1.6 ml
Bromophenol Blue	pinch

Samples were heated at either 95°C for ten minutes for detection of cytosolic proteins or 37°C for one hour for detection of membrane bound proteins. Samples were stored at -20°C once prepared.

2.3.3 Western Blot

To investigate the expression of various cellular proteins, GT1-7 protein samples were subjected to Western blot. Proteins were separated using sodium dodecyl sulphate polyacrylamide gel electrophoresis (SDS-PAGE) (Laemmli 1970) depending on their molecular weights. Several different percentages of acrylamide separating gels were used in this project to achieve different pore sizes in the gel matrices, as this can variably effect the migration of proteins through the gel due to the differing molecular weights of the proteins. Table 2.7 details the separating and stacking gels used in this project.

Table 2.7: Commonly Used Gel Recipes

Lower Gel 10% Acrylamide	**Volume required for 4 gels**
dH_2O	8.3 ml
Lower buffer	6.3 ml
30% acrylamide	7.5 ml
10% sodium dodecyl sulphate	220 µl

TEMED	22 µl
20% ammonium persulphate	110.7 µl
Lower Gel 7% Acrylamide	**Volume required for 4 gels**
dH_2O	10.55 ml
Lower buffer	6.3 ml
30% acrylamide	5.25 ml
10% sodium dodecyl sulphate	220 µl
TEMED	22 µl
20% ammonium persulphate	110.7 µl
Upper Gel 4% Acrylamide	**Volume required for 4 gels**
dH_2O	5.6 ml
Lower buffer	2.5 ml
30% acrylamide	1.7 ml
10% sodium dodecyl sulphate	100 µl
TEMED	10.7 µl
20% ammonium persulphate	100 µl

In this project, a 4% acrylamide stacking gel was used and cast with either 10- or 15-well combs to create the desired number of wells for protein sample loading. Typically, 10 µg protein was loaded from each sample. Every gel was also run with at least one lane containing 3 µl of molecular weight marker to allow determination of protein band sizes.

Gels were cast using the BioRad blotting system and once loaded were run at 135 volts for one hour and 30 minutes in 1x Tris/Glycine running buffer.

After completion of SDS-PAGE, resolved proteins were transferred to nitrocellulose or polyvinylidene fluoride (PVDF) membrane (PVDF membrane was soaked in 100% methanol for two minutes prior to use). This was achieved by creating a transfer "sandwich" by stacking sponges and filter paper either side of the gel and membrane, which were in direct contact with one another, into a transfer cassette. By passing electrical current through the set up in the correct orientation it is possible to cause the negatively charged proteins to migrate out of the gel and onto the membrane. This was performed at a constant voltage of 100 volts for one hour in transfer buffer.

Upon completion of the transfer the membranes were placed into square petri boxes and incubated in Ponceau S solution for two minutes at room temperature on a rocker to reversible stain protein bands to confirm successful transfer of the proteins to the membrane. The Ponceau dye was rinsed off thoroughly by repeated washing in tris-buffered saline with tween solution (TBST).

Membranes were blocked in a 10% w/v non-fat dried milk solution made up in TBST for one hour at room temperature on a rocker to reduce non-specific binding sites prior to primary antibody incubation. After blocking, the membranes were rinsed several times in TBST to remove any residual milk solution. Primary antibodies were applied overnight in 5% BSA w/v solution in TBST at 4°C on a rocker. The following day primary antibodies were removed and membranes were washed five times for five minutes each time in TBST solution prior to incubation with secondary antibodies. Secondary antibodies were made up in 5% w/v non-fat dried milk solution in TBST and applied for one hour at room temperature on a rocker. Following this membranes were again washed five times for five minutes each time in TBST solution.

Membranes were imaged using a Licor Odyssey scanner. Briefly, membranes were exposed to light of an appropriate wavelength to cause fluorescence emission from the secondary antibodies used and a digital image of the resulting fluorescence from the membrane was obtained. The images of the protein bands were then subjected to densitometry analysis in order to determine relative expression levels of the proteins to their appropriate controls and to a stably expressed housekeeping protein.

Table 2.8: Commonly Used Buffers

Buffer	**Components**
Lower Buffer	1.5M Tris/HCl, pH 8.8 in dH_2O
Upper Buffer	0.5M Tris/HCl, pH 6.8 in dH_2O
1x Running Buffer	0.025M Tris, 0.192M Glycine, 0.1% v/v SDS in dH_2O
Transfer Buffer	48mM Tris, 39mM Glycine, 20% v/v methanol in dH_2O
TBST	20mM Tris/HCl pH 7.4, 148 mM NaCl, 0.1% v/v Tween in dH_2O

2.3.4 Densitometry

The intensity of the pixels in each protein band obtained was determined by drawing a rectangle around each band and quantifying the signal in these boxes using the Licor Odyssey Image Studio software. A background signal was also determined by quantifying the intensity of pixels in a box of the same size as those around the bands of interest but from a blank part of the membrane with no protein bands. The background value was subtracted away from the intensity values obtained for the protein bands to exclude the contribution of autofluoresence from the membrane to the observed signal. The expression of proteins of interest was normalised to the expression of the gel loading control protein actin to account for pipetting error in gel loading. The fold change in intensity, which directly indicates protein abundance, was then calculated from untreated or vehicle treated control samples to treated samples.

2.4 Cell Lysis for Gene Expression (TRI Reagent)

Lysis of cells that would subsequently undergo gene expression analysis was performed in the RNA isolation agent TRI Reagent. To ensure sterility cells were lysed in a tissue culture hood. The assay medium was removed and a 4°C PBS rinse was performed to remove as much media as possible. Residual PBS was removed with a P1000 pipette. 1 ml of TRI reagent at 4°C was then applied directly onto the cells and this solution was

pipetted up and down thoroughly and used to rinse the base of the plastic to ensure recovery of as many cells as possible. The TRI reagent was transferred to appropriately labelled eppendorf tubes which were stored at -20°C.

2.4.1 RNA Isolation

RNA isolation was performed according to the manufacturer's instructions included with the TRI Reagent. Samples were thawed on ice at 4°C and then were allowed to stand at room temperature for five minutes to allow phase separation to ensure complete dissociation of nucleoprotein complexes. 0.2 ml of chloroform was added to each sample, which were then shaken vigorously for 15 seconds. Samples were stood at room temperature for 15 minutes then the resulting mixture was centrifuged at 12,000 *x g* for 15 minutes at 4°C. Centrifugation separates the mixture into three phases of which the clear, upper aqueous phase is RNA containing. The upper aqueous phase was transferred to a fresh eppendorf tube using a P200 pipette and 0.5 ml of isopropanol was added to this tube. The samples were stood at room temperature for ten minutes. Then they were centrifuged at 12,000 *x g* for ten minutes at 4°C. This caused the RNA to precipitate out of solution and form a pellet on the bottom on the tube. The supernatant was removed to waste and the RNA pellet was washed by adding 1 ml of 75% ethanol (in dH_2O), vortexing briefly, then centrifuging at 12,000 *x g* for five minutes at 4°C. The ethanol was removed and the RNA pellets were allowed to air dry for ten minutes under a vacuum. The RNA pellets were resuspended in 30 µl of DNase free H_2O and heated at 57°C for 15 minutes to facilitate dissolution. RNA purity and concentration was determined using a Nanodrop ND-8000 (Nanodrop).

2.4.2 cDNA Synthesis Using SuperScript™ II Reverse Transcriptase (RT)

cDNA was synthesised from isolated GT1-7 RNA according to the manufacturer's protocol included with SuperScript™ II RT. The reaction was performed in microcentrifuge tubes at a final volume of 19 µl using 1 µg RNA. Following quantification of extracted RNA using the Nanodrop, the volume of the RNA sample required to achieve to 1 µg RNA was calculated and added to a microcentrifuge tube. 3 µg random primers and 1 µl dNTP Mix (10 mM each) was added to the tube. The

volume was made up to 12 µl by adding an appropriate volume of DNase free H_2O. The mixture was heated to 65°C for five minutes and then quick chilled on ice. Tubes were briefly centrifuged and 4 µl of 5x First-Strand Buffer and 2 µl of 0.1 M DTT were added to the tubes and the contents were mixed by gentle pipetting. Tubes were incubated at 25°C for two minutes before 1 µl (200 units) of SuperScript™ II RT was added and mixed by pipetting gently up and down. Tubes were incubated at 25°C for ten minutes, then at 42°C for 50 minutes. The reaction was then inactivated by heating at 70°C for 15 minutes. Finally, the cDNA was diluted 1:10 by adding 180 µl of DNase free H_2O before being stored at -20°C.

2.4.3 TaqMan® Gene Expression Assays (Real-time PCR)

In this project, the TaqMan® real-time polymerase chain reaction (PCR; Life Technologies) assay was used for assessing gene expression in GT1-7 cells. After RNA isolation and cDNA synthesis described above, GT1-7 cDNA was subjected to PCR using primers and probes specific to several genes of interest, the expression of which was normalised to the housekeeping gene Cyclophillin A. The PCR was performed in a 96 well plate at a final reaction volume of 20 µl. The plate was loaded on ice. Each well contained a reaction mixture comprising of 1 µl of primers and probes, 10 µl master mix, 6.5 µl of RNAse free H_2O and 2.5 µl of cDNA. The plate was centrifuged for 15 seconds prior to beginning the reaction. The plate was run using a real-time PCR machine (Applied Biosystems).

2.5 Electrophysiological Recordings

Table 2.9: Electrophysiological Recording Solutions

	NaCl (mM)	**KCl (mM)**	**$MgCl_2{}_6H_2O$ (mM)**	**$CaCl_2$ (mM)**	**HEPES (mM)**	**EGTA (mM)**	**pH**
External Saline Solution	135	5	1	1	10		7.4 (NaOH)
Internal Saline Solution		140	5	3.8	10	10	7.2 (KOH)

Two main configurations of electrophysiology were used in this project to record from GT1-7 cells. These were the whole-cell patch clamp configuration and the perforated patch clamp configuration. Both modes of recording required some set up in common. On the day of recording a syringe tip was prepared. This was achieved by melting a P200 pipette tip over a methanol burner and stretching it out to make a very fine tip capable of being inserted into and filling a glass micropipette with solution. The required internal saline was filter sterilised through a 0.22 μm filter and was collected in a 1 ml syringe onto which the prepared P200 tip was added. Borosilicate glass capillary tubing with an outer diameter of 1.2 mm and and inner diameter of 0.69 mm was used to prepare glass micropipettes. The glass capillaries were fire polished at either end using a Bunsen burner to smooth the edges and then pulled and stretched horizontally using a Flaming/Brown micropipette puller (Model P97, Sutter Instrument Co., USA). This resulted in two micropipettes of equal length that then had their tips fire polished using a micro forge (MF-830, Narishige, Japan). Tip resistance was typically between 5 and 10 MΩ. Prior to use the micropipettes were half filled with the appropriate solution using the above described syringe preparation.

Before commencing recordings each day the bath and the perfusion tubing of the electrophysiology rig set up was thoroughly rinsed with 70% ethanol then MilliQ H_2O to ensure sterility prior to experiments.

22 mm^2 glass coverslips with GT1-7 cells seeded at a density of around 50-300 cells were carefully transferred using forceps into the bath on the electrophysiology rig that contained 1-2 ml of 2.5 mM glucose physiological external saline solution. The reference electrode was introduced to the bath solution along with the inlet and outlet of the gravity perfusion system.

2.5.1 Whole-Cell Patch Clamp Configuration

The glass micropipettes described above were half filled with internal saline solution and attached to the pipette holder, such that the chloride-coated, silver wire electrode was submerged in the micropipette solution. Positive pressure was applied prior to entry of the micropipette into the recording bath external saline solution. The microelectrode was lowered to just above a single GT1-7 cell using an electronic micromanipulator (Luigs & Neumann) and the pipette offset was corrected by zeroing the current in voltage clamp mode. The microelectrode was then brought into contact with the cell membrane and gentle negative pressure was applied by mouth pipetting in order to form a giga ohm (GΩ) seal between the micropipette tip and the cell membrane. This is termed cell-attached configuration. The pipette capacitance transients, formed by charging and discharging of the cell membrane with test voltage pulses, were cancelled using the fast capacitance control on the amplifier (Axopatch 200B, Axon Instruments). From the cell-attached configuration, the negative pressure was increased in order to rupture the cell membrane and enter the whole-cell patch clamp configuration, gaining access to whole-cell macroscopic currents, with the micropipette holding potential set at -70 mV. Upon adoption of the whole-cell configuration, the sudden appearance of large capacitance transients were cancelled using the whole cell capacitance and series resistance controls on the amplifier, giving an estimation of the cell membrane capacitance (pF) and the resistance between the pipette and cell interiors, termed the series resistance (R_s in MΩ). Over time (typically 10-15 minutes) in the whole-cell configuration, the intracellular contents of the cell dialyse out and exchange with the contents of the glass micropipette.

In this project, the whole-cell patch clamp configuration was exploited to conduct a voltage clamp protocol to investigate current conductance at stepped voltage pulses ranging from -90 to +30 mV, from a holding potential of -70 mV (net membrane potential steps were therefore from -160 to -40 mV) in 20 mV steps which were a duration of 400 ms with a 20 ms interval between pulses. The steady-state currents elicited by each test pulse allow determination of the reversal potential, slope conductance, total whole-cell current and voltage-dependent kinetics. Conductance density of the cell was determined by plotting the current amplitude elicited by each voltage step against the magnitude of the test pulse, producing a linear current-voltage (I-V) relationship. Linear regression analysis of the line of best fit for the I-V relationship allows the slope conductance to be determined from the gradient of this line. The reversal potential (in mV) can be determined from the point where the I-V line intercepts the x-axis. The slope conductance can then be normalised to the cell size (pF) in order to determine the conductance density of the cell (pS/pF). In the experiments in the current work, the above described voltage clamp recordings were made at intermittent intervals during a current-clamp recording (detailed subsequently). These intervals were at the beginning of recording immediately after whole-cell formation, after complete dialysis of the intracellular and pipette solutions (termed run-up) and finally after closure of K_{ATP} channels using the sulphonylurea tolbutamide (reversing the run-up state of the cell). The recordings made in whole-cell voltage clamp configuration were sampled at 2 kHz and filtered at 10 kHz using a low pass Bessel filter incorporated in the amplifier.

2.5.2 Perforated Patch Clamp Configuration

Glass microelectrodes were half filled with internal saline solution supplemented with 12.5 – 40 μg/ml Amphotericin B, an antibiotic capable of perforating the cell membrane by puncturing small holes in it that are permeable to ions but not to larger molecules. Since the perforated patch clamp configuration maintains the integrity of the cell membrane to a large extent, recordings made in this configuration are widely accepted as being more physiologically closer to intact cells than those made in whole-cell configuration.

The attainment of the cell-attached configuration and cancellation of pipette capacitance was achieved in the same manner as that detailed in the above section for whole-cell

patch clamp configuration. The amplifier was then switched from voltage clamp to current clamp mode to start recording. The current clamp mode of recording allows observation of the membrane potential (V_m) and action potential frequency of the cell being recorded from in real time, allowing accurate measurement of the effects of exposure to varying solutions and agents on V_m. Upon commencement of current clamp recording in the perforated patch clamp configuration a period of stabilisation was permitted (up to 20 minutes) while the cell membrane perforated in response to Amphotericin B and a stable resting V_m was obtained. All recordings made in this configuration were sampled at 2 kHz and filtered at 10 kHz using a low pass Bessel filter incorporated in the amplifier.

It should be mentioned that while every effort was made to only accept recordings from cells with no current injection (I=0), occasionally, negative current (up to -10 pA) was passed via the amplifier to the cells that didn't perforate to a normal resting V_m for GT1-7 cells of -40 to -60 mV.

For all electrophysiological experiments a gravity-flow perfusion system attached to a vacuum pump was used to exchange the bath solution. Bath glucose concentrations were altered by perfusing external saline supplemented with varying concentrations of glucose. This method was also employed for perfusing drugs into bath. Perfusion was manually operated using three way taps and a minimum of 10 ml of solution was perfused to ensure full exchange of the bath solution.

2.6 Primary Mouse Cortical Astrocyte Preparation

Mouse pups (postnatal day 2-4) were decapitated and heads placed on ice. An incision was made along the skull midline to allow the skin to be peeled back and the skull to be opened. The brain was removed and placed into 1 ml of ice cold Hank's Balanced Salt Solution (HBSS). Meningeal membranes were peeled away using fine forceps under a dissection microscope and the cortex was dissected out and placed in a 60 mm dish containing a small volume of ice cold HBSS to prevent the tissue from drying. Brain tissue was minced using a scalpel and 3 ml of 0.5% trypsin was added and brain tissue was transferred to a 15 ml Falcon tube and incubated in a water bath at 37°C for 20 minutes. Trypsin was neutralised by the addition of 3 ml of stock media followed by repeated pipetting to thoroughly triturate. The suspension was filtered through a 70 µm cell filter and then added to a T75 flask containing 10 ml of stock media. After

incubation at 37°C in a 5% CO_2 incubator, media was removed and a fresh 10 ml of stock media was replaced. As astrocytes are selected for by their robust adherence to plasticware, at every media change thereafter the cell culture surface was rinsed with PBS three times before replenishment of stock media. Once astrocytes reached ~80% confluency they were split into 60 mm dishes for experiments. Media was removed and a PBS rinse performed before cells were detached from the flask by incubation in 2 ml of 0.5% trypsin for five minutes at 37°C in a 5% CO_2 incubator. 3 ml of stock media was added and the suspension was centrifuged at 800 rpm for four minutes to pellet the cells. Cells were resuspended in an appropriate volume of stock media and seeded in 60 mm dishes for experiments.

2.7 Media Harvest from Astrocytes for IL-6 Secretion Measurement

Primary mouse cortical astrocyte cultures in 60 mm dishes were incubated in 3 ml of 2.5 mM glucose or 0.1 mM glucose serum-free DMEM for three hours. Media was harvested immediately at the end of the treatment time and a fresh 3 ml of 2.5 mM glucose serum-free DMEM was applied to all cultures. Cultures were incubated at 37°C in a 5% CO_2 incubator for four hours after which time this media was harvested. The amount of IL-6 secreted in the harvested supernatants was measured by Mouse IL-6 Quantikine ELISA (R&D Systems, Abingdon) according to the manufacturer's protocol.

2.8 shRNA Lentiviral Transduction

Passage 51 (p51) GT1-7 cells were plated the day before infection in a pre-PLL-coated 12 well plate at a density of 50,000 cells per well in 1 ml of stock media. Only eight wells of the plate were seeded as the infections would consist of one scrambled small hairpin RNA (shRNA) control, five different shRNAs targeting the IL-6 receptor and two cell death control wells. The optimum cell confluency for transduction is 50 – 70%. The plate was incubated at 37°C overnight in a 5% CO_2 incubator.

The media for the infection was made up on the day by supplementing 25 mM glucose, 10 % FBS containing DMEM growth media with 20 μg/ml Polybrene to encourage virus particle uptake into GT1-7 cells.

The five shRNAs targeting the IL-6 receptor and the control were the commercially available MISSION® Transduction Particles and MISSION® Non-Mammalian shRNA Control Transduction Particles respectively. Since the constructs were of varying concentrations of transducing units (TU) per ml, it was necessary to calculate what volume of each construct was required to achieve a multiplicity of infection (MOI) of 20. An example of this calculation is shown below:

shRNA 1: 1.3×10^7 TU/ml = 13, 000 TU/µl

50,000 cells/ 13,000 TU = 3.85 ul x 20 MOI = 77 µl

The media was removed from each well and replaced with 500 µl of 20 µg/ml Polybrene containing DMEM and the appropriate volume of each lentivirus was added to the appropriate wells and the plate was gently swirled to mix. Cell death control wells just received a media change with no viral particles added. The plate was incubated at 37°C overnight in a 5% CO_2 incubator for 18-24 hours.

The following day (day two) the cells were fed by adding 500 µl of 25 mM glucose, 10% FBS containing growth media to each well. On day three a full media change was performed by removing the media and replacing it with a fresh 1 ml of 25 mM glucose, 10% FBS containing growth media per well. On day four the GT1-7 cells were confluent enough to be scaled up into a 6 well plate. This was achieved by removing the media, performing a 500 µl 37°C rinse of each well and applying 500 µl trypsin per well and incubating at 37°C in a 5% CO_2 incubator for two to five minutes. The plate was tapped gently to make sure cells were dissociated from the plastic. 500 µl of GT1-7 growth media was added to each well and the suspension was pipetted up and down thoroughly before the full 1 ml of cell suspension was added to a pre-PLL-coated 6 well plate containing 2 ml of GT1-7 growth media. As there were eight wells in total, two 6 well plates were required for this scale up. The cells were fed over the following days as described on day three above, until they had reached 70-80% confluency in the six well plate. The MISSION® constructs contain a puromycin-resistance cassette conferring resistance to this antibiotic in virally infected cells. Virally infected cells were therefore selected for by replacing the media on the six well plate with GT1-7 growth media supplemented with 5 µg/ml puromycin hydrochloride. With this media change only those cells successfully infected with virus were able to survive. Confirmation that this was indeed the case came via the lack of viable cells in the cell death control wells,

which were subsequently excluded from the rest of the protocol. The GT1-7 cells were then scaled up to T25 flasks and subsequently T75 flasks via trypsinising and replating as described above. The virally infected GT1-7 cells were maintained in GT1-7 growth media supplemented with 5 μg/ml puromycin hydrochloride.

RNA was isolated from two different cultures of each of the shRNA infected GT1-7 cell lines as previously described above. cDNA was synthesised from this RNA and subjected to TaqMan RT-PCR using primers and probes specific for the IL-6Rα mRNA transcript. The expression of the mRNA for the IL-6Rα in the five shIL-6Rα infected GT1-7 cell lines was quantified and compared to the expression level in the shControl infected cell line. shIL-6Rα4-infected GT1-7 cells exhibited a ~74% reduction in expression of IL-6Rα mRNA compared to shControl infected cells. Stocks of the shRNA infected GT1-7 cells were obtained by freezing down cells from confluent T75 flasks in 10% DMSO containing GT1-7 growth media in 1.8 ml cryotubes in a Mr. Frosty™ Freezing Container (Thermo Scientific™) at -80°C prior to storage in liquid nitrogen dewars.

2.9 Seahorse Bioscience Extracellular Flux Analyser (XF24)

The Seahorse Bioscience Extracellular Flux Analyser XF24 (XF24; Seahorse Bioscience) was used to measure extracellular acidification rate (ECAR) and oxygen consumption rate (OCR), which index glycolysis (by measuring the acidification in response to lactate release) and oxidative phosphorylation respectively.

Table 2.10: Medias for Seahorse XF24 Assays

Media	**Stock**	**Supplements**
Basal	XF24	2.5 mM D-Glucose
Mito Stress Test	XF24	2.5 mM D-Glucose, 2.5 mM sodium pyruvate, 2 mM L-glutamine

2.9.1 Basal ECAR and OCR Measurements

To measure basal ECAR and OCR GT1-7 cells were treated with vehicle control (dH_2O) or 20 ng/ml IL-6 for three hours in 2.5 mM glucose serum-free DMEM. Following recovery in 2.5 mM glucose serum-containing media for approximately two hours, cells were trypsinised and counted using an automated cell counter. The cells were seeded the day before the assay at a density of 30,000 cells per well in pre-PLL-coated 24 well Seahorse XF24 culture plates in a final volume of 400 µl GT1-7 plating media. The plate was incubated at 37°C overnight in a 5% CO_2 incubator.

On the day of the assay and 18-24 hours subsequent to seeding the plating media was removed from the wells by aspiration and replaced with 500 µl of assay medium for basal measurements and incubated for one hour at 37°C in a non-CO_2 incubator to de-gas the cells. This step should remove any CO_2 from the cells and the culture plate that may interfere with the readings from the Seahorse XF24 probes. The Seahorse XF24 system uses a cartridge that can be pre-loaded with compounds that can be injected into the assay wells during experiments. In the case of basal readings, no compounds were injected, so the cartridge was simply loaded into the Seahorse XF24 and allowed to undergo the calibration phase of the assay. When cartridge calibration and the one hour de-gassing had been completed, the cell plate was also loaded into the Seahorse XF24 positioned such that it was underneath the recording probes of the cartridge. The protocol employed consisted of five repetitions of a three minute mix, two minute wait, three minute measure cycle.

2.9.2 Mito Stress Test

The commercially available Mito Stress Test (Seahorse Bioscience) was utilised for assessing functional mitochondrial measurements allowing detailed mitochondrial profiling. The test allows the measurement of key parameters of mitochondrial function including basal respiration, ATP production, proton leak, maximal respiration and spare respiratory capacity.

For this assay GT1-7 cells were treated and plated in the same way as described for basal ECAR and OCR measurements and incubated overnight at 37°C in a 5% CO_2 incubator.

On the day of the assay and 18-24 hours subsequent to seeding the plating media was removed from the wells by aspiration and replaced with 500 µl of assay medium for the Mito Stress Test and incubated for one hour at 37°C in a non-CO_2 incubator to de-gas the cells. During this time the cartridge was loaded with the appropriate drugs for the Mito Stress Test assay. The assay is conducted in a sequential fashion so the drugs were loaded in the appropriate ports of the cartridge to achieve this order. The additions made were 1 µM oligomycin to inhibit ATP synthase at complex V of the electron transport chain (ETC), 0.8 µM carbonyl cyanide-p-trifluoromethoxyphenylhydrazone (FCCP) which uncouples oxygen consumption from ATP production and finally 2 µM each of rotenone and antimycin A to inhibit complexes I and III respectively. The drug stocks loaded in the cartridge were ten times more concentrated than the working concentration desired during the assay, as the stock is diluted 1:10 upon injection into the assay wells. Once loaded the cartridge was allowed to calibrate in the Seahorse XF24. After one hour of de-gassing the cell plate was loaded into the Seahorse XF24 positioned such that it was underneath the recording probes of the cartridge. The protocol employed consisted of five repetitions of a three minute mix, two minute wait, three minute measure cycle to achieve baseline measurements of OCR prior to the addition of the first drug injection. Three mix, wait, measure cycles were then performed prior to the next drug injection and this was followed by three mix, wait, measure cycles prior to the final drug injection, which was followed by a final three cycles of the mix, wait and measurement of OCR.

Upon completion of Seahorse XF24 assays, the assay media was removed by aspiration and 120 µl of 50 mM sodium hydroxide (NaOH) was added to each well to lyse the cells. The bases of the wells were scraped with a P200 pipette tip with the end cut to widen the diameter of the tip to avoid cell clogging. The lysate was transferred to an eppendorf tube and stored at -20°C for future protein concentration determination by the Bradford protein assay method previously described, to permit normalisation of ECAR and OCR measurements to µg protein content per well.

2.10 Co-Immunoprecipitation of SUR1 with Kir6.2 and EPAC2

Co-immunoprecipitation (Co-IP) was employed to investigate interaction between the K_{ATP} channel subunits SUR1 and Kir6.2 as well as with exchange protein activated by

cAMP 2 (EPAC2) in response to antecedent treatment with IL-6. Table 2.11 details the buffers used for this protocol.

Table 2.11: Buffers for Co-Immunoprecipitation

Buffer	**Components**
Lysis Buffer	PBS supplemented with 1% Triton X-100, 1:1000 protease inhibitor cocktail (Pierce), 0.1 mM PMSF, 1 mM Na_3VO_4 (heated at 95°C for five minutes prior to addition)
Wash Buffer	PBS supplemented with 0.1% Triton X-100, 1:1000 protease inhibitor cocktail (Pierce), 0.1 mM PMSF, 1 mM Na_3VO_4 (heated at 95°C for five minutes prior to addition)
2x SDS PAGE Sample Buffer	Diluted 1:1 from 4x stock detailed above, supplemented with 5% v/v 2-mercaptoethanol and 100 mM DTT

GT1-7 cells were plated in pre-PLL-coated 100 mm culture plates in GT1-7 plating media. Once they had reached 70-80% confluency they were treated with vehicle dH_2O (control) or 20 ng/ml IL-6 for three hours in 2.5 mM glucose serum-free DMEM at 37°C in a 5% CO_2 incubator. At the end of the treatment time the media was removed and a 37°C PBS rinse performed and cells were returned to GT1-7 plating media overnight and incubated at 37°C in a 5% CO_2 incubator.

The following day protein G sepharose beads (GE Healthcare) to be used for the Co-IP were washed prior to use. 40 µl of beads were used per IP and washed five times in 1 ml PBS, recovering the beads at the end of each wash by centrifugation at 17, 000 *x g* for 30 seconds. The primary antibody used for the IP was raised against SUR1 nucleotide binding domain 2 (SUR1 NBD2). The primary antibody was immobilised on the beads for 3 hours at room temperature by incubating 4 µg of SUR1 NBD2 primary antibody

per IP with the pre-washed beads at room temperature on a rotating wheel to mix. GT1-7 cells to be used were lysed by removing the media from the plates, performing a 4°C PBS rinse and adding 500 µl of lysis buffer. Plates were scraped thoroughly to harvest the cells and the lysates were transferred to eppendorf tubes and agitated on a rotating wheel at 4°C for 30 minutes. After the beads and primary antibody had been immobilising for three hours, the beads were recovered by centrifugation at 17,000 *x g* for 30 seconds. The supernatant was removed by aspiration and the beads were equilibrated in 1 ml of lysis buffer for 30 minutes on a rotating wheel at room temperature. After the cell lysates had agitated for 30 minutes they were centrifuged at 17,000 *x g* for five minutes at 4°C. The resulting supernatants were transferred to fresh eppendorf tubes and the pellets were resuspended in 1 ml of 2x SDS-PAGE sample buffer. This material was labelled as the insoluble fraction. 30 µl of the supernatant was retained and diluted 1:1 in 2x SDS PAGE sample buffer in a separate eppendorf and labelled as the starting material, to be able to demonstrate the presence of proteins of interest in the lysate prior to the Co-IP procedure. The beads were given a final 1 ml wash in lysis buffer and were recovered by centrifugation at 17,000 *x g* for 30 seconds prior to resuspension in 100 µl lysis buffer per Co-IP reaction. 100 µl of the beads:antibody mixture was added to the supernatant from the cell lysates and labelled as the Co-IP. The Co-IP reactions were incubated at 4°C overnight on a rotating wheel.

The following day the Co-IP reactions were centrifuged at 17,000 *x g* at 4°C. The supernatant was transferred to a fresh eppendorf tube, diluted 1:1 with 2x SDS PAGE sample buffer and labelled as the unbound fraction. This would allow determination of the amount of SUR1, Kir6.2 and EPAC2 protein not bound to the beads. The beads were washed five times in 1 ml of wash buffer at 4°C on a rotating wheel for ten minutes each time, apart from the first wash which was only one minute in duration. After each wash the beads were collected by centrifugation at 17,000 *x g* for one minute and the resulting supernatant was removed by aspiration and discarded. After the final wash the beads were resuspended in 50 µl of 2x SDS PAGE sample buffer and labelled as the Co-IP fraction. All the fractions from the experiment were heated at 37°C for ten minutes prior to storage at -20°C.

2.11 Protein Expression in Co-Immunoprecipitation Fractions Measured by Western Blot

Initially it is important to evaluate the amount of each protein of interest in all fractions from the Co-IP experiment to be able to determine where the majority of each protein is recovered. However, the main comparison between fractions should be between the starting material and the Co-IP fraction to be able to determine how much of the protein of interest associates with the beads:antibody complexes after the reaction compared to before. The fractions from the Co-IP experiments were subjected to Western blot protein expression analysis as previously described above and probed with primary antibodies raised against the proteins of interest.

2.12 ATP Assay

The ATPLite assay (PerkinElmer) was purchased to measure GT1-7 cell ATP levels. GT1-7 cells were cultured in T25 flasks in plating media at a confluency of approximately 70%. Media was removed and a PBS rinse performed prior to incubation of the cells in serum-free media supplemented with vehicle dH_2O control or 20 ng/ml IL-6 for three hours at 37°C in a 5% CO_2 incubator. After this time cells were returned to plating media for three hours to recover prior to trypsinisation and seeding at a density of 10,000 cells per well in a pre-PLL-coated black 96 well plate. Cells were incubated overnight at 37°C in a 5% CO_2 incubator. 18-24 hours after the exposure to control or IL-6, cells were subjected to three hours 2.5 mM glucose serum-free DMEM (euglycaemia) or 0.1 mM glucose serum-free DMEM (hypoglycaemia) prior to cell lysis and measurement of ATP according to the manufacturer's protocol.

2.13 cAMP Assay

GT1-7 cells were seeded in 60 mm dishes at a density of 350, 000 cells per dish in plating media the day prior to study. The following day media was removed and a PBS rinse performed prior to application of 3 ml of serum-free media supplemented with vehicle dH_2O control (1:250) or 20 ng/ml IL-6 for three hours and incubation at 37°C in a 5% CO_2 incubator. After this time, media was removed and a PBS rinse performed prior to cell lysis in 350 µl of 0.1 M HCl. Lysates were centrifuged at 1000 *x g* and stored at -20°C. Lysates were assayed subsequently using the Direct cAMP ELISA kit (Enzo) using the acetylated format of the assay to enhance sensitivity. Measured cAMP

values were normalised to the protein concentration of the cell lysates as determined by Bradford assay.

2.14 Data Analysis

A number of parametric and non-parametric statistical analyses were performed depending on the data sets being analysed and whether they passed a D'Agostino-Pearson omnibus normality test. Parametric statistical tests included unpaired student's t-test and one-way analysis of variance (ANOVA) with Tukey's or Dunnett's multiple comparisons test. Non-parametric statistical tests included Mann-Whitney test, Kruskal-Wallis test, Friedman test and one sample t-test. Data are presented as mean ± standard error of the mean (SEM). Statistical significance was accepted at the 95% confidence interval with a *p* value of less than 0.05. Significance was allocated to the following *p* values: * = <0.05; ** = <0.01 and *** = <0.001.

Table 2.12: Commonly Used Chemicals and Reagents

Supplier	**Chemical/Reagent**
Sigma-Aldrich	D5671 DMEM, Interleukin-6 from mouse, poly-L-lysine (PLL), sodium fluoride (NaF), ethylenediaminetetraacetic acid (EDTA), ethylene glycol tetraacetic acid (EGTA), 2-mercaptoethanol, benzamidine, sodium orthovanadate (Na_3VO_4), phenylmethylsulphonyl fluoride (PMSF), Bradford reagent, bovine serum albumin (BSA), glycerol, bromophenol blue, Tris, Ponceau S solution, MISSION® Transduction Particles, MISSION® Non-Mammalian shRNA Control Transduction Particles, amphotericin B, tolbutamide, Polybrene, WP1066, tween

Seahorse Bioscience	XF24 DMEM,
Fisher	D-glucose, sodium chloride (NaCl), methanol, isopropanol, ethanol, chloroform
Harvard Apparatus	GC120F-10 Borosilicate glass capillary tubing
Marvel	Non-fat dried milk
Gibco	D11966 DMEM, L-glutamine, penicillin-streptomycin, 0.05% typsin-EDTA,
Ambion	DNase free H_2O
Tocris	HJC 0350
Invitrogen	SeeBlue® Plus2 molecular weight marker, SuperScript™ II Reverse Transcriptase (RT), 3 µg/ml random primers, dNTPs, 5x First Strand Buffer, 0.1 M DTT
VWR	Sodium dodecyl sulphate (SDS), 18 x 18 mm glass coverslips
Applied Biosystems	96 well plates, 2x Universal PCR Master Mix
PAA	Fetal Bovine Serum
National Diagnostics	30% Acrylamide, 1x Running Buffer
PALL	Nitrocellulose membrane
Hyclone	Fetal Bovine Serum
Falcon	35 mm culture dishes

Merck Millipore	Triton X 100, PVDF membrane, 0.22 µm filters
ThermoScientific	T75 culture flasks, T25 culture flasks, 60 mm culture dishes, 96 well plates, cryotubes, 12 well plates, 6 well plates, syringes
Novo Nordisk	NN414
Melford	Glycine

Table 2.13: List of Antibody Sources and Dilutions

Antibody	**Supplier**	**Species**	**Dilution factor**
Actin	Sigma-Aldrich	Rabbit	1:10,000
Phospho AMPK (T172)	Cell Signaling Technology	Rabbit	1:1000
Phospho p42/44 MAPK (T202/Y204)	Cell Signaling Technology	Rabbit	1:1000
Phospho PKB (S473)	Cell Signaling Technology	Rabbit	1:1000
Phospho STAT3 (Y705)	Cell Signaling Technology	Rabbit	1:1000
HSP60	Cell Signaling Technology	Rabbit	1:1000
PKM2	Cell Signaling Technology	Rabbit	1:1000
Phospho STAT3	Cell Signaling	Mouse	1:1000

(S727)	Technology		
PHB1	Cell Signaling Technology	Rabbit	1:1000
EPAC1	Cell Signaling Technology	Mouse	1:1000
EPAC2	Cell Signaling Technology	Mouse	1:1000
PDH	Cell Signaling Technology	Rabbit	1:1000
SUR1 NBD2	In House	Sheep	1:1000
NCX	Swant	Mouse	1:1000
COX IV	Cell Signaling Technology	Rabbit	1:1000
Kir6.2	In House	Sheep	1:1000
HK1	Cell Signaling Technology	Rabbit	1:1000
Phospho CREB (S133)	Cell Signaling Technology	Rabbit	1:1000
IRDye 800 anti-rabbit secondary	Rockland	Goat	1:10,000
Alexa Fluor 680 anti-mouse secondary	Life Technologies	Goat	1:10,000
Alexa Fluor 680 anti-sheep secondary	Life Technologies	Donkey	1:10,000

3 The Effects of IL-6 on Glucose Sensing in GT1-7 Cells

3.1 Introduction

As previously described, studies have demonstrated the importance of the CNS in the regulation of the CRR to hypoglycaemia (Borg et al. 1997; Borg et al. 1995; Borg et al. 1994). Glucose alters the firing rate of neurons in the VMH, which ultimately instigate an appropriate CRR (Chan & Sherwin 2013). Antecedent hypoglycaemia and diabetic disease can lead to brain adaptations that impair CRRs (Chan & Sherwin 2013). The mechanisms underlying these impairments are likely complex and their study and interpretation is complicated as VMH glucose-sensing neurons not only contain their own mechanisms for detecting hypoglycaemia but also receive multiple inputs from the periphery and other brain regions (Chan & Sherwin 2013). The advantage of the current studies is the investigation of glucose sensing in an isolated population of homogenous GE neurons, independent from glial cell and other neuronal influences. Importantly, studies have found that neuronal and glial cells have distinct responses to IL-6 stimulation (Brown et al. 2014), so it is advantageous to study these cells types in isolation when investigating molecular mechanisms in a specific population of cells.

Due to the abundance of literature documenting diverse and often conflicting effects of IL-6 on signalling pathways and physiological and pathophysiological responses in peripheral tissues such as skeletal muscle, liver and adipose, the current work and literature cited focuses for the most part solely on IL-6 action in brain and the CNS.

Importantly, IL-6 and IL-6R mRNA have been found in neurons of the VMH (Schöbitz et al. 1993). IL-6 is produced within the CNS by astrocytes and microglia (Frei et al. 1989; Nelson et al. 2002), with documented roles as a neuroprotective and neurotrophic factor (Wang et al. 2015; O. Islam et al. 2009). Under normal conditions the production of IL-6 in the CNS is highly regulated, but chronic dysregulation of IL-6 expression during inflammation and infection is thought to contribute to the pathogenesis of several neurological disorders (Nelson et al. 2002). IL-6 has been shown to be closely aligned with resistance to primary herpes virus type 1 (HSV-1) infection (Chucair-Elliott et al. 2014), accelerates nerve regeneration following trauma (Hirota et al. 1996), is neuroprotective following cerebral ischaemia or spinal cord injury (Loddick et al. 1998;

Yang et al. 2012) and promotes neuronal survival, axon outgrowth and neuronal differentiation *in vitro* (Chucair-Elliott et al. 2014; Hama et al. 1991). Neutralisation of IL-6 resulted in a loss of neuroblasts and neuronal cells undergoing differentiation in HSV-1 infected microglial and neural precursor cell (NPC) co-cultures, identifying IL-6 as a critical cytokine in preserving the neuronal differentiation cascade of NPCs (Chucair-Elliott et al. 2014).

Some studies have documented the effects of IL-6 on neuronal activity measured during electrophysiological analysis. In thalamic relay neurons, IL-6 was found to reduce the membrane resistance of these cells at the resting membrane potential, potentially by increasing K^+ leak, and also decrease the number of action potentials in the low calcium threshold spike bursts, a characteristic electrophysiological signature of thalamic relay cells, after 25 minutes exposure to IL-6 (Samios & Inoue 2014).

Fever induction caused by IL-6 is one of the best characterised central effects of the cytokine (Kluger 1991; Schöbitz et al. 1993). In the early 1960s, hypothalamic neurons sensitive to small, local temperature changes were found in anesthetised cats and dogs (Hardy et al. 1964; Nakayama et al. 1961). The neurons were further characterised as being warm-sensitive neurons which increased their firing rates with higher temperature, and cold-sensitive neurons which increased their firing rates in cooler than normal temperatures. In the medial preoptic area of the hypothalamus the proportions of warm-sensitive, cold-sensitive and thermally insensitive neurons were 30%, 10% and 60% respectively (Shibata 1990; Silva & Boulant 1986). These neurons were also responsive to peripheral thermal stimulation as well as central. These data taken together are remarkably reminiscent of glucose-sensing neurons in the hypothalamus, which have similarly been demonstrated to be either GE, GI or non-glucose sensing (Routh 2010). Xin and Blatteis demonstrated that the activities of hypothalamic neurons in slice preparations from guinea pig brains are selectively affected by human recombinant IL-6 (hrIL-6), with hrIL-6 depressing the majority of warm-sensitive neurons and exciting all cold-sensitive neurons recorded from (Xin & Blatteis 1992). Studies of chronic IL-6 exposure in rat Purkinje cerebellar neurons, using concentrations based on those seen in CSF during a variety of neurological disorders, induced changes in evoked action potential generation, membrane biophysical properties, resting Ca^{2+} levels and the membrane and Ca^{2+} signalling responses to glutamate receptor agonists (Nelson et al. 2002).

Gnv4 cells, a GnRH-expressing adult rat hypothalamic cell line, express both IL-6 and IL-6R mRNA (Igaz et al. 2006). In *in vitro* studies, the IL-6 family cytokine oncostatin M (OSM) was found to inhibit the NMDA-induced increase in GnRH gene expression in Gnv4 cells and primary rat hypothalamic neuronal cultures, suggesting that cytokines have the ability to modulate GnRH expression (Igaz et al. 2006). In GN11 cells, obtained by targeted tumourigenesis of mouse GnRH neurons, leukemia inhibitory factor (LIF) was found to promote the chemomigration of these immature neurons through independent activation of JAK/STAT3, MAPK/ERK1/2 and PI3K/PKB signalling pathways (Magni et al. 2007). Taken together, these data suggest that IL-6 may also regulate GnRH expression and release in GT1-7 cells, potentially via regulation of membrane potential.

The aims of the following studies were therefore to determine whether IL-6, elevated in response to hypoglycaemia, exerts effects on GE neurons under euglycaemic and hypoglycaemic conditions, by examining the biochemical and electrophysiological responses of GT1-7 cells upon exposure to IL-6.

3.2 Results

3.2.1 IL-6 Signalling in GT1-7 Cells

Initial experiments in the current work focused on confirming whether the cytokine interleukin-6 (IL-6) could exert biological effects on GT1-7 cells, indicated by stimulation of intracellular signalling pathways known to be regulated by IL-6. IL-6 is known to activate the PI3K, MAPK cascade and JAK/STAT cascade of signalling pathways (Eulenfeld et al. 2012). The observation that cytokines can rapidly affect neurotransmitter release and synaptic plasticity when applied *in vitro* suggests that these effects are presumably mediated through the activation of protein phosphorylation processes (Arcangelo et al. 2000).

Although Dozio *et al.* demonstrated expression of gp130 in GT1-7 cells and an increase in the phosphorylation of STAT3 in response to ciliary neurotrophic factor (CNTF) treatment (Dozio et al. 2005), whether IL-6 increases STAT3 phosphorylation in these cells has not been studied. Encouragingly, IL-6 has been shown to stimulate GnRH release from rat primary hypothalamic neuronal cultures, suggesting IL-6 can induce biological effects at least in this model (Yamaguchi et al. 1991). In the current work a

dose of 20 ng/ml IL-6 over a time course exposure of five, 30 and 180 minutes caused significant increases in STAT3 Y705 phosphorylation at all three time points compared to vehicle treated cells (Figure 3.1A; p=<0.05 at each time point).

The literature concerning the effects of cytokines on ERK1/2 in neurons of the hypothalamus is much less profound, however the effects of IL-6 on the regulation of ERK in other brain regions has been studied. Restraint stress in rats increased pERK in IL-6 positive neurons of the hypothalamus (Jankord et al. 2010). The Benfenati lab observed a suppression of both MAPK and ERK1/2 phosphorylation in response to IL-6 treatment in rat hippocampal slices (Tancredi et al. 2000). In contrast, Chang SH *et al.* found that OSM, an IL-6 family cytokine, induces expression of myeloid cell leukemia-1 (Mcl-1) via activation of ERK1/2 (Chang et al. 2015) in cortical neurons. In rat cerebellar granule neurons, IL-6 exposure for eight days induced phosphorylation of ERK1/2 (Fang et al. 2013). In the current study, there was no significant effect of 20 ng/ml IL-6 exposure for five-180 minutes on the phosphorylation of ERK1/2 at residues threonine 202 (T202) and tyrosine 204 (Y204) in GT1-7 cells (Figure 3.1B).

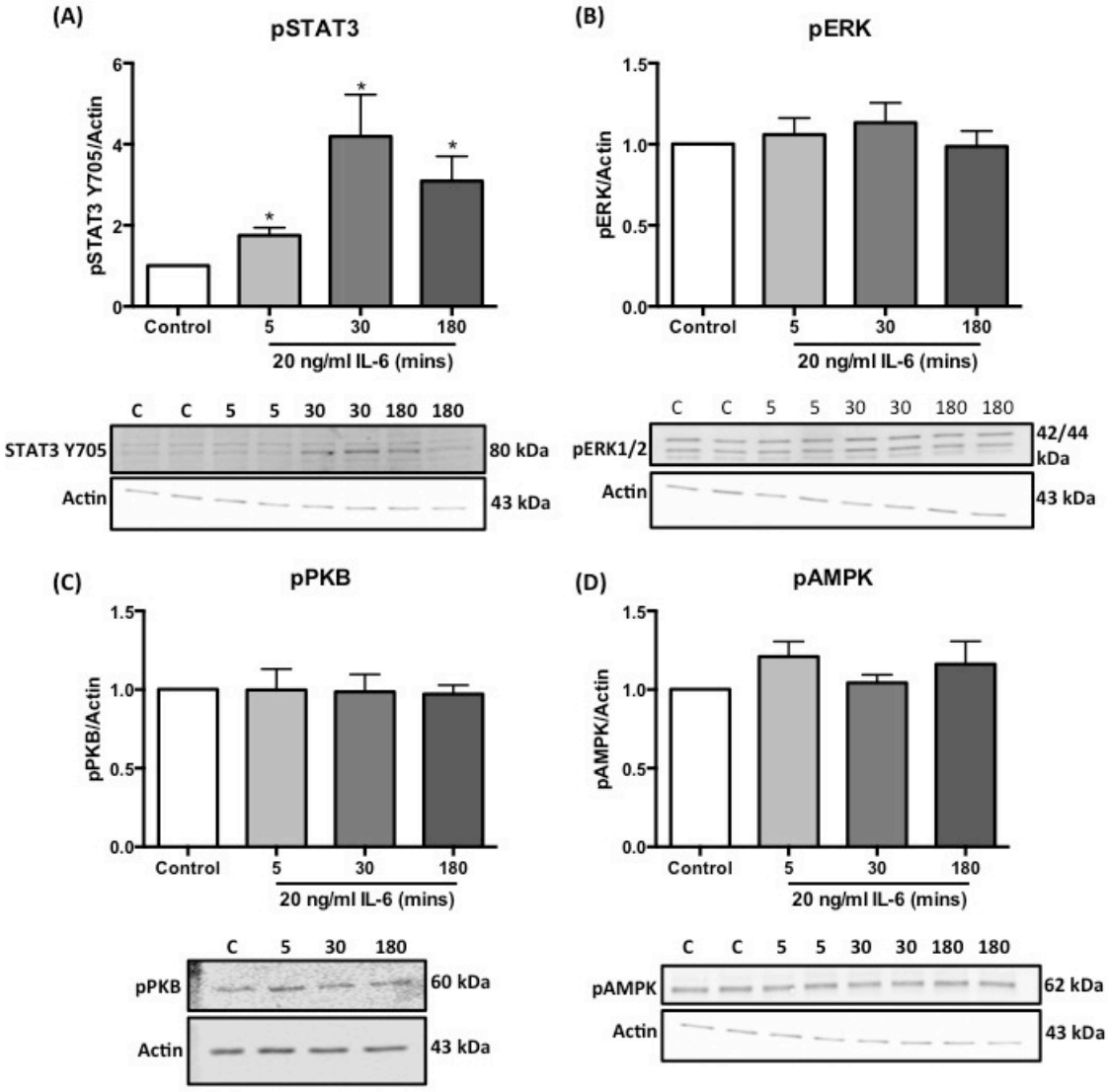

Figure 3.1 Effects of interleukin-6 (IL-6) on intracellular signalling pathways in GT1-7 cells

GT1-7 cells were serum starved for two hours in the presence of 2.5 mM glucose prior to exposure to vehicle dH_2O (Control, C) for three hours or 20 ng/ml IL-6 for the indicated times. Cells were lysed and samples prepared for Western blot analysis of protein expression of pSTAT3 Y705 **(A)**, pERK T202/Y204 **(B)**, pPKB S473 **(C)** or pAMPK T172 **(D)** (n=4-6). Fold change in phosphorylation of each protein was determined relative to Control treated cells normalised to actin and representative blots are shown. Statistical significance was determined by one sample t-test where * indicates significantly different from control (p=<0.05).

Relatively little is known about the effects of cytokine exposure on the regulation of central AMPK in either neurons or non-neuronal cell types such as astrocytes and microglia. In contrast, a wealth of literature documents effects of IL-6 on the regulation of AMPK in multiple tissues, particularly skeletal muscle, liver and adipose. Kelly *et al.* demonstrated convincingly that incubation of skeletal muscle with IL-6 caused an increase in the phosphorylation of AMPK at site T172 and an increase in activity of α2-containing AMPK (Kelly et al. 2009). The same group also demonstrated the *in vivo* importance of IL-6 in the activation of AMPK (Kelly et al. 2004). Increased AMPK T172 phosphorylation in response to IL-6 has also been observed in cultured mouse epididymal adipose tissue (Wan et al. 2012). Replacement of recombinant IL-6 protein in IL-$6^{-/-}$ mice fed a high fat diet leads to increased liver pAMPK levels compared to high fat diet control IL-$6^{-/-}$ animals, suggesting that IL-6 increases pAMPK in the liver as well (Vida et al. 2015). In contrast however, excess nutrient stress has been shown to suppress AMPK phosphorylation in the heart (Ko et al. 2009). In this study the authors acutely administered IL-6 to mimic the increased circulating levels of the cytokine observed in animals fed a high fat diet (HFD), and they observed a reduction of pAMPK levels in the heart compared to saline injected control mice. The discrepancy between the effect of IL-6 in most peripheral tissues and the heart may be due to the dose and length of exposure to IL-6, as well as tissue specific effects of the cytokine. In the current work, there was a subtle trend of 20 ng/ml IL-6 exposure for five and 180 minutes towards increasing pAMPK T172 levels compared to vehicle treated GT1-7 cells, however this did not reach statistical significance (Figure 3.1D; 5 minutes: p=0.12; 30 minutes: p=0.47; 180 minutes: p=0.35).

In a 2010 study in GT1-7 cells, Choi *et al.* observed that insulin stimulation induced the phosphorylation of PKB (also called Akt). Fang *et al.* observed increases in pPKB after eight days IL-6 exposure in rat cerebellar granule neurons (Fang 2013). In the current experiments, 20 ng/ml IL-6 exposure in GT1-7 cells for five, 30 or 180 minutes failed to affect the phosphorylation of PKB at serine 473 (S473) (Figure 3.1C).

Taken together, these data show that IL-6 increases the phosphorylation of STAT3 in GT1-7 cells with no effect on ERK1/2 or PKB phosphorylation. IL-6 was not shown to have a major effect on AMPK as there was no significant effect of IL-6 to increase pAMPK at T172. The clearly observed increase in pSTAT3 in response to IL-6 demonstrates activation of the JAK/STAT cascade suggesting that IL-6 is able to transduce a signal via the ubiquitously expressed gp130 glycoprotein and either the

membrane bound or soluble form of the IL-6 receptor. These data suggest that in GT1-7 cells IL-6 does not activate the ERK1/2 and PI3K signalling cascades as has previously been documented in other cell types (Eulenfeld et al. 2012).

3.2.2 Effects of IL-6 on GT1-7 Membrane Potential Under Euglycaemic Conditions

Several cytokines including IL-1, TNF and IFN have been demonstrated to elicit pyrogenic effects in the context of fever potentially by affecting the activity of hypothalamic thermosensitive neurons. The fact that cytokines have been demonstrated to regulate thermal sensitive neurons led to the hypothesis that IL-6 may also acutely regulate glucose-sensing neurons of the hypothalamus. Intriguingly, thermosensitive neurons were also demonstrated to be sensitive to glucose fluctuations permitting speculation that the previously demonstrated effects of cytokines on thermosensitive neurons may also be applicable to glucose-sensing neurons. To address whether this was the case, GT1-7 cells were subjected to perforated patch current clamp recordings to allow monitoring of the cell membrane potential during acute perfusion of IL-6. Exposure of GT1-7 cells to IL-6 in this way had no effect on membrane potential, which remained at a constant value throughout the experiment (Figure 3.2). In 2.5 mM glucose the mean resting membrane potential of the cells was -44.4 +- 3.9 mV and after IL-6 perfusion mean membrane potential was -46.6 +- 4.8 mV. Analysis of the pooled data from five individual recordings demonstrated that there was no effect of IL-6 on either depolarisation or hyperpolarisation of the cell membrane under euglycaemic conditions (Figure 3.2B). To confirm that the cells had K_{ATP} channels and membrane potential was sensitive to alterations in K_{ATP} activity, the K_{ATP} channel opener NN414 was delivered extracellularly at a dose of 5 μM to one of the cells, causing hyperpolarisation of the cell membrane to -65 mV and cessation of action potential firing (Figure 3.2).

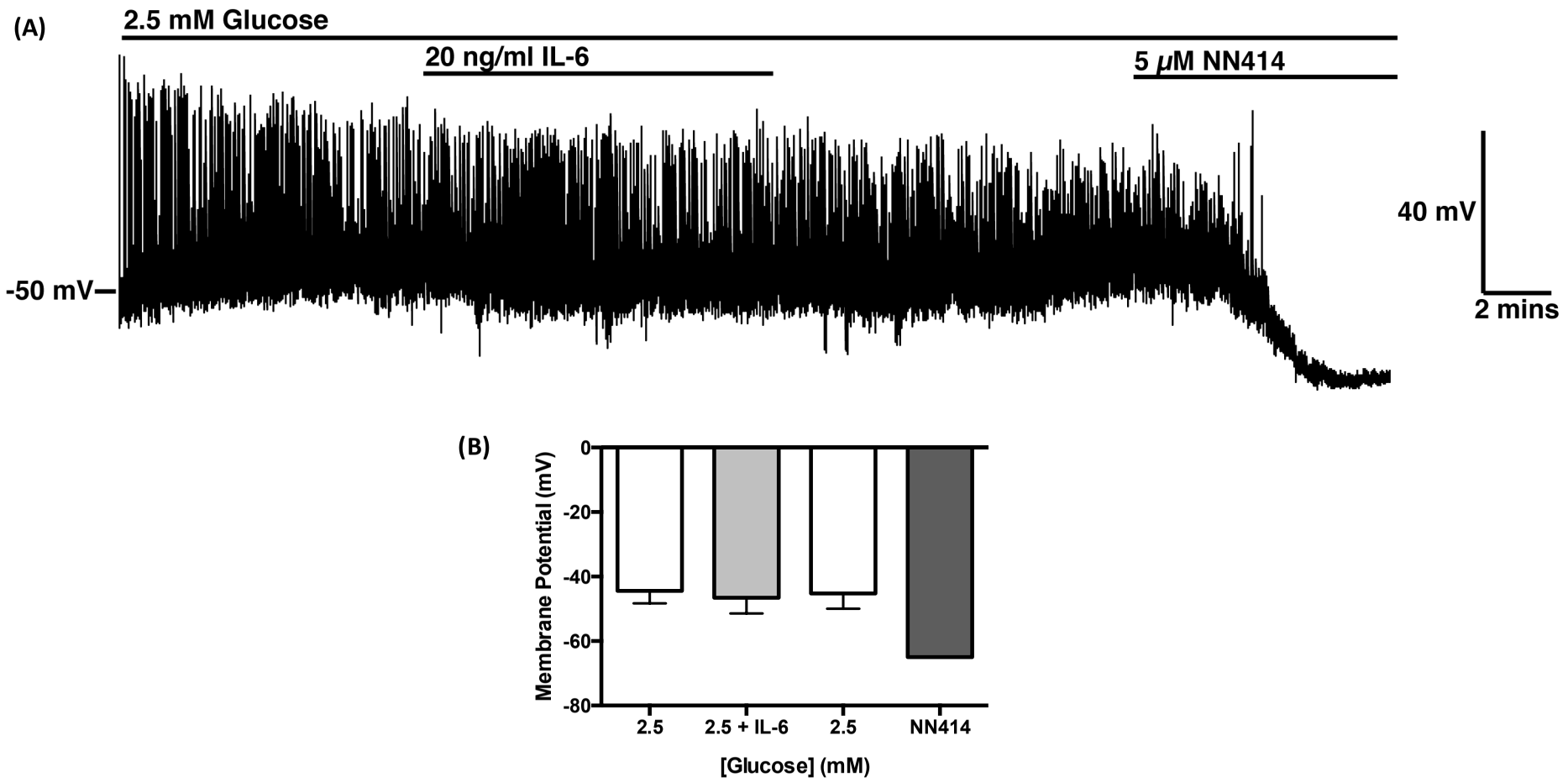

Figure 3.2 Effect of acute 20 ng/ml IL-6 exposure on GT1-7 cell membrane potential

(A) Representative perforated patch current clamp recording from a GT1-7 cell acutely exposed to 20 ng/ml IL-6 in 2.5 mM glucose physiological saline solution. The cell was also exposed to a dose of 5 μM NN414 to pharmacologically open K_{ATP} channels and induce membrane hyperpolarisation. **(B)** Bar chart demonstrating the pooled membrane potential data for n=5 cells. Data was analysed by Friedman test with Dunn's multiple comparisons test.

3.2.3 IL-6 does not Regulate GT1-7 Cell Membrane Potential Under Acute Hypoglycaemic Conditions

Although there was no effect of IL-6 on GT1-7 cell membrane potential under euglycaemic conditions I also sought to determine whether there might be an effect of IL-6 during acute hypoglycaemia to either potentiate or attenuate membrane potential hyperpolarisation in low glucose. GT1-7 cells were subjected to perforated patch clamp electrophysiology and current clamp recordings were made in order to assess membrane potential. 0.5 mM glucose physiological saline solution was perfused to induce membrane hyperpolarisation and after achievement of a stable membrane potential 20 ng/ml IL-6 was perfused in 0.5 mM glucose saline. The effect of the IL-6 addition on membrane potential was monitored for at least ten minutes prior to washout with 2.5 mM glucose saline. In the current experiments, a small but non-significant effect of IL-6 perfusion on membrane potential during acute hypoglycaemic conditions was observed (Figure 3.3). Resting membrane potential in 2.5 mM glucose averaged -51.3 +- 0.7 mV, with membrane hyperpolarisation observed to -66.3 +- 3.9 mV in 0.5 mM glucose. Addition of 20 ng/ml IL-6 in this setting resulted in further membrane hyperpolarisation to -71.7 +- 6.0 mV on average (p=0.75 vs 0.5 mM glucose).

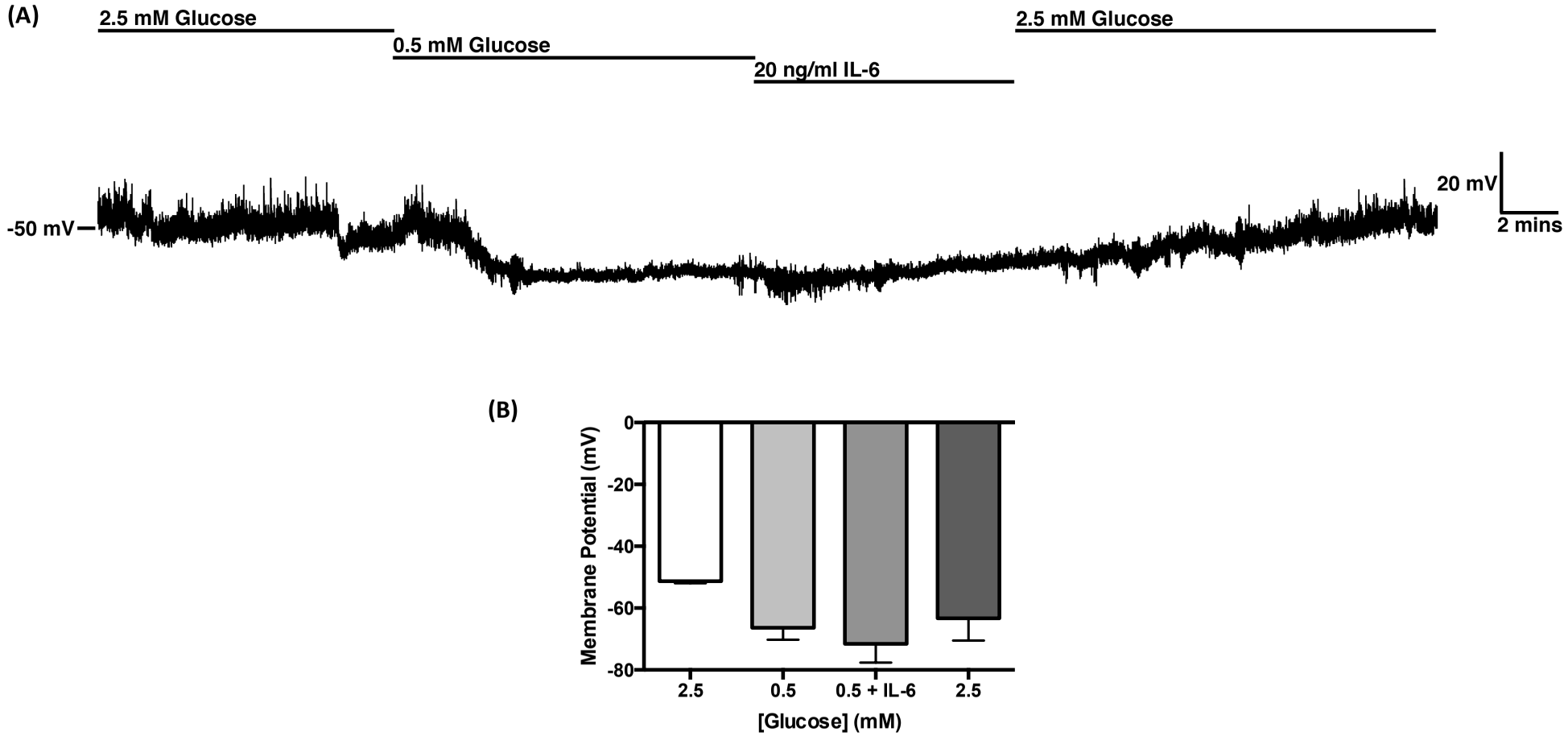

Figure 3.3 Effects of 20 ng/ml IL-6 on GT1-7 cell membrane potential during an acute 0.5 mM glucose hypoglycaemic challenge

(A) Representaative perforated patch current clamp recording from a GT1-7 cell exposed to 0.5 mM glucose followed by 20 ng/ml IL-6 during 0.5 mM glucose. Representative cell is not firing action potentials but membrane does hyperpolarise in response to 0.5 mM glucose. **(B)** Pooled data from three separate experiments. Data was analysed by Friedman test with Dunn's multiple comparisons test.

3.2.4 IL-6 is Secreted from Primary Mouse Astrocytes in the Recovery Period Following Hypoglycaemia

Although it is clear that GT1-7 cells respond to IL-6 through classical signalling cascades, whether there is a CNS source of IL-6 and/or whether peripheral IL-6 circulating in the blood stream can cross the BBB and enter the brain and the extent of its action when it gets there remains controversial. William A Banks demonstrated the appearance of radio labelled IL-6 in mouse brain tissue following peripheral injection confirming that IL-6 can cross the BBB at least in mice (Banks et al. 1994). However, in those studies only 16% of the radioactivity recovered eluted as intact IL-6. Importantly, other studies have demonstrated the capacity for a central source of IL-6 through its release from brain cell types. The immortalised mouse microglial BV2 cell line has been demonstrated to secrete IL-6 in response to glucose deprivation (S. J. Choi et al. 2013). To determine whether a local source of IL-6 is present in the brain and the relationship of IL-6 release to hypoglycaemia, primary astrocyte cultures were prepared from mouse cortex and subjected to euglycaemia control (2.5 mM glucose) or hypoglycaemia (0.1 mM glucose) for three hours. Supernatants from the cultures were harvested immediately at the end of the three hour treatment or after four hours recovery in euglycaemic conditions in order to measure IL-6 secretion at these two time points. Interestingly, IL-6 release from primary astrocytes was undetectable after three hour treatments of either euglycaemia or hypoglycaemia. However, after a four hour euglycaemic recovery period post treatments, IL-6 secretion was increased from both euglycaemic and hypoglycaemic astrocyte cultures, with a significantly greater IL-6 secretion observed from hypoglycaemia-exposed astrocytes compared to euglycaemia-exposed controls (p=<0.05, n=4). These data demonstrate that IL-6 secretion from mouse astrocytes is significantly increased during the euglycaemic recovery period following a hypoglycaemic challenge. *In vivo*, this would lead to an increase in CNS IL-6 levels following hypoglycaemia.

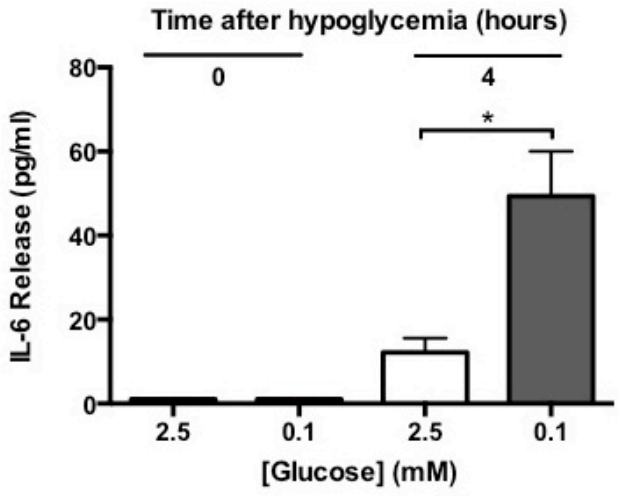

Figure 3.4 Interleukin-6 is released from mouse cortical astrocytes in the recovery period following hypoglycaemia

Mouse cortical astrocyte cultures were subjected to euglycaemia (2.5 mM glucose) or hypoglycaemia (0.1 mM glucose) for three hours in serum-free DMEM which was harvested immediately at the end of the treatment time (0 hours). Fresh euglycaemic 2.5 mM glucose serum-free DMEM was applied to the astrocyte cultures and this was harvested four hours subsequently (4 hours). The amount of IL-6 in the harvested supernatants was measured by ELISA (n=4). Hypoglycaemia for three hours resulted in significantly more IL-6 secretion in the euglycaemic recovery period following treatment than that observed from euglycaemia treated astrocyte cultures (compare 2.5 mM to 0.1 mM at four hours post treatment). Statistical significance was analysed by Mann-Whitney test where * indicates significantly different (p=<0.05). Data generated in collaboration with Kathryn Wright.

3.2.5 Antecedent IL-6 Causes Defective Glucose Sensing of Subsequent Hypoglycaemia in GT1-7 Cells

Taking together the observations that IL-6 had no major effect on GT1-7 cell membrane potential when applied acutely and that IL-6 is secreted from astrocytes in the euglycaemic recovery period following hypoglycaemia, it was hypothesised that IL-6 might exert delayed effects on GT1-7 cells. To test this hypothesis an antecedent exposure for three hours to either vehicle dH_2O (Control) or 20 ng/ml IL-6 was performed prior to a subsequent hypoglycaemic challenge in GT1-7 cells 18-24 hours later. This models whether elevated IL-6 levels, released following hypoglycaemia, effects responses of glucose-sensing neurons to subsequent hypoglycaemia. During perforated patch clamp electrophysiological analysis, vehicle treated control cells exhibited a resting membrane potential in 2.5 mM glucose of -52 +- 1 mV. These cells demonstrated a robust, significant hyperpolarisation by -10.2 +- 2.9 mV on average to a membrane potential of -65.3 +- 3.3 mV, and a silencing of neuronal firing rate in response to 0.5 mM glucose exposure. This was reversible upon reapplication of 2.5 mM glucose, with cells depolarising by 12.3 +- 5.2 mV on average to a membrane potential of -52.5 +- 3.3 mV (Figure 3.5A and C). Antecedent 20 ng/ml IL-6 treated cells had a similar resting membrane potential in 2.5 mM glucose of -51.1 +- 1.7 mV as vehicle treated control cells. However, in contrast to controls, 20 ng/ml IL-6 treated cells only hyperpolarised by 3.0 +- 1.3 mV on average and maintained firing rates during the 0.5 mM glucose exposure (Figure 3.5B and C). In 0.5 mM glucose, 20 ng/ml IL-6 treated cells only hyperpolarised to -54.4 +- 2.3 mV, and they depolarised by 3.6 +-1.8 mV on average to -50.8 +- 3.6 mV upon reapplication of 2.5 mM glucose. Antecedent IL-6 treatment resulted in a significant suppression of cell membrane hyperpolarisation in response to subsequent hypoglycaemia compared with vehicle treated control cells (Figure 3.5C). This data can also be represented as percentage reduction in the hyperpolarising response to 0.5 mM glucose in IL-6 treated cells compared to vehicle treated cells. This is quantified as a 70% reduction in hyperpolarisation by antecedent IL-6 treatment (data not shown). In summary, an antecedent exposure to IL-6 in GT1-7 cells causes a reduction in their ability to detect and respond appropriately to a 0.5 mM glucose hypoglycaemic challenge the following day (18 to 24 hours subsequently).

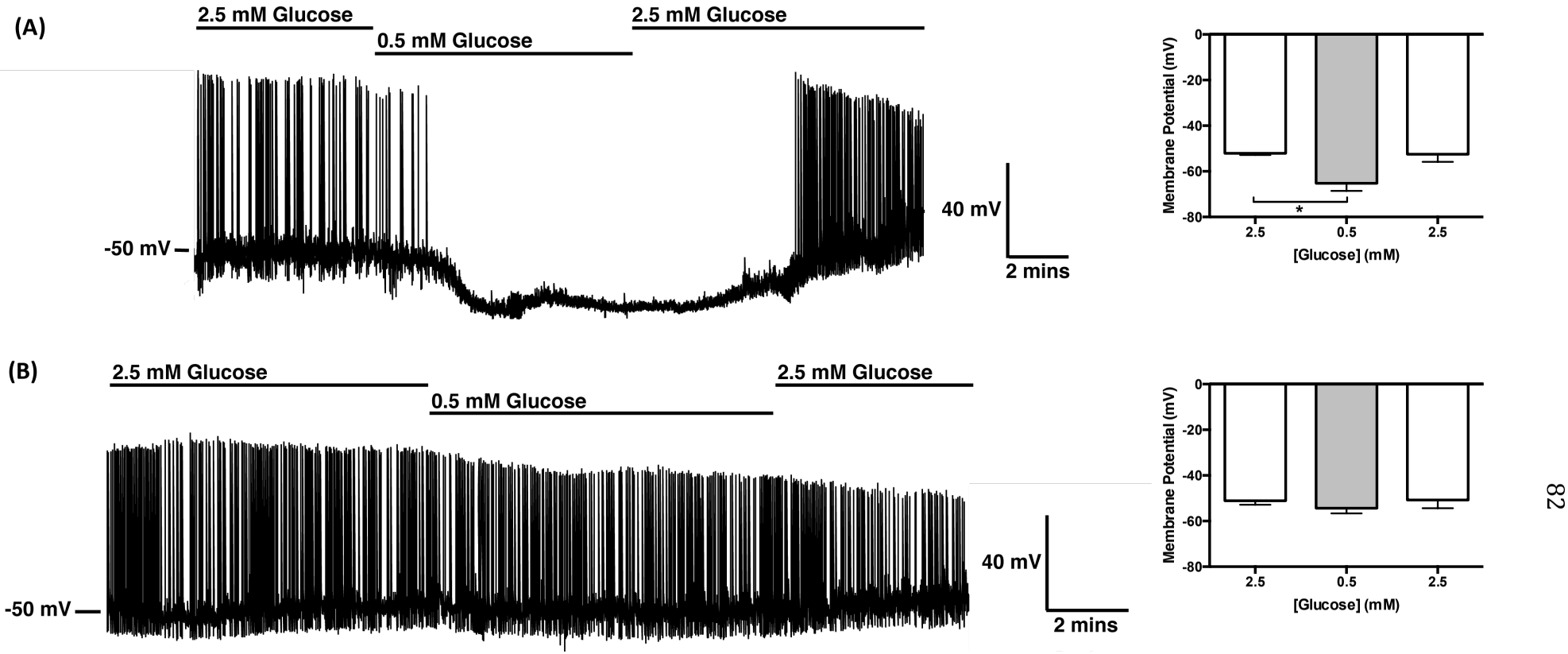

Figure 3.5 Antecedent 20 ng/ml IL-6 treatment induces defective glucose sensing of subsequent hypoglycaemia in GT1-7 cells

GT1-7 cells were exposed to either vehicle control (dH_2O) or 20 ng/ml IL-6 for three hours on day one and their electrical response to a 0.5 mM glucose hypoglycaemic challenge was assessed the following day. **(A)** Representative perforated patch current clamp recording of a vehicle treated GT1-7 cell and pooled data from n=9 cells. **(B)** Representative perforated patch current clamp recording of a 20 ng/ml IL-6 treated GT1-7 cell and pooled data from n=10 cells. **(C)** Quantification of the hyperpolarising response to 0.5 mM in control vs IL-6 treated cells. Statistical significance was analysed by one-way ANOVA in panels **(A)** and **(B)** and student's unpaired t-test in **(C)** where * indicates significantly different from 2.5 mM glucose and Control respectively (P=<0.05).

3.2.6 Antecedent IL-6 Does Not Affect K_{ATP} Channel Conductance Density in GT1-7 Cells

The effect of antecedent IL-6 treatment to impair subsequent membrane hyperpolarisation in response to a hypoglycaemic challenge may be mediated by a reduction in the ability of the K_{ATP} channel to open. When K_{ATP} channels are opened either by physiological or pharmacological manipulation an increase in macroscopic currents can be measured in the whole-cell patch clamp configuration. This technique was exploited to examine whether antecedent IL-6 treatment affected the ability of K_{ATP} channels to conduct current 18 to 24 hours later. GT1-7 cells were exposed to dH_2O vehicle (Control) or 20 ng/ml IL-6 (IL-6) for three hours on day one and the following day were subjected to electrophysiological examination in the whole-cell patch clamp configuration. A voltage clamp protocol (see methods) was employed to assess K_{ATP} channel currents under control conditions and after the cell had been dialysed with 0 ATP. Over time (usually five to 15 minutes), the presence of 0 ATP in the patch pipette will cause intracellular ATP to dialyse out of the cell relieving ATP inhibition of K_{ATP} channels. This will lead to an increase in outward currents through K_{ATP} channels that can be observed using the voltage clamp protocol. By plotting the current-voltage relationships observed the conductance density for each cell can be extrapolated and normalised to cell size. The data can then be pooled together to compare conductance density between two different treatment groups. In the current work control and IL-6 treated GT1-7 cells had comparable macroscopic currents measured at both baseline and after dialysis with 0 ATP (Figure 3.6Aii and Bii). Accordingly, there was no difference in the profile of whole-cell current clamp recordings made during dialysis with 0 ATP (Figure 3.6Ai and Bi). There was no significant difference in the conductance densities for control versus antecedent IL-6 treated cells (1.11 +- 0.16 vs 1.00 +- 0.17 pS/pF respectively), indicating that a lack of functional K_{ATP} channels in the cell membrane is not responsible for mediating defective glucose sensing induced by antecedent IL-6 treatment (Figure 3.6C). This data therefore implies that antecedent IL-6 treatment does not affect the number of available or functional K_{ATP} channels at the cell membrane 18-24 hours subsequently.

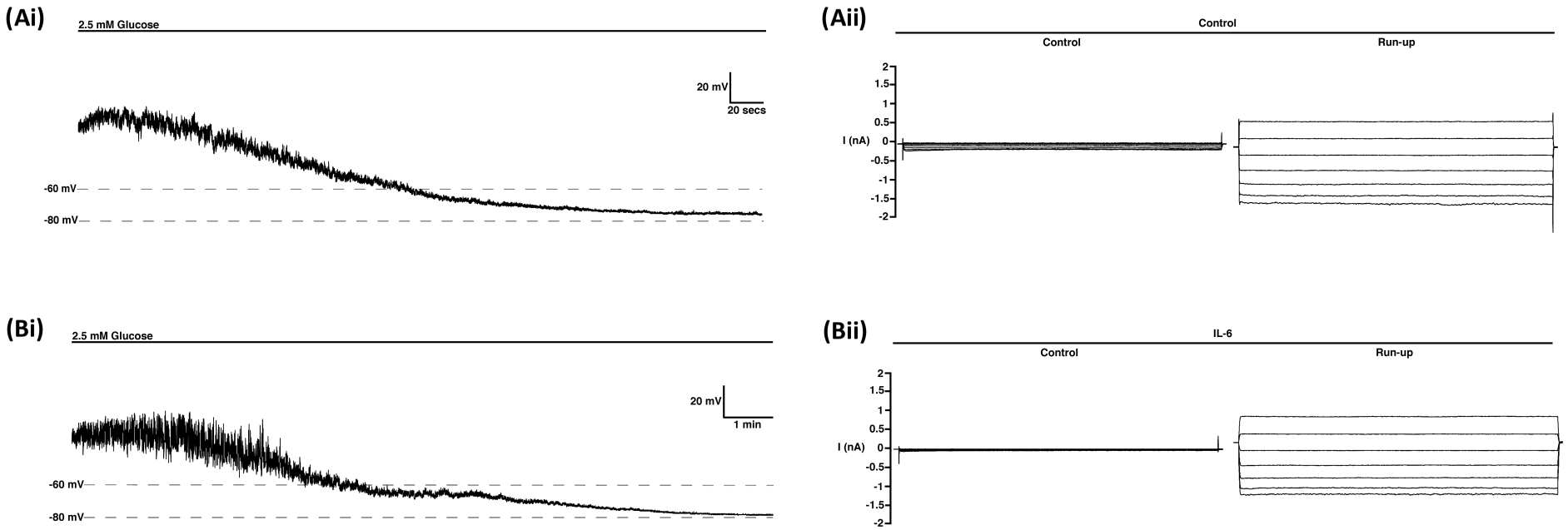

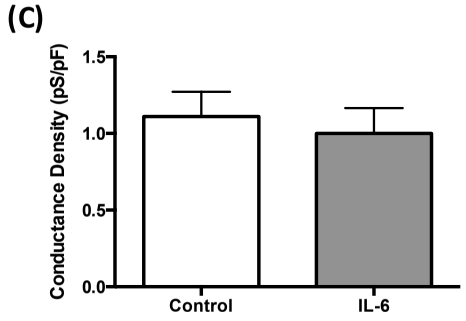

Figure 3.6 Antecedent IL-6 exposure does not alter K_{ATP} channel conductance in response to dialysis of cell with 0 ATP

(Ai) Representative whole-cell current clamp recording of an antecedent vehicle (dH_2O) treated GT1-7 cell as it is dialysed with 0 ATP in the presence of 2.5 mM glucose the day following treatment. **(Aii)** Corresponding families of currents evoked by the voltage-clamp protocol described in methods. Whole-cell macroscopic currents were examined immediately after the cell membrane was ruptured (Control) and after the cell had been dialysed with 0 ATP and reached a steady state (Run-up; n=6). **(Bi)** Representative whole-cell current clamp recording of an antecedent 20 ng/ml IL-6 treated GT1-7 cell as it is dialysed with 0 ATP in the presence of 2.5 mM glucose the day following treatment. **(Bii)** Corresponding families of currents evoked by the voltage-clamp protocol described in methods. Whole-cell macroscopic currents were examined immediately after the cell membrane was ruptured (Control) and after the cell had been dialysed with 0 ATP and reached a steady state (Run-up; n=6). **(C)** Pooled conductance densities at run-up in antecedent vehicle (Control) treated and 20 ng/ml IL-6 (IL-6) treated GT1-7 cells (n=6). In panel **(C)** statistical significance was analysed by Mann-Whitney test (P=0.57).

3.2.7 Generation of IL-6Rα Knockdown Cells

To confirm that the defective glucose sensing observed following antecedent IL-6 treatment was indeed an effect of exogenously applied IL-6, a GT1-7 cell line with stable knockdown of the IL-6 membrane bound receptor (IL-6Rα) was developed. While pharmacological intervention to impede IL-6 signalling could also have been employed in order to investigate this, the partial removal of the receptor through which IL-6 signals gave a more global inhibition of IL-6 signalling and would also be predicted to guard against activation of compensatory intracellular signalling pathways which is often observed when using pharmacological inhibition of specific signalling cascades. A panel of five commercially available shRNA sequences targeted against IL-6Rα were purchased (Sigma-Aldrich) and each shRNA was delivered to separate populations of GT1-7 cells in culture via the lentiviral delivery system (see methods for details). Additionally a scrambled shRNA sequence known not to target any mammalian genes was delivered to a population of GT1-7 cells as a control (shControl). Virally infected cells were selected for by resistance to puromycin, conferred by the inclusion of a puromycin-resistant cassette in the shRNA constructs. Stable cell lines of each genotype (shControl and shIL-6Rα1-5) were grown up and RNA from these cultures was isolated and used to synthesise cDNA which was then subjected to TaqMan® RT-PCR analysis to quantify shIL-6Rα gene expression (normalised to the house-keeping gene cyclophillin A). In Figure 3.7A the reduction in IL-6Rα gene expression in shIL-6Rα1-5 infected GT1-7 cells is shown compared to expression in shControl GT1-7 cells. shIL-6Rα4 cells were confirmed as demonstrating the most robust and reproducible knockdown of expression of the IL-6Rα gene, achieving ~75% reduction in expression compared to shControl treated cells (Figure 3.7C). The virally infected cell lines were frozen down and stored in liquid nitrogen. Upon re-suspension of shControl and shIL-6Rα4 cells (henceforth referred to as shIL-6Rα cells) in culture the expression of IL-6Rα was reconfirmed by TaqMan® RT-PCR. It should be noted that a slight decrease in the knockdown of IL-6Rα was observed in shIL-6Rα compared to shControl GT1-7 cells following the freeze thaw cycle compared to before it. The percentage expression of IL-6Rα in shIL-6Rα GT1-7 cells was quantified as 43% that of shControl cells, therefore meaning a 57% knockdown of IL-6Rα was achieved (data not shown).

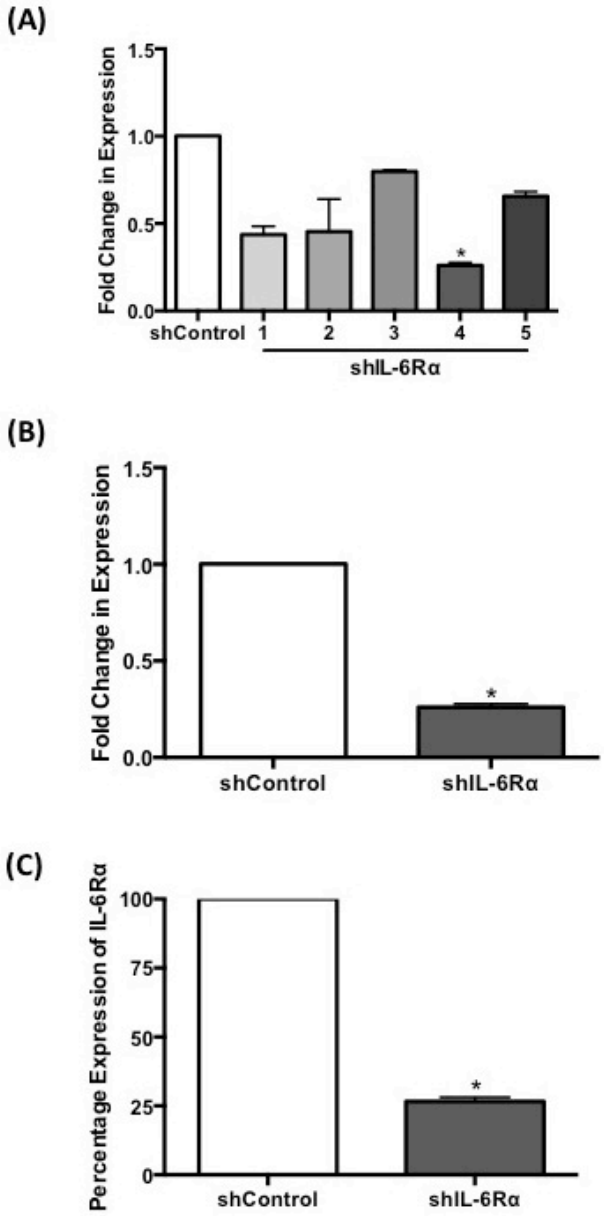

Figure 3.7 Generation of stable IL-6Rα knockdown GT1-7 cells using shRNA

A panel of five different shRNA sequences targeting the IL-6Rα (shIL-6Rα 1-5) or a scrambled control sequence (shControl) were delivered to GT1-7 cells via the lentiviral method. Stable cell lines of each transfection were cultured and after selection for virally infected cells RNA was isolated and cDNA synthesised to quantify gene expression of IL-6Rα by TaqMan® RT-PCR. **(A)** Bar chart demonstrating fold decrease in IL-6Rα mRNA expression in shIL-6Rα1-5 treated compared to shControl treated GT1-7 cells (n=2). **(B)** Direct comparison of IL-6Rα mRNA expression in shControl and shIL-6Rα4 GT1-7 cells, the shIL-6Rα sequence giving the most robust knockdown of IL-6Rα mRNA measured by TaqMan® RT-PCR (n=2). **(C)** For illustrative purposes the decrease in IL-6Rα mRNA expression in shIL-6Rα4 cells is shown as a percentage of IL-6Rα expression in shControl GT1-7 cells (n=2). Statistical significance was analysed by Kruksal-Wallis test ANOVA in panel **(A)** where * indicates significantly different from shControl ($p=<0.05$) and by one-sample t-test in panels **(B)** and **(C)** where * indicates significantly different from shControl ($p=<0.05$).

3.2.8 shControl and shIL-6Rα GT1-7 Cells Have Comparable K_{ATP} Channel Conductance

To confirm that shControl or shIL-6Rα infection didn't affect K_{ATP} channel expression or function, the two cell types were subjected to whole-cell patch clamp electrophysiology analysis. This technique was exploited to analyse whether the shRNA infections affected the ability of K_{ATP} channels to conduct current. A voltage-clamp protocol (see methods) was employed to assess K_{ATP} channel currents under control conditions and after the cell had been dialysed with 0 ATP. shControl and shIL-6Rα GT1-7 cells had comparable macroscopic currents measured at both baseline and after dialysis with 0 ATP (Figure 3.8Aii and Bii). Accordingly, there was no difference in the profile of whole-cell current clamp recordings made during dialysis with 0 ATP (Figure 3.8Ai and Bi). There was no significant difference in conductance density between shControl and shIL-6Rα cells (1.01 +- 0.21 and 1.35 +- 0.15 pS/pF respectively), confirming that shRNA mediated infection of GT1-7 cells does not affect the ability of K_{ATP} channels to conduct current (Figure 3.6C). Furthermore, the virally infected GT1-7 cells had comparable conductance densities with those observed in WT GT1-7 cells (compare Figure 3.6C with Figure 3.8C).

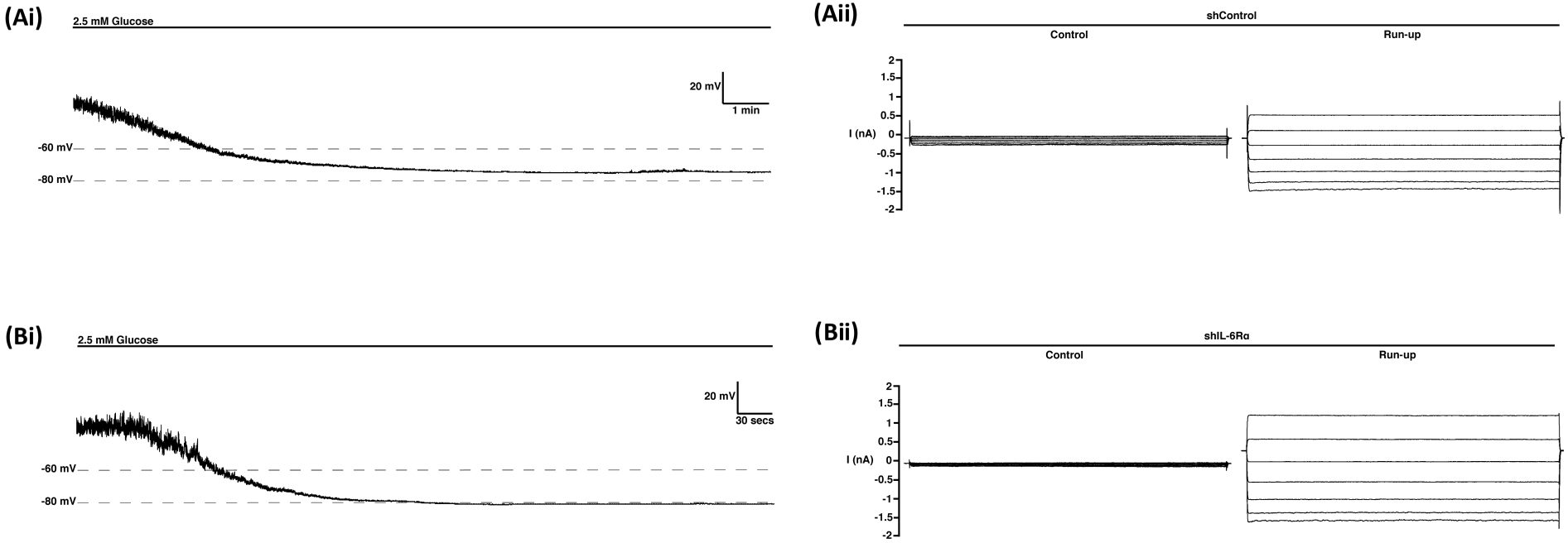

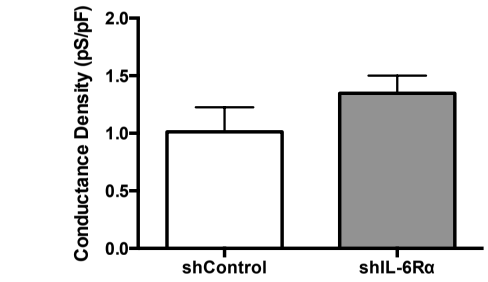

Figure 3.8 shControl and shIL-6Rα GT1-7 cells have comparable K_{ATP} channel conductance in response to dialysis of cell with 0 ATP

(Ai) Representative whole-cell current clamp recording of a shControl-infected GT1-7 cell as it is dialysed with 0 ATP in the presence of 2.5 mM glucose. **(Aii)** Corresponding families of currents evoked by the voltage-clamp protocol described in methods. Whole-cell macroscopic currents were examined immediately after the cell membrane was ruptured (Control) and after the cell had been dialysed with 0 ATP and reached a steady state (Run-up; n=5). **(Bi)** Representative whole-cell current clamp recording of a shIL-6Rα-infected GT1-7 cell as it is dialysed with 0 ATP in the presence of 2.5 mM glucose. **(Bii)** Corresponding families of currents evoked by the voltage-clamp protocol described in methods. Whole-cell macroscopic currents were examined immediately after the cell membrane was ruptured (Control) and after the cell had been dialysed with 0 ATP and reached a steady state (Run-up; n=6). **(C)** Pooled conductance densities at run-up in shControl and shIL-6Rα GT1-7 cells (n=5-6). In panel **(C)** statistical significance was analysed by Mann-Whitney test (P=0.32).

3.2.9 Antecedent IL-6 Induces Defective Glucose Sensing of Subsequent Hypoglycaemia in shControl GT1-7 Cells

To confirm that the shControl GT1-7 cells behaved physiologically the same as WT GT1-7 cells, as would be predicted, shControl cells were subjected to the antecedent IL-6 experiment previously performed in WT GT1-7 cells. shControl GT1-7 cells were exposed to vehicle dH_2O (Control) or 20 ng/ml IL-6 (IL-6) for three hours prior to undergoing a 0.5 mM glucose hypoglycaemic challenge 18-24 hours subsequently during perforated patch clamp electrophysiological analysis. Similarly to WT GT1-7 cells, vehicle treated shControl GT1-7 cells exhibited a resting membrane potential of -51.7 +- 1.9 mV in 2.5 mM glucose and these cells hyperpolarised and firing rates ceased in response to the low glucose challenge (Figure 3.9A and C). Antecedent IL-6 treatment in shControl cells prevented the hyperpolarising response and resulted in maintained firing rates during the low glucose stimulus, replicating the glucose sensing defect observed with antecedent IL-6 exposure in WT GT1-7 cells (Figure 3.9B and C). It should be noted that in vehicle treated shControl GT1-7 cells, the hyperpolarising response to 0.5 mM glucose was reduced compared to that observed in vehicle treated WT GT1-7 cells (Appendix I). In response to 0.5 mM glucose, vehicle treated shControl cells only hyperpolarised by -2.3 +- 2.2 mV to -54.0 +- 2.2 mV on average. However, this was due to over 50% (4 of 7) of the cells studied failing to detect the 0.5 mM glucose challenge (see Appendix I for details). Although this was an unexpected observation, importantly, the hyperpolarising response to 0.5 mM glucose in shControl cells exposed to antecedent IL-6 treatment was prevented in all cells studied, such that from a resting membrane potential in 2.5 mM glucose of -47.5 +- 3.1 mV, cells in fact depolarised by 2.7 +- 0.7 mV on average to a membrane potential of -44.8 +- 2.8 mV in response to 0.5 mM glucose (Figure 3.9C and Appendix I). Furthermore, separation of the vehicle treated hypoglycaemia-responsive cells from the non-responsive cells demonstrated that they hyperpolarised by -8.0 +- 2.1 mV on average in response to 0.5 mM glucose, whereas the non-responders in fact depolarised by 2.0 +- 0.7 mV on average (Appendix I). The hyperpolarising response to 0.5 mM glucose in responsive shControl cells is therefore comparable with that observed in WT cells in previous experiments (-8.0 +- 2.1 vs -10.2 +- 2.9 mV respectively). Therefore, the responses of shControl cells to antecedent vehicle and IL-6 treatments were phenotypically

comparable to WT GT1-7 cells, with antecedent IL-6 treatment inducing defective hypoglycaemia detection in shControl GT1-7 cells.

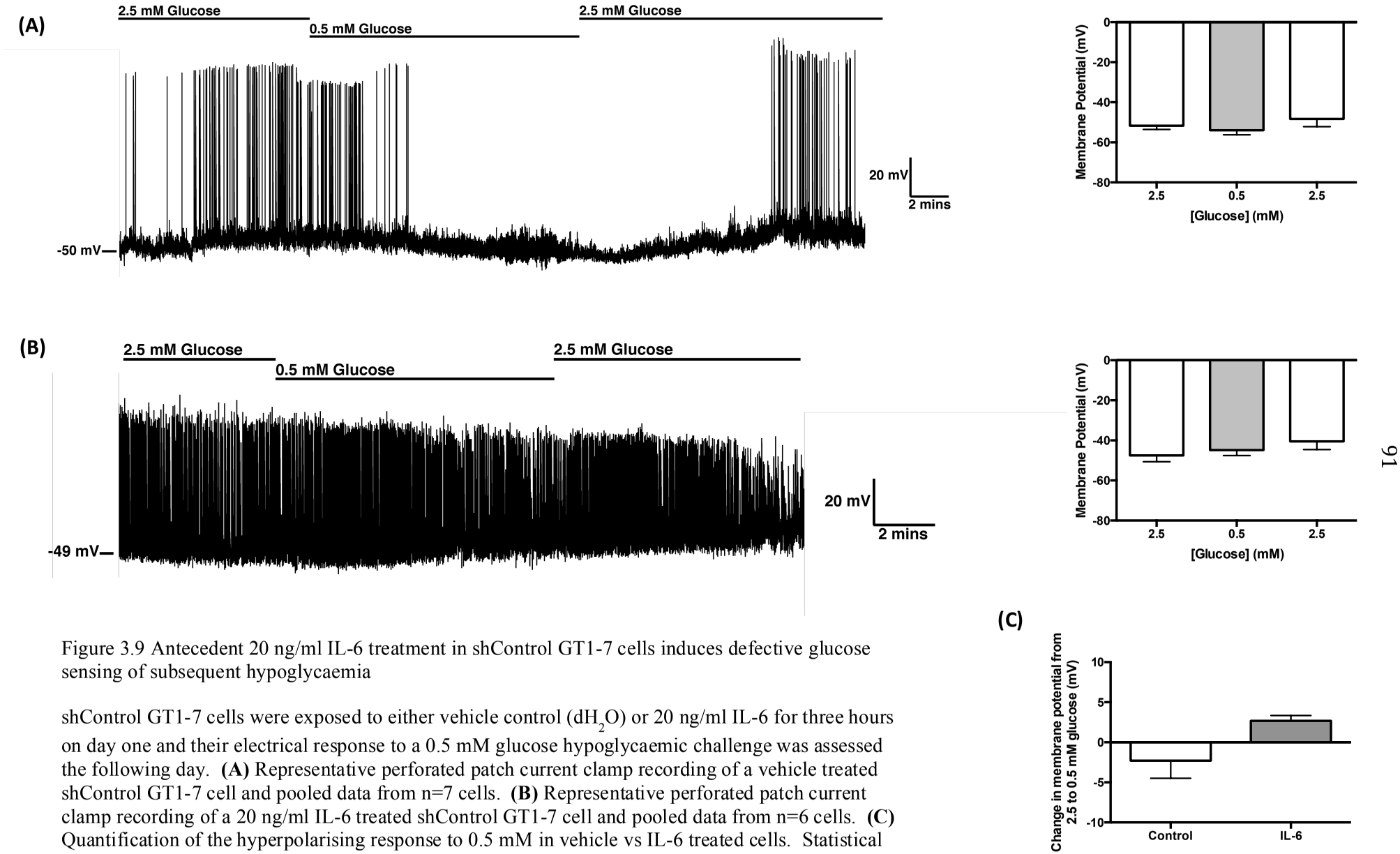

Figure 3.9 Antecedent 20 ng/ml IL-6 treatment in shControl GT1-7 cells induces defective glucose sensing of subsequent hypoglycaemia

shControl GT1-7 cells were exposed to either vehicle control (dH_2O) or 20 ng/ml IL-6 for three hours on day one and their electrical response to a 0.5 mM glucose hypoglycaemic challenge was assessed the following day. **(A)** Representative perforated patch current clamp recording of a vehicle treated shControl GT1-7 cell and pooled data from n=7 cells. **(B)** Representative perforated patch current clamp recording of a 20 ng/ml IL-6 treated shControl GT1-7 cell and pooled data from n=6 cells. **(C)** Quantification of the hyperpolarising response to 0.5 mM in vehicle vs IL-6 treated cells. Statistical significance was analysed by Friedman test in panels **(A)** and **(B)** and Mann-Whitney test in **(C)**.

3.2.10 Antecedent IL-6 Fails to Induce Defective Glucose Sensing in shIL-6Rα GT1-7 Cells

To prove that the defect in glucose sensing observed in Figure 5 was indeed mediated by IL-6, shIL-6Rα cells were treated antecedently with either vehicle (dH_2O) or 20 ng/ml IL-6 on day one prior to being subjected to a 0.5 mM glucose hypoglycaemic challenge the following day during perforated patch clamp electrophysiology. In vehicle treated shIL-6Rα cells a normal physiological response to the hypoglycaemic challenge was observed the following day during current clamp recordings with cells significantly hyperpolarising by 14 mV on average and inhibition of firing rates in response to the hypoglycaemic stimulus (Figure 3.10A and C). Importantly, antecedent IL-6 treated shIL-6Rα GT1-7 cells also exhibited a normal physiological response to the hypoglycaemic challenge the following day, also significantly hyperpolarising by 14 mV on average and ceasing firing rates in response to the hypoglycaemic stimulus (Figure 3.10B and C). Statistical analysis confirmed there was no significant difference in the hyperpolarising response to 0.5 mM glucose in IL-6 treated cells compared to vehicle treated cells (Figure 3.10C) and therefore, partial knockdown of the membrane bound IL-6α by shRNA resulted in a complete prevention of the antecedent IL-6 induced glucose sensing defect observed in WT GT1-7 cells.

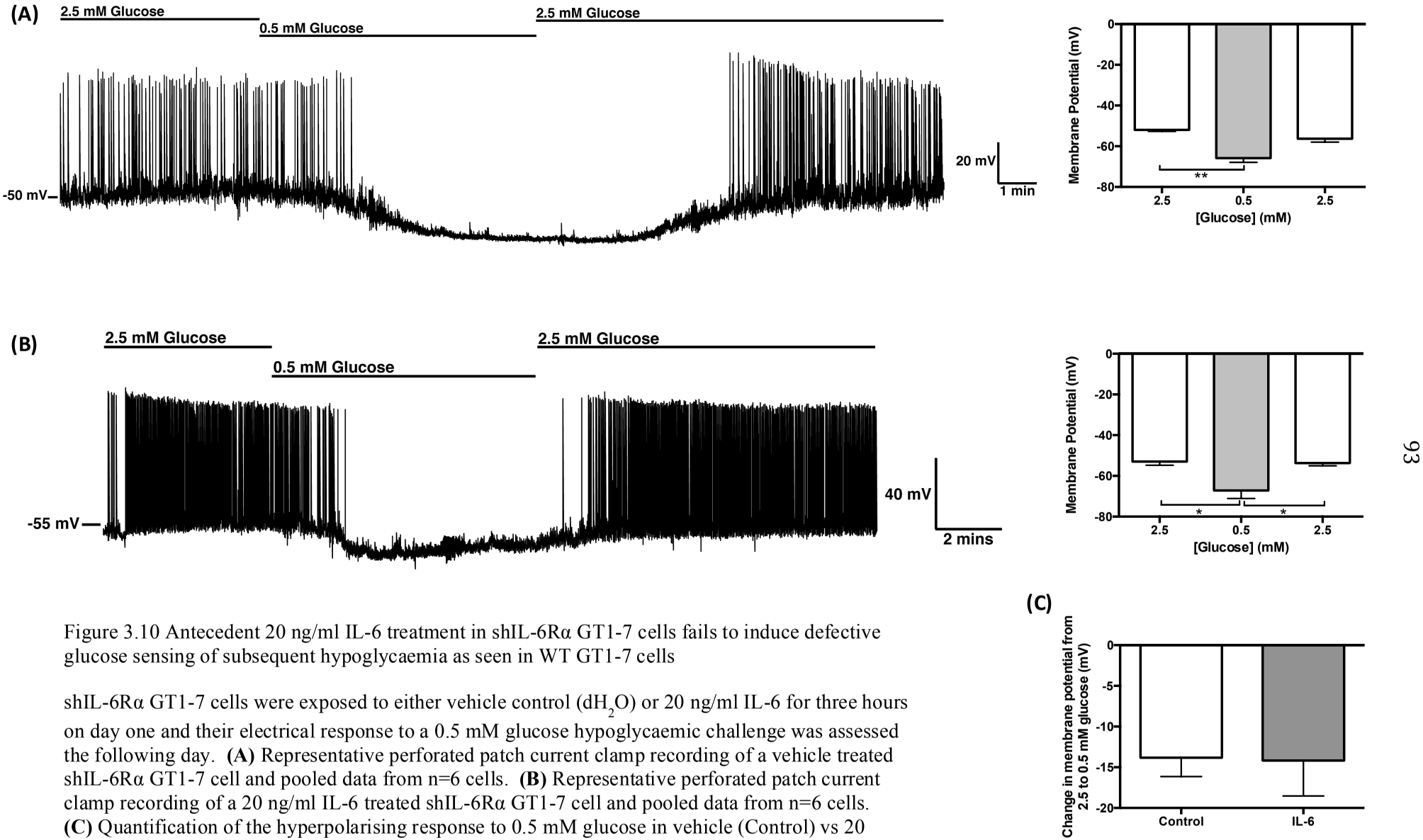

Figure 3.10 Antecedent 20 ng/ml IL-6 treatment in shIL-6Rα GT1-7 cells fails to induce defective glucose sensing of subsequent hypoglycaemia as seen in WT GT1-7 cells

shIL-6Rα GT1-7 cells were exposed to either vehicle control (dH_2O) or 20 ng/ml IL-6 for three hours on day one and their electrical response to a 0.5 mM glucose hypoglycaemic challenge was assessed the following day. **(A)** Representative perforated patch current clamp recording of a vehicle treated shIL-6Rα GT1-7 cell and pooled data from n=6 cells. **(B)** Representative perforated patch current clamp recording of a 20 ng/ml IL-6 treated shIL-6Rα GT1-7 cell and pooled data from n=6 cells. **(C)** Quantification of the hyperpolarising response to 0.5 mM glucose in vehicle (Control) vs 20 ng/ml IL-6 (IL-6) treated shIL-6Rα GT1-7 cells. Statistical significance was analysed by Friedman test in panels **(A)** and **(B)** and Mann-Whitney test in **(C)** where * and ** indicate significant differences (P=<0.05 and P=<0.01 respectively).

3.2.11 Antecedent IL-6-Induced Suppression of Glucose Sensing is Prevented in shIL-6Rα GT1-7 Cells

Figure 3.11 depicts the compiled data from the antecedent IL-6 glucose sensing experiments. For illustrative purposes, vehicle treated WT and shIL-6Rα GT1-7 cells were combined for analysis as the Control column as their hyperpolarising responses were comparable. In the Kruskal-Wallis analysis performed in this figure the effect of antecedent IL-6 treatment to suppress hyperpolarisation in response to 0.5 mM glucose in WT GT1-7 cells did not reach statistical significance, however the same treatment in shControl cells did. Importantly, antecedent IL-6 treated shIL-6Rα cells had comparable hyperpolarising responses to 0.5 mM glucose as WT GT1-7 cells, confirming that IL-6 via IL-6Rα-mediated signalling induced defective hypoglycaemia detection in GT1-7 cells.

3.2.12 Effects of IL-6 on STAT3 Phosphorylation in shControl and shIL-6Rα GT1-7 Cells

To confirm that the shRNA-mediated knockdown of IL-6Rα expression had functional consequences, shControl and shIL-6Rα GT1-7 cells were subjected to 20 ng/ml IL-6 timecourse experiments, similar to those performed in WT GT1-7 cells in Figure 3.1. 20 ng/ml IL-6 exposure in shControl cells elicited a robust increase in STAT3 Y705 phosphorylation, particularly at 30 minutes and three hours exposure to IL-6, however the increase in STAT3 Y705 phosphorylation in response to IL-6 in shIL-6Rα cells was much less pronounced (Figure 3.12A and B). In Figure 3.12C the fold increase in STAT3 Y705 phosphorylation in response to three hours 20 ng/ml IL-6 exposure from vehicle dH_2O exposure is compared in shControl and shIL-6Rα cells, and the increase observed in shIL-6Rα cells is only 42% of that observed in shControl cells. This data demonstrates that partial reduction of IL-6Rα results in an attenuation of IL-6 mediated intracellular signalling in GT1-7 cells.

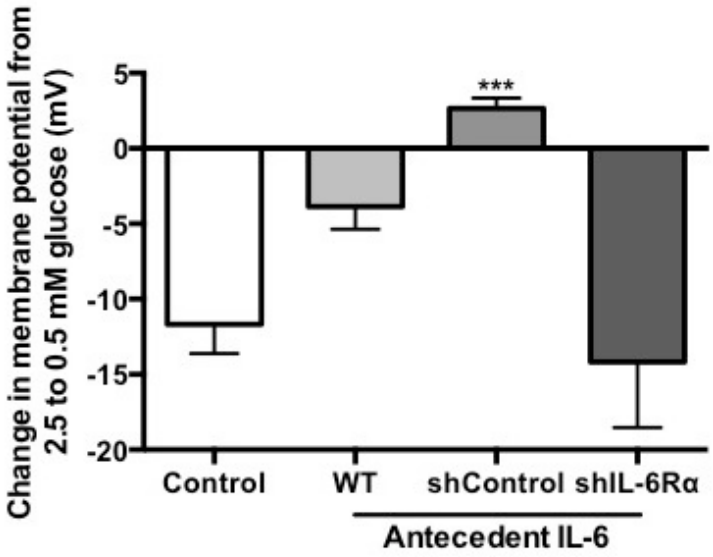

Figure 3.11 Antecedent 20 ng/ml IL-6 treatment causes an attenuation in the hyperpolarising response to subsequent 0.5 mM glucose exposure in WT GT1-7 cells but not in GT1-7 cells with partial knockdown of IL-6Rα by shRNA

WT GT1-7 and shIL-6Rα GT1-7 cells were treated with vehicle (dH_2O) or 20 ng/ml IL-6 for three hours on day one and exposed to a 0.5 mM glucose hypoglycaemic challenge the following day (18-24 hours later). Hyperpolarising responses to the low glucose stimulus were monitored during current clamp electrophysiological recordings in the perforated patch clamp configuration. The bar chart depicts the average hyperpolarising response (mV) to the hypoglycaemic stimulus in vehicle (Control) and IL-6 treated WT, shControl and shIL-6Rα GT1-7 cells. For illustrative purposes the responses to vehicle treatment have been pooled together for WT and shIL-6Rα cell genotypes as they did not differ between cell types (n=15). Antecedent IL-6 treatment is an average of n=8, n=6 and n=6 cells in WT, shControl and shIL-6Rα cells respectively. Statistical significance was analysed by Kruskal-Wallis test where *** indicates significantly different to Control ($p=<0.001$).

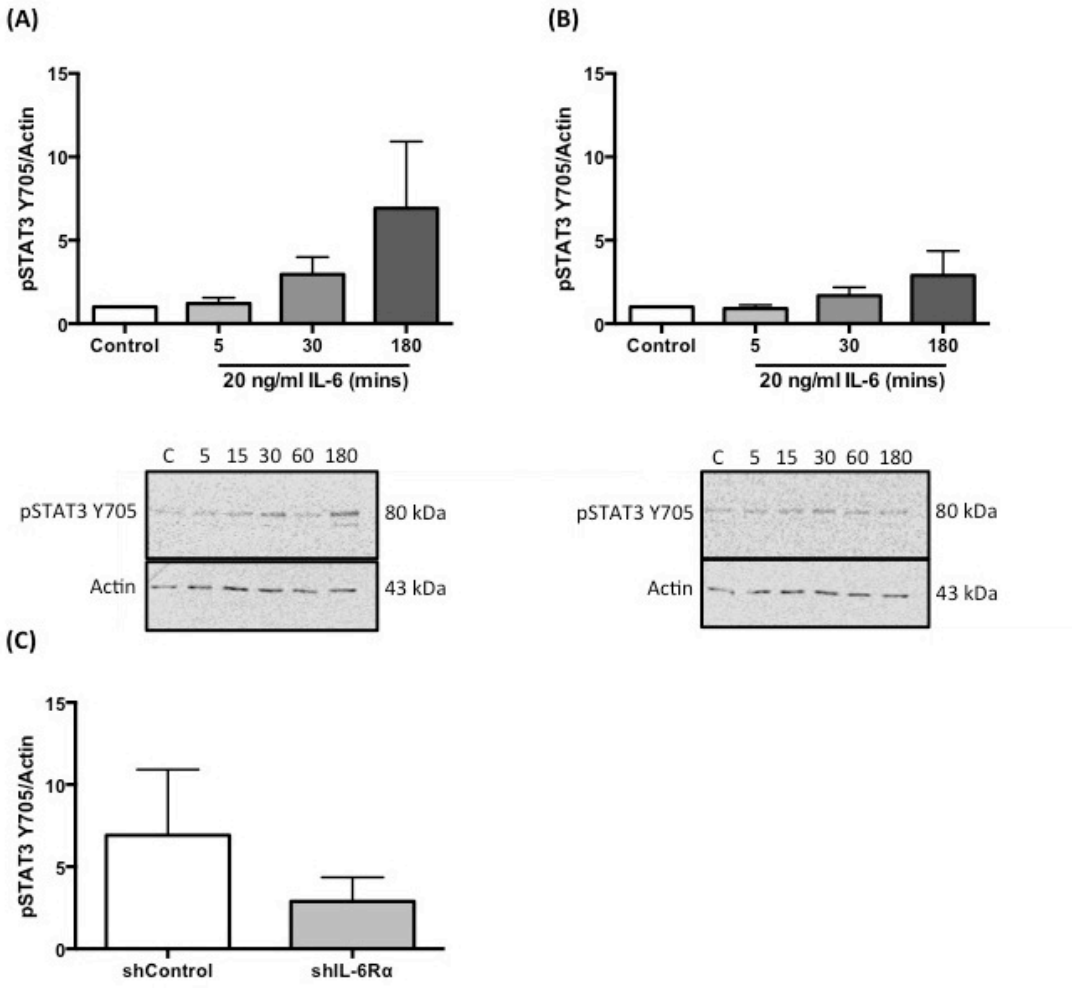

Figure 3.12 IL-6 induced STAT3 phosphorylation is reduced in shIL-6Rα GT1-7 cells compared to shControl GT1-7 cells

shControl **(A)** and shIL-6Rα **(B)** GT1-7 cells were serum starved for two hours in the presence of 2.5 mM glucose prior to exposure to 20 ng/ml IL-6 for the indicated times or vehicle dH_2O (Control) for 180 minutes. Cells were lysed and samples prepared for Western Blot analysis of pSTAT3 Y705 protein expression. Fold change in phosphorylation of STAT3 was determined compared to Control cells normalised to actin expression and representative blots are shown (n=3). **(C)** Comparison between fold increase in pSTAT3 Y705 in response to 20 ng/ml IL-6 treatment for 180 minutes in shControl and shIL-6Rα cells (n=3). Statistical significance was analysed by one sample t-test in **(A)** and **(B)** and Mann-Whitney test in **(C)**.

3.2.13 Regulation of SOCS3 Gene Expression by IL-6 in GT1-7 Cells

SOCS3 mRNA and protein is rapidly induced in response to IL-6 stimulation (Endo et al. 1997; Starr et al. 1997; Naka et al. 1997; Sasaki et al. 1999; Kershaw et al. 2013). In GT1-7 cells, after 30 minutes exposure to IL-6, no upregulation of SOCS3 mRNA expression was observed four or 24 hours later (Figure 3.13A). In order to confirm IL-6 did not induce an upregulation of SOCS3 mRNA expression earlier than four hours after exposure, GT1-7 cells were exposed to 20 ng/ml IL-6 for one, two or three hours and SOCS3 mRNA was measured at these three time points by RT-PCR. Unexpectedly, no increases in SOCS3 mRNA were observed at any of the time points and in fact, a significant suppression of SOCS3 mRNA was observed in cells exposed to IL-6 for two hours compared to vehicle treated control cells (Figure 3.13B; 2 hours IL-6: p=<0.01).

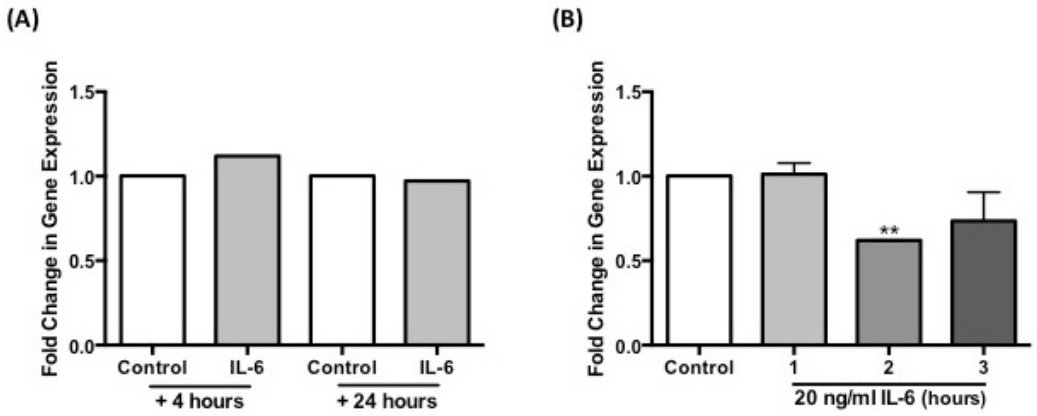

Figure 3.13 Effects of IL-6 on SOCS3 mRNA expression in GT1-7 cells

(A) GT1-7 cells were exposed to vehicle dH_2O (Control) or 20 ng/ml IL-6 for 30 minutes then lysed four or 24 hours subsequently. RNA was extracted and used to synthesise cDNA which was subjected to Taqman qRT-PCR analysis to determine SOCS3 gene expression (n=1). **(B)** GT1-7 cells were exposed to vehicle dH_2O (Control) for three hours or 20 ng/ml IL-6 for one, two or three hours and lysed. RNA was extracted and used to synthesise cDNA which was subjected to Taqman qRT-PCR analysis to determine SOCS3 gene expression. Fold change in gene expression was determined relative to Control treated cells normalised to the housekeeping gene cyclophillin A (n=2). Data was analysed by one sample t-test in **(B)** where ** indicates significantly different from Control ($p=<0.01$).

3.3 Discussion

IL-6 was found to activate the JAK/STAT3 signalling pathway in GT1-7 cells demonstrated by robust increases in the phosphorylation of STAT3 Y705 in response to IL-6 stimulation, persisting for at least three hours. Somewhat unexpectedly, IL-6 was not observed to activate other pathways classically activated in response to IL-6 stimulation, namely the MAPK/ERK pathway or PI3K/PKB pathway, which were indexed in the current work by phosphorylation of ERK1/2 and PKB respectively. Interestingly, studies have shown that IL-6 typically activates ERK1/2 in subconfluent cells, but that this response is lost in post-confluent cultures, suggesting that cell density may be a factor determining ERK1/2 responses to IL-6 stimulation (Raptis et al. 2011). Molecular studies of the IL-6Rα complex have identified that residue Y759 of gp130 is critical in controlling the balance between STAT and MAPK activation in IL-6, as it recruits SHP2 to activate MAPK signalling and is also the recruitment site of SOCS3 mediated inhibition of STAT signalling (Eulenfeld et al. 2012). Potentially in GT1-7 cells, the STAT3 signalling axis is preferentially activated over the MAPK cascade. Interestingly, in GT1-7 cells no apparent regulation of SOCS3 mRNA in response to IL-6 stimulation was observed. Literature suggests that SOCS3 mRNA and protein is rapidly upregulated in response to IL-6 stimulation of its receptor complex. In the current work the earliest time point that SOCS3 mRNA levels was measured was after one hour of IL-6 exposure. It would be of interest to investigate SOCS3 mRNA levels after a shorter exposure to IL-6 and also to investigate SOCS3 protein levels in these cells. IL-6 stimulation also failed to activate the PI3K cascade in GT1-7 cells, demonstrated by a lack of an effect of IL-6 exposure on PKB phosphorylation. The PI3K signalling cascade is also activated through the Y759 SHP2 binding site (Eulenfeld et al. 2012). Taking this data together raises the possibility that in GT1-7 cells the Y759 residue of gp130 fails to recruit SHP2 to activate MAPK and PI3K signalling pathways. Similarly, IL-6-induced phosphorylation of STAT3 Y705 might persist beyond three hours due to a lack of induction of SOCS3 and a failure of SOCS3 to be recruited to Y759 of gp130 to inhibit IL-6 induced STAT signalling. The interaction of SHP2 with Y759 of gp130 could be investigated by co-immunoprecipitation experiments in the future to determine whether these two proteins can interact in GT1-7 cells.

AMPK has been shown to be important in regulating the CRR to hypoglycaemia (McCrimmon et al. 2008) and its importance in glucose sensing capacity of hypothalamic neurons has been documented (Beall, Hamilton, et al. 2012). The effect of IL-6 exposure on pAMPK T172 was investigated in GT1-7 cells and phosphorylation of this residue was not found to be significantly regulated by IL-6. Phosphorylation of AMPK at this residue increases activity of the enzyme, suggesting that IL-6 doesn't regulate AMPK activity in GT1-7 cells. AMPK activity assays or phosphorylation status of its downstream target ACC would have given a better indication of whether IL-6 regulates this enzyme in GT1-7 cells. Given the importance of AMPK in hypoglycaemia detection, it would be of interest to investigate the activity of AMPK 18-24 hours after IL-6 exposure, as this is the time point at which defective glucose sensing following antecedent IL-6 exposure was observed. An attempt at this experiment was performed (see Appendix II). The lack of any acute effects of IL-6 on GT1-7 cell membrane potential correlates with the lack of effect of IL-6 on AMPK phosphorylation.

Acute exposure of GT1-7 cells to IL-6 during perforated patch current clamp recordings during euglycaemia was performed to see if IL-6 regulated the resting membrane potential of GT1-7 cells. No significant effects of IL-6 exposure on GT1-7 cell membrane potential were observed. A similar study involving exposure of thalamic neurons to 1 nM IL-6 found no change in resting membrane potential with IL-6 exposure compared to control treated cells (Samios & Inoue 2014), supporting the current finding of no acute regulation of membrane potential by IL-6 in GT1-7 cells.

The effect of IL-6 on membrane potential delivered during acute hypoglycaemia was also investigated, to determine whether IL-6 played a role in the regulation of glucose-sensing neuron activity during low glucose. GT1-7 neurons hyperpolarise in response to a low glucose challenge and action potential firing rates are ablated. The average data from three separate neurons suggested a trend of IL-6 to potentiate the hyperpolarising response to low glucose exposure in GT1-7 cells. Although this did not reach statistical significance, it does not completely exclude a subtle effect of IL-6 on glucose-sensing neurons. It would be of interest to study this further, as it suggests that IL-6 action may be coordinated to further enhance the response of glucose sensing neurons to hypoglycaemia upon detection of the low glucose stress. A more detailed study of the acute effect of IL-6 during a range of low glucose exposures (e.g. 0.5, 0.25, 0.1 mM) would have been required to confirm this.

IL-6 secretion from primary mouse cortical astrocytes in response to hypoglycaemia was confirmed in the current work. Plasma increases in IL-6 in response to hypoglycaemia have been confirmed in multiple studies but whether there is a CNS source of IL-6 during hypoglycaemia is less documented. Glial cells types in the brain have been shown to synthesise and release IL-6 (Gruol 2015; Dong & Benveniste 2001), and models of hypoglycaemia and oxygen and glucose deprivation simultaneously result in increased IL-6 secretion (S. J. Choi et al. 2013). In the current work, a three hour hypoglycaemic challenge in primary mouse cortical astrocytes had no immediate effect on the secretion of IL-6, with levels unchanged from euglycaemia treated cultures. However, in the euglycaemic recovery period following hypoglycaemia, IL-6 release was significantly increased from hypoglycaemia-exposed astrocyte cultures compared to euglycaemia-exposed cultures, indicating that hypoglycaemia increased IL-6 secretion from astrocytes. This data suggests that there is a local source of IL-6 in the CNS following hypoglycaemia. The delayed release of IL-6 following hypoglycaemia suggests that during hypoglycaemia the role of IL-6 in the regulation of glucose sensing machinery may be minimal, and rather that IL-6 is more likely involved in mediating the adaptive, recovery phase of hypoglycaemia to limit brain injury. This is in keeping with more recent evidence documenting a protective role of IL-6 in the response to endotoxaemia infection (Mauer et al. 2014; Mauer et al. 2015). In line with protective roles of IL-6, studies have shown IL-6 to be one of the molecular mechanisms by which hypoxic preconditioning induces tolerance to brain ischaemia (Westberg et al. 2007). A limitation here is the use of cortical astrocyte preparations rather than hypothalamic, the latter of which would serve as a better model for the physiological environment in which VMH glucose-sensing neurons would be situated, especially since cultured astrocytes have been demonstrated to exhibit brain region-specific responses (Takeda et al. 2014). Furthermore, the concentrations of IL-6 release measured from astrocytes raise a discrepancy with those concentrations used to stimulate GT1-7 cells in the current work (pg/ml range released vs ng/ml range stimulated). The 20 ng/ml IL-6 dose used was selected based on previous work investigating the effects of cytokines on neuronal cultures *in vitro* (Xin & Blatteis 1992; Qiu et al. 1995; Yamada & Hatanaka 1994; Hama et al. 1989), and importantly, CNS concentrations of IL-6 are elevated in numerous neurological diseases and injury (Gruol 2015). It is also impossible to infer what concentration of IL-6 glucose-sensing neurons would be exposed to in response to hypoglycaemia *in vivo*, however, if the glucose-

sensing neuron is surrounded by IL-6-secreting astrocytes and glial cells, the local concentration of IL-6 that the neuron sees would be considerable.

The most interesting finding of this work was that antecedent IL-6 exposure induced a defective detection of and physiological response to hypoglycaemia 18-24 hours subsequently in GT1-7 cells. IL-6 treated cells failed to hyperpolarise in response to hypoglycaemia and maintained action potential firing rates during low glucose exposure in stark contrast to vehicle treated cells which hyperpolarised and silenced appropriately in response to 0.5 mM glucose, as has been described for GE neurons of the hypothalamus (Beall, Hamilton, et al. 2012; Routh 2010). The defect in glucose sensing observed with antecedent IL-6 exposure was proven not to be due to an absence of functional K_{ATP} channels, as whole cell voltage clamp analysis 18-24 hours subsequently demonstrated comparable K_{ATP} channel conductance between vehicle and IL-6 treated cells. In keeping with this, non-glucose sensing GT1-7 cells following antecedent IL-6 exposure were capable of hyperpolarising in response to pharmacological opening of K_{ATP} channels with NN414 (Appendix III). The subsequent aims of the work were to elucidate the mechanisms by which antecedent IL-6 exposure induced defective hypoglycaemia detection and glucose sensing in GT1-7 cells.

Initial focus of mechanistic investigation was on the involvement of the JAK/STAT3 pathway since it was robustly induced in response to IL-6, as evidenced by increased phosphorylation of STAT3 Y705. Since phosphorylation of STAT3 Y705 leads to dimerisation and nuclear translocation, and given the latent onset (18-24 hours subsequently) of defective glucose sensing, it was hypothesised that STAT3-mediated gene expression was involved in mediating the effects of IL-6 to induce defective glucose sensing. As a proof of principle, expression of the IL-6Rα was partially reduced using shRNA interference to confirm that the IL-6Rα signalling complex was mediating the effects of IL-6 in GT1-7 cells. The IL-6Rα is the most upstream target involved in transducing IL-6 signalling and permitted a global impedance of IL-6 mediated signalling. Partial knockdown of the IL-6Rα prevented the defective glucose sensing phenotype induced by antecedent IL-6 exposure in GT1-7 cells, confirming that IL-6 signalling via IL-6Rα was necessary for this effect. This intervention could not determine whether IL-6 signals predominantly via the classical or trans-signalling mode of IL-6 signalling in GT1-7 cells, as given the knowledge that IL-6Rα can be shedded from the cell membrane to permit trans-signalling, knockdown of IL-6Rα could suppress both modes of signalling. shIL-6Rα cells had a markedly reduced pSTAT3

Y705 induction in response to IL-6 stimulation compared to shControl cells, and indeed WT GT1-7 cells, suggesting that this activation of STAT3 phosphorylation may be of importance for mediating the development of defective glucose sensing induced by antecedent IL-6 exposure. However, the apparent lack of regulation of SOCS3 mRNA expression by IL-6 stimulation in GT1-7 cells raises doubts over whether the induction of STAT3-mediated gene transcription is involved in mediating the effects of antecedent IL-6 on glucose sensing, as SOCS3 mRNA and protein is potently induced by IL-6 in other cell types (White & Nicola 2013). It may be that induction of SOCS3 transcription occurs very rapidly in GT1-7 cells, and an upregulation of the mRNA transcript was missed with the earliest time point studied at one hour of exposure to IL-6. In an attempt to prevent STAT3-induced gene transcription, the JAK2 inhibitor WP1066 was used to specifically prevent JAK2-mediated phosphorylation of STAT3 in response to IL-6, thereby abolishing its dimerisation, nuclear translocation and subsequent regulation of gene expression. Although WP1066 was effective at preventing acute IL-6-induced increases in phosphorylation of STAT3 at residue Y705 (Appendix IV), it was not compatible for use with the current experimental model as it exhibited cytotoxic effects on GT1-7 cells making it impossible to perform electrophysiological analysis on cells 18-24 hours after exposure to WP1066 and IL-6 (data not shown). In order to confirm if IL-6 requires transcription to mediate its negative effects on glucose sensing, antecedent IL-6 exposure could have been performed in the presence of a transcriptional inhibitor, for example dichlorobenzimidazole 1-β-D-ribofuranoside, to avoid the cytotoxic effects exhibited by JAK2 inhibition. A small molecule inhibitor of STAT3 is commercially available (Stattic, Sigma-Aldrich) and it would be of great interest to test whether treatment with this agent is capable of preventing the IL-6-induced glucose sensing defect in GT1-7 cells. Importantly, Stattic has been demonstrated to inhibit STAT3 Y705 phosphorylation and mRNA expression of STAT3 targets (Abkhezr & Dryer 2014). A particularly insightful experiment would be to investigate IL-6 regulated STAT3 DNA binding in GT1-7 cells. This could be determined by chromatin immunoprecipitation and would identify which genes were regulated by STAT3 in response to IL-6 stimulation and may therefore identify potential mediators of IL-6-induced defective glucose sensing.

Unfortunately, it wasn't confirmed in the current work how soon after three hour exposure to IL-6 negative effects on glucose sensing are first observed. The model used

involved studying the cells 18-24 hours subsequently as it was then comparable with other on-going studies in the laboratory investigating the effects of antecedent hypoglycaemia on GT1-7 cell glucose sensing capacity. The time scale in which IL-6 regulates glucose sensing in GT1-7 cells may indicate whether transcriptional regulation is required for its effects. Similarly, it wasn't confirmed how long the suppression of glucose sensing by antecedent IL-6 exposure persists for.

Although the data comparing the effects of antecedent IL-6 on glucose sensing in WT and shIL-6Rα GT1-7 cells was robust, the studies in shControl cells were less reproducible. During the current work, a decrease in glucose sensing capacity of GT1-7 cells, regardless of genotype, has been observed over time (Appendix V). Unfortunately, the shControl cell studies were performed later than those of WT and shIL-6Rα cells. Due to this, the hyperpolarising responses to low glucose in vehicle treated shControl cells were reduced in magnitude compared to those seen in WT and shIL-6Rα cells (Figures 3.5, 3.9, 3.10 and Appendix V). This made comparisons between the genotypes difficult, due to vehicle treated shControl cells having suppressed responses to low glucose, such that vehicle treated shControl cells had a hyperpolarising response to hypoglycaemia comparable in magnitude to that initially observed in IL-6 treated WT GT1-7 cells with defective glucose sensing. This meant that comparisons between shControl and the other GT1-7 cell lines were not valid. The important comparison between WT GT1-7 and shIL-6Rα GT1-7 cells is valid however, and clearly demonstrates that partial reduction of the IL-6Rα prevents IL-6-induced defective glucose sensing, as one would predict. Furthermore, the data demonstrating that antecedent IL-6 induces defective glucose sensing in shControl GT1-7 cells is clear, as no IL-6 treated shControl cells hyperpolarised in low glucose where as some vehicle treated cells did (3/7), albeit fewer and with lower magnitude than that observed in WT and shIL-6Rα cells (Appendix I and Figures 3.5, 3.9, 3.10).

GT1-7 cells and other glucose-sensing neurons have been shown to exhibit a robust increase in AMPK T172 phosphorylation in response to hypoglycaemia (Beall, Hamilton, et al. 2012; Lamy et al. 2014). When populations of GT1-7 cells were exposed to hypoglycaemia in the current work, there was an absence of an increase in AMPK T172 phosphorylation (Appendix II). Electrophysiological single cell analysis of GT1-7 cells shows that a proportion of the cells hyperpolarise in response to low glucose challenge, however, many GT1-7 cells do not (Appendix VI). However, GT1-7 cells do hyperpolarise in response to metabolic inhibition by 2-DG or oligomycin

(Appendix VI), suggesting that ATP depletion is capable of hyperpolarising these cells, but glucose deprivation alone is not. The studies investigating AMPK phosphorylation in a population of GT1-7 cells exposed to hypoglycaemia suggests that the majority of GT1-7 cells do not respond to low glucose with an upregulation of AMPK T172 phosphorylation. This is in line with electrophysiological analysis identifying a lack of hyperpolarisation in response to hypoglycaemia in many GT1-7 cells. The reason for this finding is not known, however, given that whole cell metabolic inhibition can hyperpolarise the cells (Appendix VI) the fact that glucose deprivation alone isn't sufficient to induce membrane hyperpolarisaiton, points to the availability of alternate fuel substrates to provide ATP when glucose is reduced. It has been reported that lactate is able to modulate metabolic and neuronal activity, and that elevated levels are critical for maintaining glucose metabolism under hypoglycaemia, preserving neuronal function (Herzog et al. 2013). Ketone infusion has been demonstrated to reduce hormonal responses to hypoglycaemia, consistent with the hypothesis that human neurons can utilise ketones as a fuel source (Amiel et al. 1991). There are no other fuels present in the media during electrophysiological experiments, therefore GT1-7 cells may have internal fuel stores that can maintain activity during glucose deprivation. In support of this, preliminary studies have identified fat droplets in GT1-7 cells (data not shown). This would provide an alternate energy source for GT1-7 cells to utilise during glucose deprivation, and although IL-6 stimulates lipolysis in adipose tissue (Hoene & Weigert 2007), fatty acids are only used poorly as fuel in the brain (Schönfeld & Reiser 2013). Clearly, the population of GT1-7 cells used in the current work appear to have heterogeneous responses to hypoglycaemia, making studies difficult. In the future it would be of interest to attempt to sort the cells based on their AMPK T172 phosphorylation response to hypoglycaemia to try to isolate a more pure population of hypoglycaemia-responsive GE cells, as the current studies suggest that the GT1-7 cell population are heterogeneous, at least in their response to glucose deprivation.

Taken together, these data demonstrate that antecedent exposure of GT1-7 cells to IL-6 attenuates their glucose sensing capacity the following day, resulting in a failure of these cells to hyperpolarise in response to a hypoglycaemic challenge. The effect of IL-6 was confirmed to be mediated via its receptor complex, with the transcription factor STAT3 potentially playing a role, as Y705 phosphorylation and therefore activation of STAT3 was reduced in cells lacking the IL-6Rα, which were resistant to IL-6-induced defective glucose sensing. The lack of induction of SOCS3 mRNA in response to IL-6

stimulation and STAT3 activation in these cells questioned whether IL-6 negatively regulated glucose sensing via transcriptionally mediated changes, even though the time scale of the induction of defective glucose sensing suggested that this might be the case. The absence of an increase of SOCS3 mRNA in response to IL-6 stimulation contradicts other studies, and should be repeated to confirm this observation. The expression of SOCS3 protein should also be determined in response to IL-6 stimulation, as this would give a more functional readout of the negative regulation of STAT3 signalling via SOCS3. It raised the possibility that IL-6 activation of STAT3 results in stimulation of an alternate pathway by which IL-6 signals, independent from the well-described classical IL-6-JAK-STAT-SOCS3 axis. Interestingly, cAMP response element-binding protein (CREB) has been identified as a downstream mediator of the effects of the IL-6 family cytokine OSM in rat cortical neurons, although its induction was stimulated by ERK1/2 rather than JAKs (Chang et al. 2015). This is consistent with data in neural stem cells, where IL-6 is proposed to activate neurogenesis via the MAPK/CREB cascade whereas it activates gliogenesis via the JAK/STAT signalling pathway (O. Islam et al. 2009). Another study suggested that phosphorylation of STAT3 and CREB by peripheral inflammation in primary afferent neurons may be mediated via the OSM receptor (OSMR) (Tamura et al. 2005), indicating that IL-6 family cytokines can activate CREB phosphorylation in neurons.

The investigation of the JAK/STAT, MAPK and PI3K intracellular signalling cascades classically activated by IL-6 did not suggest a major involvement of any of these pathways in the mediation of the action of IL-6 to suppress glucose sensing and membrane hyperpolarisation to hypoglycaemia 18-24 hours after exposure. The following studies therefore investigated other potential mechanisms that may mediate the effects of IL-6, with attention focussed next on IL-6 regulation of whole cell metabolism.

4 The Role of Cell Metabolism in the Regulation of Glucose Sensing by IL-6

4.1 Introduction

The next focus of the current work was to determine the mechanisms by which antecedent IL-6 exposure induced defective glucose sensing. The failure of GT1-7 cells to hyperpolarise appropriately to a low glucose stimulus following antecedent IL-6 exposure is associated with a maintenance of a depolarised cell membrane and action potential firing rates during the hypoglycaemic challenge. This suggests that K_{ATP} channels maintain a closed state during the low glucose exposure, and this was supported by the finding that pharmacological opening of K_{ATP} channels with 5 μM NN414 induced membrane hyperpolarisation and silencing of firing rates in cells that had been antecedently exposed to IL-6, confirming that K_{ATP} channels were still functional (Appendix III). It was hypothesised that an increase in ATP-mediated inhibition of K_{ATP} channels might be responsible for the effect of antecedent IL-6 exposure to induce defective glucose sensing in GT1-7 cells.

The brain relies on glucose metabolism to maintain its function, and has a high demand for ATP, with neurons demonstrating the highest demand for energy compared to other brain cell types. The mitochondria are the major site of brain cellular ATP generation, with over 90% of ATP generation occurring via oxidative phosphorylation of substrates in the mitochondria (Schönfeld & Reiser 2013). In neurons, glucose undergoes glycolysis, yielding a small amount of ATP and the generation of pyruvate, which becomes the main hydrogen source for mitochondrial oxidative phosphorylation (Schönfeld & Reiser 2013).

Roles for IL-6 in the regulation of whole body metabolism and energy homeostasis have been described. Immune cell accumulation in adipose tissue during obesity has been well documented, and is associated with a pro-inflammatory phenotype of the infiltrating cells and release of cytokines, including IL-6 (Pal et al. 2014). IL-6 has been demonstrated to reduce insulin signalling in liver and adipose (Lagathu et al. 2003; Rotter et al. 2003; Siegmund et al. 2004), but its administration has also been shown to enhance glucose tolerance and insulin sensitivity in skeletal muscle and liver (Holmes et

al. 2007). Muscle derived IL-6 has been demonstrated to regulate metabolic factors in mouse inguinal white adipose tissue (iWAT), affecting iWAT mass through regulation of glucose uptake capacity as well as lipogenic and lipolytic factors (Knudsen et al. 2015).

IL-6 deficient mice develop mature onset obesity (V. Wallenius et al. 2002) suggesting that IL-6 is involved in the regulation of body weight. Wallenius *et al.* showed that CNS administration of IL-6 increased energy expenditure and reduced body fat mass in rats, implicating a role of central IL-6 to regulate whole body metabolism (K. Wallenius et al. 2002) Jansson et al. 2003). Li *et al.* showed that chronic elevation of IL-6 in the CNS reduces body weight gain and visceral adiposity by a mechanism involving sympathetic induction of UCP1 in brown adipose tissue (BAT) in rats (Li et al. 2002). IL-6 has been demonstrated to exert effects in the ARC resulting in regulation of body fat, with speculation that IL-6 can inhibit obesity partly by inhibiting orexigenic NPY expression (Schéle et al. 2013), providing a potential molecular mechanism by which the development of obesity in IL-$6^{-/-}$ mice may be mediated. Furthermore, astroglial IL-6 production has been implicated as the mechanism by which amylin interacts with leptin signalling in the VMH to increase its effect on weight loss (Le Foll et al. 2015).

While IL-6 regulation of peripheral metabolism and effects of CNS IL-6 to regulate energy expenditure and body weight have been described, studies documenting the roles of IL-6 in neuronal and glial cell metabolism are lacking. When Brown *et al.* challenged developing mouse neurons with IL-6 they responded by increasing their consumption of resources from the media, suggesting that IL-6 exposure increased neuronal metabolism in this model (Brown et al. 2014).

Very recently, Chang and colleagues demonstrated that the IL-6 family cytokine OSM increases mitochondrial respiration indexed by increased OCR in cortical neurons measured using the XF24 (Chang et al. 2015). Likewise, others have demonstrated that IL-17 can modulate mitochondrial function in sensory neurons from rats. IL-17 was shown to enhance mitochondrial bioenergetic function via ERK and PI3K signalling pathways, with increased protein level and activity of ETC components (Habash et al. 2015). These studies suggest that cytokines can regulate mitochondrial function in neurons, although whether IL-6 also can has not been investigated.

The current experiments were therefore designed to investigate whether IL-6 regulates GT1-7 cell metabolism. The XF24 was employed to study GT1-7 cell metabolism. By indexing oxygen consumption rate (OCR) and extracellular acidification rate (ECAR), the XF24 permits measurement of the two major pathways of ATP generation, mitochondrial oxidative phosphorylation and glycolysis respectively. OCR measures the cell's utilisation of oxygen that is mainly consumed by the mitochondria during oxidative phosphorylation of substrates to generate ATP. ECAR measures the acidification rate of the extracellular media, driven by lactate accumulation from glycolysis, giving an indirect measure of glycolytic rates. The question of whether IL-6 exposure altered metabolism in GT1-7 cells was addressed using the XF24 to measure OCR and ECAR. Further indications of regulation of metabolism and ATP production by IL-6 included biochemical investigation of expression of metabolically relevant proteins and genes and direct measurement of cellular ATP production by ELISA.

4.2 Results

4.2.1 Effects of Antecedent IL-6 on Oxygen Consumption and Extracellular Acidification Rates 24 Hours Subsequently

In the following studies I examined the hypothesis that the reduction in the hyperpolarising response to 0.5 mM glucose in GT1-7 cells antecedently exposed to IL-6 may be due to increased ATP-mediated inhibition of K_{ATP} channels, preventing channel opening, potassium efflux and therefore membrane hyperpolarisation. To study this I used the XF24 to examine GT1-7 whole cell bioenergetics after vehicle or IL-6 treatment. Since the defective glucose sensing observation had been made 18-24 hours subsequent to IL-6 treatment, measurements of cellular metabolism were made at the same time point post treatment. The XF24 gives two read outs of cellular metabolism, namely OCR and ECAR. OCR measures the oxygen consumption of the cells and therefore provides an index of mitochondrial respiration and oxidative phosphorylation. ECAR provides an indirect measure of cellular glycolysis by measuring the acidification of the extracellular media by lactate that accumulates from glycolysis (Appendix VII). In the current work, GT1-7 cells were exposed to vehicle dH_2O (Control) or 20 ng/ml IL-6 (IL-6) for three hours before being returned to plating media for two hours prior to cell counting and seeding at a density of 30,000 cells per well in

Seahorse XF24 culture plates. 18-24 hours subsequently cells were transferred to assay medium containing 2.5 mM glucose, consistent with substrate availability during electrophysiological analyses, and OCR and ECAR were measured every eight minutes for a total of 40 minutes. The final measurements taken at 40 minutes gave the most stable results so these were averaged and plotted to determine OCR and ECAR in the two treatment groups. Antecedent IL-6 treatment trended towards increasing OCR (p=0.21) 18-24 hours subsequently compared to vehicle treated cells with no effect observed on ECAR (p=0.72) (Figure 4.1A and B). The slight increase in OCR is suggestive of an increase in oxygen consumption directed towards mitochondrial respiration (Figure 4.1B). Although the effect of IL-6 exposure on OCR did not reach statistical significance it was deemed a large enough increase to be worthwhile studying in further detail using the commercially available Mito Stress Test Kit.

4.2.2 Effect of Antecedent IL-6 on the Profile of OCR During Mito Stress Tests

The XF Mito Stress Test Kit provides a complete mitochondrial profile and reveals critical information not evident in basal metabolism measurements. The kit allows the measurement of key parameters of mitochondrial function including basal respiration, ATP production, proton leak and spare respiratory capacity. The assay consists of serial injections of the compounds oligomycin, FCCP and a mix of rotenone and antimycin A to measure ATP production, spare respiratory capacity and non-mitochondrial respiration respectively. Proton leak can then be determined using these parameters. GT1-7 cells were treated with vehicle dH_2O (Control) or 20 ng/ml IL-6 (IL-6) for three hours before being returned to plating media for two hours prior to cell counting and seeding at a density of 30,000 cells per well in Seahorse XF24 culture plates. 18-24 hours later the cells underwent the Mito Stress Test and OCR was measured throughout. The assay protocol involved measuring OCR every eight minutes. Initially, five OCR measurements were made to achieve a stable basal OCR. To allow for inter-plate comparison of the Mito Stress Test data each OCR measurement is reported as a percentage of the 40 minute basal OCR measurement, giving a percentage change from baseline for each data point (Figure 4.2).

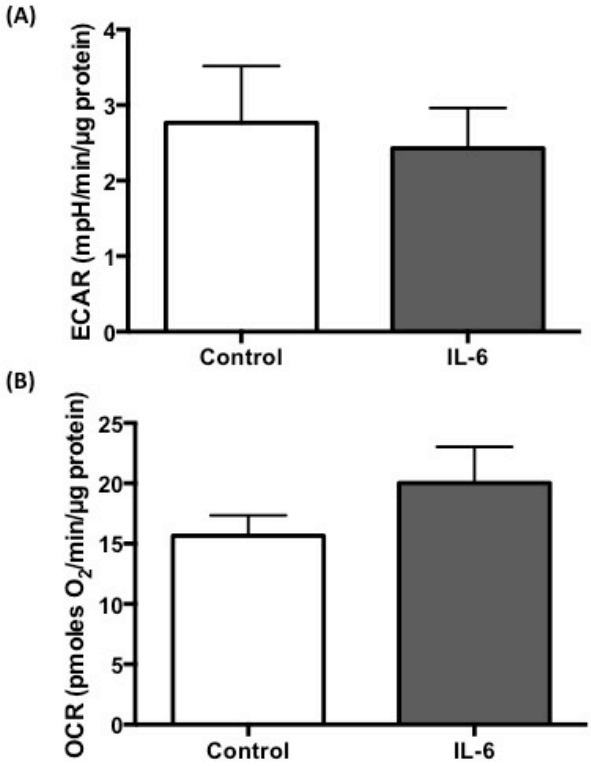

Figure 4.1 Antecedent IL-6 treatment trends towards increasing basal oxygen consumption rate (OCR) 24 hours subsequently with no effect on extracellular acidification rate (ECAR)

WT GT1-7 cells were exposed to dH_2O vehicle (Control) or 20 ng/ml IL-6 (IL-6) for three hours prior to seeding for Seahorse analysis the following day. 24 hours after treatment cells were transferred to assay medium containing 2.5 mM glucose and OCR and ECAR were measured over a 40 minute period using the Seahorse Bioscience Extracellular Flux Analyser 24. **(A)** Basal ECAR at the 40 minute time point of the assay (n=25 for both treatments). **(B)** Basal OCR at the 40 minute time point of the assay (n=31 for Control and n=32 for IL-6). Statistical significance was analysed by unpaired student's t-test with p=0.21 in **(A)** and p=0.72 in **(B)**.

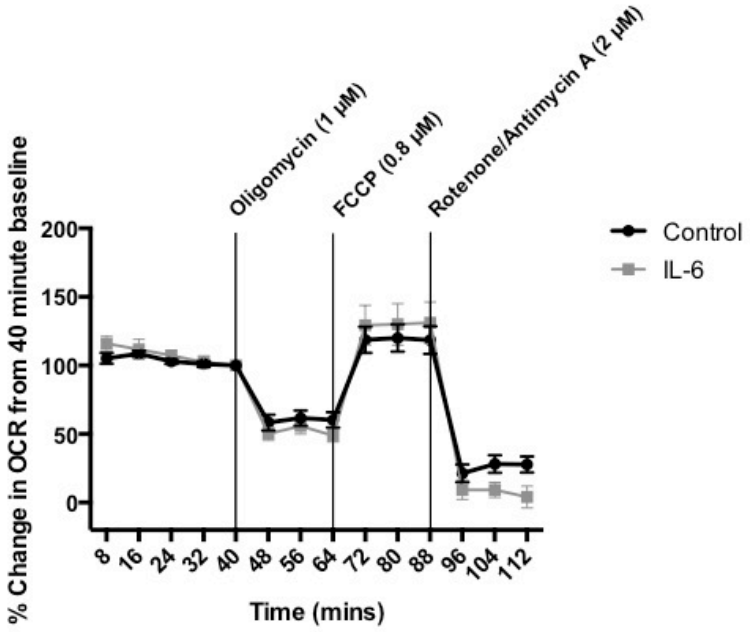

Figure 4.2 Profile of oxygen consumption rate (OCR) during a Mito Stress Test in GT1-7 cells

WT GT1-7 cells were treated with vehicle dH_2O (Control) or 20 ng/ml IL-6 (IL-6) for three hours prior to seeding for subsequent Mito Stress Tests using the Seahorse Bioscience XF24 the following day (18-24 hours after treatment). OCR was measured every eight minutes for a total of 112 minutes with sequential drug additions of the ATP synthase inhibitor Oligomycin (1 μM), the electron transfer chain (ETC) accelerator FCCP (0.8 μM) and ETC complex I and III inhibitors Rotenone (2 μM) and Antimycin A (2 μM) respectively. To allow for inter-plate comparison, OCRs were normalised to a 100% baseline at the final basal measurement made at the 40 minute time point and all other OCR measurments were calculated as percentage change from this baseline. Data represents n=35 individual wells from seven plates.

Upon inhibition of the ATP synthase with 1 μM oligomycin a reduction in OCR is observed in both control and IL-6 treated cells, allowing determination of the percentage of cellular oxygen consumption directed towards mitochondrial ATP production. FCCP is an uncoupling agent that disrupts ATP synthesis by transporting hydrogen ions across the mitochondrial membrane instead of the proton channel of ATP synthase. Collapse of the mitochondrial membrane potential leads to rapid consumption of energy and oxygen in the absence of ATP generation causing an increase in OCR. This allows determination of spare respiratory capacity, defined as the quantitative difference between maximal uncontrolled OCR and the initial basal OCR. The spare respiratory capacity demonstrates the ability of cells to respond to stress under conditions of increased energy demand and is influenced by the bioenergetic capacity of mitochondria. The third and final injection is a mix of rotenone and antimycin A, complex I and III inhibitors respectively, that shut down mitochondrial respiration enabling calculation of non-mitochondrial respiration driven by processes outside the mitochondria. The profile of OCR in response to the compound injections during a Mito Stress Test is depicted in Figure 4.2.

4.2.3 Effects of Antecedent IL-6 on Respiration Parameters Measured During Mito Stress Tests

Figure 4.3 demonstrates the quantification of the parameters measured during Mito Stress Tests in WT GT1-7 cells treated antecedently with vehicle dH_2O (Control) or 20 ng/ml IL-6 (IL-6). Upon inhibition of ATP synthase with oligomycin there is a reduction in OCR, with the decrease observed approximating the proton current flowing through the ATP synthase and therefore ATP production. IL-6 treated GT1-7 cells direct slightly more oxygen towards ATP production than vehicle treated GT1-7 cells, although this does not reach statistical significance (Figure 4.3A). Upon addition of the mitochondrial uncoupling agent FCCP, OCR is increased maximally, allowing determination of the spare respiratory capacity of the cells.

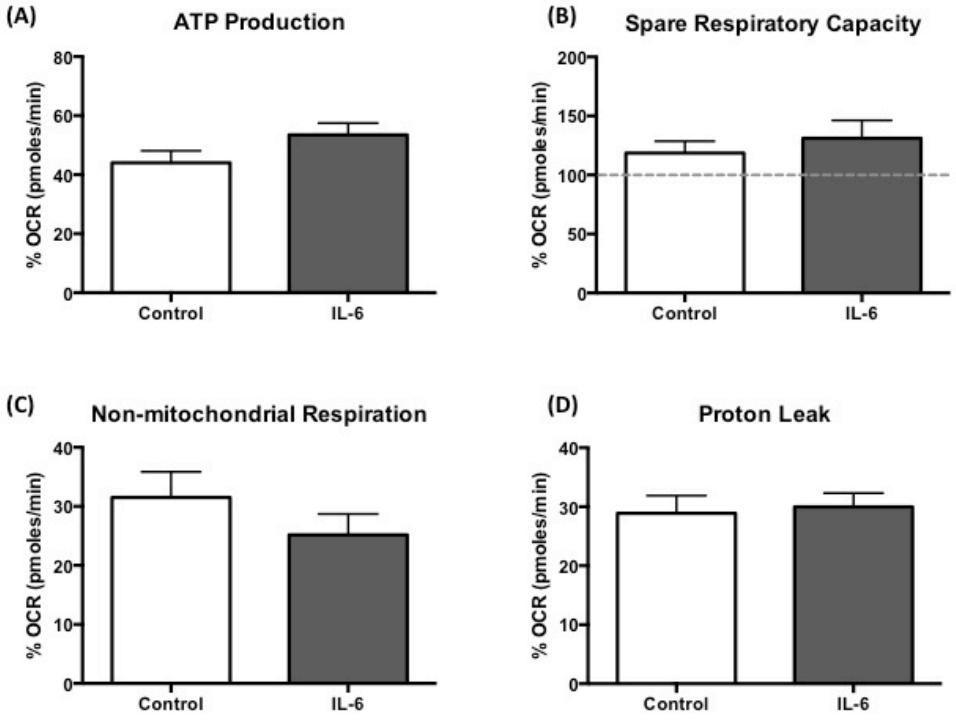

Figure 4.3 Effects of IL-6 on cellular respiration parameters measured during Mito Stress Tests in GT1-7 cells.

WT GT1-7 cells were treated with vehicle dH_2O (Control) or 20 ng/ml IL-6 (IL-6) for three hours prior to being seeded for Mito Stress Tests using the Seahorse Bioscience XF24 the following day (18-24 hours after treatment). **(A)** Percentage of cellular oxygen consumption (OCR) directed towards mitochondrial ATP production measured upon inhibition of ATP synthase by 1 μM oligomycin (n=29-34). **(B)** Percentage increase in OCR indexing spare respiratory capacity upon acceleration of the electron transport chain (ETC) by 0.8 μM FCCP (n=35). **(C)** Percentage of OCR directed towards non-mitochondrial respiration calculated upon inhibition of ETC complexes I and III by 2 μM rotenone and 2 μM antimycin A respectively (n=23-31). **(D)** Percentage of OCR required to maintain the mitochondrial protein leak (n=22-27). Statistical significance was analysed by unpaired student's t-test.

After IL-6 treatment there was a slight increase in spare respiratory capacity in GT1-7 cells compared to vehicle control cells, suggesting that IL-6 exposure enhances mitochondrial bioenergetics under conditions of increased energy demand in GT1-7 cells, although again this did not reach statistical significance (Figure 4.3B). The complex I and III inhibitors rotenone and antimycin A respectively reduce OCR by completely blocking the ETC, allowing determination of the percentage of cellular OCR directed towards non-mitochondrial respiration. In IL-6 treated GT1-7 cells, a smaller percentage of cellular oxygen consumption is directed towards non-mitochondrial respiration compared to control cells, therefore indicating that an increase in mitochondrial OCR may occur in GT1-7 cells following IL-6 treatment (Figure 4.3C). The proton current generated by basal respiration involves proton re-entry to the mitochondria via two parallel pathways, namely via ATP synthase and via the proton leak. The residual OCR after inhibition of ATP synthase with oligomycin is attributable to the mitochondrial proton leak. By subtracting the non-mitochondrial respiration OCR from the oligomycin-inhibited OCR gives a more accurate estimation of the OCR directed towards maintaining the proton leak. There was no difference observed in the OCR directed towards maintaining the mitochondrial proton leak between control and IL-6 treated GT1-7 cells, suggesting that IL-6 treatment does not alter mitochondrial uncoupling or the proton current (Figure 4.3D). Taken together these data suggest that antecedent IL-6 treatment does not have any significant effects on mitochondrial respiration in GT1-7 cells, but trends towards increasing the bioenergetic capacity of mitochondria.

4.2.4 Effect of Antecedent IL-6 on GT1-7 Cell ATP Levels Under Euglycaemic and Hypoglycaemic Conditions 24 Hours Subsequently

The Seahorse studies did not identify a clear effect of IL-6 on whole cell bioenergetics. To further investigate whether the subtle effects of antecedent IL-6 exposure might impact on ATP production an assay was performed to directly measure whole cell ATP levels using a commercially available ATP assay (ATPLite, PerkinElmer). GT1-7 cells were exposed to vehicle dH_2O (Control) or 20 ng/ml IL-6 (IL-6) for three hours prior to seeding in a 96 well plate at a density of 10,000 cells per well. 24 hours later the cells

were subjected to three hours of 2.5 mM glucose euglycaemia (2.5 mM) or 0.1 mM glucose hypoglycaemia (0.1 mM) prior to cell lysis and ATP measurement according to the manufacturer's protocol. As predicted, in vehicle treated control cells, hypoglycaemia exposure reduced the total level of cellular ATP compared to euglycaemia (0.302 +- 0.036 vs 0.402 +- 0.009 μM ATP/10^4 cells respectively; p=0.0022) (Figure 4.4A). This would be expected due to a decrease in glucose uptake and subsequent glycolysis and mitochondrial oxidative phosphorylation. Intriguingly, antecedent IL-6 treatment led to a small, yet significant decrease in ATP levels under euglycaemic conditions compared to vehicle treated control cells (0.323 +- 0.03 vs 0.402 +- 0.009 μM ATP/10^4 cells respectively; p=0.016) (Figure 4.4A). This meant that ATP levels at euglycaemia in antecedent IL-6 treated cells were comparable with ATP levels under hypoglycaemia in vehicle treated cells (p=0.57). In response to hypoglycaemia in antecedent IL-6 treated cells a small, non-significant decrease in ATP levels was observed compared to euglycaemic levels (0.2508 +- 0.026 vs 0.323 +- 0.03 μM ATP/10^4 cells respectively, p=0.093). Hypoglycaemia reduced ATP levels to a similar percentage of euglycaemic levels in both control treated and IL-6 treated cells (75.0 and 77.6 % respectively), confirming a comparable percentage decrease in ATP levels upon hypoglycaemia exposure (Figure 4.4B).

4.2.5 Antecedent IL-6 Treatment Does Not Effect Expression of Mitochondrial Proteins 24 hours Subsequently

In the next series of studies I asked whether antecedent IL-6 treatment affected mitochondrial number. In order to give an indication of whether antecedent IL-6 treatment of GT1-7 cells induces an increase in mitochondrial number, GT1-7 cells were exposed to vehicle dH_2O (Control) or 20 ng/ml IL-6 (IL-6) for three hours and lysed 24 hours subsequently and subjected to Western blot analysis of mitochondrial protein expression. Cytochrome c oxidase or complex IV (COX IV) is the last enzyme in the mitochondrial ETC, prohibitin 1 (PHB1) is a mitochondrial protein required for optimal ETC activity (Han et al. 2014) and heat shock protein 60 (HSP60) is a mitochondrially expressed stress protein (Grundtman et al. 2011). No significant increase in protein expression of either COX IV, PHB1 nor HSP60 was observed in antecedent IL-6 treated cells compared to Control treated cells, suggesting that

antecedent IL-6 treatment does not increase or decrease the number of functional mitochondria in GT1-7 cells (Figure 4.5A-C).

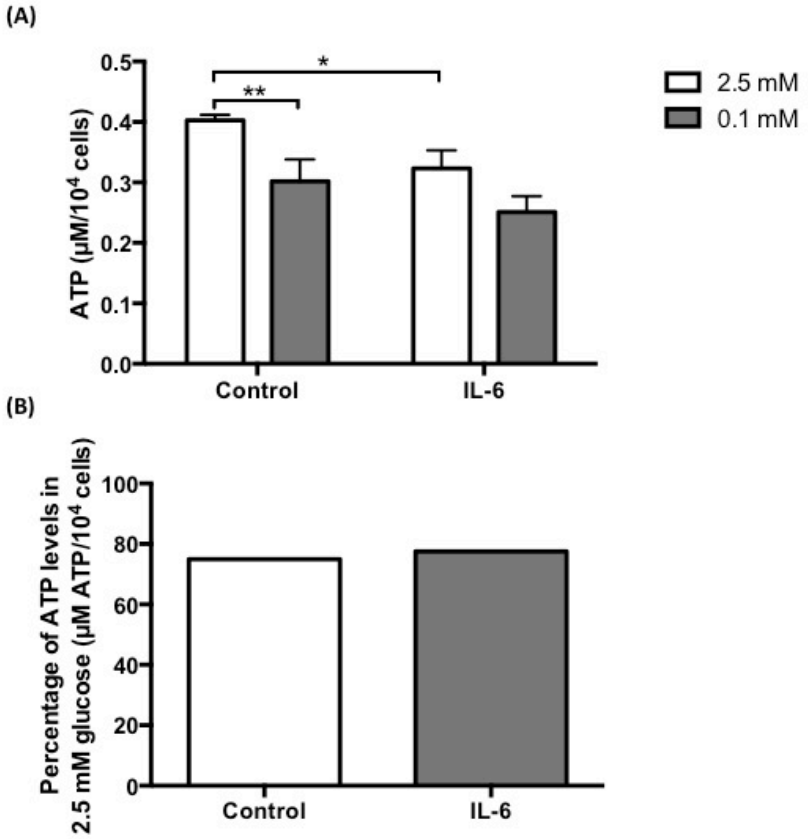

Figure 4.4 Effect of antecedent IL-6 treatment on ATP levels under euglycaemic and hypoglycaemic conditions in GT1-7 cells

GT1-7 cells were exposed to vehicle dH_2O (Control) or 20 ng/ml IL-6 (IL-6) for three hours prior to seeding in a 96 well plate at a density of 10,000 cells per well in euglycaemic plating media (2.5 mM glucose). **(A)** 24 hours later cells were exposed to 2.5 mM glucose euglycaemia (2.5 mM) or 0.1 mM glucose hypoglycaemia (0.1 mM) for three hours prior to cell lysis and ATP measurement (n=6 per group). **(B)** The percentage of 2.5 mM glucose ATP levels was determined under hypoglycaemic conditions in control vs IL-6 cells, demonstrating a similar percentage reduction in response to hypoglycaemia in both treatment groups. Data was analysed by Mann-Whitney test in **(A)** where * or ** indicate significantly different ($p=<0.05$ or $p=<0.01$ respectively). Data generated in collaboration with Kathryn Wright.

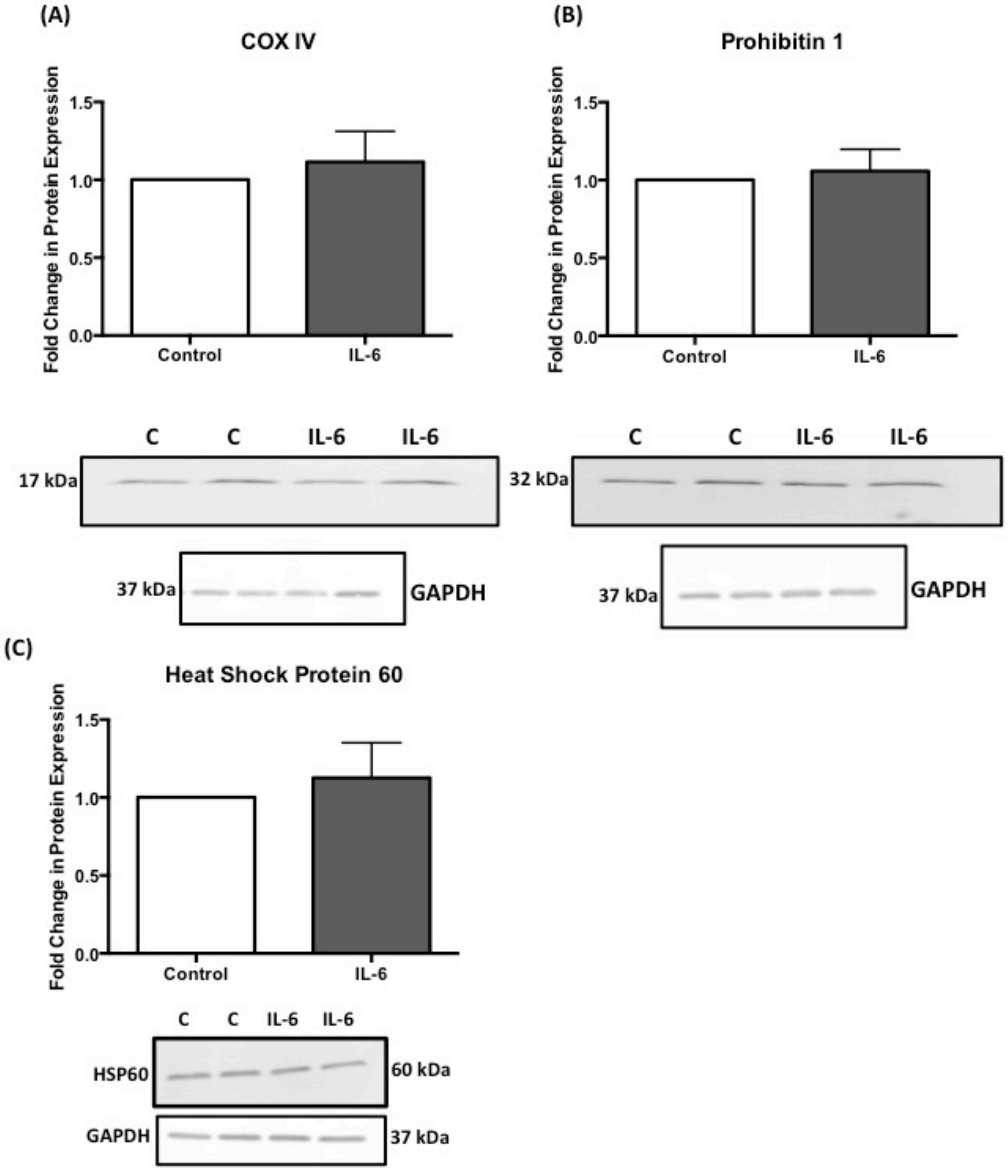

Figure 4.5 Antecedent IL-6 treatment does not effect expression of mitochondrial proteins 24 hours subsequently

GT1-7 cells were exposed to vehicle dH_2O (Control, C) or 20 ng/ml IL-6 (IL-6) for three hours and were lysed 24 hours later and processed for Western blot analysis of mitochondrial protein expression of **(A)** complex IV **(**COX IV), **(B)** prohibitin 1 (PHB1) or **(C)** heat shock protein 60 (HSP60). Fold change in protein expression relative to Control cells was determined and representative blots are shown (n=9). Representative GAPDH blots for the samples are also shown. Statistical significance was analysed by one sample t-test.

4.2.6 Antecedent IL-6 Exposure Does Not Regulate the Expression of Glycolytic Proteins 24 Hours Subsequently in GT1-7 Cells

The lack of any alterations in ECAR following antecedent IL-6 treatment in GT1-7 cells (Figure 4.1A) suggested that IL-6 does not affect glycolysis when administered in this manner. In an effort to confirm this observation, GT1-7 cells were exposed to vehicle dH_2O (Control) or 20 ng/ml IL-6 (IL-6) for three hours and lysed 24 hours subsequently and subjected to Western blot analysis of expression of several glycolytic proteins. Hexokinase 1 (HK1), pyruvate dehydrogenase (PDH) and pyruvate kinase muscle 2 (PKM2) are key enzymes of the glycolytic pathway (Li et al. 2014). No significant differences in expression of any of the four proteins investigated was observed following antecedent IL-6 treatment compared to vehicle control treated GT1-7 cells, suggesting that IL-6 administration in this manner does not regulate glycolysis in these cells (Figure 4.6A-C).

4.2.7 Effects of Antecedent IL-6 Exposure on Mitochondrial Gene Expression

To strengthen the observation that antecedent IL-6 had no effect on the expression of mitochondrial proteins, whether IL-6 regulated expression of key genes involved in mitochondrial regulation was also investigated. GT1-7 cells were exposed to vehicle dH_2O (Control) or 20 ng/ml IL-6 for 30 minutes and lysed four or 24 hours subsequently and gene expression was measured. Peroxisome proliferator-activated receptor γ co-activator 1α (PGC1α) is a positive regulator of mitochondrial biogenesis and respiration (Austin & St-Pierre 2012) and uncoupling protein 2 (UCP2) is a mitochondrial anion carrier protein which uncouples oxidative phosphorylation from ATP production by dissipating the proton gradient generated across the mitochondrial inner membrane (Toda & Diano 2014). No significant alterations in PGC1α or UCP2 expression were observed either four or 24 hours after IL-6 exposure compared to vehicle treated control cells (Figure 4.7C and D).

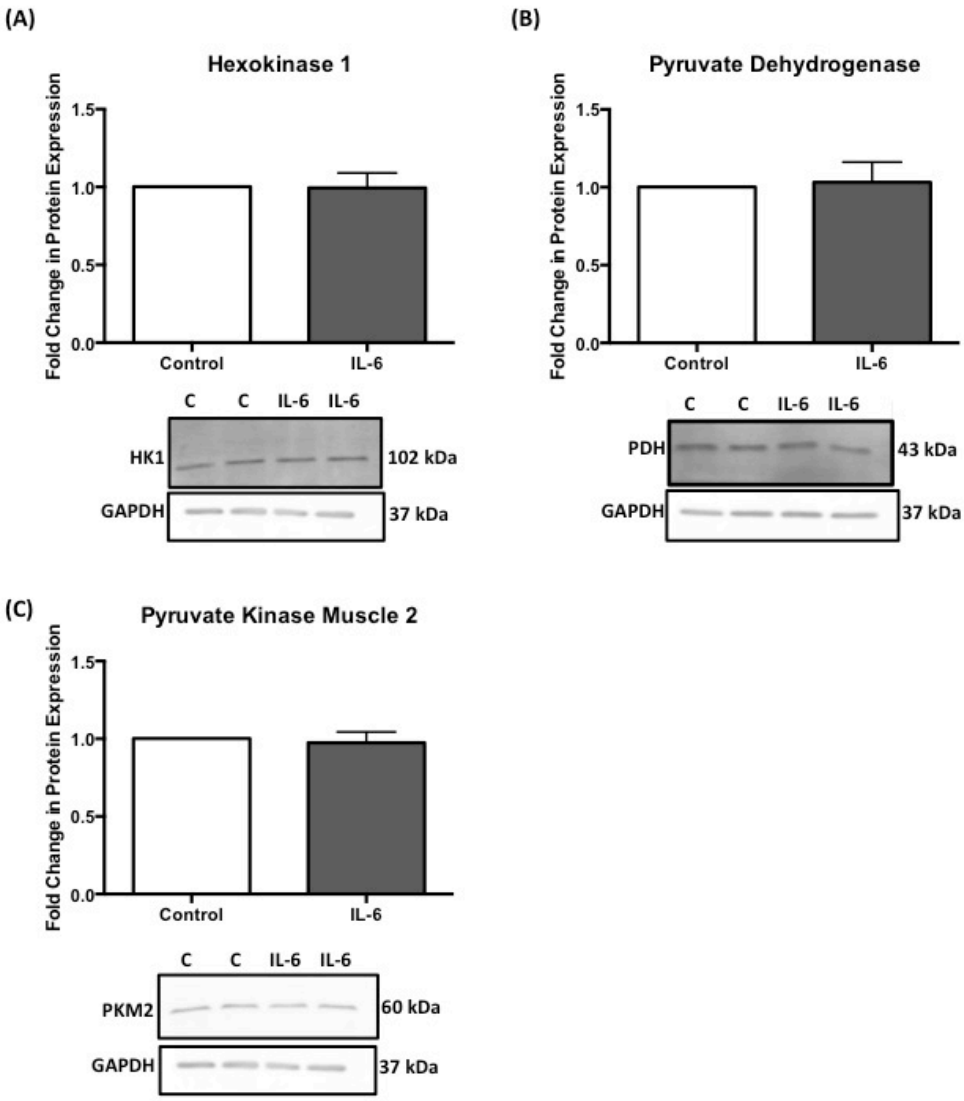

Figure 4.6 Antecedent IL-6 treatment does not effect expression of glycolytic proteins 24 hours subsequently

GT1-7 cells were exposed to vehicle dH_2O (Control, C) or 20 ng/ml IL-6 (IL-6) for three hours on day one and 24 hours later were lysed and processed for Western blot analysis of glycolytic protein expression of **(A)** hexokinase 1 (HK1), **(B)** pyruvate dehydrogenase (PDH) or **(C)** pyruvate kinase muscle 2 (PKM2). Fold change in protein expression relative to Control cells was determined and representative blots are shown (n=9). Representative GAPDH blots for the samples are also shown. Statistical significance was analysed by one sample t-test.

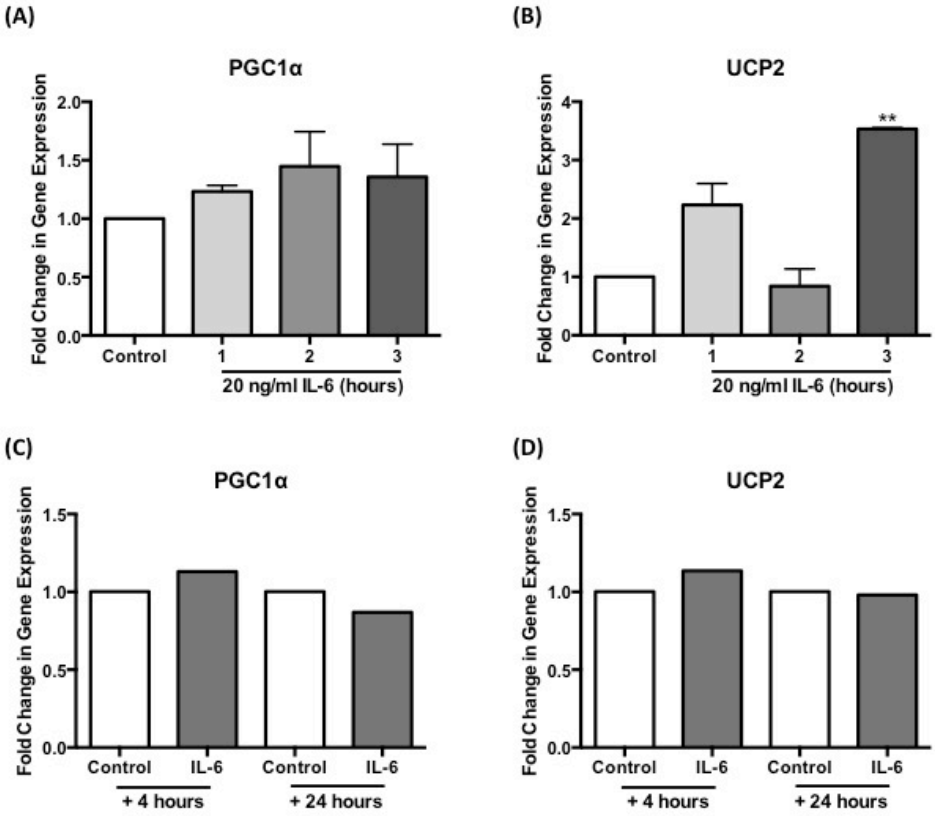

Figure 4.7 Effect of IL-6 on gene expression of mitochondrial genes PGC1α and UCP2

(A) and **(B)** GT1-7 cells were treated with vehicle dH_2O (Control) for three hours or 20 ng/ml IL-6 for one, two or three hours and lysed. RNA was extracted and used to synthesise cDNA which was subjected to Taqman qRT-PCR analysis to analyse gene expression of **(A)** PGC1α (n=2) or **(B)** UCP2 (n=2). Fold change in expression was determined relative to the expression of each gene in Control cells. **(C)** and **(D)** GT1-7 cells were treated with vehicle dH_2O (Control) or 20 ng/ml IL-6 for 30 minutes and lysed four or 24 hours subsequently. RNA was extracted and used to synthesise cDNA which was subjected to Taqman qRT-PCR analysis to analyse gene expression of **(C)** PGC1α (n=1) or **(D)** UCP2 (n=1). Fold change in expression was determined relative to the expression of each gene in Control cells. Data was analysed by one sample t-test in **(A)** and **(B)** where ** indicates $p=<0.01$.

To confirm that any effects of IL-6 on the regulation of PGC1α or UCP2 weren't missed due to the length of exposure to IL-6 or the time points at which gene expression was analysed, separate experiments were performed in which GT1-7 cells were exposed to vehicle dH_2O for three hours (Control) or 20 ng/ml IL-6 for one, two or three hours and lysed and gene expression was measured. No significant effect of IL-6 at the three time points studied on PGC1α mRNA expression was observed (Figure 4.7A), however, robust increases in UCP2 mRNA were observed after one hour and three hours exposure to IL-6 (Figure 4.7B). Interestingly, UCP2 mRNA expression after two hours IL-6 exposure was comparable with expression levels observed in Control treated cells, potentially indicating a biphasic induction of UCP2 mRNA expression in response to IL-6 stimulation in GT1-7 cells (Figure 4.7B)

4.2.8 Effects of IL-6 on Phosphorylation of STAT3 S727 in GT1-7 Cells

STAT3 is phosphorylated at residue Y705 in response to IL-6 stimulation of its receptor complex leading to nuclear translocation of STAT3 dimers and regulation of target gene expression (Wolf et al. 2014). STAT3 can also be phosphorylated at residue S727, which specifically targets STAT3 to the mitochondria where it plays a role in mitochondrial respiration (Meier & Larner 2014). To further investigate whether IL-6 regulates mitochondrial function in GT1-7 cells, the phosphorylation status of STAT3 S727 was investigated in response to IL-6 exposure. GT1-7 cells were exposed to vehicle dH_2O for three hours (Control) or 20 ng/ml IL-6 for 30 minutes or three hours and lysed and samples were prepared for Western blot analysis of phosphorylation of STAT3 at residues Y705 and S727. A separate population of GT1-7 cells were antecedently exposed to 20 ng/ml IL-6 for three hours and lysed 24 hours subsequently to determine whether antecedent IL-6 treatment affects the phosphorylation status of either of the stated STAT3 residues 24 hours subsequently. Exposure of GT1-7 cells to 20 ng/ml IL-6 for 30 minutes or three hours robustly stimulated the phosphorylation of STAT3 at residue Y705 (Figure 4.8A). These IL-6-induced increases in pSTAT3 Y705 were comparable with those observed in the initial IL-6 time course experiments performed in the previous chapter (Figure 3.1A). Antecedent exposure to IL-6 did not affect pSTAT3 Y705 levels 24 hours subsequently as levels were comparable with vehicle treated control cells (Figure 4.8A).

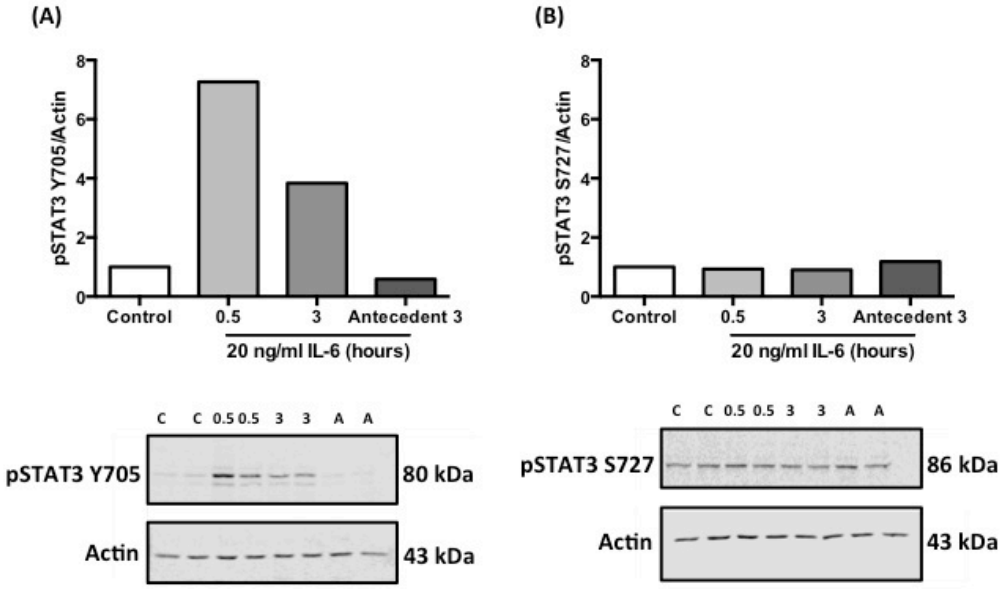

Figure 4.8 Effects of IL-6 on phosphorylation of STAT3 S727 in GT1-7 cells

GT1-7 cells were exposed to vehicle dH_2O (Control, C) for three hours or 20 ng/ml IL-6 for 30 minutes (0.5), three hours (3) or for three hours on day one and allowed to recover for 24 hours (Antecedent 3, A) then lysed and samples prepared for Western blot analysis of protein expression of pSTAT3 Y705 **(A)** and pSTAT3 S727 **(B)**. Fold change in phosphorylation of each residue was determined relative to Control treated cells normalised to actin with representative blots shown for each residue (n=1)

In contrast the same treatments had no effects on the phosphorylation status of STAT3 S727 (Figure 4.8B). Exposure to 20 ng/ml IL-6 for 30 minutes, three hours or antecedently for three hours did not affect the pSTAT3 S727 levels relative to vehicle treated control cells (Figure 4.8B). Taken together these data demonstrate that IL-6 exposure robustly increases the phosphorylation of STAT3 Y705 with no effect on STAT3 S727 phosphorylation. The lack of an increase in the phosphorylation of STAT3 S727 in response to IL-6 exposure suggests that IL-6 does not induce mitochondrial targeting of STAT3 molecules in GT1-7 cells.

4.2.9 The JAK2 Inhibitor WP1066 Prevents IL-6-Induced Phosphorylation of STAT3 Y705 but has no Effect on STAT3 S727 in GT1-7 Cells

To validate the observations regarding IL-6 regulation of STAT3 phosphorylation at residues Y705 and S727 in GT1-7 cells, the JAK2 inhibitor WP1066 was utilised to prevent the IL-6 induced phosphorylation of STAT3 Y705. Pre-exposure of GT1-7 cells to 0.5, 1 or 5 μM WP1066 for 60 minutes dose-dependently prevented subsequent 20 ng/ml IL-6-induced phosphorylation of STAT3 Y705 (Figure 4.9A). 0.5 or 1 μM WP1066 pre-exposure for 60 minutes in GT1-7 cells had no effect on subsequent STAT3 S727 phosphorylation following 20 ng/ml IL-6 exposure for 30 minutes (Figure 4.9B). There was a trend for 5 μM WP1066 pre-exposure for 60 minutes to enhance subsequent 20 ng/ml IL-6 exposure for 30 minutes to increase pSTAT3 S727 levels in GT1-7 cells, although this experiment was only performed once and would need to be repeated to consolidate this finding (Figure 4.9B). Together these data demonstrate that IL-6-induced increases in STAT3 Y705 phosphorylation occur in a JAK2-dependent manner, as pre-exposure with the JAK2 inhibitor WP1066 dose-dependently decreased IL-6-induced pSTAT3 Y705 levels. The lack of an effect of IL-6 on the regulation of pSTAT3 S727 was confirmed, and the level of pSTAT3 S727 does not appear to be regulated by JAK2, as WP1066 failed to effect STAT3 S727 phosphorylation status.

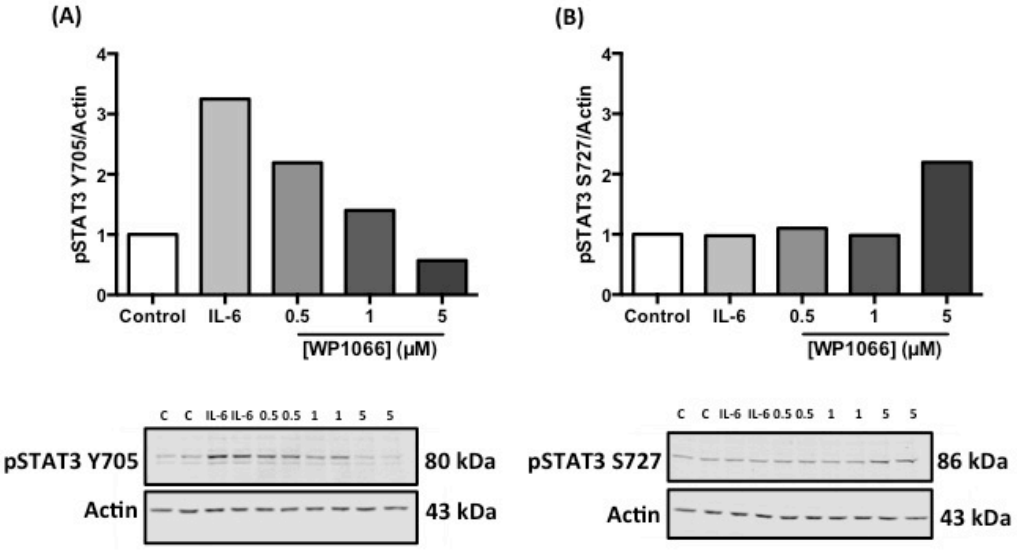

Figure 4.9 The JAK2 inhibitor WP1066 prevents IL-6 induced phosphorylation of Y705 of STAT3 but has no effect on phosphorylation of S727 of STAT3 in GT1-7 cells

GT1-7 cells were exposed to vehicles DMSO and dH_2O (Control, C) for 90 minutes, DMSO vehicle and 20 ng/ml IL-6 for 60 minutes and 30 minutes respectively (IL-6) or 0.5, 1 or 5 μM WP1066 for 60 minutes and 20 ng/ml IL-6 for 30 minutes (0.5, 1 and 5 respectively) then lysed and samples prepared for Western blot analysis of protein expression of pSTAT3 Y705 **(A)** and pSTAT3 S727 **(B)**. Fold change in phosphorylation of each residue was determined relative to Control treated cells normalised to actin with representative blots shown for each residue (n=1).

4.3 Discussion

The present results investigated the effects of IL-6 exposure on indices of GT1-7 cell metabolism. Overall, the data indicate that IL-6 does not have any significant effects to regulate metabolism in these cells. Subtle effects of IL-6 to increase mitochondrial oxygen consumption were observed, although no effects on the expression of mitochondrial genes and proteins were observed, and perhaps most conclusively, direct measurement of ATP showed no differences between vehicle treated and IL-6 treated GT1-7 cells.

There is some evidence that cytokines can act to increase neuronal oxidative phosphorylation (Habash et al. 2015). Direct effects of IL-6 on oxidative phosphorylation in neurons have not been described, although have been addressed in an adipocyte cell line (Hahn et al. 2014). When GT1-7 cells were exposed to IL-6 for three hours and studied 18-24 hours subsequently, in keeping with the model developed in the previous chapter, there was a subtle increase in mitochondrial OCR, suggestive of increased ATP production. In the adipocyte study mentioned, IL-6 only had an effect to increase basal respiration when administered for 96 hours (Hahn et al. 2014). An earlier study of the same adipocyte cell line found that IL-6 treatment reduced mitochondrial function with a reduction in ATP production (Ji et al. 2011). It may be that a much more chronic exposure to IL-6 is required to induce alterations in mitochondrial metabolism in GT1-7 cells. IL-6 preconditioning of neural stem cells has been shown to induce superoxide dismutase 2 (SOD2) expression, leading to beneficial effects on mitochondrial function by the reduction of oxidative stress (Sakata et al. 2012). In contrast however, IL-6 has been shown to induce expression of free radicals in the brain (Behrens et al. 2008) one of which, NO, is a potent inhibitor of COX IV (Brown 1995; Giuffrè et al. 1996) and therefore induces mitochondrial dysfunction. Administration of antioxidants in a rat model of sepsis improved mitochondrial respiration and decreased IL-6 levels, suggesting an association between IL-6 and mitochondrial dysfunction (Lowes et al. 2013). The literature regarding the role of IL-6 in the regulation of neuronal metabolism is therefore mixed and warrants further investigation.

Studies have shown that IL-6 can enhance glycolysis in mouse embryonic fibroblasts and human cell lines, with IL-6 induced activation of STAT3 enhancing the expression

of the glycolytic enzymes HK2 and 6-phosphofructo-2-kinase/fructose-2,6-bisphosphatase-3 (PFKFB3) (Ando et al. 2010). The IL-6 family cytokine LIF was found to down-regulate expression of HK2 and increase the expression of fructose 1, 6 bisphosphatase 1 in AtT-20 corticotrope cells, while in GH_3 somatolactotrope cells LIF induced expression of 6-phosphofructokinase C, suggesting opposite effects of LIF on glycolysis in the two cell types (Abbud et al. 2004). IL-6 subtly increased glycolysis in hepatocytes, indexed by an increase in lactate release over control treated cells (Vaartjes et al. 1990). However, neurons have a relatively low glycolytic capacity caused by a lack of activity of the glycolysis-promoting enzyme PFKFB (Bolaños et al. 2010; Pellerin & Magistretti 2012). In the present studies no significant effect of IL-6 on ECAR, a measure of lactate acidification of the extracellular media, was observed. Further insight into the role of IL-6 in the regulation of glycolysis could have been gained by performing assays to measure glucose uptake and HK activity.

There are reports demonstrating that ATP can induce astrocytes to produce and release IL-6 (Noguchi et al. 2013) but whether IL-6 stimulation of CNS cell types regulates ATP levels has not been studied. In the study investigating OSM effects in cortical neurons, Chang *et al.* demonstrated stimulation of ATP production by OSM indexed by increased OCR measured using the XF24, but a direct measurement of ATP in this study was not made (Chang et al. 2015). In a recent study by Yang *et al.* IL-6 enhanced mitochondrial membrane potential in CD4 cells but this was uncoupled from oxidative phosphorylation and therefore ATP synthesis (Yang et al. 2015). In the current experiments, a significant reduction in ATP levels at euglycaemia was observed in IL-6 treated cells compared to vehicle treated control cells, such that ATP levels at euglycaemia following IL-6 treatment were comparable with levels observed under hypoglycaemia following vehicle treatment. Based on the defective glucose sensing phenotype of GT1-7 cells following antecedent IL-6 exposure, it was hypothesised that an increase in, or maintenance of, ATP levels may be responsible for maintaining the closed state of K_{ATP} channels during subsequent hypoglycaemia. After exposure to hypoglycaemia following antecedent IL-6 treatment, a decrease in ATP levels was observed compared to euglycaemia, importantly of similar magnitude to that observed in vehicle treated cells, suggesting that ATP levels do fall in response to hypoglycaemia even after IL-6 treatment. It is unlikely therefore that increased ATP production or maintenance of ATP levels is mediating the effects of IL-6 to induce defective glucose

sensing. It is important to note however that ATP levels were measured following exposure to 0.1 mM glucose for three hours, a much more profound hypoglycaemic challenge than the 0.5 mM glucose exposure for 15 minutes employed during electrophysiological analysis. This discrepancy is due to differences in sensitivity of the techniques. GT1-7 cells have been demonstrated to respond to low glucose challenge in a dose-dependent manner (Beall, Hamilton, et al. 2012), and based on this 0.5 mM glucose was selected as the glucose concentration that induced a robust membrane hyperpolarisation in the majority of cells. Electrophysiology permits a highly sensitive, rapid measure of single cell membrane responses to hypoglycaemia. In contrast, the ATP assay involves making a measurement from a population of cells that likely exhibit a heterogeneous response to hypoglycaemia, and therefore, a more robust hypoglycaemic exposure was employed to ensure a decrease in ATP levels was observed in response to hypoglycaemia in vehicle treated cells. To indicate whether ATP levels are maintained at hypoglycaemia during electrophysiological recordings following antecedent IL-6 exposure, ATP levels should be measured after 15 minutes exposure to 0.5 mM glucose, making the two studies directly comparable. The more profound hypoglycaemic challenge induced for the ATP assay may have over ridden any IL-6-induced adaptations conferring GT1-7 cells an ability to preserve cellular ATP levels during subsequent hypoglycaemia.

Expression of mitochondrial protein expression was investigated in GT1-7 cells 24 hours after IL-6 exposure to indicate whether IL-6 increased the number of mitochondria. No effects of IL-6 exposure were observed on the expression levels of COX IV, PHB1 or HSP60. This is in accordance with the study by Hahn *et al.* where they found no change in COX IV protein expression in 3T3-L1 adipocytes in response to IL-6 exposure for 24, 48 or 96 hours (Hahn et al. 2014). Four weeks of IL-6 overexpression in a mouse model of cancer cachexia reduced muscle COX IV protein expression by 57%, but no effect of IL-6 overexpression for 10 weeks on COX IV expression was observed in WT mice (White et al. 2011). In the current study, PHB1 simply served as a mitochondrial protein whose expression could be quantified to give an indication of mitochondrial number, however, it has been shown to be upregulated by eight hours IL-6 exposure in an intestinal epithelial cell line, with STAT3 binding to the promoter region of the PHB1 gene observed (Theiss et al. 2007). Another study showed that IL-6 protected cardiomyocytes from hydrogen peroxide induced injury by

upregulation of PHB1 via STAT3 phosphorylation (Jia et al. 2012). Consistent with the expression levels of PHB1 being unchanged by IL-6 exposure, expression of another mitochondrial protein, HSP60, was also unchanged by IL-6 stimulation in GT1-7 cells, supporting the suggestion that IL-6 does not affect mitochondrial number.

The lack of an effect of IL-6 on ECAR measurements suggested that IL-6 did not regulate glycolytic rate in GT1-7 cells. The protein expression of three key glycolytic enzymes was investigated to confirm the Seahorse findings. No induction of HK1, PDH or PKM2 was observed 24 hours after IL-6 exposure in GT1-7 cells, indicating that this treatment had no effect on glycolysis. HK1 is expressed in all mammalian tissues, with high expression observed in the brain (Wilson 2003). HK expression was found to be increased in brain following recurrent hypoglycaemia (Osundiji et al. 2011). Its expression has been demonstrated in GT1-7 cells (Beall, Hamilton, et al. 2012) and in the current work its expression was not regulated by antecedent IL-6 exposure. IL-6 regulates the phosphorylation of PDH in mouse skeletal muscle but not total protein expression of PDH, consistent with the observations in the current work (Biensø et al. 2014). Examining the phosphorylation status of PDH would have given an indication of its activity, and therefore substrate delivery to the mitochondria, which could be addressed in future studies. Antecedent IL-6 exposure did not regulate expression of PKM2 measured 24 hours later, and IL-6 regulation of PKM2 has not been described elsewhere.

PGC1α and UCP2 are two key genes involved in mitochondrial regulation. PGC1α is the major regulator of mitochondrial biogenesis (Austin & St-Pierre 2012). Its expression was investigated in response to IL-6 stimulation to further investigate whether IL-6 regulated mitochondrial number in GT1-7 cells. In a recent study, IL-6 gene delivery has been shown to upregulate mRNA and protein expression of PGC1α and mRNA expression of UCP2 in BAT (Ma et al. 2015). In the current work antecedent IL-6 exposure did not regulate the expression of PGC1α 24 hours subsequently, indicating that IL-6 does not affect mitochondrial biogenesis when administered in this manner, and therefore that increased mitochondrial number is unlikely to mediate the effects of IL-6 to induce defective glucose sensing in GT1-7 cells. This finding was further verified by exposure to IL-6 for one, two or three hours failing to significantly affect expression of PGC1α mRNA in GT1-7 cells. It is important to note however that in the antecedent IL-6 exposure model used to

investigate mRNA expression, IL-6 exposure was only for a duration of 30 minutes rather than the previously used three hour model, and therefore is not directly comparable with the electrophysiological and Seahorse studies. In porcine adipocytes, IL-6 was found to upregulate PGC1α mRNA expression but only at 50 ng/ml or 100 ng/ml for 48 hours, suggesting that a more chronic exposure to IL-6 may regulate PGC1α (Yang et al. 2008).

UCP2 is a major regulator of mitochondrial ATP production, as it uncouples oxidative phosphorylation from ATP production by dissipating the proton gradient generated across the mitochondrial inner membrane (Toda & Diano 2014). UCP2 has been shown to be important in the CNS in the regulation of food intake, energy expenditure, glucose homeostasis and reward behaviours (Toda & Diano 2014). In the antecedent IL-6 exposure model, no effect of IL-6 exposure on mRNA expression of UCP2 24 hours subsequently was observed. Interestingly however, robust increases in UCP2 mRNA expression were observed when GT1-7 cells were exposed to IL-6 for one or three hours, suggesting that acutely IL-6 may increase mitochondrial uncoupling and therefore reduce ATP production. Intriguingly, IL-6 exposure for two hours did not increase UCP2 mRNA levels compared to vehicle treatment, indicative of a biphasic regulation of UCP2 mRNA expression by IL-6 in GT1-7 cells. The acute effects of IL-6 on UCP2 mRNA expression are pronounced, however they do not correlate with the functional XF24 data where antecedent IL-6 exposure did not affect mitochondrial proton leak OCR compared to vehicle treated cells, although these measurements were not made at the same time point. It would be of interest to perform the XF24 analysis after either a one or three hour exposure to IL-6, to see if the effects of IL-6 exposure for these times on UCP2 mRNA levels have functional consequences on mitochondrial bioenergetics. A rat *in vivo* study showed that chronic IL-6 administration for 14 days increased UCP2 protein expression in skeletal muscle, supporting a role for IL-6 in the regulation of UCP2 (Holmes et al. 2008). 50 ng/ml and 100 ng/ml IL-6 for 48 hours increased UCP2 mRNA in porcine adipocytes (Yang et al. 2008). An increase in UCP2 mRNA may only be of physiological relevance if the message is transcribed into functional protein that can exert biological effects. UCP2 protein expression in response to IL-6 stimulation could be determined by Western blot analysis to investigate if the IL-6 effects of mRNA are consistent with an increase in protein expression.

S727 phosphorylation of STAT3 assigns the protein mitochondrial regulatory functions independent of its transcriptional activity (Reich 2009). To further investigate whether IL-6 exerts metabolic regulation, particularly via mitochondrial metabolism, the phosphorylation of S727 of STAT3 was investigated. Experiments demonstrated that IL-6 does not regulate the phosphorylation of STAT3 S727 in GT1-7 cells, with an induction of STAT3 Y705 providing a positive control for IL-6 stimulation of GT1-7 cells. Furthermore, inhibition of JAK2 with WP1066 prevented Y705 phosphorylation of STAT3 induced by IL-6 but had no effect on S727 phosphorylation, which remained at a basal level in response to IL-6 alone, or in response to IL-6 after pretreatment with WP1066. This is in keeping with data demonstrating that ERK, JNK and PKCδ are involved in the phosphorylation of S727 of STAT3 rather than JAKs (Eulenfeld et al. 2012). The lack of an increase in STAT3 S727 phosphorylation in response to IL-6 stimulation of GT1-7 cells suggests that there is no induction of mitochondrial targeting of STAT3, further complementing the above data indicating that IL-6 does not exert significant regulatory effects on GT1-7 cell metabolism.

Comparisons can be made between the current work and the recent study by Chang *et al.* investigating OSM exposure in rat cortical neurons (Chang et al. 2015). In their study, they described an OSM pathway to increase mitochondrial ATP production via a JAK1/2-STAT1/3 and CREB mediated induction of Mcl-1. In the current work, IL-6 has been demonstrated to increase STAT3 phosphorylation via JAK2, and also increase CREB phosphorylation (data in following chapter). The increases in mitochondrial OCR in response to IL-6 were only moderate in this work, however based on the OSM pathway described, it would be of interest to investigate Mcl-1 expression as another indicator of enhanced mitochondrial respiratory capacity. In the Chang *et al.* paper, the OSM effects on mitochondrial function were shown to confer neuroprotection against 3-NP-induced toxicity. In GT1-7 cells the IL-6 effects described may confer protection against hypoglycaemic stress, with the adverse complication of inducing defective glucose sensing.

The data presented in this chapter do not implicate a role for IL-6 in the regulation of GT1-7 whole cell bioenergetics or metabolism. Functional XF24 assays failed to identify a significant effect of IL-6 on either OCR or ECAR 24 hours subsequently. This finding was supported by studies showing no change in expression of mitochondrial or glycolytic protein expression, suggesting that IL-6 did not increase

mitochondrial number in GT1-7 cells. IL-6 acutely increased expression of UCP2 at the mRNA level, but the effect did not persist 24 hours subsequently, the time point at which cells were studied electrophysiologically. A lack of alteration in OCR directed towards maintaining the mitochondrial leak in XF24 studies complemented this observation. Investigation of the phosphorylation status of the S727 site of STAT3 ruled out a mitochondrial targeting of this signal transducing molecule in response to IL-6 stimulation in GT1-7 cells, further invalidating a role for IL-6 in the regulation of metabolism in GT1-7 cells. Furthermore, direct measurement of cellular ATP levels 24 hours after IL-6 exposure demonstrated a decrease in ATP in response to hypoglycaemia. This suggested that enhanced ATP production or maintenance of ATP levels during acute hypoglycaemia exposure was unlikely to mediate the closed state of K_{ATP} channels and conserved membrane depolarisation observed in the prior electrophysiological studies during hypoglycaemia following antecedent IL-6 treatment. Taken together these data suggest that antecedent IL-6 exposure does not result in defective hypoglycaemia detection 24 hours later by altering whole cell bioenergetics or metabolism. The findings do not rule out an acute regulation of metabolism by IL-6, as functional measurements of bioenergetics and ATP levels were only made 24 hours after exposure to IL-6. Similarly, a more chronic exposure to the cytokine (e.g. over 24 hours) may also modulate cellular metabolism, as has been observed elsewhere (Hahn et al. 2014). Therefore, studies were performed to address other potential mechanisms by which antecedent IL-6 exposure may mediate its effects on glucose sensing, with focus turning more directly on the K_{ATP} channel.

5 The Role of EPAC2 in the Regulation of Glucose Sensing by IL-6

5.1 Introduction

A role for IL-6 in the regulation of GT1-7 cell metabolism and ATP production was not confirmed, suggesting that IL-6-induced suppression of GT1-7 glucose sensing ability was mediated by an alternative mechanism. Attention was focused on more direct mechanisms of K_{ATP} channel regulation.

Aside from intracellular nucleotide modulation of the K_{ATP} channel, other regulators of channel function, such as post translational modifications, have been described (Dzeja & Terzic 1998; Yang et al. 2014). Hormonal regulation of K_{ATP} has also been uncovered, with leptin regulating channel trafficking (Holz et al. 2013) and β-estradiol decreasing K_{ATP} channel activity in beta-cells (Soriano et al. 2011). Discovered in 1998 (de Rooij et al. 1998; Kawasaki et al. 1998) exchange proteins activated by cAMP (EPACs), of which there exists two isoforms, EPAC1 and EPAC2, are guanine-nucleotide-exchange factors for the Ras-like small GTPases Rap1 and Rap2 (Breckler et al. 2011). They function as intracellular sensors that, along with the classic protein kinases As (PKAs), transduce the effects of the second messenger cyclic AMP (cAMP). Both PKAs and EPACs have roles in energy homeostasis (Almahariq et al. 2014). Importantly, an EPAC2-selective activator has been shown to potentiate first and second phase insulin secretion from mouse, rat and human pancreatic beta-cells (Kelly et al. 2009; Chepurny et al. 2009). The importance of EPAC2 in GLP-1-induced insulin secretion was demonstrated with the finding that in $EPAC2^{-/-}$ mice the effects of the GLP-1 analogue E4 to enhance insulin secretion were significantly reduced (Song et al. 2013). Interestingly, EPAC2 may potentially participate in the CRR to hypoglycaemia by promoting the production of glucagon, as EPAC2 has been demonstrated to regulate pro-glucagon gene expression in intestinal cells, pancreatic alpha-cells and hypothalamic neurons (Lotfi et al. 2006; D. Islam et al. 2009; Dalvi et al. 2012). EPAC has been shown to regulate K_{ATP} channel ATP-sensitivity in human pancreatic beta-cells and rat INS-1 cells (G. Kang et al. 2008). This is an important finding as it means that EPAC can modulate the function of K_{ATP} channels independently of a change in absolute ATP levels. The same group subsequently demonstrated that EPAC was capable of facilitating sulphonylurea-mediated inhibition of K_{ATP} channels in human

pancreatic beta-cells and rat INS-1 cells (Leech et al. 2010). Of particular interest was the recent demonstration that EPAC interacts directly with the SUR1 subunit of K_{ATP} channels in mouse synaptosomes (Zhao et al. 2013). Taking together the observations that EPAC potentiates insulin secretion and regulates pancreatic beta-cell K_{ATP} activity, and interacts directly with SUR1 in mouse synaptosomes, it was hypothesised that an increase in EPAC expression or activity may mediate the effects of antecedent IL-6 exposure to induce defective hypoglycaemia detection in GT1-7 cells.

To test this hypothesis, firstly the expression of the two isoforms of EPAC proteins was determined in GT1-7 cells and subsequently it was investigated whether IL-6 could regulate the cAMP signalling pathway in these cells. Immunoprecipitation experiments were performed to identify if EPAC interacted with the K_{ATP} channel in GT1-7 cells and electrophysiology was employed to assess the effects of EPAC on K_{ATP} channel activity.

5.2 Results

5.2.1 IL-6 Increases CREB Phosphorylation in GT1-7 Cells

In the aforementioned work of Kelly and co-workers, a robust increase in the phosphorylation of CREB was observed in skeletal muscle incubated with IL-6. This was associated with an increase in cAMP, and they proceeded to demonstrate that the action of IL-6 to increase α2 AMPK activity was dependent on increases in the intracellular levels of cAMP, as an adenyl cyclase inhibitor prevented these effects of IL-6 (Kelly et al. 2009). In the current work in GT1-7 cells, exposure to 20 ng/ml IL-6 for five-180 minutes increased the phosphorylation of CREB at serine 133 (S133) and this effect almost reached statistical significance upon exposure to IL-6 for 30 minutes (Figure 5.1). Interestingly, the observed increase in pCREB does not appear to lead to increased AMPK activity as has been shown in skeletal muscle (Kelly et al. 2009) as there was no significant effect of IL-6 to increase pAMPK at T172 in GT1-7 cells (Chapter 3, Figure 3.1D).

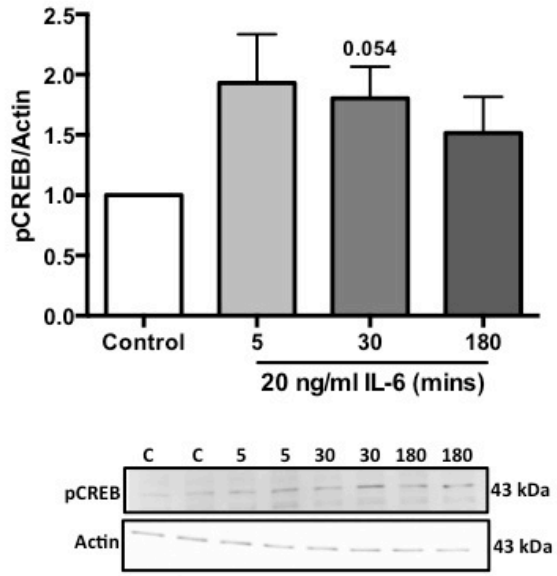

Figure 5.1 IL-6 increases pCREB S133 phosphorylation in GT1-7 cells

GT1-7 cells were serum starved for two hours in the presence of 2.5 mM glucose prior to exposure to vehicle dH_2O (Control, C) for three hours or 20 ng/ml IL-6 for the indicated times. Cells were lysed and samples prepared for Western blot analysis of protein expression of pCREB S133 (n=4). Fold change in phosphorylation was determined relative to Control treated cells normalised to actin and a representative blot is shown. Statistical significance was determined relative to control by one sample t-test with p values approaching significance displayed above the appropriate bars on the graph.

5.2.2 IL-6 Exposure Leads to a Subtle Increase in cAMP in GT1-7 Cells

Given the increase in pCREB levels observed with IL-6 treatment, it would be expected that upstream of CREB, an increase in levels of cellular cAMP would be observed. To investigate this, GT1-7 cells were exposed to vehicle dH_2O (Control) or 20 ng/ml IL-6 (IL-6) for three hours prior to lysis and cAMP measurement using a commercially available assay (Direct cAMP ELISA, Enzo). IL-6 trended towards increasing cellular cAMP levels compared to vehicle treated control cells, although this did not reach statistical significance (p=0.41) (Figure 5.2). The trend towards an increase in cAMP in IL-6 treated cells is supported by the observation that IL-6 also leads to increases in pCREB levels, and taking these data together suggest that IL-6 increases the cAMP-pCREB signalling axis in GT1-7 cells.

5.2.3 EPAC2, But Not EPAC1, is Expressed in GT1-7 Cells But its Expression is Not Regulated by IL-6

The major intracellular functions of cAMP are transduced by PKA and EPACs. Interestingly, the roles of both PKA, and more recently EPACs, in energy homeostasis have been studied (Almahariq et al. 2014). Crucially, EPAC2 has been shown to play a critical role in the potentiation of insulin secretion from mouse, rat and human pancreatic beta-cells (Chepurny et al. 2009; Almahariq et al. 2014; Chepurny et al. 2010). This led to the hypothesis that EPAC2 may mediate functions of IL-6-induced increases in cAMP, potentially involving a regulation of K_{ATP} channels and therefore membrane excitability in GT1-7 cells.

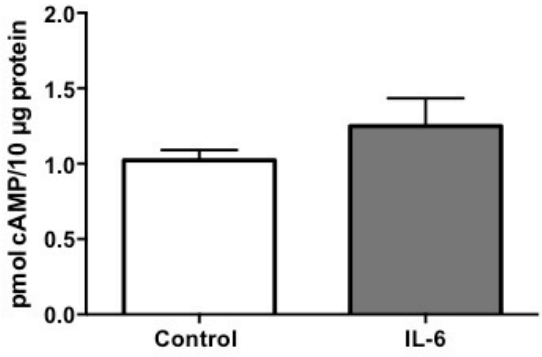

Figure 5.2 IL-6 exposure leads to a subtle increase in cAMP in GT1-7 cells

GT1-7 cells were exposed to vehicle dH_2O (Control) or 20 ng/ml IL-6 (IL-6) for three hours prior to cell lysis and cAMP measurement using a commercially available assay, performed according to the manufacturer's protocol (Direct cAMP ELISA, Enzo) (n=5). Data was analysed by Mann-Whitney test ($p=0.41$). Data generated in collaboration with Kathryn Wright.

Initially, the protein expression of the two EPAC isoforms, EPAC1 and EPAC2, and whether their expression was regulated by IL-6 was determined in GT1-7 cells. GT1-7 cells were exposed to vehicle dH_2O (Control) or 20 ng/ml IL-6 (IL-6) for three hours and were lysed 24 hours subsequently, in keeping with the antecedent IL-6 exposure model in which the negative effects of IL-6 on GT1-7 glucose sensing were observed. Samples were prepared and subjected to Western blot analysis of protein expression of EPAC1 and EPAC2. In GT1-7 cells, EPAC1 protein expression was undetected, however EPAC2 was expressed (Figure 5.3A and B). To confirm that the antibody used to detect EPAC1 was indeed capable of doing so, a mouse brain sample was run alongside GT1-7 samples and EPAC1 expression was detectable in mouse brain tissue (Figure 5.3A). There was no difference observed in EPAC2 expression between vehicle treated and IL-6 treated cells, demonstrating that antecedent IL-6 exposure does not regulate the expression level of EPAC2 protein 24 hours subsequently in GT1-7 cells (Figure 5.3B).

5.2.4 A Proportion of EPAC2 is Associated with K_{ATP} Channels in GT1-7 Cells

Given the existing data demonstrating that EPAC regulates K_{ATP} channel activity in human beta-cells and rat INS-1 cells (G. Kang et al. 2006; G. Kang et al. 2008; Leech et al. 2010), and that EPAC is able to bind directly to SUR1 in mouse synaptosomes (Zhao et al. 2013), the question was posed whether EPAC2 associates with the K_{ATP} channel in GT1-7 cells. To answer this question GT1-7 cells were treated with vehicle dH_2O (Control) or 20 ng/ml IL-6 (IL-6) for three hours and lysed 24 hours subsequently and subjected to a immunoprecipitation (IP) experiment whereby the SUR1 subunit of the K_{ATP} channel was immunoprecipitated out of the cell lysates using a SUR1 NBD2 specific monoclonal antibody. The aims of the experiment were to determine firstly whether EPAC2 co-immunoprecipitates with SUR1 from GT1-7 cells, thereby confirming an interaction between EPAC2 and the K_{ATP} channel, and secondly whether the degree of interaction between the two was regulated by IL-6. The results demonstrated that EPAC2 co-immunoprecipitated with the K_{ATP} channel in GT1-7 cells (Figure 5.4A, IP fractions). However, quantification of this interaction by densitometry demonstrated that there was no significant difference in the amount of EPAC2 associated with the channel in IL-6 treated cells compared to vehicle treated control cells (p=0.33, Figure 5.4B).

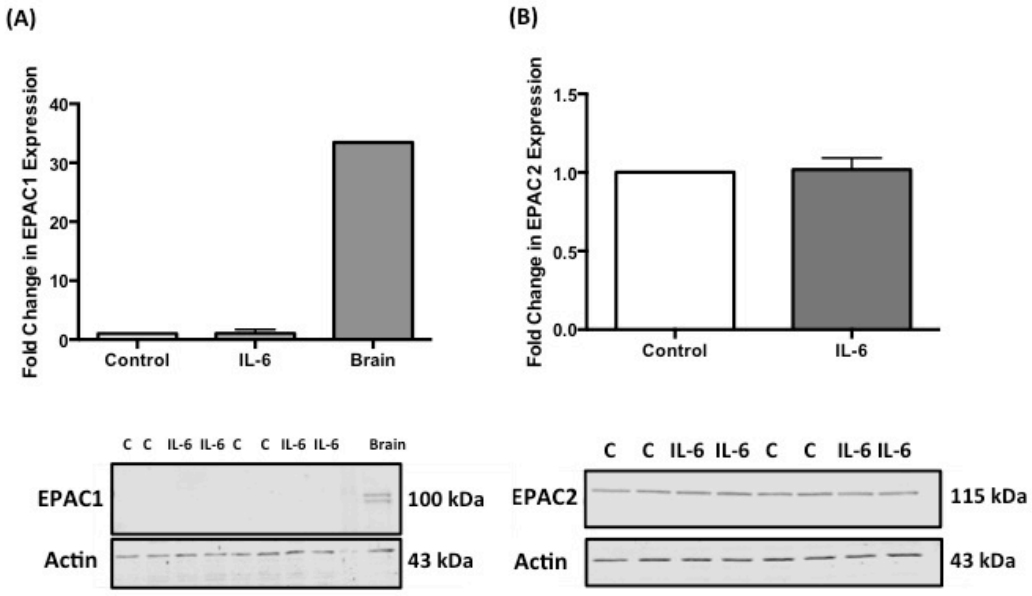

Figure 5.3 EPAC2 but not EPAC1 protein is expressed in GT1-7 cells but its expression is not regulated by IL-6

GT1-7 cells were exposed to vehicle dH_2O (Control, C) or 20 ng/ml IL-6 (IL-6) for three hours and were lysed 24 hours subsequently and samples were prepared for Western blot analysis of EPAC1 **(A)** and EPAC2 **(B)** protein expression (n=2). A mouse brain sample expressing EPAC1 was used as a positive control for EPAC1 expression. Data in **(B)** was analysed by one sample t-test (p=0.84).

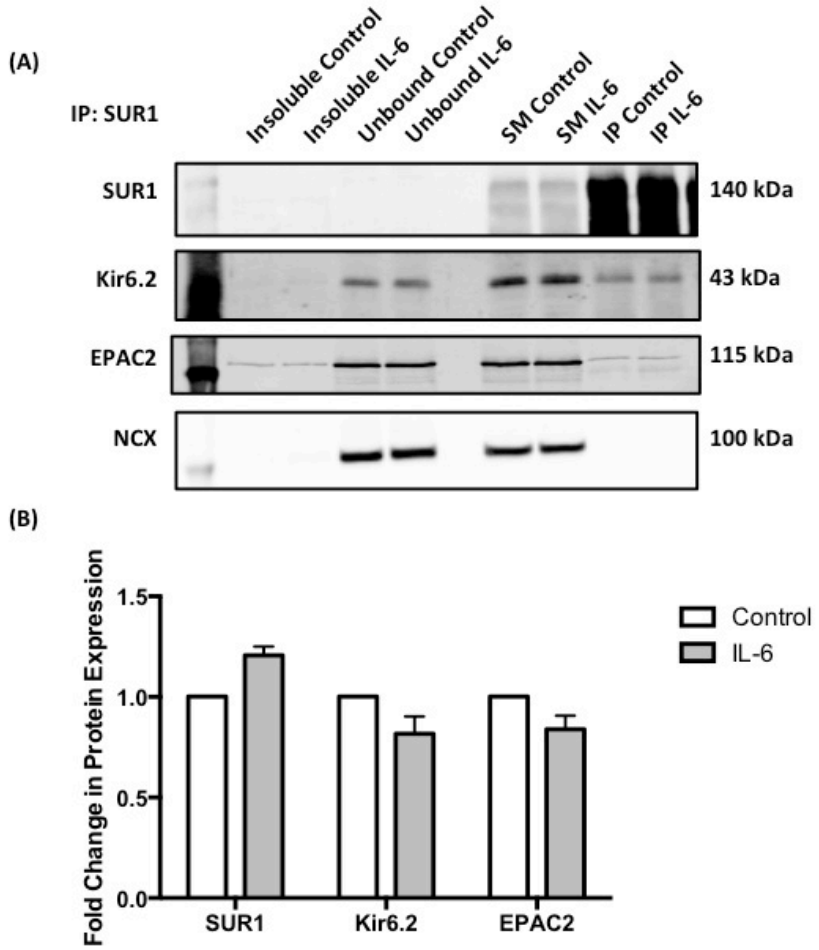

Figure 5.4 A proportion of EPAC2 is associated with K_{ATP} channels in GT1-7 cells but the amount of association is not regulated by IL-6

GT1-7 cells were exposed to vehicle dH_2O (Control) or 20 ng/ml IL-6 (IL-6) for three hours on day 1 and lysed 24 hours subsequently and an immunoprecipitation (IP) experiment was performed from the lysates using a mouse SUR1 NBD2 specific monoclonal antibody (detailed in Methods). Fractions were obtained throughout the protocol and subsequently subjected to Western blot analysis to determine expression of SUR1, Kir6.2, EPAC2 and sodium-calcium exchanger (NCX) in each fraction (n=2). NCX served as a negative control, a protein known not to interact with SUR1 or Kir6.2 of the K_{ATP} channel. The insoluble fraction was obtained by resuspending the pellet from the centrifuged cell lysates in sample buffer before starting the IP (Insoluble). A portion of the supernatant from this centrifugation step was used as the Starting Material fraction (SM). After overnight incubation IP reactions were centrifuged and a proportion of the supernatant was obtained as the unbound fraction (Unbound). Finally, the IP fraction (IP) consisted of the complex of antibody and capture beads and any associated proteins. Representative Western blots for each protein of interest are shown in **(A)** with quantification of the fold change in abundance of each protein in the IL-6 treated IP fractions relative to vehicle treated control cells in **(B)** (n=2). Data was analysed for each protein in **(B)** by one sample t-test relative to control.

In the current experiments, fractions were taken at several intervals throughout the IP. Initially, a representative fraction of the supernatant from the cell lysates following centrifugation was taken prior to starting the IP to demonstrate presence of proteins in the sample at the beginning of the procedure from which the IP would be performed (Starting Material). The pellet from this centrifugation step served as the fraction allowing determination of any protein that was not soluble in the cell lysate (Insoluble). Following the overnight reaction, IPs were centrifuged to pellet the complex of capture beads, antibody and associated proteins (IP), while the supernatant contained any protein that did not form this complex (Unbound). After Western blot analysis of protein expression in the above fractions the amount of EPAC2 protein co-immunoprecipitated from GT1-7 cell lysates could be determined and compared between control and IL-6 treated reactions. The sodium calcium exchanger (NCX) served as a negative control in the current work as it is a cell membrane localised protein that does not interact with the K_{ATP} channel, and its utility as a negative control was confirmed by an absence of any NCX expression in the IP fractions, with all NCX remaining in the Unbound fraction (Figure 5.4A).

The results from the IP experiment confirm that SUR1 is associated with Kir6.2 in GT1-7 cells, forming functional K_{ATP} channels, and that a proportion of EPAC2 is associated with the K_{ATP} channel in GT1-7 cells. Furthermore, antecedent IL-6 treatment did not affect the association of EPAC2 with the channel 24 hours subsequently in these cells.

5.2.5 EPAC2 Inhibition Prevents Antecedent IL-6-Induced Defective Glucose Sensing in GT1-7 Cells

EPAC2 expression and association with K_{ATP} was confirmed in GT1-7 cells, and although antecedent IL-6 treatment did not regulate the expression level or association of EPAC2 with K_{ATP} channels, the possibility remained that IL-6 potentially regulates EPAC2 activity. The key question to address therefore was whether the effect of antecedent IL-6 to induce defective detection of subsequent hypoglycaemia in GT1-7 cells was mediated by EPAC2. Studies have demonstrated that enhanced EPAC activity increases the ATP-mediated inhibition of K_{ATP} channels (G. Kang et al. 2008). In the current work, the potent, selective EPAC2 inhibitor HJC 0350 was used to selectively inhibit EPAC2 activity in GT1-7 cells during antecedent vehicle dH_2O (Control) or 20 ng/ml IL-6 treatment (IL-6) for three hours. Treated cells were assayed

electrophysiologically 18-24 hours subsequently and were subjected to a 0.5 mM glucose hypoglycaemic challenge during perforated patch current clamp recording. Control cells were exposed only to the vehicles in which HJC 0350 and IL-6 were delivered for three hours, which were DMSO at a dilution of 1:1000 and dH_2O at 1:250 respectively. When subjected to a hypoglycaemic challenge 18-24 hours subsequently, vehicle treated cells hyperpolarised from an average resting membrane potential in 2.5 mM glucose of -56.1 +- 2.2 mV, by -3.4 +- 2.2 mV on average to -59.6 +- 1.6 mV, and ceased action potential firing rates upon detection of the hypoglycaemic stimulus (Figure 5.5A and C). Importantly, GT1-7 cells treated antecedently with 0.5 μM HJC 0350 and 20 ng/ml IL-6 for three hours exhibited a similar resting membrane potential in 2.5 mM glucose of -53.3 +-2.1 mV, and also hyperpolarised by -3.0 +- 2.5 mV on average to -56.3 +- 3.8 mV, and ceased action potential firing rates, thereby demonstrating physiological responses to hypoglycaemia comparable to those observed in vehicle treated cells (Figure 5.5B and C). This is in stark contrast to the defective glucose sensing response of GT1-7 cells exposed to antecedent IL-6 treatment alone as described in Chapter 3 (Chapter 3, Figure 3.5B and C). These data suggest that EPAC2 is a potential mediator of the defective glucose sensing induced by antecedent IL-6 treatment, as co-application of the EPAC2 inhibitor HJC 0350 during antecedent IL-6 exposure prevents the development of defective glucose sensing of subsequent hypoglycaemia in GT1-7 cells.

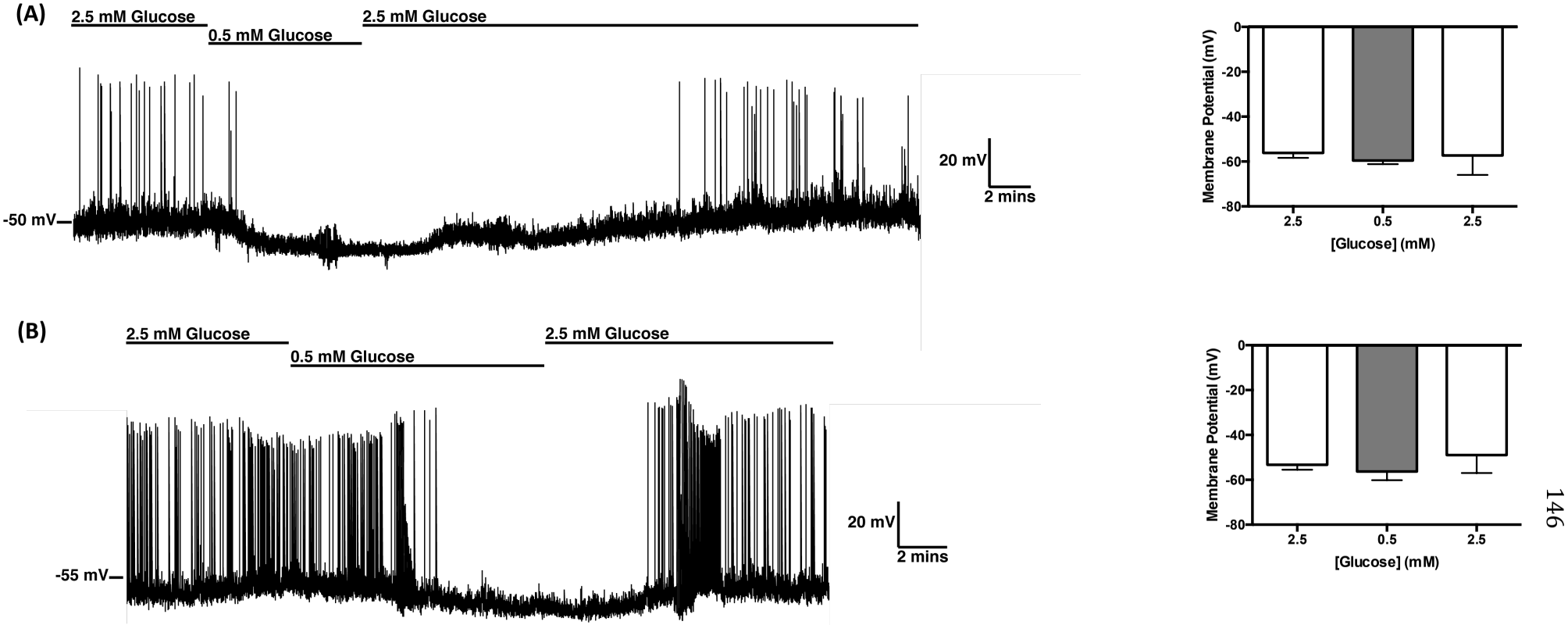

Figure 5.5 Co-application of the EPAC2 inhibitor HJC 0350 prevents antecedent IL-6-induced defective glucose sensing in GT1-7 cells

GT1-7 cells were exposed to 1:1000 DMSO + 1:250 dH_2O (Vehicle) or 0.5 μM HJC 0350 + 20 ng/ml IL-6 (HJC + IL-6) for three hours on day one and their electrical response to a 0.5 mM glucose hypoglycaemic challenge was assessed the following day. **(A)** Representative perforated patch current clamp recording of a Vehicle treated GT1-7 cell and pooled data from n=7 cells. **(B)** Representative perforated patch current clamp recording of a HJC + IL-6 treated GT1-7 cell and pooled data from n=6 cells. **(C)** Quantification of the hyperpolarising response to 0.5 mM in Vehicle vs HJC + IL-6 treated cells. Statistical significance was analysed by Friedman test in panels **(A)** and **(B)** and Mann-Whitney test in **(C)**.

It was noted that the mean hyperpolarising responses to hypoglycaemia were reduced in magnitude in GT1-7 cells studied in Figure 5.5 compared to those studied in Chapter 3 Figure 3.5 (compare Figure 5.5C with Figure 3.5C). This was shown to be due to a number of the vehicle treated cells studied in Figure 14 failing to hyperpolarise appropriately to the low glucose stimulus (Appendix VIII). Of seven vehicle treated cells studied, only two hyperpolarised appropriately in response to 0.5 mM glucose, resulting in a 28.6% hypoglycaemia-responsive population of cells. Separation of the hypoglycaemia-responsive and non-responsive cells demonstrated that the responsive cells hyperpolarised by -11.5 +- 2.5 mV on average in response to 0.5 mM glucose, exhibiting hyperpolarising responses to low glucose comparable to those in WT GT1-7 from previous studies (Chapter 3, Figure 3.5C). The cells antecedently treated with 0.5 μM HJC 0350 and 20 ng/ml IL-6 (HJC + IL-6) had variable hyperpolarising responses to subsequent 0.5 mM glucose challenge, exhibiting a mean hyperpolarising response of -3.0 +- 2.5 mV, suggesting that HJC 0350 only partially prevents the glucose sensing defect induced by antecedent IL-6 treatment. Analysis of individual cell responses to 0.5 mM glucose indicated that HJC 0350 co-treatment with IL-6 exhibited variable degrees of prevention of the defective glucose sensing phenotype induced by IL-6 (Appendix VIII).

5.3 Discussion

The lack of effect of IL-6 on whole cell metabolism in GT1-7 cells led to investigations focusing more on an effect of IL-6 to regulate K_{ATP} directly or via one of its interacting proteins. Studies have identified EPAC as a regulator of K_{ATP} function in pancreatic beta-cells and an interaction between EPAC and SUR1 of K_{ATP} has been described in mouse synaptosomes (G. Kang et al. 2006; G. Kang et al. 2008; Leech et al. 2010; Zhao et al. 2013). The data in the current results confirmed that IL-6 stimulation of GT1-7 cells leads to increases in cAMP and phosphorylation of its downstream target CREB. Furthermore, EPAC2 is expressed in GT1-7 cells and associates with K_{ATP} channels. Administration of an EPAC2 selective inhibitor during antecedent exposure to IL-6 partially prevented the glucose sensing defects observed with IL-6 treatment alone.

EPAC2 transduces the effects of cAMP and is an important regulator of insulin secretion in beta-cells via its regulation of K_{ATP} (G. Kang et al. 2006; G. Kang et al. 2008; Leech et al. 2010). IL-6 stimulation in the current work increased both cAMP

levels and CREB phosphorylation, albeit nonsignificantly. The cAMP measurement was performed after exposure to vehicle or IL-6 for three hours. However, IL-6-induced increases in CREB phosphorylation occurred more rapidly, with larger increases in phosphorylation observed after five and 30 minutes exposure to IL-6 than after three hours. It would be worthwhile measuring cAMP levels in response to a shorter exposure of IL-6, in case a more robust increase occurs prior to the three hour time point studied. In support of this notion, exposure to 50 ng/ml IL-6 for 15 minutes increased cAMP content in C2C12 myocytes (Kelly et al. 2009). In rat hepatocytes, exposure to 10 ng/ml IL-6 for 30 minutes increased the phosphorylation of CREB (Chou et al. 2013). In Chang and colleagues' study investigating OSM functions in cortical neurons, a robust increase in pCREB was observed upon exposure to 100 ng/ml of the IL-6 family cytokine for two to eight hours (Chang et al. 2015). IL-18, an IL-1 family cytokine, administered at a dose of 50 ng/ml for three to 12 hours increases pCREB in rat cortical neurons (Jiang et al. 2014) and a study in superficial dorsal horn neurons demonstrated IL-6-induced increases in CREB phosphorylation upon exposure to 10 ng/ml of the cytokine for 30 minutes (Kawasaki et al. 2008). The hyper IL-6 fusion protein, consisting of IL-6 fused to its specific receptor, induced increases in pCREB in neural stem cells when given at a dose of 100 ng/ml for ten minutes (O. Islam et al. 2009). IL-6 has been shown to rapidly increase both cAMP levels and CREB phosphorylation in C2C12 cells, and also led to increases in pCREB and cAMP content in rat skeletal muscle when quantified one hour after i.p administration of 2.5 μg IL-6 to rats *in vivo* (Kelly et al. 2009). The current data and the cited literature provides strong evidence that IL-6 can activate the cAMP/pCREB signalling axis in GT1-7 cells.

Whether IL-6 regulates EPAC has not been studied. EPAC regulation of K_{ATP} channel activity has been well described (G. Kang et al. 2006; G. Kang et al. 2008; Leech et al. 2010), implicating it as a potential mediator of the effects of IL-6 on glucose sensing observed in the current work. The results here demonstrated EPAC2, but not EPAC1, expression in GT1-7 cells, consistent with the predominant expression of EPAC2 in the brain (Kawasaki et al. 1998). Association of EPAC2 with the K_{ATP} channel in GT1-7 cells was demonstrated by co-immunoprecipitation, consistent with previous findings (Zhao et al. 2013). In the current work, densitometry quantification on Western blot analyses of protein expression in the IP fractions was performed and suggested that IL-6 did not regulate the association of EPAC2 with the K_{ATP} channel either positively or

negatively. However, it should be noted that this is not a very sensitive way of quantifying protein-protein interactions and the analysis was only performed on two independent IP experiments. A more sensitive measure of protein-protein interaction could be exploited to better understand whether IL-6 regulates the interaction of EPAC2 with the K_{ATP} channel in GT1-7 cells, such as fluorescence resonance energy transfer (FRET). Also, by selectively expressing only the SUR1 or Kir6.2 proteins with EPAC2 in a cell-based system it could be determined whether EPAC2 interacts specifically with the SUR1 or Kir6.2 subunit of K_{ATP} channels. Furthermore, EPAC is found at many cellular locations such as the plasma membrane, nuclear membrane, cytosol and mitochondria (Breckler et al. 2011). Depending on their cellular localisation and molecular partners, EPACs can activate different downstream effectors (Breckler et al. 2011). In line with this, the spatial regulation of EPACs is important for their function. Imaging studies could be employed to investigate the spatial localisation of EPAC2 in GT1-7 cells and may be able to determine whether IL-6 regulates the localisation of EPAC2. It would be of particular interest if IL-6 exposure induced a membrane targeting of EPAC2, as this would potentially make an interaction between EPAC2 and K_{ATP} channels more likely.

Importantly, inhibition of EPAC2 during IL-6 pre-exposure prevented the development of defective hypoglycaemia detection observed in antecedent IL-6 treated cells. The dose of HJC 0350 used was based on its published half maximal inhibitory concentration (IC_{50}) of 0.3 μM for competing with 8-NBD-cAMP for binding of EPAC2; which is about 133-fold more potent than cAMP for binding EPAC2 (Chen et al. 2013). In order to determine whether IL-6 requires EPAC2 function to mediate its negative regulation of glucose sensing, HJC 0350 was administered at the same time as IL-6 for three hours. The results from this study demonstrated a prevention of the defective glucose sensing phenotype induced by IL-6 in prior experiments. This data suggests that IL-6 mediates an alteration in EPAC2 function that persists for at least 18-24 hours resulting in altered K_{ATP} channel function in response to subsequent hypoglycaemia. Since EPAC2 has been demonstrated to regulate K_{ATP} channel activity in beta-cells acutely (G. Kang et al. 2006; G. Kang et al. 2008; Leech et al. 2010), it would be of interest to investigate the effects of EPAC2 inhibition and activation on GT1-7 cell membrane potential under euglycaemic conditions. Further investigation of the temporal effects of IL-6 on glucose sensing capacity in GT1-7 cells would be

interesting as well, in particular to determine a) how soon after IL-6 exposure defective glucose sensing is observed and b) how long defective glucose sensing induced by IL-6 persists for. Similarly, determining whether EPAC2 inhibition-mediated prevention of IL-6-induced defective glucose sensing is reversible or temporary would warrant further investigation.

The finding that EPAC2 inhibition during IL-6 pre-exposure prevented the development of defective hypoglycaemia detection, in conjunction with other work, suggests that IL-6 may induce defective hypoglycaemia detection and hyperpolarising responses to low glucose in GT1-7 cells via EPAC2-mediated enhancement of ATP-mediated inhibition of K_{ATP} channels. No increase in EPAC2 protein, or association of EPAC2 with K_{ATP} channels, was observed upon IL-6 treatment, however this doesn't rule out that IL-6 may enhance EPAC2 activity. An assay is available to measure Rap1 activity, which is the downstream target of EPAC, giving an indication of EPAC activity, and it would be of great interest to determine whether IL-6 increases EPAC activity in GT1-7 cells. Due to the absence of an increase in ATP production or EPAC2 expression following antecedent IL-6 treatment, together with the observation that EPAC2 inhibition prevents IL-6 induced defective glucose sensing, it is tempting to speculate that IL-6 may increase EPAC2 activity, leading to enhanced sensitivity of K_{ATP} channels to ATP-mediated inhibition, resulting in the defective glucose sensing phenotype. This may occur via a direct interaction of EPAC2 with NBD2 of SUR1 (Shibasaki et al. 2004a; Shibasaki et al. 2004b). EPAC2 binding to SUR1 might influence allosteric interactions of NBD1 with its partner NBD2, with such interactions dictating the MgADP-dependent stimulation of K_{ATP} channel activity (Gribble, Tucker et al. 1997). At the same time, SUR1 recruitment of EPAC2 to the cell membrane permits interaction of EPAC2 with the Rap GTPases (G. Kang et al. 2006). In this way, EPAC is involved in a signalling complex comprising EPAC1, Rap2B and PLC-ε in human embryonic kidney (HEK) cells (Schmidt et al. 2001). PLC-ε catalyses the hydrolysis of membrane-bound PIP2, and because PIP2 stimulates the activity of K_{ATP} channels in part by reducing the channel's sensitivity to ATP (Baukrowitz et al. 1998; Shyng & Nichols 1998; Nichols 2006), a cAMP signalling mechanism that uses EPAC, RAP and PLC-ε to reduce levels of PIP2 in the plasma membrane would be expected to increase the sensitivity of K_{ATP} channels to ATP (G. Kang et al. 2008). Investigating the affinity of K_{ATP} for ATP-

mediated inhibition following antecedent IL-6 treatment, which could be assessed electrophysiologically, would be of great interest for future research.

Another avenue for future research is encouraged by work demonstrating that cAMP elevation can inhibit activation of the JAK-STAT pathway in response to an IL-6/sIL-6Rα trans-signalling complex by promoting the accumulation of SOCS3 in vascular endothelial cells. Intriguingly, this was demonstrated to occur via a PKA-independent mechanism and was mimicked by activation of EPAC (Sands et al. 2006). The authors suggested that this data represented a new function for EPAC that is consistent with the predominantly anti-inflammatory effects of cAMP induction observed for endothelial cells (Sands et al. 2006; Blease et al. 1998). In hypothalamic slices, the cAMP elevating agent forskolin has also been shown to increase SOCS3 at the protein and mRNA level via an EPAC-dependent pathway (Fukuda et al. 2011). SOCS3 is an inhibitor of leptin signalling and the authors went on to demonstrate that activation of cAMP-Epac signalling directly densensitised POMC neurons to leptin (Fukuda et al. 2011). Furthermore, chronic exposure of mice to high fat diet resulted in obesity and leptin resistance, with increased Rap1 activity observed in the hypothalamus, suggesting that the hypothalamic EPAC-Rap1 pathway is activated in response to high fat exposure (Fukuda et al. 2011). Future work further elucidating the cross talk between cAMP and IL-6 signalling would be of interest to see how these signalling pathways interact, as the data cited suggests that EPAC2 may be a negative regulator of IL-6 mediated JAK/STAT signalling, initiating a negative feedback loop upon elevation of cAMP levels.

IL-6 stimulation of GT1-7 cells results in an increase in the cAMP/pCREB pathway, which may be associated with an increase in EPAC2 activity. In turn, this enhanced EPAC2 activity may regulate the sensitivity of the K_{ATP} channel to ATP-mediated inhibition, resulting in the maintenance of cell membrane depolarisation and action potential firing rates and associated defects in hyperpolarising responses to subsequent low glucose challenge. Future work should address the regulation of EPAC2 activity by exposure to IL-6 to increase understanding of this proposed mechanism in GT1-7 cells.

6 General Discussion

This work identified IL-6 as a novel regulator of hypothalamic glucose-sensing neurons, with the major observation that antecedent IL-6 exposure in GT1-7 neurons resulted in a suppression of hypoglycaemia detection and membrane hyperpolarisation in response to 0.5 mM glucose challenge 18-24 hours subsequently, affording cells the capacity to maintain neuronal activity during subsequent glucose deprivation. Based on the mechanisms studied in an attempt to elucidate how IL-6 elicits these effects, EPAC2 was identified as a potential mediator of defective glucose sensing, with the inference that the effect of IL-6 is potentially achieved by increasing the affinity of K_{ATP} channels for ATP-mediated channel inhibition. Based on these findings it will be of future importance to address the contribution and role of EPAC2 in hypothalamic glucose sensing further, as both IL-6 and EPAC2 may be potential therapeutic targets whose inhibition may combat defective hypoglycaemia detection and therefore help restore CRRs in patients with defective CRR due to recurrent hypoglycaemia.

The acute effects of IL-6 on GT1-7 cell membrane potential were studied but no regulation of resting membrane potential was observed by IL-6 under euglycaemic conditions. Acute hypoglycaemia hyperpolarises GT1-7 cells resulting in silencing of action potential activity, and in this setting IL-6 did not significantly affect membrane potential, suggesting that IL-6 does not regulate glucose-sensing neurons acutely. Interestingly, IL-6 secretion from primary mouse cortical astrocytes was observed to occur in the recovery period following hypoglycaemia rather than during hypoglycaemia itself, with significantly more IL-6 release observed from hypoglycaemic cultures compared to euglycaemic cultures following a four hour euglycaemic recovery period. Investigation of whether IL-6 exerted delayed effects on GT1-7 cells led to the observation that antecedent exposure to IL-6 attenuated hyperpolarising responses to subsequent hypoglycaemia, resulting in maintenance of neuronal activity. This finding implicated a role for IL-6 in the induction of physiological cellular adaptations resulting in a defective glucose sensing phenotype of GT1-7 cells. Importantly, partial reduction of the IL-6Rα prevented the effects of antecedent IL-6 treatment to induce defective glucose sensing, confirming that IL-6 activation of its receptor complex is required for the initiation of any downstream effects regulating glucose sensing.

Mechanistic investigation of the effects of IL-6 on glucose sensing focussed initially on the involvement of the JAK/STAT3 signalling pathway which was robustly induced in GT1-7 cells upon exposure to IL-6, evidenced by increases in the phosphorylation of STAT3. In GT1-7 cells lacking the IL-6Rα, a reduction in the phosphorylation of STAT3 was observed in cells that were protected from IL-6-induced defective glucose sensing, implicating a role for activation of STAT3 in the transduction of the IL-6 effects on glucose sensing. Given the latent onset (18-24 hours subsequently) of the defective glucose sensing phenotype, and that STAT3 phosphorylation leads to dimerisation and translocation to the nucleus, the hypothesis that STAT3-mediated gene transcription was required to induce the effects of IL-6 on glucose sensing was tested. STAT3 inhibition with the JAK2 inhibitor WP1066 prior to antecedent IL-6 exposure was effective at blocking IL-6-induced phosphorylation of STAT3, and therefore its transcriptional activity, however, by the time cells were due to be studied electrophysiologically 18-24 hours subsequently, inhibition of STAT3 had exerted cytotoxic effects on GT1-7 cells resulting in cell death. A limitation of the current work was that an alternative way of inhibiting STAT3-mediated gene transcription was not attempted, as alternatives for targeting this, such as small molecule inhibitors, are available and should be studied in the future.

A role for an IL-6-induced increase in cellular ATP production via increased cellular metabolism was not confirmed, and therefore did not support the hypothesis that an increase in ATP production leading to enhanced inhibition of K_{ATP} channels was responsible for mediating the IL-6-induced glucose sensing defect. However, a role for the cAMP/EPAC2 pathway was implicated, with cAMP assays confirming increases in cAMP in response to IL-6 and phosphorylation of CREB by IL-6 exposure indicating activation of cAMP signalling cascades. Inhibition of EPAC2 during antecedent IL-6 exposure partially prevented the induction of defective glucose sensing, implicating a role for EPAC2 in mediating the effects of IL-6. This is hypothesised to occur via an EPAC2-mediated increase in the sensitivity of K_{ATP} channels to inhibition by ATP, and future studies should focus on elucidating if this is the case.

A limitation of this work was the lack of confirmation of the role of STAT3 in mediating the effects of IL-6 on glucose sensing. Initial studies suggested an involvement of STAT3 in this observation, but were not followed up effectively. There are also limitations induced by inconsistencies between the electrophysiological and

biochemical studies. The hypoglycaemic challenge in electrophysiological experiments was 0.5 mM glucose for a 15 minute duration. In contrast, many of the functional assays performed, such as ATP measurement, were following a hypoglycaemic challenge of 0.1 mM glucose for three hours. Electrophysiology allows a highly sensitive measurement of single cell neuronal activity. In contrast, assays performing measurements from cell populations exhibiting heterogeneous responses are less robust, and therefore a more profound hypoglycaemic challenge was performed for these assays. In doing this however, subtle effects of IL-6 on measured parameters may have been missed. It will be important to re-assess the functional measurements of ATP and cAMP content in GT1-7 cells after exposure to a 15 minute 0.5 mM glucose hypoglycaemic challenge in order to be more consistent with the electrophysiological studies.

Further limitations of the current work are associated with the model used to perform these studies. The GT1-7 cell line provided an attractive model to study the effects of IL-6 on glucose sensing. As a homogenous population of GE neurons, which recapitulates the glucose sensing machinery expressed in GE neurons of the VMH (Beall, Hamilton, et al. 2012; Ogunnowo-Bada et al. 2014), it permitted the study of mechanisms regulating glucose sensing in isolation from glial cell influences and other central and peripheral innervation. Unfortunately, during the current work, heterogeneous responses to low glucose exposure were observed in these cells, complicating experiments and interpretation of the data obtained. It will be of significant importance in the future to confirm whether antecedent IL-6 exposure results in similar suppression of glucose sensing in other models. An ideal experimental model to validate this would be to utilise a reporter mouse that has fluorescent tagging of GE neurons of the VMH. This could potentially be achieved by selectively tagging a component of the glucose sensing machinery in, for example, SF-1-expressing neurons of the VMH, as these have been identified to be glucose-sensing cells (Y.-H. Choi et al. 2013; Silver & Erecińska 1998; Tong et al. 2007). Hypothalamic slices could then be obtained from these animals and fluorescent cells could be examined electrophysiologically to determine whether antecedent IL-6 exposure regulates glucose sensing in similar ways to those observed in the current work.

The inference of the IL-6-induced suppression of glucose sensing would be an associated suppression of CRR to hypoglycaemia (Chan & Sherwin 2013). Whether this

is the case could be studied *in vivo* by measuring CRR hormone release in response to acute hypoglycaemia following antecedent VMH IL-6 microinjection. If antecedent IL-6 treatment suppressed CRR hormonal secretion in response to hypoglycaemia this would suggest that IL-6 could induce impaired CRR to hypoglycaemia. Together with data demonstrating IL-6 regulation of glucose-sensing neurons in hypothalamic slices, this would help elucidate whether IL-6 induced defective glucose sensing in a more physiological model of the VMH and whether this had functional consequences in terms of whole body CRR to hypoglycaemia *in vivo*. If the experiments above are successful, a further level of investigation could involve attempting to specifically knockout the IL-6Rα, or impede IL-6 action pharmacologically, in glucose-sensing neurons of the VMH and see if this could prevent any effects of antecedent IL-6 treatment on either glucose sensing or CRR hormone secretion to acute hypoglycaemia.

The current work highlights the potential physiological role of factors released in the recovery period following hypoglycaemia. Hypoglycaemic clamp studies in humans have shown increases in plasma IL-6 levels after one-two hours of hypoglycaemia exposure (Ceriello et al. 2013a). However, temporal IL-6 release in brain in response to hypoglycaemia has not been the focus of many studies. IL-6 mRNA accumulation in rat cortical mixed glial cells occurred as early as 15 minutes after exposure to glucose deprivation, but secretion was not measured in this study (Wang et al. 2001). The current work demonstrates that IL-6 is released from astrocytes only in the euglycaemic recovery period following hypoglycaemia. The importance of controlled regulation of the recovery period following hypoglycaemia has been demonstrated, at least in terms of glucose concentration, in a study demonstrating that hyperglycaemia exposure during recovery from hypoglycaemia worsens endothelial function and increases oxidative stress and inflammation in both healthy individuals and patients with T1D (Ceriello et al. 2013b). This data also suggests that the secretion of inflammatory mediators such as IL-6 in the recovery period following hypoglycaemia may be influenced by glucose concentration. The essential role of IL-6 produced locally by resident brain cells for post-stoke angiogenesis has been demonstrated (Gertz et al. 2012). IL-6 promoted early transcriptional changes in angiogenesis-related gene networks after brain ischaemia, which led to increased angiogenesis after experimental stroke (Gertz et al. 2012). Therefore, IL-6 affords long-term, functional protection, assigning an important role of

neuroinflammation for post-stroke recovery (Gertz et al. 2012). It may be speculated that IL-6 exerts similar neuroprotective effects during recovery from hypoglycaemia.

The current work suggests that the inflammatory response associated with hypoglycaemia may be of functional, physiological relevance in the CNS and also strengthens the hypothesis that pro-inflammatory states associated with diseases such as obesity, T2D and cancer, and increases in IL-6 in particular, are more than just a biomarker for disease state (Mauer et al. 2015; Ataie-Kachoie et al. 2014; Kristiansen & Mandrup-Poulsen 2005). Particularly in the CNS, IL-6 released following hypoglycaemia appears to play a key role in the regulation of hypothalamic glucose-sensing neurons. The data presented here suggest that IL-6 exposure can impair neuronal responses to subsequent hypoglycaemia and implicate a role for EPAC2 in this observation. Therefore, IL-6 and EPAC2 are identified as two novel factors regulating glucose-sensing neurons, and warrant further study to determine their importance in the regulation of hypothalamic glucose sensing. If their roles can be confirmed and validated in more physiological models, then they provide two potential targets for therapeutic intervention to restore defective CRRs associated with recurrent hypoglycaemia in patients with T1D. Given the pleiotropic roles of IL-6 (Mauer et al. 2015; Pal et al. 2014), specifically targeting and inhibiting only its action to suppress hypothalamic glucose sensing would be challenging, and a risk given the many physiologically beneficial roles of IL-6 reported (Scheller et al. 2011; Gertz et al. 2012). Antibodies neutralising IL-6 signalling have been used to great effect to treat chronic inflammatory disorders such as rheumatoid arthritis (Kang et al. 2014), so effective pharmacology is available, but whether it would be a useful intervention in this setting is questionable. EPAC2 on the other hand provides an exciting novel target that may be exploited therapeutically. In the current work a potent, selective inhibitor of EPAC2 was demonstrated to prevent the IL-6-induced suppression of hypothalamic glucose sensing responses to hypoglycaemia. Given the physiological importance of EPAC in the brain and CNS (Laurent et al. 2012) and other tissues including heart (Métrich et al. 2010), as well as its documented roles in the immune system (Shirshev 2011), axonal growth (Peace & Shewan 2011) and tissue fibrosis (Insel et al. 2012), targeting of EPAC2 activity specifically in GE VMH neurons would be difficult. Nevertheless, it would be of interest to pursue the relevance of modulation of EPAC2 activity in the context of defective CRRs to hypoglycaemia further.

Several potential mediators of brain adaptations to recurrent hypoglycaemia that result in defective CRRs to subsequent hypoglycaemia have been identified (Chan & Sherwin 2013), and the current work identifies IL-6 and EPAC2 as two novel, potential mediators of suppressed glucose sensing, at least in GT1-7 cells. Confirmation of these findings is required in other models and certainly in an *in vivo* setting, but they may be exciting, therapeutically exploitable targets for future research to focus on. The recovery period following hypoglycaemia should also be the attention of future research as the current results implicate functional, regulatory roles for secreted factors released during this period.

7 Concluding Statements

The current work identifies the importance of the recovery period following hypoglycaemia and the potential significance of functional effects exerted by factors secreted during this time. It is demonstrated that IL-6 can exert a suppressive effect on subsequent hypoglycaemia detection in GT1-7 cells, an effect that may also be true in GE neurons of the hypothalamus. IL-6 exposure activates the cAMP signalling axis leading to phosphorylation and therefore activation of CREB as well as activating the JAK/STAT3 signalling cascade in GT1-7 cells. Finally, EPAC2 appears to mediate the effect of IL-6 to induce defective detection of subsequent hypoglycaemia and associated hyperpolarising responses to low glucose.

Future work should address whether IL-6 increases the activity of EPAC2 in GT1-7 cells and whether the sensitivity of the K_{ATP} channel to inhibition by ATP is altered following antecedent IL-6 exposure. Finally, it would be of interest to determine how activation of CREB and STAT3 link in with EPAC2 activity and the regulation of K_{ATP} channel activity.

8 Appendices

8.1 Appendix I

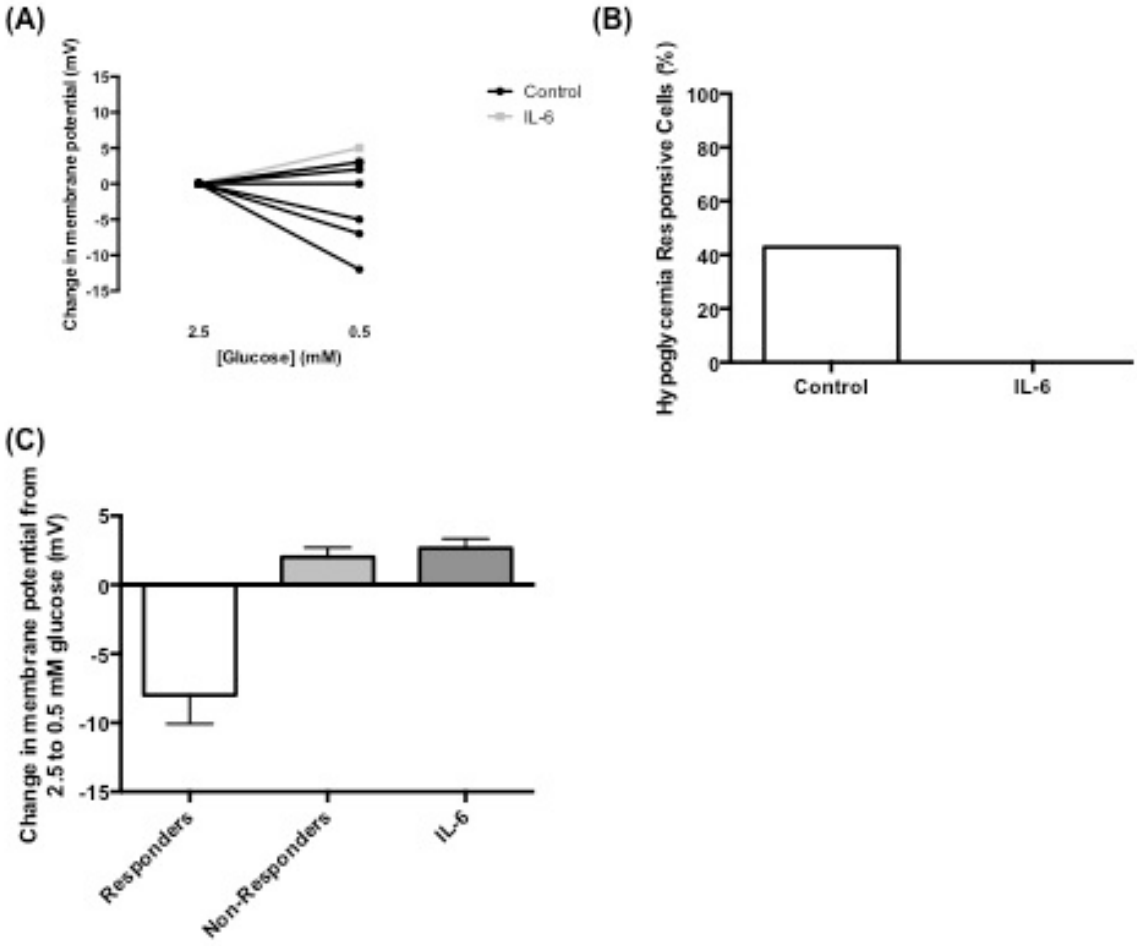

Figure 8.1 A percentage of vehicle dH_2O (Control) treated shControl cells are unresponsive to hypoglycaemia

shControl GT1-7 cells were exposed to either vehicle dH_2O (control) or 20 ng/ml IL-6 (IL-6) for three hours on day one and their electrical response to a 0.5 mM glucose hypoglycaemic challenge was assessed the following day during perforated patch current clamp recordings. **(A)** 4 of the 7 control cells studied failed to hyperpolarise in response to 0.5 mM glucose. **(B)** The percentage of control treated hypoglycaemia-responsive cells was quantified as 43%, while no hypoglycaemia-responsive cells were observed following antecedent IL-6 exposure. **(C)** Separation of vehicle treated cells that responded (responders) or failed to respond (non-responders) to 0.5 mM glucose demonstrated that responders hyperpolarised by -8.0 +- 2.1 mV on average compared to non-responders that demonstrated a depolarisation of 2.0 +- 0.7 mV on average in response to 0.5 mM glucose challenge (n=3 and n=4 respectively). All six of the antecedent IL-6 treated shControl cells studied failed to respond to hypoglycaemia, and depolarised by 2.7 +- 0.7 mV on average in response to 0.5 mM glucose

8.2 Appendix II

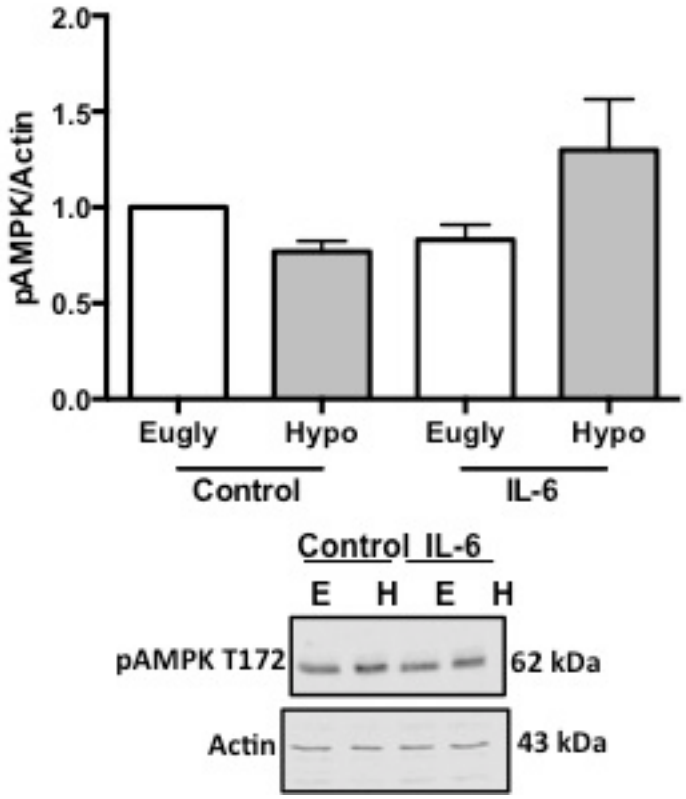

Figure 8.2 Hypoglycaemia fails to induce phosphorylation of AMPK in GT1-7 cells

GT1-7 cells were exposed to vehicle dH_2O (Control) or 20 ng/ml IL-6 (IL-6) for three hours and 24 hours subsequently were exposed to 2.5 mM glucose (Eugly) or 0.1 mM glucose (Hypo) for 15 minutes. Cells were lysed and samples prepared for Western blot analysis of expression of pAMPK T172 (n=3). Data was analysed by one-way ANOVA with Dunnett's multiple comparisons test.

8.3 Appendix III

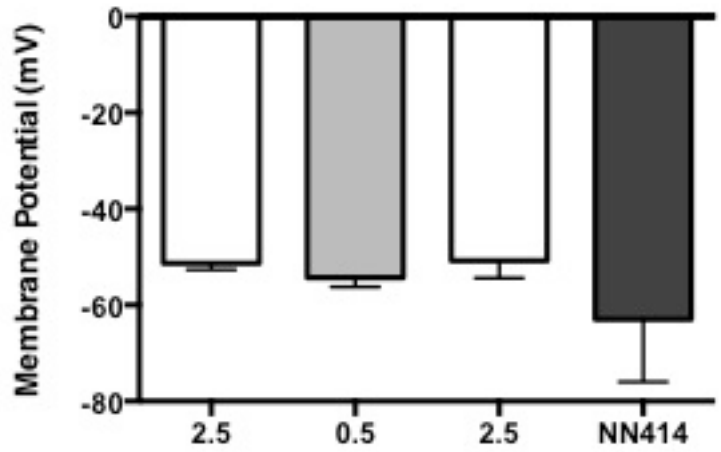

Figure 8.3 Antecedent 20 ng/ml IL-6 treated GT1-7 cells hyperpolarise in response to response to NN414

Pharmacological opening of K_{ATP} channels with 5 μM NN414 resulted in membrane hyperpolarisation of GT1-7 cells with defective hyperpolarising responses to hypoglycaemia following antecedent IL-6 treatment (n=10; n=2 for NN414 treatment).

8.4 Appendix IV

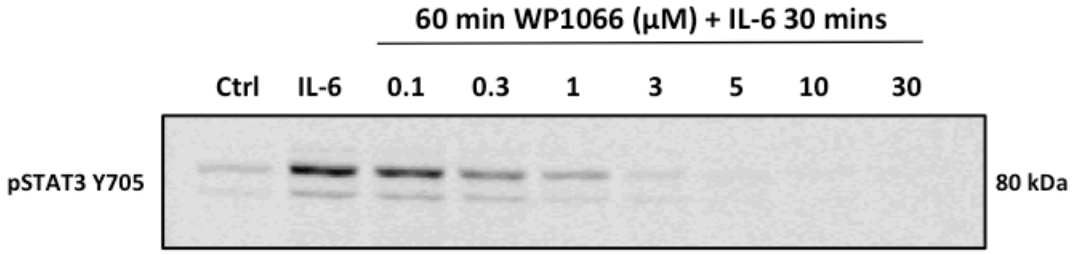

Figure 8.4 Pre-incubation with WP1066 dose-dependently prevents IL-6-induced phosphorylation of STAT3 Y705

GT1-7 cells were pre-treated with vehicle DMSO at 1:1000 for 60 minutes prior to exposure to vehicle dH_2O at 1:250 for 30 minutes (Ctrl), or pre-treated with vehicle DMSO at 1:1000 for 60 minutes prior to exposure to 20 ng/ml IL-6 for 30 minutes (IL-6) or pre-treated with 0.1 – 30 μM WP1066 for 60 minutes prior to exposure to 20 ng/ml IL-6 for 30 minutes. Cells were lysed and samples prepared for Western blot analysis of expression of pSTAT3 Y705.

8.5 Appendix V

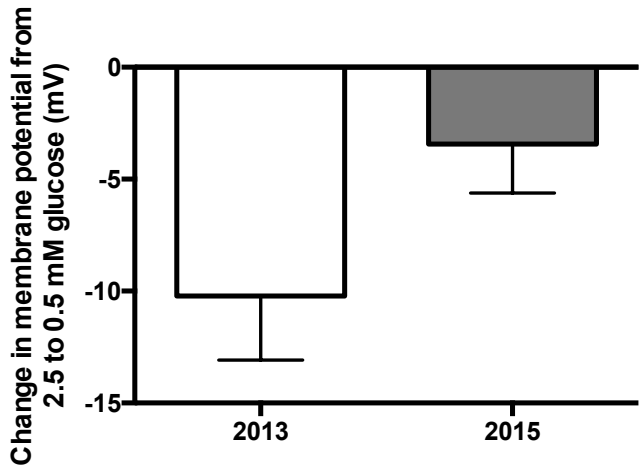

Figure 8.5 A suppression of the hyperpolarising response to 0.5 mM glucose was observed over time in vehicle treated WT GT1-7 cells

WT GT1-7 cells were exposed to vehicle control (dH_2O) for three hours on day one and their electrical response to a 0.5 mM glucose challenge was assessed the following day (18-24 hours subsequently) during perforated patch current clamp electrophysiological recordings. Data represents the hyperpolarising response to 0.5 mM glucose exposure in studies performed in 2013 (n=9) and 2015 (n=7). Data was analysed by Mann-Whitney test (P=0.11).

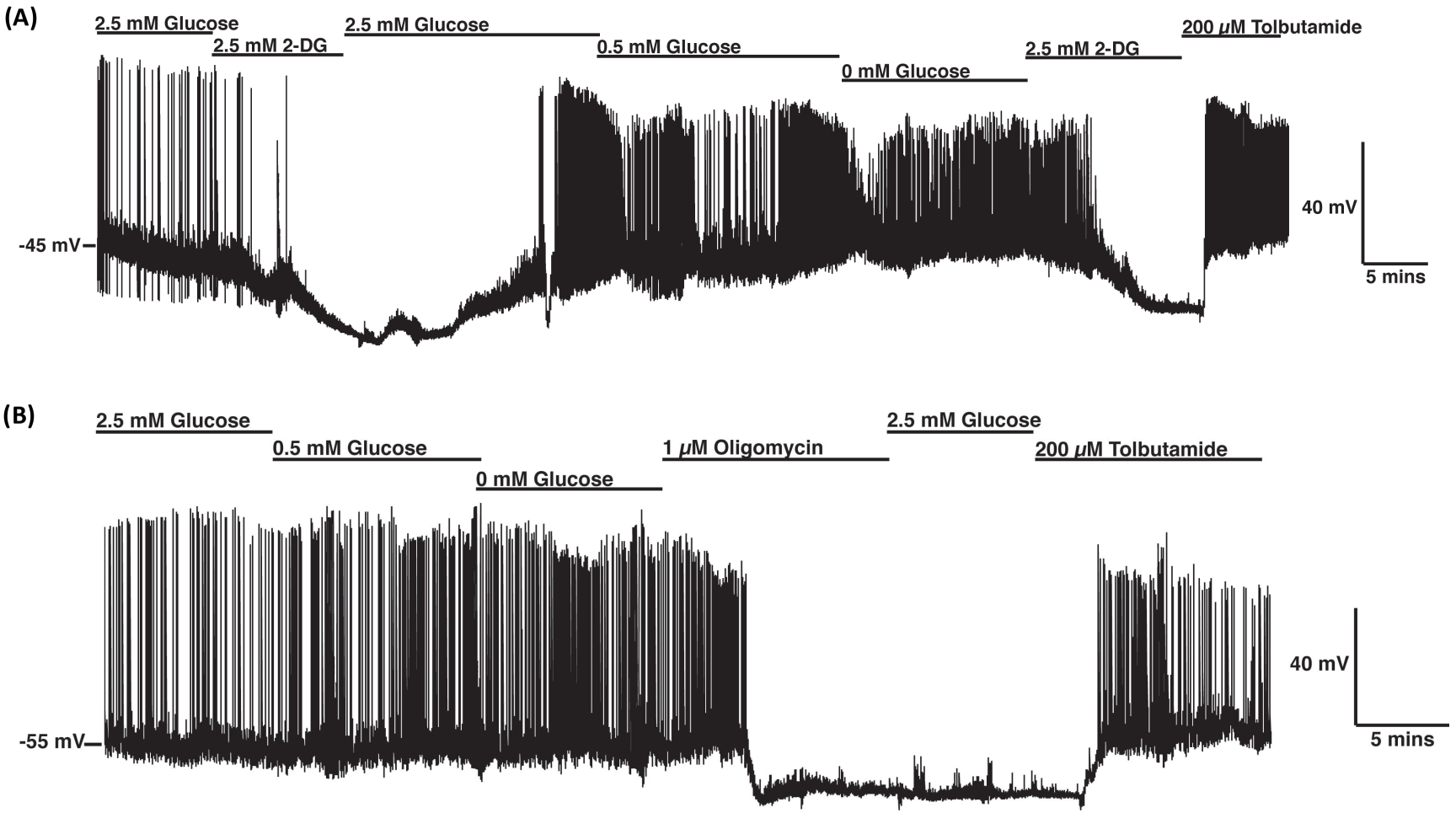

Figure 8.6 A proportion of GT1-7 cells fail to hyperpolarise to a low glucose challenge but do respond to metabolic inhibition by 2.5 mM 2-DG or 1 μM oligomycin

(A) A representative perforated patch current clamp recording demonstrating that a proportion of GT1-7 cells hyperpolarise in response to metabolic inhibition by 2-DG exposure but fail to hyperpolarise in response to low glucose. **(B)** A representative perforated patch current clamp recording demonstrating that a proportion of GT1-7 cells hyperpolarise in response to metabolic inhibition by 1 μM oligomycin but fail to hyperpolarise in response to low glucose.

8.7 Appendix VII

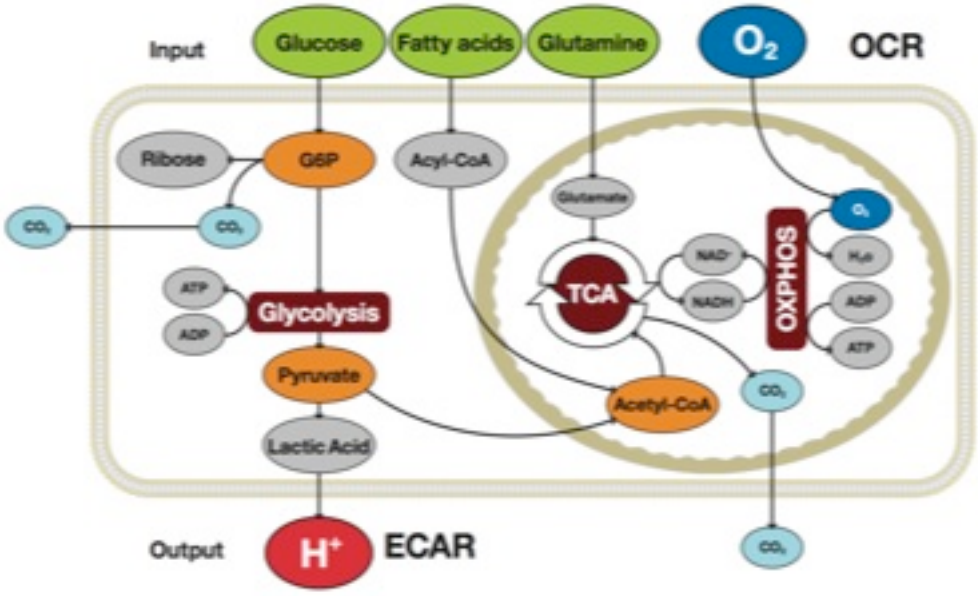

Figure 8.7 Cellular bioenergetic pathways measured using the Seahorse Bioscience Extracellular Flux Analyser

Oxygen consumption rate (OCR) provides an index of mitochondrial respiration and oxidative phosphorylation, whereas the extracellular acidification rate (ECAR) provides a measure of glycolysis. Schematic obtained and adapted from www.seahorsebio.com/learning/image-library.php

8.8 Appendix VIII

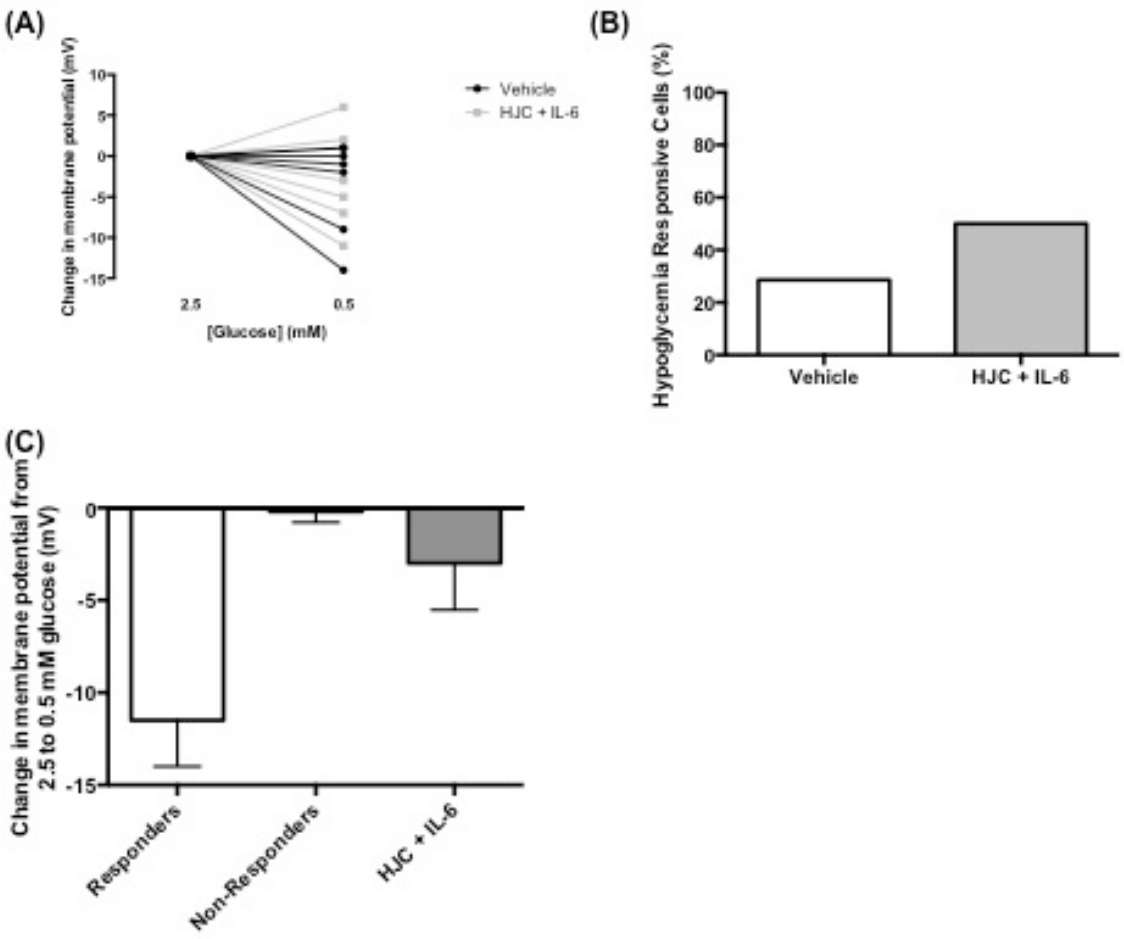

Figure 8.8 A percentage of vehicle treated WT GT1-7 cells were unresponsive to hypoglycaemia in the HJC 0350 studies

WT GT1-7 cells were exposed to either DMSO at 1:1000 + dH_2O at 1:250 (Vehicle) or 0.5 μM HJC 0350 + 20 ng/ml IL-6 (HJC + IL-6) for three hours on day one and their electrical response to a 0.5 mM glucose hypoglycaemic challenge was assessed the following day during perforated patch current clamp recordings. **(A)** Five of the seven vehicle treated cells failed to hyperpolarise in response to 0.5 mM glucose. **(B)** The percentage of vehicle treated hypoglycaemia-responsive cells was quantified as 28.6% while 50% of HJC + IL-6 treated cells were hypoglycaemia-responsive in terms of exhibiting a hyperpolarising response to 0.5 mM glucose. **(C)** Separation of vehicle treated cells that responded (responders) or failed to respond (non-responders) to 0.5 mM glucose demonstrated that responders hyperpolarised by -11.5 +- 2.5 mV on average compared to non-responders that demonstrated a -0.2 +- 0.6 mV hyperpolarisation on average in response to 0.5 mM glucose (n=2 and n=5 respectively). HJC + IL-6 treated cells hyperpolarised by -3.0 +- 2.5 mV on average in response to 0.5 mM glucose (n=6).

9 References

Abbud, R. A., Kelleher, R. & Melmed, S., 2004. Cell-specific pituitary gene expression profiles after treatment with leukemia inhibitory factor reveal novel modulators for proopiomelanocortin expression. *Endocrinology*, 145(2), pp.867–880.

Abkhezr, M. & Dryer, S. E., 2014. STAT3 Regulates steady-state expression of synaptopodin in cultured mouse podocytes. *Molecular Pharmacology*, 87(2), pp.231-239.

Acosta-Martínez, M. & Levine, J. E., 2007. Regulation of KATP channel subunit gene expression by hyperglycemia in the mediobasal hypothalamus of female rats. *American Journal of Physiology. Endocrinology and Metabolism*, 292(6), pp.E1801–E1807.

Agorastos, A. et al., 2014. Circadian rhythmicity, variability and correlation of interleukin-6 levels in plasma and cerebrospinal fluid of healthy men. *Psychoneuroendocrinology*, 44, pp.71–82.

Aguilar-Bryan, L. & Bryan, J., 1999. Molecular biology of adenosine triphosphate-sensitive potassium channels. *Endocrine Reviews*, 20(2), pp.101–135.

Ahmed, S., Pakozdi, A. & Koch, A. E., 2006. Regulation of interleukin-1beta-induced chemokine production and matrix metalloproteinase 2 activation by epigallocatechin-3-gallate in rheumatoid arthritis synovial fibroblasts. *Arthritis and Rheumatism*, 54(8), pp.2393–2401.

Almahariq, M., Mei, F. C. & Cheng, X., 2014. Cyclic AMP sensor EPAC proteins and energy homeostasis. *Trends in Endocrinology and Metabolism*, 25(2), pp.60–71.

Alquier, T. et al., 2007. Role of hypothalamic adenosine 5'-monophosphate-activated protein kinase in the impaired counterregulatory response induced by repetitive neuroglucopenia. *Endocrinology*, 148(3), pp.1367–1375.

Amiel, S. A. et al., 1991. Ketone infusion lowers hormonal responses to hypoglycaemia: evidence for acute cerebral utilization of a non-glucose fuel. *Clinical science (London, England:1979)*, 81(2), pp.189–194.

Amoroso, S. et al., 1990. Glucose, sulfonylureas, and neurotransmitter release: role of ATP-sensitive K+ channels. *Science (New York, N.Y.)*, 247(4944), pp.852–854.

Anand, B. K. et al., 1964. Activity of single neurons in the hypothalamic feeding centers: effect of glucose. *American Journal of Physiology*, 207, pp.1146–1154.

Ando, M. et al., 2010. Interleukin 6 enhances glycolysis through expression of the glycolytic enzymes hexokinase 2 and 6-phosphofructo-2-kinase/fructose-2,6-bisphosphatase-3. *Journal of Nihon Medical School = Nihon Ika Daigaku Zasshi*, 77, pp.97–105.

D'Arcangelo, G. et al., 2000. Interleukin-6 inhibits neurotransmitter release and the spread of excitation in the rat cerebral cortex. *The European Journal of Neuroscience*, 12(4), pp.1241–1252.

Arluison, M., Quignon, M., Nguyen, P., et al., 2004. Distribution and anatomical localization of the glucose transporter 2 (GLUT2) in the adult rat brain—an immunohistochemical study. *Journal of Chemical Neuroanatomy*, 28(3), pp.117–136.

Arluison, M., Quignon, M., Thorens, B., et al., 2004. Immunocytochemical localization of the glucose transporter 2 (GLUT2) in the adult rat brain. II. Electron microscopic study. *Journal of Chemical Neuroanatomy*, 28(3), pp.137–146.

Ashcroft, F. M., 1988. Adenosine 5'-triphosphate-sensitive potassium channels. *Annual Review of Neuroscience*, 11, pp.97–118.

Ashcroft, F. M. & Rorsman, P., 1990. ATP-sensitive K+ channels: a link between B-cell metabolism and insulin secretion. *Biochemical Society Transactions*, 18(1), pp.109–111.

Ashford, M. L., Boden, P. R. & Treherne, J. M., 1990. Tolbutamide excites rat glucoreceptive ventromedial hypothalamic neurones by indirect inhibition of ATP-K+ channels. *British Journal of Pharmacology*, 101(3), pp.531–540.

Asschert, J. G. et al., 1999. Differential regulation of IL-6 promoter activity in a human ovarian-tumor cell line transfected with various p53 mutants: involvement of AP-1. *International Journal of Cancer*, 81(2), pp.236–242.

Ataie-Kachoie, P. et al., 2014. Gene of the month: interleukin 6 (IL-6). *Journal of Clinical Pathology*, 67(11), pp.932–937.

Ataie-Kachoie, P., Morris, D. L. & Pourgholami, M. H., 2013. Minocycline suppresses interleukine-6, its receptor system and signaling pathways and impairs migration, invasion and adhesion capacity of ovarian cancer cells: in vitro and in vivo studies. *PLoS One*, 8(4), pp.e60817.

Austin, S. & St-Pierre, J., 2012. PGC1α and mitochondrial metabolism - emerging concepts and relevance in ageing and neurodegenerative disorders. *Journal of Cell Science*, 125(21), pp.4963–4971.

Balfour, R. H., Hansen, A. M. & Trapp, S., 2006. Neuronal responses to transient hypoglycaemia in the dorsal vagal complex of the rat brainstem. *The Journal of Physiology*, 570, pp.469–484.

Balfour, R. H. & Trapp, S., 2007. Ionic currents underlying the response of rat dorsal vagal neurones to hypoglycaemia and chemical anoxia. *The Journal of Physiology*, 579(Pt 3), pp.691–702.

Banks, W. A., Kastin, A. J. & Gutierrez, E. G., 1994. Penetration of interleukin-6 across the murine blood-brain barrier. *Neuroscience Letters*, 179, pp.53–56.

Banzet, S. et al., 2009. Control of gluconeogenic genes during intense/prolonged exercise: hormone-independent effect of muscle-derived IL-6 on hepatic tissue and PEPCK mRNA. *Journal of Applied Physiology (Bethesda, Md.:1985)*, 107(6), pp.1830–1839.

Bauer, J. et al., 1989. Regulation of interleukin-6 receptor expression in human monocytes and hepatocytes. *FEBS Letters*, 249(1), pp.27–30.

Baukrowitz, T. et al., 1998. PIP2 and PIP as determinants for ATP inhibition of KATP channels. *Science (New York, N.Y.)*, 282(5391), pp.1141–1144.

Beall, C. et al., 2010. Loss of AMP-activated protein kinase α2 subunit in mouse β-cells impairs glucose-stimulated insulin secretion and inhibits their sensitivity to hypoglycaemia. *Biochemical Journal*, 429(2), pp.323–333.

Beall, C., Hamilton, D. L., et al., 2012. Mouse hypothalamic GT1-7 cells demonstrate AMPK-dependent intrinsic glucose-sensing behaviour. *Diabetologia*, 55(9), pp.2432–2444.

Beall, C., Ashford, M. L. & McCrimmon, R. J., 2012. The physiology and pathophysiology of the neural control of the counterregulatory response. *American Journal of Physiology. Regulatory, Integrative and Comparative Physiology*, 302(2), pp.R215–R223.

Behrens, M. M., Ali, S. S. & Dugan, L. L., 2008. Interleukin-6 mediates the increase in NADPH-oxidase in the ketamine model of schizophrenia. *Journal of Neuroscience*, 28(51), pp.13957–13966.

Benrick, A., Wallenius, V. & Asterholm, I. W., 2012. Interleukin-6 mediates exercise-induced increase in insulin sensitivity in mice. *Experimental Physiology*, 97(11), pp.1224–1235.

Biensø, R. S. et al., 2014. Effects of IL-6 on pyruvate dehydrogenase regulation in mouse skeletal muscle. *Pflügers Archiv - European Journal of Physiology*, 466(8), pp.1647–1657.

Biggers, D. W. et al., 1989. Role of brain in counterregulation of insulin-induced hypoglycemia in dogs. *Diabetes*, 38(1), pp.7–16.

Bingham, E. M. et al., 2002. The role of insulin in human brain glucose metabolism: an 18fluoro-deoxyglucose positron emission tomography study. *Diabetes*, 51(12), pp.3384–3390.

Blease, K., Burke-Gaffney, A. & Hellewell, P. G., 1998. Modulation of cell adhesion molecule expression and function on human lung microvascular endothelial cells by inhibition of phosphodiesterases 3 and 4. *British Journal of Pharmacology*, 124(1), pp.229–237.

Bolaños, J. P., Almeida, A. & Moncada, S., 2010. Glycolysis: a bioenergetic or a survival pathway? *Trends in Biochemical Sciences*, 35(3), pp.145–149.

Bonito, N. A. et al., 2014. Control of gp130 expression by the mitogen-activated protein kinase ERK2. *Oncogene*, 33(17), pp.2255–2263.

Borg, M. A. et al., 1997. Local ventromedial hypothalamus glucose perfusion blocks counterregulation during systemic hypoglycemia in awake rats. *The Journal of Clinical Investigation*, 99(2), pp.361–365.

Borg, M. A. et al., 2003. Local lactate perfusion of the ventromedial hypothalamus suppresses hypoglycemic counterregulation. *Diabetes*, 52(3), pp.663–666.

Borg, W. P. et al., 1995. Local ventromedial hypothalamus glucopenia triggers counterregulatory hormone release. *Diabetes*, 44(2), pp.180–184.

Borg, W. P. et al., 1994. Ventromedial hypothalamic lesions in rats suppress counterregulatory responses to hypoglycemia. *The Journal of Clinical Investigation*, 93(4), pp.1677–1682.

Böttger, E. et al., 2013. Expression of interleukin-6 family receptors in NK92 cells is regulated by cytokines and not through direct interaction with plasmodium falciparum-infected erythrocytes. *Journal of Interferon & Cytokine Research : The Official Journal of the International Society for Interferon and Cytokine Research*, 33(2), pp.65–71.

Boyle, P. J. et al., 1994. Adaptation in brain glucose uptake following recurrent hypoglycemia. *Proceedings of the National Academy of Sciences of the United States of America*, 91(20), pp.9352–9356.

Bradford, M. M., 1976. A rapid and sensitive method for the quantitation of microgram quantities of protein utilizing the principle of protein-dye binding. *Analytical Biochemistry*, 72, pp.248–254.

Breckler, M. et al., 2011. Rap-linked cAMP signaling Epac proteins: compartmentation, functioning and disease implications. *Cellular Signalling*, 23(8), pp.1257–1266.

Briscoe, V. J., Ertl, A. C., Tate, D. B., Dawling, S., et al., 2008. Effects of a selective serotonin reuptake inhibitor, fluoxetine, on counterregulatory responses to hypoglycemia in healthy individuals. *Diabetes*, 57(9), pp.2453–2460.

Briscoe, V. J., Ertl, A. C., Tate, D. B. & Davis, S. N., 2008. Effects of the selective serotonin reuptake inhibitor fluoxetine on counterregulatory responses to hypoglycemia in individuals with type 1 diabetes. *Diabetes*, 57(12), pp.3315–3322.

Briski, K. P. & Patil, G. D., 2005. Induction of fos immunoreactivity labeling in rat forebrain metabolic loci by caudal fourth ventricular infusion of the monocarboxylate transporter inhibitor, alpha-cyano-4-hydroxycinnamic acid. *Neuroendocrinology*, 82(1), pp.49–57.

Brown, A. M., Baltan Tekkök, S. & Ransom, B. R., 2004. Energy transfer from astrocytes to axons: the role of CNS glycogen. *Neurochemistry International*, 45(4), pp.529–536.

Brown, G., 1995. Nitric oxide regulates mitochondrial respiration and cell functions by inhibiting cytochrome oxidase. *FEBS Letters*, 369(2-3), pp.136–139.

Brown, J. A. et al., 2014. Metabolic consequences of interleukin-6 challenge in developing neurons and astroglia. *Journal of Neuroinflammation*, 11(1), pp.183.

Burdakov, D. et al., 2006. Tandem-pore k(+) channels mediate inhibition of orexin neurons by glucose. *Neuron*, 50(5), pp.711–722.

Cai, F. et al., 2007. Glucose regulates AMP-activated protein kinase activity and gene expression in clonal, hypothalamic neurons expressing proopiomelanocortin: additive effects of leptin or insulin. *Journal of Endocrinology*, 192(3), pp.605–614.

Canabal, D. D. et al., 2007. Glucose, insulin, and leptin signaling pathways modulate nitric oxide synthesis in glucose-inhibited neurons in the ventromedial hypothalamus. *American Journal of Physiology. Regulatory, Integrative and Comparative Physiology*, 292, pp.R1418–R1428.

Canada, S. E. et al., 2011. Brain glycogen supercompensation in the mouse after recovery from insulin-induced hypoglycemia. *Journal of Neuroscience Research*, 89(4), pp.585–591.

Carey, A. L. et al., 2006. Interleukin-6 increases insulin-stimulated glucose disposal in humans and glucose uptake and fatty acid oxidation in vitro via AMP-activated protein kinase. *Diabetes*, 55(10), pp.2688-2697.

Ceriello, A. et al., 2013a. Glucagon-like peptide 1 reduces endothelial dysfunction, inflammation, and oxidative stress induced by both hyperglycemia and hypoglycemia in type 1 diabetes. *Diabetes Care*, 36(8), pp.2346–2350.

Ceriello, A. et al., 2013b. Vitamin C further improves the protective effect of glucagon-like peptide-1 on acute hypoglycemia-induced oxidative stress, inflammation, and endothelial dysfunction in type 1 diabetes. *Diabetes Care*, 36(12), pp.4104–4108.

Chalaris, A. et al., 2011. The soluble interleukin 6 receptor: generation and role in inflammation and cancer. *European Journal of Cell Biology*, 90(6-7), pp.484–494.

Chan, C. B. et al., 2004. Uncoupling protein 2 and islet function. *Diabetes*, 53(February), pp.S136–S142.

Chan, O. et al., 2007. ATP-sensitive K(+) channels regulate the release of GABA in the ventromedial hypothalamus during hypoglycemia. *Diabetes*, 56(4), pp.1120–1126.

Chan, O. et al., 2006. Blockade of GABA(A) receptors in the ventromedial hypothalamus further stimulates glucagon and sympathoadrenal but not the hypothalamo-pituitary-adrenal response to hypoglycemia. *Diabetes*, 55(4), pp.1080–1087.

Chan, O. et al., 2008. Increased GABAergic tone in the ventromedial hypothalamus contributes to suppression of counterregulatory responses after antecedent hypoglycemia. *Diabetes*, 57(5), pp.1363–1370.

Chan, O. et al., 2013. Lactate-induced release of gaba in the ventromedial hypothalamus contributes to counterregulatory failure in recurrent hypoglycemia and diabetes. *Diabetes*, 62(12), pp.4239–4246.

Chan, O. & Sherwin, R., 2013. Influence of VMH fuel sensing on hypoglycemic responses. *Trends in endocrinology and metabolism: TEM*, 24(12), pp.616–624.

Chandrasekar, B. et al., 1999. Regulation of CCAAT/enhancer binding protein, interleukin-6, interleukin-6 receptor, and gp130 expression during myocardial ischemia/reperfusion. *Circulation*, 99(3), pp.427–433.

Chang, S.-H. et al., 2015. Oncostatin M-dependent Mcl-1 induction mediated by JAK1/2-STAT1/3 and CREB contributes to bioenergetic improvements and protective effects against mitochondrial dysfunction in cortical neurons. *Biochimica et Biophysica Acta (BBA) - Molecular Cell Research*, 1853(10), pp.2306–2325.

Chen, B., Tsui, S. & Smith, T. J., 2005. IL-1β induces IL-6 expression in human orbital fibroblasts: identification of an anatomic-site specific phenotypic attribute relevant to thyroid-associated ophthalmopathy. *The Journal of Immunology*, 175(2), pp.1310–1319.

Chen, H. et al., 2013. Identification and characterization of small molecules as potent and specific EPAC2 antagonists. *Journal of Medicinal Chemistry*, 56(3), pp.952–962.

Chen, P. et al., 2011. Identification of urocortin 3 afferent projection to the ventromedial nucleus of the hypothalamus in rat brain. *The Journal of Comparative Neurology*, 519(10), pp.2023–2042.

Chepurny, O. G. et al., 2009. Enhanced Rap1 activation and insulin secretagogue properties of an acetoxymethyl ester of an Epac-selective cyclic AMP analog in rat INS-1 cells: studies with 8-pCPT-2'-O-Me-cAMP-AM. *Journal of Biological Chemistry*, 284(16), pp.10728–10736.

Chepurny, O. G. et al., 2010. PKA-dependent potentiation of glucose-stimulated insulin secretion by Epac activator 8-pCPT-2'-O-Me-cAMP-AM in human islets of Langerhans. *American Journal of Physiology. Endocrinology and Metabolism*, 298(3), pp.E622–E633.

Choi, S.-E. et al., 2004. IL-6 protects pancreatic islet beta cells from pro-inflammatory cytokines-induced cell death and functional impairment in vitro and in vivo. *Transplant Immunology*, 13(1), pp.43–53.

Choi, S.-J. et al., 2013. Hypoxia antagonizes glucose deprivation on interleukin 6 expression in an Akt dependent, but HIF-1/2α independent manner. *PLoS One*, 8(3), pp.e58662.

Choi, Y.-H. et al., 2013. Revisiting the ventral medial nucleus of the hypothalamus: the roles of SF-1 neurons in energy homeostasis. *Frontiers in Neuroscience*, 7(May), pp.1–9.

Chou, C.-H. et al., 2013. IL-6 regulates Mcl-1L expression through the JAK/PI3K/Akt/CREB signaling pathway in hepatocytes: implication of an anti-apoptotic role during liver regeneration. *PLoS One*, 8(6), pp.e66268.

Chucair-Elliott, A. J. et al., 2014. Microglia-induced IL-6 protects against neuronal loss following HSV-1 infection of neural progenitor cells. *Glia,* 62(9), pp.1418-1434.

Claret, M. et al., 2007. AMPK is essential for energy homeostasis regulation and glucose sensing by POMC and AgRP neurons. *Journal of Clinical Investigation*, 117(8), pp.2325–2336.

Coles, B. et al., 2007. Classic interleukin-6 receptor signaling and interleukin-6 trans-signaling differentially control angiotensin II-dependent hypertension, cardiac signal transducer and activator of transcription-3 activation, and vascular hypertrophy in vivo. *The American Journal of Pathology*, 171(1), pp.315–325.

Contartese, A. et al., 2012. A novel CB2 agonist, COR167, potently protects rat brain cortical slices against OGD and reperfusion injury. *Pharmacological Research*, 66(6), pp.555–563.

Content, J. et al., 1982. Secretory proteins induced in human fibroblasts under conditions used for the production of interferon beta. *Proceedings of the National Academy of Sciences of the United States of America*, 79(9), pp.2768-2772.

Coppola, A. et al., 2007. A central thermogenic-like mechanism in feeding regulation: an interplay between arcuate nucleus T3 and UCP2. *Cell Metabolism*, 5(1), pp.21–33.

Cotero, V. E. & Routh, V. H., 2009. Insulin blunts the response of glucose-excited neurons in the ventrolateral-ventromedial hypothalamic nucleus to decreased glucose. *American Journal of Physiology. Endocrinology and Metabolism*, 296(5), pp.E1101–E1109.

Crawford, R. M. et al., 2001. Creatine kinase is physically associated with the cardiac ATP-sensitive K+ channel. *FASEB Journal*, 16(1), pp.102–104.

Cressman, D. E. et al., 1996. Liver failure and defective hepatocyte regeneration in interleukin-6-deficient mice. *Science (New York, N.Y.)*, 274(5291), pp.1379–1383.

Cryer, P. E., 1997. Hierarchy of physiological responses to hypoglycemia: relevance to clinical hypoglycemia in type I (insulin dependent) diabetes mellitus. *Hormone and Metabolic Research*, 29(3), pp.92–96.

Cryer, P. E., 2013. Hypoglycemia-associated autonomic failure in diabetes. *Handbook of Clinical Neurology*, 117, pp.295–307.

Dalvi, P. S. et al., 2012. Direct regulation of the proglucagon gene by insulin, leptin, and cAMP in embryonic versus adult hypothalamic neurons. *Molecular Endocrinology*, 26(8), pp.1339–1355.

Van Damme, J. et al., 1987. Purification and characterization of human fibroblast-derived hybridoma growth factor identical to T-cell-derived B-cell stimulatory factor-2 (interleukin-6). *European Journal of Biochemistry/FEBS*, 168(3), pp.543–550.

Deeney, J. T., Prentki, M. & Corkey, B. E., 2000. Metabolic control of beta-cell function. *Seminars in Cell and Developmental Biology*, 11, pp.267–275.

Dendorfer, U., Oettgen, P. & Libermann, T. A., 1994. Multiple regulatory elements in the interleukin-6 gene mediate induction by prostaglandins, cyclic AMP, and lipopolysaccharide. *Molecular and Cellular Biology*, 14(7), pp.4443–4454.

Detimary, P., Jonas, J. C. & Henquin, J. C., 1995. Possible links between glucose-induced changes in the energy state of pancreatic B cells and insulin release. *Journal of Clinical Investigation*, 96(4), pp.1738–1745.

Detimary, P. et al., 1998. The changes in adenine nucleotides measured in glucose-stimulated rodent islets occur in beta cells but not in alpha cells and are also observed in human islets. *Journal of Biological Chemistry*, 273(51), pp.33905–33909.

Dong, Y. & Benveniste, E. N., 2001. Immune function of astrocytes. *Glia*, 36(2), pp.180–190.

Donnelly, L. A. et al., 2005. Frequency and predictors of hypoglycaemia in type 1 and insulin-treated type 2 diabetes: a population-based study. *Diabetic Medicine*, 22(6), pp.749–755.

Donovan, C. M. & Watts, A. G., 2014. Peripheral and central glucose sensing in hypoglycemic detection. *Physiology (Bethesda, Md.)*, 29(5), pp.314–324.

Dotson, S. et al., 2008. Hypoglycemia increases serum interleukin-6 levels in healthy men and women. *Diabetes Care*, 31(6), pp.1222–1223.

Dozio, E. et al., 2005. Expression of functional ciliary neurotrophic factor receptors in immortalized gonadotrophin-releasing hormone-secreting neurones. *Journal of Neuroendocrinology*, 17(5), pp.286–291.

Duchen, M. R., Smith, P. A. & Ashcroft, F. M., 1993. Substrate-dependent changes in mitochondrial function, intracellular free calcium concentration and membrane channels in pancreatic beta-cells. *Biochemical Journal*, 294, pp.35–42.

Duelli, R. et al., 1999. Increase in flucose transporter densities of Glut3 and decrease of glucose utilization in rat brain after one week of hypoglycemia. *Brain Research*, 12(381), pp.254–262.

Dunn-Meynell, A. A. et al., 2002. Glucokinase is the likely mediator of glucosensing in both glucose-excited and glucose-inhibited central neurons. *Diabetes*, 51(7), pp.2056–2065.

Dunne, M. J. et al., 2004. Hyperinsulinism in infancy: from basic science to clinical disease. *Physiological Reviews*, 84(1), pp.239–275.

Dzeja, P. P. & Terzic, A., 1998. Phosphotransfer reactions in the regulation of ATP-sensitive K+ channels. *The FASEB Journal*, 12(7), pp.523–529.

Eizirik, D. L. & Mandrup-Poulsen, T., 2001. A choice of death - the signal-transduction of immune-mediated beta-cell apoptosis. *Diabetologia*, 44(12), pp.2115–2133.

Ellingsgaard, H. et al., 2011. Interleukin-6 enhances insulin secretion by increasing glucagon-like peptide-1 secretion from L cells and alpha cells. *Nature Medicine*, 17(11), pp.1481–1489.

Endo, T. A. et al., 1997. A new protein containing an SH2 domain that inhibits JAK kinases. *Nature*, 387(6636), pp.921–924.

Ernst, M., Gearing, D. P. & Dunn, A. R., 1994. Functional and biochemical association of Hck with the LIF/IL-6 receptor signal transducing subunit gp130 in embryonic stem cells. *The EMBO Journal*, 13(7), pp.1574–1584.

Erta, M., Quintana, A. & Hidalgo, J., 2012. Interleukin-6, a major cytokine in the central nervous system. *International Journal of Biological Sciences*, 8(9), pp.1254–1266.

Eulenfeld, R. et al., 2012. Interleukin-6 signalling: more than Jaks and STATs. *European Journal of Cell Biology*, 91(6-7), pp.486–495.

Evans, M. L. et al., 2004. Hypothalamic ATP-sensitive K + channels play a key role in sensing hypoglycemia and triggering counterregulatory epinephrine and glucagon responses. *Diabetes*, 53(10), pp.2542–2551.

Fan, X. et al., 2009. Hypothalamic AMP-activated protein kinase activation with AICAR amplifies counterregulatory responses to hypoglycemia in a rodent model of type 1 diabetes. *American Journal of Physiology. Regulatory, Integrative and Comparative Physiology*, 296(6), pp.R1702–R1708.

Fan, Z. & Makielski, J. C., 1997. Anionic phospholipids activate ATP-sensitive potassium channels. *Journal of Biological Chemistry*, 272(9), pp.5388–5395.

Fang, X. et al., 2013. Neuroprotection of interleukin-6 against NMDA-induced neurotoxicity is mediated by JAK / STAT3 , MAPK / ERK , and PI3K / AKT signaling pathways. *Cell and Molecular Neurobiology*, 33(2), pp.241–251.

Febbraio, M. A., 2014. Role of interleukins in obesity: implications for metabolic disease. *Trends in Endocrinology & Metabolism*, 25(6), pp.312–319.

Feltbower, R., 2008. Acute complications and drug misuse are important causes of death for children and young adults with type 1 diabetes. *Diabetes care*, 31(5), pp.922–926.

Fioramonti, X. et al., 2010. Ventromedial hypothalamic nitric oxide production is necessary for hypoglycemia detection and counterregulation. *Diabetes*, 59(2), pp.519–528.

Fischer, P. et al., 2004. The role of the inhibitors of interleukin-6 signal transduction SHP2 and SOCS3 for desensitization of interleukin-6 signalling. *The Biochemical Journal*, 378(Pt 2), pp.449–460.

Flanagan-Cato, L. M., Calizo, L. H. & Daniels, D., 2001. The synaptic organization of VMH neurons that mediate the effects of estrogen on sexual behavior. *Hormones and Behavior*, 40(2), pp.178–182.

Le Foll, C. et al., 2015. Amylin-induced central IL-6 production enhances ventromedial hypothalamic leptin signaling. *Diabetes*, 64(5), pp.1621–1631.

Fong, Y. et al., 1989. Endotoxemia elicits increased circulating beta 2-IFN/IL-6 in man. *Journal of Immunology*, 142(7), pp.2321–2324.

Fraley, G. S. & Ritter, S., 2003. Immunolesion of norepinephrine and epinephrine afferents to medial hypothalamus alters basal and 2-deoxy-D-glucose-induced neuropeptide Y and agouti gene-related protein messenger ribonucleic acid expression in the arcuate nucleus. *Endocrinology*, 144(1), pp.75–83.

Frei, K. et al., 1989. On the cellular source and function of interleukin 6 produced in the central nervous system in viral diseases. *European Journal of Immunology*, 19(4), pp.689–694.

Friederichs, K. et al., 2001. Interleukin-6-induced proliferation of pre-B cells mediated by receptor complexes lacking the SHP2/SOCS3 recruitment sites revisited. *European Journal of Biochemistry/FEBS*, 268(24), pp.6401–6407.

Frizzell, R. T. et al., 1993. Counterregulation during hypoglycemia is directed by widespread brain regions. *Diabetes*, 42(9), pp.1253–1261.

Fukada, T. et al., 1998. STAT3 orchestrates contradictory signals in cytokine-induced G1 to S cell-cycle transition. *The EMBO Journal*, 17(22), pp.6670–6677.

Fukada, T. et al., 1996. Two signals are necessary for cell proliferation induced by a cytokine receptor gp130: involvement of STAT3 in anti-apoptosis. *Immunity*, 5(5), pp.449–460.

Fukuda, M. et al., 1988. Correlation between minimal secretory capacity of pancreatic beta-cells and stability of diabetic control. *Diabetes*, 37(1), pp.81–88.

Fukuda, M. et al., 2011. Induction of leptin resistance by activation of cAMP-Epac signaling. *Cell Metabolism*, 13(3), pp.331–339.

Gale, S. M., Castracane, V. D. & Mantzoros, C. S., 2004. Energy homeostasis, obesity and eating disorders: recent advances in endocrinology. *The Journal of Nutrition*, 134(2), pp.295–298.

Galloway, P. J. et al., 2000. Insulin-induced hypoglycemia induces a rise in C-reactive protein. *Diabetes Care*, 23(6), pp.861-862.

García, M. et al., 2003. Hypothalamic ependymal-glial cells express the glucose transporter GLUT2, a protein involved in glucose sensing. *Journal of Neurochemistry*, 86(3), pp.709–724.

Geiger, P. C. et al., 2007. IL-6 increases muscle insulin sensitivity only at superphysiological levels. *American Journal of Physiology. Endocrinology and Metabolism*, 292(6), pp.E1842–E1846.

George, P. S. et al., 2015. Diazoxide improves hormonal counterregulatory responses to acute hypoglycemia in long-standing type 1 diabetes. *Diabetes*, 64(6), pp.2234–2241.

Gerich, J. E. et al., 1973. Lack of glucagon response to hypoglycemia in diabetes: evidence for an intrinsic pancreatic alpha cell defect. *Science (New York, N.Y.)*, 182(4108), pp.171–173.

Gertz, K. et al., 2012. Essential role of interleukin-6 in post-stroke angiogenesis. *Brain*, 135(6), pp.1964–1980.

Gesuete, R. et al., 2011. Glial cells drive preconditioning-induced blood-brain barrier protection. *Stroke*, 42(5), pp.1445–1453.

Giuffrè, A. et al., 1996. On the mechanism of inhibition of cytochorme c oxidase by nitric oxide. *Journal of Biological. Chemistry*, 271(52), pp.33404–33408.

Glaser, B. et al., 1994. Familial hyperinsulinism maps to chromosome 11p14-15.1, 30 cM centromeric to the insulin gene. *Nature Genetics*, 7(2), pp.185–188.

Gloyn, A. L. et al., 2004. Activating mutations in the gene encoding the ATP-sensitive potassium-channel subunit Kir6.2 and permanent neonatal diabetes. *The New England Journal of Medicine*, 350(18), pp.1838–1849.

Gloyn, A. L., Siddiqui, J. & Ellard, S., 2006. Mutations in the genes encoding the pancreatic beta-cell KATP channel subunits Kir6.2 (KCNJ11) and SUR1 (ABCC8) in diabetes mellitus and hyperinsulinism. *Human Mutation*, 27(3), pp.220-231.

Gogitidze Joy, N. et al., 2010. Effects of acute hypoglycemia on inflammatory and pro-atherothrombotic biomarkers in individuals with type 1 diabetes and healthy individuals. *Diabetes care*, 33(7), pp.1529–1535.

González, J. A. et al., 2008. Metabolism-independent sugar sensing in central orexin neurons. *Diabetes*, 57(10), pp.2569–2576.

Gonzàlez, J. A., Reimann, F. & Burdakov, D., 2009. Dissociation between sensing and metabolism of glucose in sugar sensing neurones. *The Journal of Physiology*, 587(Pt 1), pp.41–48.

Gough, D. J., Koetz, L. & Levy, D. E., 2013. The MEK-ERK pathway is necessary for serine phosphorylation of mitochondrial STAT3 and ras-mediated transformation. *PLoS One*, 8(11), pp.1–9.

Gray, S. et al., 1990. Distinct patterns of expression of two VAMP genes within the rat brain. *Journal of Neuroscience*, 10(4), pp.1380–1387.

Di Gregorio, G. B. et al., 2004. Lipid and carbohydrate metabolism in mice with a targeted mutation in the IL-6 gene: absence of development of age-related obesity. *American Journal of Physiology. Endocrinology and Metabolism*, 287(1), pp.E182–E187.

Gribble, F. M. et al., 1998. Mechanism of cloned ATP-sensitive potassium channel activation by oleoyl-CoA. *Journal of Biological Chemistry*, 273(41), pp.26383–26387.

Gribble, F. M., Ashfield, R., et al., 1997. Properties of cloned ATP-sensitive K + currents expressed in Xenopus oocytes. *The Journal of Physiology*, 498, pp.87–98.

Gribble, F. M., Tucker, S. J. & Ashcroft, F. M., 1997. The essential role of the Walker A motifs of SUR1 in K-ATP channel activation by Mg-ADP and diazoxide. *The EMBO Journal*, 16(6), pp.1145–1152.

Gribble, F. M., Tucker, S. J. & Ashcroft, F. M., 1997. The interaction of nucleotides with the tolbutamide block of cloned ATP-sensitive K+ channel currents expressed in Xenopus oocytes: a reinterpretation. *The Journal of Physiology*, 504(1), pp.35–45.

Grundtman, C. et al., 2011. Heat shock protein 60 and immune inflammatory responses in atherosclerosis. *Arteriosclerosis, Thrombosis, and Vascular Biology*, 31(5), pp.960–968.

Gruol, D. L., 2015. IL-6 regulation of synaptic function in the CNS. *Neuropharmacology*, 96(Pt A), pp.42–54.

Guillod-Maximin, E. et al., 2004. Acute intracarotid glucose injection towards the brain induces specific c-fos activation in hypothalamic nuclei: involvement of astrocytes in cerebral glucose-sensing in rats. *Journal of Neuroendocrinology*, 16(5), pp.464–471.

Gunaje, J. J. & Bhat, G. J., 2000. Distinct mechanisms of inhibition of interleukin-6-induced Stat3 signaling by TGF-beta and alpha-thrombin in CCL39 cells. *Molecular Cell Biology Research Communications: MCBRC*, 4(3), pp.151–157.

Guschin, D. et al., 1995. A major role for the protein tyrosine kinase JAK1 in the JAK/STAT signal transduction pathway in response to interleukin-6. *The EMBO Journal*, 14(7), pp.1421–1429.

Habash, T. et al., 2015. The proinflammatory cytokine, interleukin-17A, augments mitochondrial function and neurite outgrowth of cultured adult sensory neurons derived from normal and diabetic rats. *Experimental Neurology*, 273, pp.177–189.

Haegeman, G. et al., 1986. Structural analysis of the sequence coding for an inducible 26-kDa protein in human fibroblasts. *European Journal of Biochemistry/FEBS*, 159(3), pp.625–632.

Hahn, W. S. et al., 2014. Proinflammatory cytokines differentially regulate adipocyte mitochondrial metabolism, oxidative stress, and dynamics. *American Journal of Physiology. Endocrinology and Metabolism*, 306(9), pp.E1033–E1045.

Hama, T. et al., 1989. Interleukin-6 as a neurotrophic factor for promoting the survival of cultured basal forebrain cholinergic neurons from postnatal rats. *Neuroscience Letters*, 104(3), pp.340–344.

Hama, T. et al., 1991. Interleukin-6 improves the survival of mesencephalic catecholaminergic and septal cholinergic neurons from postnatal, two-week-old rats in cultures. *Neuroscience*, 40(2), pp.445–452.

Han, J. et al., 2014. Prohibitin 1 modulates mitochondrial function of Stat3. *Cellular Signalling*, 26(10), pp.2086–2095.

Hardie, D. G. & Carling, D., 1997. The AMP-activated protein kinase-fuel gauge of the mammalian cell? *European Journal of Biochemistry/FEBS*, 246(2), pp.259–273.

Hardy, J. D., Hellon, R. F. & Sutherland, K., 1964. Temperature-sensitive neurones in the dog's hypothalamus. *The Journal of Physiology*, 175, pp.242-253.

Hausherr, A. et al., 2007. Inhibition of IL-6-dependent growth of myeloma cells by an acidic peptide repressing the gp130-mediated activation of Src family kinases. *Oncogene*, 26(34), pp.4987–4998.

Heinrich, P. C. et al., 1998. Interleukin-6-type cytokine signalling through the gp130/Jak/STAT pathway. *The Biochemical Journal*, 334(Pt 2), pp.297–314.

Heinrich, P. C. et al., 2003. Principles of interleukin (IL)-6-type cytokine signalling and its regulation. *The Biochemical Journal*, 374(Pt 1), pp.1–20.

Heller, S. R. & Cryer, P. E., 1991. Reduced neuroendocrine and symptomatic responses to subsequent hypoglycemia after 1 episode of hypoglycemia in nondiabetic humans. *Diabetes*, 40(2), pp.223–226.

Herzog, R. I. et al., 2008. Effect of acute and recurrent hypoglycemia on changes in brain glycogen concentration. *Endocrinology*, 149(4), pp.1499–1504.

Herzog, R. I. et al., 2013. Lactate preserves neuronal metabolism and function following antecedent recurrent hypoglycemia. *The Journal of Clinical Investigation*, 123(5), pp.1988–1998.

Hideshima, T. et al., 2001. Biologic sequelae of interleukin-6 induced PI3-K/Akt signaling in multiple myeloma. *Oncogene*, 20(42), pp.5991–6000.

Hirano, T. et al., 1986. Complementary DNA for a novel human interleukin (BSF-2) that induces B lymphocytes to produce immunoglobulin. *Nature*, 324(6092), pp.73–76.

Hirano, T. et al., 1985. Purification to homogeneity and characterization of human B-cell differentiation factor (BCDF or BSFp-2). *Proceedings of the National Academy of Sciences of the United States of America*, 82(16), pp.5490–5494.

Hirota, H. et al., 1996. Accelerated nerve regeneration in mice by upregulated expression of interleukin (IL) 6 and IL-6 receptor after trauma. *The Journal of Experimental Medicine*, 183(6), pp.2627–2634.

Hiscock, N. et al., 2004. Skeletal myocytes are a source of interleukin-6 mRNA expression and protein release during contraction: evidence of fiber type specificity. *FASEB Journal: Official Publication of the Federation of American Societies for Experimental Biology*, 18(9), pp.992–994.

Hoebel, B. G., 1965. Hypothalamic lesions by electrocauterization: disinhibition of feeding and self-stimulation. *Science*, 149(3682), pp.452–453.

Hoene, M. & Weigert, C., 2007. The role of interleukin-6 in insulin resistance , body fat distribution and energy balance. *Obesity Reviews*, 9(1), pp.20–29.

Hoge, J. et al., 2013. IL-6 controls the innate immune response against listeria monocytogenes via classical il-6 signaling. *The Journal of Immunology*, 190(2), pp.703–711.

Holmes, A. G. et al., 2008. Prolonged interleukin-6 administration enhances glucose tolerance and increases skeletal muscle PPARα and UCP2 expression in rats. *Journal of Endocrinology*, 198(2), pp.367–374.

Holz, G. G., Chepurny, O. G. & Leech, C. A., 2013. Leptin-stimulated KATP channel trafficking: a new paradigm for β-cell stimulus-secretion coupling? *Islets*, 5(5), pp.229–232.

Honke, N. et al., 2014. The p38-mediated rapid down-regulation of cell surface gp130 expression impairs interleukin-6 signaling in the synovial fluid of juvenile idiopathic arthritis patients. *Arthritis & Rheumatology*, 66(2), pp.470–478.

Huopio, H. et al., 2000. Dominantly inherited hyperinsulinism caused by a mutation in the sulfonylurea receptor type 1. *The Journal of Clinical Investigation*, 106(7), pp.897–906.

Igaz, P. et al., 2006. Effects of cytokines on gonadotropin-releasing hormone (GnRH) gene expression in primary hypothalamic neurons and in GnRH neurons immortalized conditionally. *Endocrinology*, 147(2), pp.1037–1043.

Insel, P. A. et al., 2012. cAMP and Epac in the regulation of tissue fibrosis. *British Journal of Pharmacology*, 166(2), pp.447–456.

Islam, D. et al., 2009. Epac is involved in cAMP-stimulated proglucagon expression and hormone production but not hormone secretion in pancreatic alpha- and

intestinal L-cell lines. *American Journal of Physiology. Endocrinology and Metabolism*, 296(1), pp.E174–E181.

Islam, O. et al., 2009. Interleukin-6 and neural stem cells: more than gliogenesis. *Molecular Biology of the Cell*, 20(1), pp.188–199.

Itoh, M. et al., 2000. Role of Gab1 in heart, placenta, and skin development and growth factor- and cytokine-induced extracellular signal-regulated kinase mitogen-activated protein kinase activation. *Molecular and Cellular Biology*, 20(10), pp.3695–3704.

Iwasaki, H. et al., 2011. The IκB kinase complex regulates the stability of cytokine-encoding mRNA induced by TLR–IL-1R by controlling degradation of regnase-1. *Nature Immunology*, 12(12), pp.1167–1175.

Jankord, R. et al., 2010. Stress activation of IL-6 neurons in the hypothalamus. *American Journal of Physiology. Regulatory, Integrative and Comparative Physiology*, 299(1), pp.R343–R351.

Jansson, J. O. et al., 2003. On the site and mechanism of action of the anti-obesity effects of interleukin-6. *Growth Hormone & IGF Research*, 13, pp.S28–S32.

Jee, S. H. et al., 2004. Interleukin-6 Induced basic fibroblast growth factor-dependent angiogenesis in basal cell carcinoma cell line via JAK/STAT3 and PI3-Kinase/Akt pathways. *Journal of Investigative Dermatology*, 123(6), pp.1169–1175.

Jetton, T. L. et al., 1994. Analysis of upstream glucokinase promoter activity in transgenic mice and identification of glucokinase in rare neuroendocrine cells in the brain and gut. *The Journal of Biological Chemistry*, 269(5), pp.3641–3654.

Ji, C. et al., 2011. IL-6 induces lipolysis and mitochondrial dysfunction, but does not affect insulin-mediated glucose transport in 3T3-L1 adipocytes. *Journal of Bioenergetics and Biomembranes*, 43(4), pp.367–375.

Jia, Y. et al., 2012. Interleukin 6 protects H2O2-induced cardiomyocytes injury through upregulation of prohibitin via STAT3 phosphorylation. *Cell Biochemistry and Function*, 30(5), pp.426–431.

Jiang, H. L. et al., 2014. The role of central nervous system on hypoglycemia and the feasibility of the brain theory in traditional Chinese medicine on treatment of diabetes mellitus. *Journal of Integrative Medicine*, 12(1), pp.1–6.

John, S. A. et al., 2003. Molecular mechanism for ATP-dependent closure of the K+ channel Kir6.2. *The Journal of Physiology*, 552(Pt 1), pp.23–34.

Jones, S. A., Scheller, J. & Rose-John, S., 2011. Therapeutic straergies for the clinical blockade of IL-6/gp130 signaling. *Journal of Clinical Investigation,* 121(9), pp.3375-3383.

Jostock, T. et al., 2001. Soluble gp130 is the natural inhibitor of soluble interleukin-6 receptor transsignaling responses. *European Journal of Biochemistry*, 268(1), pp.160–167.

Kakei, M. et al., 1986. The ATP-sensitivity of K + channels in rat pancreatic B-cells is modulated by ADP. *FEBS Letters*, 208(1), pp.63–66.

Kang, G. et al., 2006. cAMP sensor Epac as a determinant of ATP-sensitive potassium channel activity in human pancreatic β cells and rat INS-1 cells. *The Journal of Physiology*, 573(3), pp.595–609.

Kang, G. et al., 2008. Role of the cAMP sensor Epac as a determinant of K_{ATP} channel ATP sensitivity in human pancreatic β-cells and rat INS-1 cells. *The Journal of Physiology*, 586(5), pp.1307–1319.

Kang, L. et al., 2006. Glucokinase is a critical regulator of ventromedial hypothalamic neuronal glucosensing. *Diabetes*, 55(2), pp.412–420.

Kang, L. et al., 2004. Physiological and molecular characteristics of rat hypothalamic ventromedial nucleus glucosensing neurons. *Diabetes,* 53(3), pp.549–559.

Kang, L. et al., 2008. Prior hypoglycemia enhances glucose responsiveness in some ventromedial hypothalamic glucosensing neurons. *American Journal of Physiology. Regulatory, Integrative and Comparative Physiology*, 294(3), pp.R784–R792.

Kang, S., Tanaka, T. & Kishimoto, T., 2014. Therapeutic uses of anti-interleukin-6 receptor antibody. *International Immunology*, 27(1), pp.21–29.

Kaptein, A., Paillard, V. & Saunders, M., 1996. Dominant negative Stat3 mutant inhibits interleukin-6-induced Jak-STAT signal transduction. *Journal of Biological Chemistry*, 271(11), pp.5961–5964.

Kawasaki, H. et al., 1998. A family of cAMP-binding proteins that directly activate Rap1. *Science (New York, N.Y.)*, 282(5397), pp.2275–2279.

Kawasaki, Y. et al., 2008. Cytokine mechanisms of central sensitization: distinct and overlapping role of interleukin-1β, interleukin-6, and tumor necrosis factor-α in regulating synaptic and neuronal activity in the superficial spinal cord. *Journal of Neuroscience*, 28(20), pp.5189–5194.

Kelly, M. et al., 2004. AMPK activity is diminished in tissues of IL-6 knockout mice: the effect of exercise. *Biochemical and Biophysical Research Communications*, 320(2), pp.449–454.

Kelly, M. et al., 2009. Activation of AMP-activated protein kinase by interleukin-6 in rat skeletal muscle: association with changes in cAMP, energy state, and endogenous fuel mobilization. *Diabetes*, 58(9), pp.1953–1960.

Kershaw, N. J. et al., 2013. SOCS3 binds specific receptor–JAK complexes to control cytokine signaling by direct kinase inhibition. *Nature Structural & Molecular Biology*, 20(4), pp.469–476.

Kim, H. J. et al., 2004. Differnetial effects of interluekin-6 and -10 on skeletal muscle and liver insulin action in vivo. *Diabetes,* 53(4), pp.1060-1067.

King, B. M., 2006. The rise, fall, and resurrection of the ventromedial hypothalamus in the regulation of feeding behavior and body weight. *Physiology and Behavior*, 87(2), pp.221–244.

Kiranadi, B., Bangham, J. A. & Smith, P. A., 1991. Inhibition of electrical activity in mouse pancreatic beta-cells by the ATP/ADP translocase inhibitor, bongkrekic acid. *FEBS Letters*, 283(1), pp.93–96.

Klouche, M. et al., 1999. Novel path to activation of vascular smooth muscle cells: up-regulation of gp130 creates an autocrine activation loop by IL-6 and its soluble receptor. *Journal of Immunology (Baltimore, Md.:1950)*, 163(8), pp.4583–4589.

Kluger, M. J., 1991. Fever: role of pyrogens and cryogens. *Physiological Reviews*, 71(1), pp.93–127.

Knudsen, J. G. et al., 2015. Skeletal muscle interleukin-6 regulates metabolic factors in iWAT during HFD and exercise training. *Obesity*, 23(8), pp.1616–1624.

Ko, H. J. et al., 2009. Nutrient stress activates inflammation and reduces glucose metabolism by suppressing AMP-activated protein kinase in the heart. *Diabetes*, 58(11), pp.2536–2546.

Kohase, M. et al., 1987. A cytokine network in human diploid fibroblasts: interactions of beta-interferons, tumor necrosis factor, platelet-derived growth factor and interleukin-1. *Molecular and Cellular Biology*, 7(1), pp.273–280.

Kohno, D. & Yada, T., 2012. Arcuate NPY neurons sense and integrate peripheral metabolic signals to control feeding. *Neuropeptides*, 46(6), pp.315–319.

Kolb, H. & Mandrup-Poulsen, T., 2005. An immune origin of type 2 diabetes? *Diabetologia*, 48(6), pp.1038–1050.

Kong, D. et al., 2010. Glucose stimulation of hypothalamic MCH neurons involves KATP channels, is modulated by UCP2, and regulates peripheral glucose homeostasis. *Cell Metabolism*, 12(5), pp.545–552.

Kortylewski, M. et al., 1999. Interleukin-6 and oncostatin M-induced growth inhibition of human A375 melanoma cells is STAT-dependent and involves upregulation of the cyclin-dependent kinase inhibitor p27/Kip1. *Oncogene*, 18(25), pp.3742–3753.

Kraakman, M. J. et al., 2015. Blocking IL-6 trans-signaling prevents high-fat diet-induced adipose tissue macrophage recruitment but does not improve insulin resistance. *Cell Metabolism*, 21(3), pp.403–416.

Krippeit-Drews, P. et al., 2003. Phosphocreatine as a determinant of KATP channel activity in pancreatic beta-cells. *Pflugers Archiv*, 445(5), pp.556–562.

Kristiansen, O. P. & Mandrup-Poulsen, T., 2005. Interluekin-6 and diabetes: the good, the bad, or the indifferent? *Diabetes*, 54(December), pp.S114-S124.

Laakso, M. & Kuusisto, J., 2014. Insulin resistance and hyperglycaemia in cardiovascular disease development. *Nature Reviews. Endocrinology*, 10(5), pp.293–302.

Laemmli, U. K., 1970. Cleavage of structural proteins during the assembly of the head of bacteriophage T4. *Nature*, 227(5259), pp.680–685.

Lagathu, C. et al., 2003. Chronic interleukin-6 (IL-6) treatment increased IL-6 secretion and induced insulin resistance in adipocyte: prevention by rosiglitazone. *Biochemical and Biophysical Research Communications*, 311(2), pp.372–379.

Lamy, C. M. et al., 2014. Hypoglycemia-activated GLUT2 neurons of the nucleus tractus solitarius stimulate vagal activity and glucagon secretion. *Cell Metabolism*, 19(3), pp.527–538.

Lang, F. & Föller, M., 2014. Regulation of ion channels and transporters by AMP-activated kinase (AMPK). *Channels*, 8(1), pp.20–28.

Lang, R. et al., 2003. SOCS3 regulates the plasticity of gp130 signaling. *Nature Immunology*, 4(6), pp.546–550.

Larsson, O. et al., 1996. Activation of the ATP-sensitive K+ channel by long chain acyl-CoA. A role in modulation of pancreatic beta-cell glucose sensitivity. *Journal of Biological Chemistry*, 271(18), pp.10623–10626.

Laurent, A.-C. et al., 2012. Role of Epac in brain and heart. *Biochemical Society Transactions*, 40(1), pp.51–57.

Leech, C. A. et al., 2010. Facilitation of beta-cell KATP channel sulfonylurea sensitivity by a cAMP analog selective for the cAMP-regulated guanine nucelotide exchange factor Epac. *Islets*, 2(2), pp.72–81.

Lehmann, U. et al., 2003. SHP2 and SOCS3 contribute to Tyr-759-dependent attenuation of interleukin-6 signaling through gp130. *Journal of Biological Chemistry*, 278(1), pp.661–671.

Lei, H. & Gruetter, R., 2006. Effect of chronic hypoglycaemia on glucose concentration and glycogen content in rat brain: a localized 13C NMR study. *Journal of Neurochemistry*, 99(1), pp.260–268.

Lenzen, S., 2014. A fresh view of glycolysis and glucokinase regulation: history and current status. *Journal of Biological Chemistry*, 289(18), pp.12189–12194.

Levin, B. E., 1999. Arcuate NPY neurons and energy homeostasis in diet-induced obese and resistant rats. *American Journal of Physiology*, 276(2 Pt 2), pp.R382–R387.

Levin, B. E. et al., 2008. Ventromedial hypothalamic glucokinase is an important mediator of the counterregulatory response to insulin-induced hypoglycemia. *Diabetes*, 57(5), pp.1371–1379.

Li, B., Lee, K. & Martin, R. J., 2006. Overexpression of glucose transporter 2 in GT1-7 cells inhibits AMP-activated protein kinase and agouti-related peptide expression. *Brain Research*, 1118(1), pp.1–5.

Li, G. et al., 2002. Induction of uncoupling protein 1 by central interleukin-6 gene delivery is dependent on sympathetic innervation of brown adipose tissue and underlies one mechanism of body weight reduction in rats. *Neuroscience,* 115(3) pp.879-889.

Li, W. et al., 2003. Regulation of noradrenergic function by inflammatory cytokines and depolarization. *Journal of Neurochemistry*, 86(3), pp.774–783.

Libermann, T. A. & Baltimore, D., 1990. Activation of interleukin-6 gene expression through the NF-κB transcription factor. *Molecular and Cellular Biology*, 10(5), pp.2327–2334.

Loddick, S. A., Turnbull, A. V. & Rothwell, N. J., 1998. Cerebral interleukin-6 is neuroprotective during permanent focal cerebral ischemia in the rat. *Journal of Cerebral Blood Flow And Metabolism: Official Journal of the International Society of Cerebral Blood Flow and Metabolism*, 18(2), pp.176–179.

Lotfi, S. et al., 2006. Role of the exchange protein directly activated by cyclic adenosine 5'-monophosphate (Epac) pathway in regulating proglucagon gene expression in intestinal endocrine l cells. *Endocrinology*, 147(8), pp.3727–3736.

Lowes, D. A. et al., 2013. Antioxidants that protect mitochondria reduce interleukin-6 and oxidative stress, improve mitochondrial function, and reduce biochemical markers of organ dysfunction in a rat model of acute sepsis. *British Journal of Anaesthesia*, 110(3), pp.472–480.

Lust, J. A. et al., 1992. Isolation of an mRNA encoding a soluble form of the human interleukin-6 receptor. *Cytokine*, 4(2), pp.96–100.

Lynch, R. M. et al., 2000. Localization of glucokinase gene expression in the rat brain. *Diabetes*, 49(5), pp.693–700.

Ma, Y. et al., 2015. Interleukin-6 gene transfer reverses body weight gain and fatty liver in obese mice. *Biochimica et Biophysica Acta (BBA) - Molecular Basis of Disease*, 1852(5), pp.1001–1011.

Magistretti, P. J. et al., 1999. Energy on demand. *Science*, 283(5401), pp.496–497.

Magni, P. et al., 2007. Leukemia inhibitory factor induces the chemomigration of immortalized gonadotropin-releasing hormone neurons through the independent activation of the Janus kinase/signal transducer and activator of transcription 3, mitogen-activated protein kinase/extracellularly regulated kinase 1/2, and phosphatidylinositol 3-kinase/Akt signaling pathways. *Molecular Endocrinology (Baltimore, Md.)*, 21(5), pp.1163–1174.

Markworth, E., Schwanstecher, C. & Schwanstecher, M., 2000. ATP4- mediates closure of pancreatic beta-cell ATP-sensitive potassium channels by interaction with one of four identical sites. *Diabetes*, 49(9), pp.1413–1418.

Marty, N. et al., 2005. Regulation of glucagon secretion by glucose transporter type 2 (glut2) and astrocyte-dependent glucose sensors. *The Journal of Clinical Investigation*, 115(12), pp.3545–3553.

Marty, N., Dallaporta, M. & Thorens, B., 2007. Brain glucose sensing, counterregulation, and energy homeostasis. *Physiology (Bethesda, Md.)*, 22 pp.241–251.

Mason, G. F. et al., 2006. Increased brain monocarboxylic acid transport and utilization in type 1 diabetes. *Diabetes*, 55(4), pp.929–934.

Masuda, K. et al., 2013. Arid5a controls IL-6 mRNA stability, which contributes to elevation of IL-6 level in vivo. *Proceedings of the National Academy of Sciences of the United States of America*, 110(23), pp.9409–9414.

Matsusaka, T. & Fujikawa, K., 1993. Transcription factors NF-IL6 and NFκB synergistically activate transcription of the inflammatory cytokines, interleukin 6 and interleukin 8. *Proceedings of the National Academy of Sciences of the United States of America,* 90(21), pp.10193–10197.

Matsushita, K. et al., 2009. Zc3h12a is an RNase essential for controlling immune responses by regulating mRNA decay. *Nature*, 458(7242), pp.1185–1190.

Matthews, V. B. et al., 2010. Interleukin-6-deficient mice develop hepatic inflammation and systemic insulin resistance. *Diabetologia*, 53(11), pp.2431–2441.

Mauer, J. et al., 2014. Signaling by IL-6 promotes alternative activation of macrophages to limit endotoxemia and obesity-associated resistance to insulin. *Nature Immunology*, 15(5), pp.423-430.

Mauer, J., Denson, J. L. & Brüning, J. C., 2015. Versatile functions for IL-6 in metabolism and cancer. *Trends in Immunology*, 36(2), pp92-101.

Mayer, J., 1953. Glucostatic mechanism of regulation of food intake. *New England Journal of Medicine*, 249(1), pp.13–16.

McCrimmon, R. J. et al., 2005. Activation of ATP-sensitive K+ channels in the ventromedial hypothalamus amplifies counterregulatory hormone responses to hypoglycemia in normal and recurrently hypoglycemic rats. *Diabetes*, 54(11), pp.3169–3174.

McCrimmon, R. J. et al., 2006. Corticotrophin-releasing factor receptors within the ventromedial hypothalamus regulate hypoglycemia-induced hormonal counterregulation. *Journal of Clinical Investigation.*, 116(6), pp.1723–1730.

McCrimmon, R. J. et al., 2008. Key role for AMP-activated protein kinase in the ventromedial hypothalamus in regulating counterregulatory hormone responses to acute hypoglycemia. *Diabetes*, 57(2), pp.444–450.

McCrimmon, R. J. et al., 2004. Potential role for AMP-activated protein kinase in hypoglycemia sensing in the ventromedial hypothalamus. *Diabetes*, 53(8), pp.1953–1958.

McCrimmon, R. J. & Sherwin, R. S., 2010. Hypoglycemia in type 1 diabetes. *Diabetes*, 59(10), pp.2333–2339.

McFarland-Mancini, M. M. et al., 2010. Differences in wound healing in mice with deficiency of IL-6 versus IL-6 receptor. *The Journal of Immunology*, 184(12), pp.7219–7228.

Meier, J. A. & Larner, A. C., 2014. Toward a new STATe: the role of STATs in mitochondrial function. *Seminars in Immunology*, 26(1), pp.20–28.

Mellon, P. L. et al., 1990. Immortalization of hypothalamic GnRH neurons by genetically targeted tumorigenesis. *Neuron*, 5(1), pp.1–10.

Métrich, M. et al., 2010. Role of the cAMP-binding protein Epac in cardiovascular physiology and pathophysiology. *Pflügers Archiv - European Journal of Physiology*, 459(4), pp.535–546.

Miki, T. et al., 2001. ATP-sensitive K+ channels in the hypothalamus are essential for the maintenance of glucose homeostasis. *Nature Neuroscience*, 4(5), pp.507–512.

Miki, T. et al., 1998. Defective insulin secretion and enhanced insulin action in KATP channel-deficient mice. *Proceedings of the National Academy of Sciences of the United States of America*, 95(18), pp.10402–10406.

Miki, T. & Seino, S., 2005. Roles of K channels as metabolic sensors in acute metabolic changes. *Journal of Molecular and Cellular Cardiology*, 38(6), pp.917–925.

Millán, C. et al., 2010. Glial glucokinase expression in adult and post-natal development of the hypothalamic region. *ASN Neuro*, 2(3), pp.135–145.

Mokan, M. et al., 1994. Hypoglycemia unawareness in IDDM. *Diabetes Care*, 17(12), pp.1397–1403.

Mounien, L. et al., 2010. Glut2-dependent glucose-sensing controls thermoregulation by enhancing the leptin sensitivity of NPY and POMC neurons. *The FASEB Journal: Official Publication of the Federation of American Societies for Experimental Biology*, 24(6), pp.1747–1758.

Müllberg, J. et al., 1993. The soluble interleukin-6 receptor is generated by shedding. *European Journal of Immunology*, 23(2), pp.473–480.

Müller-Newen, G. et al., 1996. Purification and characterization of the soluble interleukin-6 receptor from human plasma and identification of an isoform generated through alternative splicing. *European Journal of Biochemistry/FEBS*, 236(3), pp.837–842.

Murai, K. K. & Pasquale, E. B., 2011. Eph receptors and ephrins in neuron-astrocyte communication at synapses. *Glia*, 59(11), pp.1567–1578.

Murphy, B. A. et al., 2009. AMP-activated protein kinase and nitric oxide regulate the glucose sensitivity of ventromedial hypothalamic glucose-inhibited neurons. *American Journal of Physiology: Cell Physiology*, 297(3), pp.C750–C758.

Murphy, B. A. et al., 2009. Fasting enhances the response of arcuate neuropeptide Y-glucose-inhibited neurons to decreased extracellular glucose. *American Journal of Physiology. Cell Physiology*, 296(4), pp.C746–C756.

Myers, M. P. et al., 2001. TYK2 and JAK2 are substrates of protein-tyrosine phosphatase 1B. *The Journal of Biological Chemistry*, 276(51), pp.47771–47774.

Naka, T. et al., 1997. Structure and function of a new STAT-induced STAT inhibitor. *Nature*, 387(6636), pp.924–929.

Nakayama, T., Eisenman, J. S. & Hardy, J. D., 1961. Single unit activity of anterior hypothalamus during local heating. *Science (New York, N.Y.)*, 134(3478), pp.560–561.

Nelson, T. E., Ur, C. L. & Gruol, D. L., 2002. Chronic interleukin-6 exposure alters electrophysiological properties and calcium signaling in developing cerebellar purkinje neurons in culture. *Journal of Neurophysiology*, 88(1), pp.475–486.

Neurath, K. M. et al., 2006. AMP-dependent protein kinase alpha 2 isoform promotes hypoxia-induced VEGF expression in human glioblastoma. *Glia*, 53(7), pp.733–743.

Neurath, M. F. & Finotto, S., 2011. IL-6 signaling in autoimmunity, chronic inflammation and inflammation-associated cancer. *Cytokine & Growth Factor Reviews*, 22(2), pp.83–89.

Nichols, C. G. et al., 1996. Adenosine diphosphate as an intracellular regulator of insulin secretion. *Science*, 272(5269), pp.1785–1787.

Nichols, C. G., 2006. KATP channels as molecular sensors of cellular metabolism. *Nature*, 440(7083), pp.470–476.

Nicholson, S. E. et al., 2000. Suppressor of cytokine signaling-3 preferentially binds to the SHP-2-binding site on the shared cytokine receptor subunit gp130. *Proceedings of the National Academy of Sciences of the United States of America*, 97(12), pp.6493–6498.

Nieto-Vazquez, I. & Ferna, S., 2008. Dual role of interleukin-6 in regulating insulin sensitivity in murine skeletal muscle. *Diabetes*, 57(12), pp.3211–3221.

Niu, F. et al., 2009. Trichostatin A enhances OGD-astrocyte viability by inhibiting inflammatory reaction mediated by NF-κB. *Brain Research Bulletin*, 78(6), pp.342–346.

Noguchi, Y. et al., 2013. Astrocytes protect neurons against methylmercury via ATP/P2Y1 receptor-mediated pathways in astrocytes. *PLoS One*, 8(2), pp.e57898.

Nowell, M. A. et al., 2003. Soluble IL-6 receptor governs IL-6 activity in experimental arthritis: blockade of arthritis severity by soluble glycoprotein 130. *The Journal of Immunology*, 171(6), pp.3202–3209.

O'Malley, D. et al., 2006. Sodium-coupled glucose cotransporters contribute to hypothalamic glucose sensing. *Diabetes*, 55(12), pp.3381–3386.

O'Neill, H. M. et al., 2013. IL-6 is not essential for exercise-induced increases in glucose uptake IL-6 is not essential for exercise-induced increases in glucose uptake. *Journal of Applied Physiology*, 114(9), pp.1151–1157.

Ogunnowo-Bada, E. O. et al., 2014. Brain glucose sensing, glucokinase and neural control of metabolism and islet function. *Diabetes, Obesity and Metabolism*, 16(S1), pp.26–32.

Oh, Y. S. et al., 2011. Interleukin-6 treatment induces beta-cell apoptosis via STAT-3-mediated nitric oxide production. *Diabetes/Metabolism Research and Reviews*, 27, pp.813–819.

Oomura, Y. & Yoshimatsu, H., 1984. Neural network of glucose monitoring system. *Journal of the Autonomic Nervous System*, 10(3-4), pp.359–372.

Osundiji, M. A. et al., 2010. Brain glucosamine boosts protective glucoprivic feeding. *Endocrinology*, 151(4), pp.1499–1508.

Osundiji, M. A. et al., 2012. Brain glucose sensors play a significant role in the regulation of pancreatic glucose-stimulated insulin secretion. *Diabetes*, 61(2), pp.321–328.

Osundiji, M. A. et al., 2011. Recurrent hypoglycemia increases hypothalamic glucose phosphorylation activity in rats. *Metabolism*, 60(4), pp.550–556.

Pal, M., Febbraio, M. A. & Whitham, M., 2014. From cytokine to myokine: the emerging role of interleukin-6 in metabolic regulation. *Immunology and Cell Biology*, 92(4), pp.331–339.

Pan, L. et al., 2014. Astrocytic toll-like receptor 3 is associated with ischemic preconditioning-induced protection against brain ischemia in rodents. *PLoS One*, 9(6), pp.e99526.

Paranjape, S. A. et al., 2010. Influence of insulin in the ventromedial hypothalamus on pancreatic glucagon secretion in vivo. *Diabetes*, 59(6), pp.1521–1527.

Patil, G. D. & Briski, K. P., 2005. Lactate is a critical "sensed" variable in caudal hindbrain monitoring of CNS metabolic stasis. *American Journal of Physiology. Regulatory, Integrative and Comparative Physiology*, 289(6), pp.R1777–R1786.

Patil, G. D. & Briski, K. P., 2005. Transcriptional activation of nucleus tractus solitarii/area postrema catecholaminergic neurons by pharmacological inhibition

of caudal hindbrain monocarboxylate transporter function. *Neuroendocrinology*, 81(2), pp.96–102.

Peace, A. G. & Shewan, D. A., 2011. New perspectives in cyclic AMP-mediated axon growth and guidance: the emerging epoch of Epac. *Brain Research Bulletin*, 84(4-5), pp.280–288.

Pedersen, B. K. & Febbraio, M.A., 2007. Point-counterpoint: interleukin-6 does/does not have a beneficial role in insulin sensitivity and glucose homeostasis. *Journal of Applied Physiology (Bethesda, Md.:1985)*, 102(2), pp.814–816.

Pellerin, L. et al., 2007. Activity-dependent regulation of energy metabolism by astrocytes: an update. *Glia*, 55(12), pp.1251–1262.

Pellerin, L. & Magistretti, P. J., 2012. Sweet sixteen for ANLS. *Journal of Cerebral Blood Flow and Metabolism*, 32(7), pp.1152–1166.

Pickup, J., 2004. Inflammation and activated innate immunity in the pathogenesis of type 2 diabetes. *Diabetes Care*, 27(3), pp.813–823.

Pluskey, S. et al., 1995. Potent stimulation of SH-PTP2 phosphatase activity by simultaneous occupancy of both SH2 domains. *The Journal of Biological Chemistry*, 270(7), pp.2897–2900.

Pranada, A. L. et al., 2004. Real time analysis of STAT3 nucleocytoplasmic shuttling. *Journal of Biological Chemistry*, 279(15), pp.15114–15123.

Qiu, Z., Parsons, K. L. & Gruol, D. L., 1995. Interleukin-6 selectively enhances the intracellular calcium response to NMDA in developing CNS neurons. *Journal of Neuroscience.*, 15(10), pp.6688–6699.

Ramsay, A. J. et al., 1994. The role of interleukin-6 in mucosal IgA antibody responses in vivo. *Science (New York, N.Y.)*, 264(5158), pp.561–563.

Raptis, L. et al., 2011. The R(h)oads to Stat3: Stat3 activation by the Rho GTPases. *Experimental Cell Research*, 317(13), pp.1787–1795.

Ray, A., LaForge, K. S. & Sehgal, P. B., 1990. On the mechanism for efficient repression of the interleukin-6 promoter by glucocorticoids: enhancer, TATA box, and RNA start site (Inr motif) occlusion. *Molecular and Cellular Biology*, 10(11), pp.5736–5746.

Ray, A. et al., 1988. Activation of the human "beta 2-interferon/hepatocyte-stimulating factor/interleukin 6" promoter by cytokines, viruses, and second messenger agonists. *Biochemistry*, 85(18), pp.6701–6705.

Razavi Nematollahi, L. et al., 2009. Proinflammatory cytokines in response to insulin-induced hypoglycemic stress in healthy subjects. *Metabolism*, 58(4), pp.443–448.

Redzic, Z. B. et al., 2015. Differential effects of paracrine factors on the survival of cells of the neurovascular unit during oxygen glucose deprivation. *International Journal of Stroke*, 10(3), pp.407–414.

Reich, N. C., 2009. STAT3 revs up the powerhouse. *Science Signaling*, 2(90), pp.pe61.

Richards, P. J. et al., 2006. Functional characterization of a soluble gp130 isoform and its therapeutic capacity in an experimental model of inflammatory arthritis. *Arthritis and Rheumatism*, 54(5), pp.1662–1672.

Ritter, R. C., Slusser, P. G. & Stone, S., 1981. Glucoreceptors controlling feeding and blood glucose: location in the hindbrain. *Science (New York, N.Y.)*, 213(4506), pp.451–452.

Ritter, S., Bugarith, K. & Dinh, T. T., 2001. Immunotoxic destruction of distinct catecholamine subgroups produces selective impairment of glucoregulatory

responses and neuronal activation. *Journal of Comparative Neurology*, 432(2), pp.197–216.

Ritter, S., Dinh, T. T. & Zhang, Y., 2000. Localization of hindbrain glucoreceptive sites controlling food intake and blood glucose. *Brain Research*, 856(1-2), pp.37–47.

Rodig, S. J. et al., 1998. Disruption of the Jak1 gene demonstrates obligatory and nonredundant roles of the Jaks in cytokine-induced biologic responses. *Cell*, 93(3), pp.373–383.

Roncero, I. et al., 2004. Expression of glucose transporter isoform GLUT-2 and glucokinase genes in human brain. *Journal of Neurochemistry*, 88(5), pp.1203–1210.

De Rooij, J. et al., 1998. Epac is a Rap1 guanine-nucleotide-exchange factor directly activated by cyclic AMP. *Nature*, 396(6710), pp.474–477.

Rose-John, S., 2012. IL-6 trans-signaling via the soluble IL-6 receptor: importance for the pro-inflammatory activities of IL-6. *International Journal of Biological Sciences,* 8(9), pp.1237-1247.

Rose-John, S. et al., 1990. Studies on the structure and regulation of the human hepatic interleukin-6 receptor. *European Journal of Biochemistry*, 190(2990), pp.79–83.

Rossato, M. et al., 2012. IL-10-induced microRNA-187 negatively regulates TNF-α, IL-6, and IL-12p40 production in TLR4-stimulated monocytes. *Proceedings of the National Academy of Sciences of the United States of America*, 109(45), pp.E3101–E3110.

Rotter Sopasakis, V. et al., 2004. Short-term infusion of interleukin-6 does not induce insulin resistance in vivo or impair insulin signalling in rats. *Diabetologia*, 47(11), pp.1879–1887.

Rotter, V., Nagaev, I. & Smith, U., 2003. Interleukin-6 (IL-6) induces insulin resistance in 3T3-L1 adipocytes and is, like IL-8 and tumor necrosis factor-α, overexpressed in human fat cells from insulin-resistant subjects. *Journal of Biological Chemistry*, 278(46), pp.45777–45784.

Routh, V. H., 2010. Glucose sensing neurons in the ventromedial hypothalamus. *Sensors*, 10(10), pp.9002–9025.

Rowe, I. C., Boden, P. R. & Ashford, M. L., 1996. Potassium channel dysfunction in hypothalamic glucose-receptive neurones of obese Zucker rats. *The Journal of Physiology*, 497(Pt 2), pp.365–377.

Sakata, H. et al., 2012. Interleukin 6-preconditioned neural stem cells reduce ischaemic injury in stroke mice. *Brain*, 135(11), pp.3298–3310.

Sakura, H. et al., 1995. Cloning and functional expression of the cDNA encoding a novel ATP-sensitive potassium channel subunit expressed in pancreatic beta-cells, brain, heart and skeletal muscle. *FEBS Letters*, 377(3), pp.338–344.

Samios, V. N. & Inoue, T., 2014. Interleukin-1β and interleukin-6 affect electrophysiological properties of thalamic relay cells. *Neuroscience Research*, 87, pp.16–25.

Sanders, N. M. et al., 2007. Antecedent hindbrain glucoprivation does not impair the counterregulatory response to hypoglycemia. *Diabetes*, 56(1), pp.217–223.

Sanders, N. M. et al., 2008. The selective serotonin reuptake inhibitor sertraline enhances counterregulatory responses to hypoglycemia. *American Journal of Physiology. Endocrinology and Metabolism*, 294(5), pp.E853–E860.

Sands, W. A. et al., 2006. Exchange protein activated by cyclic AMP (Epac)-mediated induction of suppressor of cytokine signaling 3 (SOCS-3) in vascular endothelial cells. *Molecular and Cellular Biology*, 26(17), pp.6333–6346.

Sasaki, A. et al., 1999. Cytokine-inducible SH2 protein-3 (CIS3/SOCS3) inhibits Janus tyrosine kinase by binding through the N-terminal kinase inhibitory region as well as SH2 domain. *Genes to Cells*, 4(6), pp.339–351.

Schaeffer, M. et al., 2001. Signaling through a novel domain of gp130 mediates cell proliferation and activation of Hck and Erk kinases. *Molecular and Cellular Biology*, 21(23), pp.8068–8081.

Schaper, F. et al., 1998. Activation of the protein tyrosine phosphatase SHP2 via the interleukin-6 signal transducing receptor protein gp130 requires tyrosine kinase Jak1 and limits acute-phase protein expression. *The Biochemical Journal*, 335(Pt 3), pp.557–565.

Schaper, F. & Rose-John, S., 2015. Interleukin-6: biology, signaling and strategies of blockade. *Cytokine & Growth Factor Reviews*, 26(5), pp.475–487.

Schéle, E. et al., 2013. Inter-relation between interleukin (IL)-1, IL-6 and body fat regulating circuits of the hypothalamic arcuate nucleus. *Journal of Neuroendocrinology*, 25(6), pp.580–589.

Scheller, J. et al., 2011. The pro- and anti-inflammatory properties of the cytokine interleukin-6. *Biochimica et Biophysica Acta*, 1813(5), pp.878–888.

Schiemann, W. P., Bartoe, J. L. & Nathanson, N. M., 1997. Box 3-independent signaling mechanisms are involved in leukemia inhibitory factor receptor alpha- and gp130-mediated stimulation of mitogen-activated protein kinase. Evidence for participation of multiple signaling pathways which converge at Ras. *The Journal of Biological Chemistry*, 272(26), pp.16631–16636.

Schmid-Antomarchi, H. et al., 1987. The receptor for antidiabetic sulfonylureas controls the activity of the ATP-modulated K+ channel in insulin-secreting cells. *Journal of Biological Chemistry*, 262(33), pp.15840–15844.

Schmidt, M. et al., 2001. A new phospholipase-C-calcium signalling pathway mediated by cyclic AMP and a Rap GTPase. *Nature Cell Biology*, 3(11), pp.1020–1024.

Schmitz, J. et al., 2000. SOCS3 exerts its inhibitory function on interleukin-6 signal transduction through the SHP2 recruitment site of gp130. *Journal of Biological Chemistry*, 275(17), pp.12848–12856.

Schöbitz, B. et al., 1993. Cellular localization of interleukin 6 mRNA and interleukin 6 receptor mRNA in rat brain. *The European Journal of Neuroscience*, 5(11), pp.1426–1435.

Schönfeld, P. & Reiser, G., 2013. Why does brain metabolism not favor burning of fatty acids to provide energy? - Reflections on disadvantages of the use of free fatty acids as fuel for brain. *Journal of Cerebral Blood Flow & Metabolism*, 33(10), pp.1493–1499.

Schulze, D. et al., 2003. Phosphatidylinositol 4,5-bisphosphate (PIP 2) modulation of ATP and pH sensitivity in Kir channels. *Journal of Biological Chemistry*, 278(12), pp.10500–10505.

Schwartz, G. J., 2000. The role of gastrointestinal vagal afferents in the control of food intake: current prospects. *Nutrition*, 16(10), pp.866–873.

Seghers, V. et al., 2000. Sur1 knockout mice. a model for K(ATP) channel-independent regulation of insulin secretion. *Journal of Biological Chemistry*, 275(13), pp.9270–9277.

Sehgal, P. B. et al., 1988. Regulation of the acute phase and immune responses in viral diseases. *The Journal of Experimental Medicine,* 167(6), pp.1951–1956.

Sehgal, P. B. & Sagar, A. D., 1980. Heterogeneity of poly(I) x poly(C)-induced human fibroblast interferon mRNA species. *Nature*, 288(5786), pp.95–97.

Seino, S., 1999. ATP-sensitive potassium channels: a model of heteromultimeric potassium channel/receptor assemblies. *Annual Review of Physiology*, 61(88), pp.337–362.

Seino, S. et al., 2000. Diverse roles of K(ATP) channels learned from Kir6.2 genetically engineered mice. *Diabetes*, 49(3), pp.311–318.

Shi, H. et al., 2004. Suppressor of cytokine signaling 3 is a physiological regulator of adipocyte insulin signaling. *Journal of Biological Chemistry*, 279(33), pp.34733–34740.

Shibasaki, T. et al., 2004a. Interaction of ATP sensor, cAMP sensor, Ca2+ sensor, and voltage-dependent Ca2+ channel in insulin granule exocytosis. *Journal of Biological Chemistry*, 279(9), pp.7956–7961.

Shibasaki, T., Sunaga, Y. & Seino, S., 2004b. Integration of ATP, cAMP, and Ca2+ signals in insulin granule exocytosis. *Diabetes*, 53(Suppl 3), pp.S59–S62.

Shibata, M., 1990. Hypothalamic neuronal responses to cytokines. *The Yale Journal of Biology and Medicine*, 63(2), pp.147–156.

Shimizu, H. et al., 1990. Involvement of a NF-kappa B-like transcription factor in the activation of the interleukin-6 gene by inflammatory lymphokines. *Molecular and Cellular Biology*, 10(2), pp.561–568.

Shiota, C., 2002. Sulfonylurea receptor type 1 knock-out mice have intact feeding-stimulated insulin secretion despite marked impairment in their response to glucose. *Journal of Biological Chemistry*, 277(40), pp.37176–37183.

Shirazi, R. et al., 2013. Glucagon-like peptide 1 receptor induced suppression of food intake, and body weight is mediated by central IL-1 and IL-6. *Proceedings of the National Academy of Sciences of the United States of America*, 110(40), pp.16199–16204.

Shirshev, S. V., 2011. Role of Epac proteins in mechanisms of cAMP-dependent immunoregulation. *Biochemistry (Moscow)*, 76(9), pp.981–998.

Shyng, S. et al., 2000. Modulation of nucleotide sensitivity of ATP-sensitive potassium channels by phosphatidylinositol-4- phosphate 5-kinase. *Proceedings of the National Academy of Sciences of the United States of America*, 97(2), pp.937–941.

Shyng, S., Ferrigni, T. & Nichols, C. G., 1997. Regulation of KATP channel activity by diazoxide and MgADP. Distinct functions of the two nucleotide binding folds of the sulfonylurea receptor. *Journal of General Physiology*, 110(6), pp.643–654.

Shyng, S. L. & Nichols, C. G., 1998. Membrane phospholipid control of nucleotide sensitivity of KATP channels. *Science (New York, N.Y.)*, 282(5391), pp.1138–1141.

Siegmund, B. et al., 2004. Development of intestinal inflammation in double IL-10- and leptin-deficient mice. *Journal of Leukocyte Biology*, 76(4), pp.782–786.

Silva, N. L. & Boulant, J. A, 1986. Effects of testosterone, estradiol, and temperature on neurons in preoptic tissue slices. *American Journal of Physiology*, 250(4 Pt 2), pp.R625–R632.

Silver, I. A. & Erecińska, M., 1998. Glucose-induced intracellular ion changes in sugar-sensitive hypothalamic neurons. *Journal of Neurophysiology*, 79(4), pp.1733–1745.

Simpson, I. A. et al., 1999. Blood-brain barrier glucose transporter: effects of hypo- and hyperglycemia revisited. *Journal of Neurochemistry*, 72(1), pp.238–247.

Skrivarhaug, T. et al., 2006. Long-term mortality in a nationwide cohort of childhood-onset type 1 diabetic patients in Norway. *Diabetologia*, 49(2), pp.298–305.

Snyers, L., De Wit, L. & Content, J., 1990. Glucocorticoid up-regulation of high-affinity interleukin 6 receptors on human epithelial cells. *Proceedings of the National Academy of Sciences of the United States of America*, 87(7), pp.2838–2842.

Sodenkamp, J. et al., 2012. Therapeutic targeting of interleukin-6 trans-signaling does not affect the outcome of experimental tuberculosis. *Immunobiology*, 217(10), pp.996–1004.

Song, W. J. et al., 2013. Pancreatic β-cell response to increased metabolic demand and to pharmacologic secretagogues requires EPAC2A. *Diabetes*, 62(8), pp.2796–2807.

Song, Z. & Routh, V.H., 2006. Recurrent hypoglycemia reduces the glucose sensitivity of glucose-inhibited neurons in the ventromedial hypothalamus nucleus. *American Journal of Physiology. Regulatory, Integrative and Comparative Physiology*, 291(5), pp.R1283–R1287.

Soriano, S. et al., 2011. Regulation of KATP channel by 17β-estradiol in pancreatic β-cells. *Steroids*, 76(9), pp.856–860.

Southern, C., Schulster, D. & Green, I. C., 1990. Inhibition of insulin secretion from rat islets of Langerhans by interleukin-6. An effect distinct from that of interleukin-1. *The Biochemical Journal*, 272(1), pp.243–245.

Stanley, S. et al., 2013. Profiling of glucose-sensing neurons reveals that GHRH neurons are activated by hypoglycemia. *Cell Metabolism*, 18(4), pp.596–607.

Starr, R. et al., 1997. A family of cytokine-inducible inhibitors of signalling. *Nature*, 387(6636), pp.917–921.

Steensberg, A. et al., 2000. Production of interleukin-6 in contracting human skeletal muscles can account for the exercise-induced increase in plasma interleukin-6. *The Journal of Physiology*, 529(Pt 1), pp.237–242.

Stouthard, J. M., Oude Elferink, R. P. & Sauerwein, H. P., 1996. Interleukin-6 enhances glucose transport in 3T3-L1 adipocytes. *Biochemical and Biophysical Research Communications*, 220(2), pp.241–245.

Study, U. H., 2007. Risk of hypoglycaemia in types 1 and 2 diabetes: effects of treatment modalities and their duration. *Diabetologia*, 50(6), pp.1140–1147.

Suh, S. W. et al., 2007. Astrocyte glycogen sustains neuronal activity during hypoglycemia: studies with the glycogen phosphorylase inhibitor CP-316,819 ([R-R*,S*]-5-chloro-N-[2-hydroxy-3-(methoxymethylamino)-3-oxo-1-(phenylmethyl)propyl]-1H-indole-2-carboxamide). *The Journal of Pharmacology and Experimental Therapeutics*, 321(1), pp.45–50.

Taborsky Jr, G. J., Ahrén, B. & Havel, P. J., 1998. Autonomic mediation of glucagon secretion during hypoglycemia implications for impaired α-cell responses in type 1 diabetes. *Diabetes*, 47(7), pp.995–1005.

Takahashi-Tezuka, M. et al., 1998. Gab1 acts as an adapter molecule linking the cytokine receptor gp130 to ERK mitogen-activated protein kinase. *Molecular and Cellular Biology*, 18(7), pp.4109–4117.

Takeda, T. et al., 2014. Primary cerebral and cerebellar astrocytes display differential sensitivity to extracellular sodium with significant effects on apoptosis. *Cell Biochemistry and Function*, 32(4), pp.395–400.

Tamura, S., Morikawa, Y. & Senba, E., 2005. Up-regulated phosphorylation of signal transducer and activator of transcription 3 and cyclic AMP-responsive element binding protein by peripheral inflammation in primary afferent neurons possibly through oncostatin M receptor. *Neuroscience*, 133(3), pp.797–806.

Tancredi, V. et al., 2000. The inhibitory effects of interleukin-6 on synaptic plasticity in the rat hippocampus are associated with an inhibition of mitogen-activated protein kinase ERK. *Journal of Neurochemistry*, 75(2), pp.634–643.

Tanuma, N. et al., 2000. Protein-tyrosine phosphatase PTPεC inhibits Jak-STAT signaling and differentiation induced by interleukin-6 and leukemia inhibitory factor in M1 leukemia cells. *Journal of Biological Chemistry*, 275(36), pp.28216–28221.

Tarasov, A., Dusonchet, J. & Ashcroft, F., 2004. Metabolic regulation of the pancreatic beta-cell ATP-sensitive K+ channel: a pas de deux. *Diabetes*, 53(Suppl 3), pp.113–122.

Tenhumberg, S. et al., 2008. Structure-guided optimization of the interleukin-6 trans-signaling antagonist sgp130. *The Journal of Biological Chemistry*, 283(40), pp.27200–27207.

Theiss, A. L. et al., 2007. Interleukin-6 transcriptionally regulates prohibitin expression in intestinal epithelial cells. *Journal of Biological Chemistry*, 282(17), pp.12804–12812.

Thorens, B., 2012. Sensing of glucose in the brain. *Handbook of Experimental Pharmacology*, 209, pp.277–294.

Thorens, B. et al., 2000. Transgenic reexpression of GLUT1 or GLUT2 in pancreatic β cells rescues GLUT2-null mice from early death and restores normal glucose-stimulated insulin secretion. *Journal of Biological Chemistry*, 275(31), pp.23751–23758.

Tian, Z. J. & An, W., 2004. ERK1/2 contributes negative regulation to STAT3 activity in HSS-transfected HepG2 cells. *Cell Research*, 14(2), pp.141–147.

Toda, C. & Diano, S., 2014. Mitochondrial UCP2 in the central regulation of metabolism. *Best Practice & Research Clinical Endocrinology & Metabolism*, 28(5), pp.757–764.

Tong, Q. et al., 2007. Synaptic glutamate release by ventromedial hypothalamic neurons is part of the neurocircuitry that prevents hypoglycemia. *Cell Metabolism*, 5(5), pp.383–393.

Tsujii, S. & Bray, G. A., 1990. Effects of glucose, 2-deoxyglucose, phlorizin, and insulin on food intake of lean and fatty rats. *American Journal of Physiology*, 258(3 Pt 1), pp.E476–E481.

Tucker, S. J. et al., 1998. Molecular determinants of KATP channel inhibition by ATP. *The EMBO Journal*, 17(12), pp.3290–3296.

Vaartjes, W. J., de Haas, C. G. & Houweling, M., 1990. Acute effects of interleukin 1alpha and 6 on intermediary metabolism in freshly isolated rat hepatocytes. *Biochemical and Biophysical Research Communications*, 169(2), pp.623–628.

Verberne, A. J., Sabetghadam, A. & Korim, W. S., 2014. Neural pathways that control the glucose counterregulatory response. *Frontiers in Neuroscience*, 8(2), pp.38.

Vida, M. et al., 2015. Chronic administration of recombinant IL-6 upregulates lipogenic enzyme expression and aggravates high-fat-diet-induced steatosis in IL-6-deficient mice. *Disease Models & Mechanisms*, 8(7), pp.721–731.

Waage, A., 1989. Local production of tumor necrosis factor alpha, interleukin 1, and interleukin 6 in meningococcal meningitis. Relation to the inflammatory response. *Journal of Experimental Medicine*, 170(6), pp.1859–1867.

Wadt, K. A. et al., 1998. Ciliary neurotrophic factor potentiates the beta-cell inhibitory effect of IL-1beta in rat pancreatic islets associated with increased nitric oxide synthesis and increased expression of inducible nitric oxide synthase. *Diabetes*, 47(10), pp.1602-1608.

Wallenius, K. et al., 2002. Intracerebroventricular interleukin-6 treatment decreases body fat in rats. *Biochemical and Biophysical Research Communications*, 293(1), pp.560–565.

Wallenius, V. et al., 2002. Interleukin-6-deficient mice develop mature-onset obesity. *Nature Medicine*, 8(1), pp.75–79.

Wan, Z. et al., 2012. IL-6 is not necessary for the regulation of adipose tissue mitochondrial content. *PLoS One*, 7(12), pp.e51233.

Wang, C. et al., 2002. Compromised ATP binding as a mechanism of phosphoinositide modulation of ATP-sensitive K+ channels. *FEBS Letters*, 532(1-2), pp.177-182.

Wang, M. J. et al., 2001. Resveratrol inhibits interleukin-6 production in cortical mixed glial cells under hypoxia/hypoglycemia followed by reoxygenation. *Journal of Neuroimmunology*, 112(1-2), pp.28–34.

Wang, R. et al., 2004. The regulation of glucose-excited neurons in the hypothalamic arcuate nucleus by glucose and feeding-relevant peptides. *Diabetes*, 53(8), pp.1959–1965.

Wang, W. Y. et al., 2015. Role of pro-inflammatory cytokines released from microglia in Alzheimer's disease. *Annals of Translational Medicine*, 3(10), pp.136.

Wang, Y. & Fuller, G. M., 1994. Phosphorylation and internalization of gp130 occur after IL-6 activation of Jak2 kinase in hepatocytes. *Molecular Biology of the Cell*, 5(7), pp.819–828.

Wasserman, D. H., 2009. Four grams of glucose. *American Journal of Physiology. Endocrinology and Metabolism*, 296(1), pp.E11–E21.

Watts, A. G. & Donovan, C. M., 2010. Sweet talk in the brain: glucosensing, neural networks, and hypoglycemic counterregulation. *Frontiers in Neuroendocrinology*, 31(1), pp.32–43.

Wegrzyn, J. et al., 2009. Function of mitochondrial Stat3 in cellular respiration. *Science (New York, N.Y.)*, 323(5915), pp.793–797.

Weissenbach, J. et al., 1980. Two interferon mRNAs in human fibroblasts: in vitro translation and escherichia coli cloning studies. *Proceedings of the National Academy of Sciences of the United States of America* , 77(12), pp.7152–7156.

Wellen, K. E. & Hotamisligil, G. S., 2005. Inflammation, stress, and diabetes. *The Journal of Clinical Investigation*, 115(5), pp.1111–1119.

Westberg, J. A. et al., 2007. Hypoxic preconditioning induces neuroprotective stanniocalcin-1 in brain via IL-6 signaling. *Stroke*, 38(3), pp.1025–1030.

White, C. A. & Nicola, N. A., 2013. SOCS3: an essential physiological inhibitor of signaling by interleukin-6 and G-CSF family cytokines. *JAK-STAT*, 2(4), pp.e25045.

White, J. P. et al., 2011. Muscle oxidative capacity during IL-6-dependent cancer cachexia. *American Journal of Physiology. Regulatory, Integrative and Comparative Physiology*, 300(5), pp.R201–R211.

Wilson, J. E., 2003. Isozymes of mammalian hexokinase: structure, subcellular localization and metabolic function. *Journal of Experimental Biology*, 206(12), pp.2049–2057.

Wolf, J., Rose-John, S. & Garbers, C., 2014. Interleukin-6 and its receptors: a highly regulated and dynamic system. *Cytokine*, 70(1), pp.11–20.

Wright, R. J. et al., 2007. Plasma endothelin response to acute hypoglycaemia in adults with type 1 diabetes. *Diabetic Medicine*, 24(9), pp.1039–1042.

Wright, R. J., Newby, D. E. & Stirling, D., 2010. Effects of acute insulin-induced hypoglycemia on indices of inflammation: putative mechanism for aggravating vascular disease in diabetes. *Diabetes Care*, 33(7), pp.1591-1597.

Wueest, S. et al., 2014. Interleukin-6 contributes to early fasting-induced free fatty acid mobilization in mice. *American Journal of Physiology. Regulatory, Integrative and Comparative Physiology*, 306(11), pp.R861–R867.

Wunderlich, F. T. et al., 2010. Interleukin-6 signaling in liver-parenchymal cells suppresses hepatic inflammation and improves systemic insulin action. *Cell Metabolism*, 12(3), pp.237–249.

Xiang, H.-F. et al., 2014. Isoflurane protects against injury caused by deprivation of oxygen and glucose in microglia through regulation of the toll-like receptor 4 pathway. *Journal of Molecular Neuroscience*, 54(4), pp.664–670.

Xie, L., Horie, M. & Takano, M., 1999. Phospholipase C-linked receptors regulate the ATP-sensitive potassium channel by means of phosphatidylinositol 4,5-bisphosphate metabolism. *Proceedings of the National Academy of Sciences of the United States of America*, 96(26), pp.15292–15297.

Xin, L. & Blatteis, C. M., 1992. Hypothalamic neuronal responses to interleukin-6 in tissue slices: effects of indomethacin and naloxone. *Brain Research Bulletin*, 29(1), pp.27–35.

Yamada, M. & Hatanaka, H., 1994. Interleukin-6 protects cultured rat hippocampal neurons against glutamate-induced cell death. *Brain Research*, 643(1-2), pp.173–180.

Yamaguchi, M. et al., 1991. Interleukin-6 stimulates gonadotropin-releasing hormone secretion from rat hypothalamic cells. *Hormone Research*, 35(6), pp.252–256.

Yan, L. J., 2014. Pathogenesis of chronic hyperglycemia: from reductive stress to oxidative stress. *Journal of Diabetes Research*, 2014, pp.137919.

Yang, C. S. et al., 2010. Hypothalamic AMP-activated protein kinase regulates glucose production. *Diabetes*, 59(10), pp.2435–2443.

Yang, P. et al., 2012. IL-6 promotes regeneration and functional recovery after cortical spinal tract injury by reactivating intrinsic growth program of neurons and enhancing synapse formation. *Experimental Neurology*, 236(1), pp.19–27.

Yang, R. et al., 2015. Mitochondrial Ca^{2+} and membrane potential, an alternative pathway for Interleukin 6 to regulate CD4 cell effector function. *eLife*, 4, pp.1–22.

Yang, X. et al., 1999. Hypothalamic glucose sensor similarities to and differences from pancreatic beta-cell mechanisms. *Diabetes*, 48(9), pp.1763–1772.

Yang, X. J. et al., 2004. Metabolic pathways that mediate inhibition of hypothalamic neurons by glucose. *Diabetes*, 53(1), pp.67–73.

Yang, Y. et al., 2008. Interleukin-6 stimulates lipolysis in porcine adipocytes. *Endocrine*, 33(3), pp.261–269.

Yang, Y., Jin, X. & Jiang, C., 2014. S-glutathionylation of ion channels: insights into the regulation of channel functions, thiol modification crosstalk, and mechanosensing. *Antioxidants & Redox Signaling*, 20(6), pp.937–951.

Yasukawa, H. et al., 2003. IL-6 induces an anti-inflammatory response in the absence of SOCS3 in macrophages. *Nature Immunology*, 4(6), pp.551–556.

Yasukawa, K. et al., 1987. Structure and expression of human β cell stimulatory factor-2 (BSF-2/IL-6) gene. *The EMBO Journal*, 6(10), pp.2939–2945.

Yettefti, K. et al., 1995. Sensitivity of nucleus tractus solitarius neurons to induced moderate hyperglycemia, with special reference to catecholaminergic regions. *Journal of the Autonomic Nervous System*, 51(3), pp.191–197.

Yoshimura, A. et al., 1995. A novel cytokine-inducible gene CIS encodes an SH2-containing protein that binds to tyrosine-phosphorylated interleukin 3 and erythropoietin receptors. *The EMBO Journal*, 14(12), pp.2816–2826.

Young, J. K., Baker, J. H. & Montes, M. I., 2000. The brain response to 2-deoxy glucose is blocked by a glial drug. *Pharmacology Biochemistry and Behavior*, 67(2), pp.233–239.

Yuen, D. Y. et al., 2009. Interleukin-6 attenuates insulin-mediated increases in endothelial cell signaling but augments skeletal muscle insulin action via differential effects on tumor necrosis factor-α expression. *Diabetes*, 58(5), pp.1086–1095.

Zhang, H. et al., 2011. Hypoxia-inducible factor directs POMC gene to mediate hypothalamic glucose sensing and energy balance regulation. *PLoS Biology*, 9(7), pp.e1001112.

Zhao, K. et al., 2013. EPAC inhibition of SUR1 receptor increases glutamate release and seizure vulnerability. *Journal of Neuroscience*, 33(20), pp.8861–8865.

Zhou, L. et al., 2010. The medial amygdalar nucleus: a novel glucose-sensing region that modulates the counterregulatory response to hypoglycemia. *Diabetes*, 59(10), pp.2646–2652.

Zhu, W. et al., 2010. Glucose prevents the fall in ventromedial hypothalamic GABA that is required for full activation of glucose counterregulatory responses during hypoglycemia. *American Journal of Physiology. Endocrinology and Metabolism*, 298(5), pp.E971–E977.

Zierler, K., 1999. Whole body glucose metabolism. *American Journal of Physiology. Endocrinology and Metabolism*, 276(3), pp.E409–E426.

Zingman, L. V. et al., 2001. Signaling in channel/enzyme multimers: ATPase transitions in SUR module gate ATP-sensitive K+ conductance. *Neuron*, 31(2), pp.233–245.